

# Ant Colony Optimisation-based Algorithms for Optical Burst Switching Networks

Andrew Scott Gravett

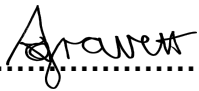
Submitted in fulfilment of the requirements for the degree of Magister Scientiae in  
the Faculty of Science at the Nelson Mandela Metropolitan University

April 2017

Supervisors: Mathys C. du Plessis & Timothy B.  
Gibbon

## DECLARATION

I, Andrew Scott Gravett (s210153563), hereby declare that the dissertation for MSc Computer Science and Information Systems is my own work and that it has not previously been submitted for assessment or completion of any postgraduate qualification to another University or for another qualification.

  
.....  
Andrew Scott Gravett

Official use:

In accordance with Rule G5.6.3,

**5.6.3** A treatise/dissertation/thesis must be accompanied by a written declaration on the part of the candidate to the effect that it is his/her own work and that it has not previously been submitted for assessment to another University or for another qualification. However, material from publications by the candidate may be embodied in a treatise/dissertation/thesis.

# Acknowledgements

I would like to express my sincere gratitude to my supervisors Mathys du Plessis and Timothy Gibbon for their guidance, support and expertise. In addition, I am grateful to Michael Louwrens and Timothy Lee Son for providing advice and support required for this research to have been possible. I would also like to thank Jean Rademakers and Grant Woodford in managing the systems that were used for experimentation, my family for their support and the positive feedback received from the Journal reviewers.

The financial assistance of the National Research Foundation (NRF) and Cisco towards this research is hereby acknowledged (UID number: 103083).

All opinions expressed and conclusions arrived at, are those of the authors and are not necessarily to be attributed to the NRF or Cisco.

# Abstract

This research developed two novel distributed algorithms inspired by Ant Colony Optimisation (ACO) for a solution to the problem of dynamic Routing and Wavelength Assignment (RWA) with wavelength continuity constraint in Optical Burst Switching (OBS) networks utilising both the traditional International Telecommunication Union (ITU) Fixed Grid Wavelength Division Multiplexing (WDM) and Flexible Spectrum scenarios.

The growing demand for more bandwidth in optical networks require more efficient utilisation of available optical resources. OBS is a promising optical switching technique for the improved utilisation of optical network resources over the current optical circuit switching technique. The development of newer technologies has introduced higher rate transmissions and various modulation formats, however, introducing these technologies into the traditional ITU Fixed Grid does not efficiently utilise the available bandwidth.

Flexible Spectrum is a promising approach offering a solution to the problem of improving bandwidth utilisation, which comes with a potential cost. Transmissions have the potential for impairment with respect to the increased traffic and lack of large channel spacing. Proposed routing algorithms should be aware of the linear and non-linear Physical Layer Impairments (PLIs) in order to operate closer to optimum performance. The OBS resource reservation protocol does not cater for the loss of transmissions, Burst Control Packets (BCPs) included, due to physical layer impairments. The protocol was adapted for use in Flexible Spectrum.

Investigation of the use of a route and wavelength combination, from source to destination node pair, for the RWA process was proposed for ACO-based approaches to enforce the establishment and use of complete paths for greedy exploitation in Flexible Spectrum was conducted. The routing tuple for the RWA process is the tight coupling of a route and wavelength in combination intended to promote the greedy exploitation of successful paths for transmission requests. The application

of the routing tuples differs from traditional ACO-based approaches and prompted the investigation of new pheromone calculation equations.

The two novel proposed approaches were tested and experiments conducted comparing with and against existing algorithms (a simple greedy and an ACO-based algorithm) in a traditional ITU Fixed Grid and Flexible Spectrum scenario on three different network topologies. The proposed Flexible Spectrum Ant Colony (FSAC) approach had a markably improved performance over the existing algorithms in the ITU Fixed Grid WDM and Flexible Spectrum scenarios, while Upper Confidence Bound Routing and Wavelength Assignment (UCBRWA) algorithm was able to perform well in the traditional ITU Fixed Grid WDM scenario, but underperformed in the Flexible Spectrum scenario. The results show that the distributed ACO-based FSAC algorithm significantly improved the burst transmission success probability, providing a good solution in the Flexible Spectrum network environment undergoing transmission impairments.

# Contents

<b>1</b>	<b>RESEARCH CONTEXT</b>	<b>1</b>
1.1	Introduction . . . . .	1
1.2	Background . . . . .	1
1.3	Motivation . . . . .	3
1.4	Research Objectives . . . . .	4
1.5	Methodology . . . . .	5
1.6	Scope . . . . .	6
1.7	Dissertation Layout . . . . .	6
<b>2</b>	<b>BACKGROUND AND PROBLEM DESCRIPTION</b>	<b>9</b>
2.1	Introduction . . . . .	9
2.2	Optical Networks . . . . .	10
2.3	Routing . . . . .	11
2.3.1	Routing and Wavelength Assignment . . . . .	11
2.3.2	Rudimentary Assignment Processes . . . . .	14
2.4	Optical Switching . . . . .	16
2.4.1	Optical Switching Techniques . . . . .	16
2.4.2	Optical Burst Switching . . . . .	17
2.4.3	Signalling Protocol . . . . .	19
2.5	Flexible Spectrum . . . . .	19
2.5.1	Flexible Spectrum Drivers . . . . .	20

2.5.2	Flexible Spectrum Approach . . . . .	21
2.5.3	Routing and Spectrum Assignment . . . . .	23
2.5.4	Spectrum Fragmentation . . . . .	25
2.6	Physical Layer Impairments . . . . .	27
2.6.1	Linear and Non-Linear Effects . . . . .	27
2.6.2	Transmission Penalty Equation . . . . .	28
2.7	Conclusion . . . . .	30
<b>3</b>	<b>LITERATURE REVIEW</b>	<b>31</b>
3.1	Introduction . . . . .	31
3.2	Ant Colony Optimisation . . . . .	31
3.2.1	Introduction . . . . .	32
3.2.2	Ant Colony Optimisation Process . . . . .	32
3.2.3	Simple Ant Colony Optimisation Algorithm . . . . .	34
3.2.4	Ant Colony Optimisation applied to RWA . . . . .	35
3.2.5	Ant Colony Routing and Wavelength Assignment . . . . .	36
3.2.5.1	Initialisation . . . . .	37
3.2.5.2	Routing and Wavelength Assignment . . . . .	38
3.2.5.3	State Transition Rule . . . . .	39
3.2.5.4	Global Update . . . . .	39
3.2.5.5	Local Update . . . . .	40
3.3	Upper Confidence Bound . . . . .	41
3.4	Conclusion . . . . .	42
<b>4</b>	<b>PROPOSED APPROACHES</b>	<b>44</b>
4.1	Introduction . . . . .	44
4.2	Impairment Adaptation for OBS . . . . .	44
4.3	Flexible Spectrum Ant Colony Algorithm . . . . .	47
4.3.1	Introduction . . . . .	47
4.3.2	Pheromone Information . . . . .	47

4.3.3	Pheromone Table . . . . .	48
4.3.4	FSAC Initialisation . . . . .	48
4.3.5	Routing and Wavelength Assignment . . . . .	49
4.3.6	Calculation of Pheromones . . . . .	53
4.3.6.1	Pheromone Calculation GU-1 . . . . .	53
4.3.6.2	Pheromone Calculation GU-2 . . . . .	53
4.3.6.3	Pheromone Calculation GU-3 . . . . .	54
4.3.6.4	Pheromone Calculation GU-4 . . . . .	54
4.3.6.5	Pheromone Calculation GU-5 . . . . .	54
4.3.6.6	Pheromone Calculation GU-6 . . . . .	54
4.3.6.7	Pheromone Calculation GU-7 . . . . .	55
4.3.6.8	Pheromone Calculation GU-8 . . . . .	55
4.3.6.9	Pheromone Calculation GU-9 . . . . .	55
4.3.6.10	Pheromone Calculation GU-10 . . . . .	56
4.4	Upper Confidence Bound Routing and Wavelength Assignment . . . . .	56
4.4.1	Introduction . . . . .	56
4.4.2	Routing Table . . . . .	57
4.4.3	Initialisation . . . . .	58
4.4.4	Routing and Wavelength Assignment . . . . .	58
4.4.5	Global Update . . . . .	60
4.5	Conclusion . . . . .	60
<b>5</b>	<b>EVALUATION ON FIXED GRID</b>	<b>62</b>
5.1	Introduction . . . . .	62
5.2	Experimental Procedure . . . . .	62
5.2.1	Performance Measures . . . . .	63
5.2.2	Network Topologies . . . . .	63
5.2.3	Comparison Algorithms . . . . .	65
5.2.4	Procedure . . . . .	66



5.3	Small Topology Results . . . . .	67
5.3.1	Comparison of FSAC Pheromone Calculations . . . . .	67
5.3.1.1	Relative Performance of Pheromone Calculations . . . . .	67
5.3.1.2	Timewise Performance of Pheromone Calculations . . . . .	69
5.3.1.3	Overall Performance of Pheromone Calculations . . . . .	72
5.3.2	Comparison Against Existing Algorithms . . . . .	73
5.3.2.1	Relative Performance Comparison . . . . .	73
5.3.2.2	Timewise Performance Comparison . . . . .	74
5.3.2.3	Overall Performance Analysis . . . . .	77
5.4	Medium Topology Results . . . . .	78
5.4.1	Comparison of FSAC Pheromone Calculations . . . . .	78
5.4.1.1	Relative Performance of Pheromone Calculations . . . . .	78
5.4.1.2	Timewise Performance of Pheromone Calculations . . . . .	80
5.4.1.3	Overall Performance of Pheromone Calculations . . . . .	82
5.4.2	Comparison Against Existing Algorithms . . . . .	83
5.4.2.1	Relative Performance Comparison . . . . .	84
5.4.2.2	Timewise Performance Comparison . . . . .	85
5.4.2.3	Overall Performance Analysis . . . . .	88
5.5	Large Topology Results . . . . .	89
5.5.1	Comparison of FSAC Pheromone Calculations . . . . .	90
5.5.1.1	Relative Performance of Pheromone Calculations . . . . .	90
5.5.1.2	Timewise Performance of Pheromone Calculations . . . . .	91
5.5.1.3	Overall Performance of Pheromone Calculations . . . . .	94
5.5.2	Comparison Against Existing Algorithms . . . . .	95
5.5.2.1	Relative Performance Comparison . . . . .	95
5.5.2.2	Timewise Performance Comparison . . . . .	97
5.5.2.3	Overall Performance Analysis . . . . .	100
5.6	Umbrella Analysis . . . . .	101
5.7	Conclusion . . . . .	102

## 6 EVALUATION ON FLEXIBLE SPECTRUM AND IMPAIRMENTS 104

6.1	Introduction . . . . .	104
6.2	Experimental Procedure . . . . .	105
6.2.1	Performance Measures . . . . .	105
6.2.2	Network Topologies . . . . .	106
6.2.3	Comparison Algorithms . . . . .	107
6.2.4	Procedure . . . . .	108
6.3	Small Topology Results . . . . .	110
6.3.1	Comparison of FSAC Pheromone Calculations . . . . .	110
6.3.1.1	Relative Performance of Pheromone Calculations . .	110
6.3.1.2	Timewise Performance of Pheromone Calculations . .	112
6.3.1.3	Overall Performance of Pheromone Calculations . . .	115
6.3.2	Comparison Against Existing Algorithms . . . . .	115
6.3.2.1	Relative Performance Comparison . . . . .	115
6.3.2.2	Timewise Performance Comparison . . . . .	116
6.3.2.3	Overall Performance Analysis . . . . .	119
6.4	Medium Topology Results . . . . .	121
6.4.1	Comparison of FSAC Pheromone Calculations . . . . .	121
6.4.1.1	Relative Performance of Pheromone Calculations . .	121
6.4.1.2	Timewise Performance of Pheromone Calculations . .	122
6.4.1.3	Overall Performance of Pheromone Calculations . . .	125
6.4.2	Comparison Against Existing Algorithms . . . . .	126
6.4.2.1	Relative Performance Comparison . . . . .	126
6.4.2.2	Timewise Performance Comparison . . . . .	127
6.4.2.3	Overall Performance Analysis . . . . .	130
6.5	Large Topology Results . . . . .	131
6.5.1	Comparison of FSAC Pheromone Calculations . . . . .	131
6.5.1.1	Relative Performance of Pheromone Calculations . .	132
6.5.1.2	Timewise Performance of Pheromone Calculations . .	133

6.5.1.3	Overall Performance of Pheromone Calculations . . .	135
6.5.2	Comparison Against Existing Algorithms . . . . .	136
6.5.2.1	Relative Performance Comparison . . . . .	137
6.5.2.2	Timewise Performance Comparison . . . . .	138
6.5.2.3	Overall Performance Analysis . . . . .	142
6.6	Umbrella Analysis . . . . .	142
6.7	Conclusion . . . . .	144
<b>7</b>	<b>CONCLUSION</b>	<b>145</b>
7.1	Introduction . . . . .	145
7.2	Overview of Results and Outcomes of Research Objectives . . . . .	145
7.3	Contributions . . . . .	147
7.4	Limitations . . . . .	150
7.5	Recommendation for Future Investigation . . . . .	150
7.6	Summary . . . . .	151
	<b>Appendices</b>	<b>161</b>
<b>A</b>	<b>Appendix FSAC Fixed Grid Dataset</b>	<b>162</b>
<b>B</b>	<b>Appendix FSAC Flexible Spectrum Dataset</b>	<b>169</b>
<b>C</b>	<b>Appendix Fixed Grid Comparison Dataset</b>	<b>176</b>
<b>D</b>	<b>Appendix Flexible Spectrum Comparison Dataset</b>	<b>180</b>
<b>E</b>	<b>IEEE (SSCI) 2016 Paper</b>	<b>184</b>
<b>F</b>	<b>Photonic Network Communications</b>	<b>185</b>

# List of Figures

2.1	Available optical channels for a path composed of two links that satisfy the WCC (Shen and Yang, 2011). . . . .	13
2.2	Frequency grid structures for Fixed, Flexi-Grid and Grid-Less (Flexible Spectrum) (Shen and Yang, 2011). . . . .	22
2.3	Spectrum Continuity of established paths(Capucho and Resendo, 2013). 24	
2.4	Available spectrum for a route between nodes A and E (Wright et al., 2013). . . . .	26
2.5	Spectrum fragmentation over a network’s lifespan (Wright et al., 2013). 27	
3.1	Shortest Path Finding capability of ant colonies (Blum, 2007). . . . .	33
5.1	Small 6-Node network topology . . . . .	64
5.2	Medium 11-Node network topology . . . . .	64
5.3	Large 14-Node network topology . . . . .	65
5.4	Burst Success Ratio for FSAC PCs on the small network topology with 8 wavelengths. . . . .	68
5.5	Burst Success Ratio for FSAC PCs over time at a load of 15. . . . .	69
5.6	Burst Success Ratio for FSAC PCs over time at a load of 30. . . . .	70
5.7	Burst Success Ratio for FSAC PCs over time at a load of 45. . . . .	71
5.8	Burst Success Ratio on the small network topology with 8 wavelengths. 73	
5.9	Burst Success Ratio over time at a load of 15. . . . .	75
5.10	Burst Success Ratio over time at a load of 30. . . . .	76
5.11	Burst Success Ratio for FSAC PCs over time at a load of 45. . . . .	77

5.12	Burst Success Ratio for FSAC PCs on the medium network topology with 12 wavelengths. . . . .	79
5.13	Burst Success Ratio for FSAC PCs over time at a load of 20. . . . .	81
5.14	Burst Success Ratio for FSAC PCs over time at a load of 40. . . . .	82
5.15	Burst Success Ratio for FSAC PCs over time at a load of 60. . . . .	83
5.16	Burst Success Ratio on the medium network topology with 12 wave- lengths. . . . .	84
5.17	Burst Success Ratio over time at a load of 20. . . . .	86
5.18	Burst Success Ratio over time at a load of 40. . . . .	87
5.19	Burst Success Ratio over time at a load of 60. . . . .	88
5.20	Burst Success Ratio for FSAC PCs on the large network topology with 16 wavelengths. . . . .	90
5.21	Burst Success Ratio for FSAC PCs over time at a load of 20. . . . .	92
5.22	Burst Success Ratio for FSAC PCs over time at a load of 40. . . . .	93
5.23	Burst Success Ratio for FSAC PCs over time at a load of 60. . . . .	94
5.24	Burst Success Ratio on the large network topology with 16 wavelengths.	95
5.25	Burst Success Ratio over time at a load of 20. . . . .	97
5.26	Burst Success Ratio over time at a load of 40. . . . .	98
5.27	Burst Success Ratio over time at a load of 60. . . . .	99
6.1	Small 6-Node network topology . . . . .	106
6.2	Medium 11-Node network topology . . . . .	107
6.3	Large 14-Node network topology . . . . .	108
6.4	Burst Success Ratio for FSAC PCs on the small network topology. . .	111
6.5	Burst Success Ratio for FSAC PCs over time at a load of 30. . . . .	112
6.6	Burst Success Ratio for FSAC PCs over time at a load of 60. . . . .	113
6.7	Burst Success Ratio for FSAC PCs over time at a load of 90. . . . .	114
6.8	Burst Success Ratio on the small network topology. . . . .	116
6.9	Burst Success Ratio over time at a load of 30. . . . .	118

6.10	Burst Success Ratio over time at a load of 60. . . . .	119
6.11	Burst Success Ratio over time at a load of 90. . . . .	120
6.12	Burst Success Ratio for FSAC PCs on the medium network topology.	121
6.13	Burst Success Ratio for FSAC PCs over time at a load of 30. . . . .	123
6.14	Burst Success Ratio for FSAC PCs over time at a load of 60. . . . .	124
6.15	Burst Success Ratio for FSAC PCs over time at a load of 90. . . . .	125
6.16	Burst Success Ratio on the medium network topology. . . . .	126
6.17	Burst Success Ratio over time at a load of 30. . . . .	128
6.18	Burst Success Ratio over time at a load of 60. . . . .	129
6.19	Burst Success Ratio over time at a load of 90. . . . .	130
6.20	Burst Success Ratio for FSAC PCs on the large network topology. . .	132
6.21	Burst Success Ratio for FSAC PCs over time at a load of 30. . . . .	134
6.22	Burst Success Ratio for FSAC PCs over time at a load of 60. . . . .	135
6.23	Burst Success Ratio for FSAC PCs over time at a load of 90. . . . .	136
6.24	Burst Success Ratio on the large network topology. . . . .	137
6.25	Burst Success Ratio over time at a load of 30. . . . .	139
6.26	Burst Success Ratio over time at a load of 60. . . . .	140
6.27	Burst Success Ratio over time at a load of 90. . . . .	141

# List of Tables

3.1	ACRWA Pheromone Table (Triay and Cervello-Pastor, 2010) . . . . .	38
4.1	FSAC Pheromone Table for node $A$ , $PT_A$ . . . . .	49
4.2	Routing Table . . . . .	58
5.1	Overall performance of the FSAC PCs on the small network topology with 8 wavelengths. . . . .	72
5.2	Success ratio and 95% confidence interval at a specific load on the small network topology with 8 wavelengths. . . . .	74
5.3	Overall Algorithm performance on the small network topology with 8 wavelengths. . . . .	74
5.4	Overall performance of the FSAC PCs on the medium network topology with 12 wavelengths. . . . .	80
5.5	Success ratio and 95% confidence interval at a specific load on the medium network topology with 12 wavelengths. . . . .	85
5.6	Overall Algorithm performance on the medium network topology with 12 wavelengths. . . . .	85
5.7	Overall performance of the FSAC PCs on the large network topology with 16 wavelengths. . . . .	91
5.8	Success ratio and 95% confidence interval at a specific load on the large network topology with 16 wavelengths. . . . .	96
5.9	Overall Algorithm performance on the large network topology with 16 wavelengths. . . . .	96

5.10	Overall Pheromone Calculation performance on all the tested network topologies. . . . .	101
5.11	Overall Algorithm performance on all the tested network topologies. .	101
6.1	Overall performance of the FSAC PCs on the small network topology.	110
6.2	Success ratio and 95% confidence interval at a specific load on the small network topology. . . . .	117
6.3	Overall Algorithm performance on the small network topology. . . . .	117
6.4	Overall performance of the FSAC PCs on the medium network topology.	122
6.5	Success ratio and 95% confidence interval at a specific load on the medium network topology. . . . .	127
6.6	Overall Algorithm performance on the medium network topology. . .	127
6.7	Overall performance of the FSAC PCs on the large network topology.	133
6.8	Success ratio and 95% confidence interval at a specific load on the large network topology. . . . .	138
6.9	Overall Algorithm performance on the large network topology. . . . .	138
6.10	Overall Pheromone Calculation performance on all the tested network topologies. . . . .	143
6.11	Overall Algorithm performance on all the tested network topologies. .	143
A.1	Fixed Grid dataset of the Success ratio for FSAC PCs on the small network topology . . . . .	163
A.2	Fixed Grid dataset of the Success ratio for FSAC PCs on the medium network topology . . . . .	165
A.3	Fixed Grid dataset of the Success ratio for FSAC PCs on the large network topology . . . . .	167
B.1	Flexible Spectrum dataset of the Success ratio for FSAC PCs on the small network topology . . . . .	170



B.2	Flexible Spectrum dataset of the Success ratio for FSAC PCs on the medium network topology . . . . .	172
B.3	Flexible Spectrum dataset of the Success ratio for FSAC PCs on the large network topology . . . . .	174
C.1	Fixed Grid dataset of the Success ratio for all the tested algorithms on the small network topology . . . . .	176
C.2	Fixed Grid dataset of the Success ratio for all the tested algorithms on the medium network topology . . . . .	177
C.3	Fixed Grid dataset of the Success ratio for all the tested algorithms on the large network topology . . . . .	178
D.1	Flexible Spectrum dataset of the Success ratio for all the tested algorithms on the small network topology . . . . .	180
D.2	Flexible Spectrum dataset of the Success ratio for all the tested algorithms on the medium network topology . . . . .	181
D.3	Flexible Spectrum dataset of the Success ratio for all the tested algorithms on the large network topology . . . . .	182

## List of Abbreviations

---

<b>Abbreviation</b>	<b>Term</b>
<b>ACO</b>	Ant Colony Optimisation
<b>UCB</b>	Upper Confidence Bound
<b>RWA</b>	Routing and Wavelength Assignment
<b>RSA</b>	Routing and Spectrum Assignment
<b>WCC</b>	Wavelength Continuity Constraint
<b>SCC</b>	Spectrum Continuity Constraint
<b>OCS</b>	Optical Circuit Switching
<b>OPS</b>	Optical Packet Switching
<b>OBS</b>	Optical Burst Switching
<b>WDM</b>	Wavelength Division Multiplexing
<b>DWDM</b>	Dense Wavelength Division Multiplexing
<b>BCP</b>	Burst Control Packet
<b>BCP-RA</b>	Burst Control Packet Release Acknowledgement
<b>BCP-FA</b>	Burst Control Packet Failure Acknowledgement
<b>BCP-TA</b>	Burst Control Packet Traversal Acknowledgement
<b>ITU</b>	International Telecommunication Union
<b>PLI</b>	Physical Layer Impairment
<b>JIT</b>	Just-In-Time
<b>JET</b>	Just-Enough-Time
<b>SPR</b>	Shortest Path Routing
<b>ACRWA</b>	Ant Colony Routing and Wavelength Assignment
<b>UCBRWA</b>	Upper Confidence Bound Routing and Wavelength Assignment
<b>FSAC</b>	Flexible Spectrum Ant Colony

---

# Chapter 1

## RESEARCH CONTEXT

### 1.1 Introduction

There is an ever growing demand for more bandwidth in optical transport networks (Yao et al., 2000). The telecommunication industry has been forced to upgrade its infrastructure and seek out new techniques to increase the capacity of optical transport networks (Imran and Aziz, 2014). Advances in Wavelength Division Multiplexing (WDM) technology has dramatically increased the network capacity (Yao et al., 2000). There is an increasingly growing amount of traffic driven by the high-definition video distribution services, cloud computing among many others with increasing high-speed broadband penetration through both fixed and mobile terminals (Wright et al., 2013; Jinno et al., 2009). Research is required to address the demand for more bandwidth.

### 1.2 Background

Current optical networks primarily employ Optical Circuit Switching (OCS) which is well suited for persistent high bandwidth traffic that does not vary much over time (Ngo et al., 2006). In OCS networks, an all optical path between the source and destination node is established prior to the transmission of data in a static

manner (Jue et al., 2009). The bandwidth is not efficiently utilised as the resources are reserved when not in use, especially when carrying varying traffic over time (Jue et al., 2009).

Optical Packet Switching (OPS) and Optical Burst Switching (OBS) are optical switching technologies developed to overcome the static and inefficient allocation of network resources by existing OCS networks (Agrawal et al., 2005). OBS is a technical compromise between OCS and OPS in a flexible yet feasible way as it does not require optical buffering or packet-level processing as is the case with OPS (Galdino et al., 2010). OBS is a technology that offers a more flexible and dynamic optical network compared to traditional OCS networks. However, OBS does suffer from burst losses due to a lack of cost effective optical buffers and resource reservation schemes. The Routing and Wavelength Assignment (RWA) process is especially difficult in an optical network with no wavelength converters and buffers within the core increasing the risk of burst losses.

Ant Colony Optimisation (ACO) algorithms have been extensively applied to solve routing problems within telecommunication networks (Ngo et al., 2006). ACO is a biologically inspired system based on the social and foraging behaviour patterns of ants seeking an optimal path between their food source and colony (Dorigo and Di Caro, 1999). This behaviour has been imitated and adapted for use in solving various graph based computational problems. Several ACO algorithms have been used for solving the routing and wavelengths assignment problem in OBS networks (Triay and Cervello-Pastor, 2009; Pedro et al., 2009; Donato et al., 2012). ACO is of particular interest as it is able to run continuously, adapting to changes in the network state and traffic load in real time which provides a dynamic solution to the RWA problem.

Currently, optical channels are fixed, providing a reliable solution which minimizes inter-channel collisions and crosstalk. This however, limits the performance and flexibility of the optical network. There is thus a requirement for more advanced approaches toward more spectrum-efficient technologies (Shen and Yang, 2011; Wen

et al., 2013). A promising alternative is represented by flexible optical networking which is expected to provide enhanced spectrum management with respect to the Fixed Grid of traditional WDM systems and be able to “scale to match” the capacity requirements of future systems (Manousakis and Ellinas, 2016). The flexible component refers to the ability of the optical network to dynamically adjust its optical resources in an optimum and elastic way according to the continuously varying traffic conditions and demands (Waldman et al., 2013). Flexible Spectrum offers a flexible and dynamic spectrum assignment solution in order to effectively increase the capacity in optical transport networks (Capucho and Resendo, 2013; Klinkowski and Walkowiak, 2011). There is a potential penalty associated with the use of Flexible Spectrum. The removal of the traditional International Telecommunication Union (ITU) Fixed Grid to improve spectrum utilization can possibly increase the effects of transmission impairments. Therefore, a requirement for the effective management and utilization of the network resources is needed.

### 1.3 Motivation

The bandwidth demand is increasing in optical networks. Currently used techniques do not use full potential of optical networks. OBS is one of the most promising proposed optical switching techniques to exploit the advantages of optical communication networks (Aguas et al., 2015). In the last few years, OBS has been successfully implemented on a number of testbeds demonstrating the architecture and protocols (Barpanda et al., 2014). OBS is the most likely optical switching technique to be implemented in the near future (Coulibaly et al., 2015).

With the introduction of higher transmission rates and various modulations, the traditional ITU Fixed Grid approach is unable to efficiently utilise bandwidth. The fixed channel spacing is able to achieve high capacity optical transmissions with larger channel spacing. However, bandwidth efficiency is decreased when a mix of transmission rates are used (Chino et al., 2016). Flexible Spectrum is able to

increase the spectral efficiency (Amar et al., 2014).

Flexible Spectrum is a promising approach, but it does come with a potential cost. Transmissions have the potential for impairment with respect to the increased traffic and lack of large channel spacing. Proposed routing algorithms should be aware of the linear and non-linear Physical Layer Impairments (PLIs) in order to operate closer to optimum performance (Johannisson and Agrell, 2014).

## 1.4 Research Objectives

The previous section provided a brief motivation for this study, the following research objectives were identified:

- **Improve on current algorithms for OBS networks.** This objective involves the development of new algorithms that are more effective than existing solutions.
- **Provide for Flexible Spectrum in the developed approaches.** The current OBS protocols and routing algorithms do not cater for Flexible Spectrum. The protocols and algorithms would need to be adapted in order to support this approach.
- **Consider PLIs in Flexible Spectrum.** Current research is mainly conducted on idealised scenarios which do not accurately represent the real world. This research investigates the more realistic scenarios in which PLIs are taken into account.
- **Evaluate and refine the proposed ACO-based approaches.** The final objective of this study is to evaluate the newly created algorithms in order to determine whether the previous objectives were achieved and to measure the contribution of this study.

The next section is concerned with the process that was followed to achieve this research.

## 1.5 Methodology

A literature study was performed on ACO and ACO-based approaches for RWA in optical networks, focusing on OBS. Flexible Spectrum was identified as a promising approach toward improved spectral efficiency, however, there is a potential for transmission impairments due to linear and non-linear effects. A method for modelling PLI's in Flexible Spectrum was identified and used in simulation. Appropriate ACO-based approaches were investigated, adapted for use in Flexible Spectrum and implemented. It was noted that the investigated ACO-based approaches were not successful in the Flexible Spectrum environment. In conclusion, the approaches were not able find and repeatedly make use of good solutions.

An investigation into the use of a route and wavelength combination was conducted to overcome this problem. This enforced the establishment and use of complete paths for greedy exploitation in Flexible Spectrum. The results obtained from this approach displayed an improvement over the initial ACO-based implementations. The use of a route and wavelength combination differed from traditional ACO-based approaches. New pheromone calculation equations were proposed for the use of route and wavelength combinations, leading to the development of the novel Flexible Spectrum Ant Colony approach. Further investigation into the use of Upper Confidence Bound (UCB) to provide a balance between the exploration and exploitation in the RWA process was also conducted. A hybridisation of UCB and ACO lead to the development of the novel UCBRWA approach to select an appropriate route and wavelength combination for the RWA process.

The novel proposed approaches were tested and experiments conducted comparing with and against existing algorithms (a simple greedy and an ant based algorithm) in a traditional ITU Fixed Grid and Flexible Spectrum scenario on three

different network topologies.

## 1.6 Scope

The scope of this research does not include an exhaustive parameter study. There are many parameters to test that could potentially impact the performance of the algorithms tested in this research significantly. The parameters used in this study were informed through the parameters used by other researchers, determined through a series of preliminary experiments, and expert knowledge.

## 1.7 Dissertation Layout

Chapters 2 and 3 present the the background to the problem statement, introducing the relevant literature and motivations for the proposed approaches. The proposed approaches are introduced and discussed in detail within Chapter 4. Chapters 5 and 6 discuss the experimental work conducted in order to measure the proposed approaches against existing algorithms. Details of the experimental method are presented and discussed within each chapter. Chapter 7 presents the conclusions drawn from this work. The chapters address the following issues:

- **Chapter 2:** The applicable background theory of Optical Networks, RWA, Optical Switching techniques, Flexible Spectrum and PLIs are discussed.
- **Chapter 3:** Related work and literature of ACO-based algorithms for RWA are presented. The application of UCB is detailed.
- **Chapter 4:** The developed novel ACO-based approaches FSAC and UCBRWA are presented and discussed. New pheromone calculations are explored for the use of routing tuples. The adapted OBS reservation protocol for Flexible Spectrum is detailed.



- **Chapter 5:** This chapter covers the experimental work performed in an existing technology (traditional ITU Fixed Grid). Experimental methods are discussed and details of the experiments are provided. Results of the experimental work are presented and discussed comparing the proposed approaches with existing algorithms.
- **Chapter 6:** This chapter covers the experimental work performed in a future technology (Flexible Spectrum with PLIs). Experimental methods are discussed and details of the experiments are provided. Results of the experimental work are presented and discussed comparing the proposed approaches with existing algorithms.
- **Chapter 7:** In this chapter an overview is presented of the experimental work together with discussions and outcomes of the research objectives. The contributions and limitations of this work are detailed with recommendations for future research proposed.
- **Appendix A:** Presents the tabulated results collected for the FSAC algorithm pheromone updates on Fixed Grid.
- **Appendix B:** Presents the tabulated results collected for the FSAC algorithm pheromone updates on Flexible Spectrum.
- **Appendix C:** Presents the tabulated results collected for proposed approaches and existing algorithms on Fixed Grid.
- **Appendix D:** Presents the tabulated results collected for proposed approaches and existing algorithms on Flexible Spectrum.
- **Appendix E:** The conference paper that was accepted and presented at the 2016 IEEE Symposium Series on Computational Intelligence (IEEE SSCI 2016).

- **Appendix F:** The journal paper that was submitted to Photonic Network Communications and is under review.

# Chapter 2

## BACKGROUND AND PROBLEM DESCRIPTION

### 2.1 Introduction

This chapter will discuss Optical Networks, past and present (Section 2.2). Routing (Section 2.3) covers the process of allocating a route and wavelength for an incoming transmission request in an optical network, introducing the importance of the WCC and presenting rudimentary methods for RWA. Current techniques for the transmission of data within optical networks is discussed in Section 2.4, introducing new optical switching techniques that have been proposed to make more efficient use of optical network resources than the current OCS technique. A detailed description of OBS and the manner in which it functions is provided in Section 2.4.2. Section 2.5 details new techniques developed for optical networks to enhance the manner in which optical spectrum is allocated, moving from the traditional ITU Fixed Grid to Flexi-Grid and Grid-Less (Flexible Spectrum) techniques. The above mentioned techniques, Flexi-Grid and Grid-Less, better cater for the use of mixed transmission rates and modulations. The process of allocating a route and spectrum for an incoming transmission request in Flexible Spectrum is be covered, including the

importance of the SCC and the challenges Flexible Spectrum introduces in terms of Spectrum Fragmentation and PLIs. A detailed description of the PLIs covering the linear and non-linear impairments is provided, including an equation for modelling the associated effects in Section 2.6.

## 2.2 Optical Networks

An optical network is a high capacity telecommunication network that is based on optical technology and components. The optical network is composed of a collection of nodes and switches which are connected by means of optical fiber. Driven by the sustained growth of data traffic volume, a new approach is required to fulfil the traffic demands placed upon the optical network. Due to the limitations in technology at the time, signal frequencies had to be widely separated. The fused biconic tapered coupler system typically made use of 1310 nm and 1550 nm (1310 nm, 1500 nm and 1625 nm bands have very low signal loss) signals providing 5 Gb/s on a single fiber (Bourouha et al., 2002). This system provided double the bandwidth, in contrast to modern networks which can transmit an individual signal at 10 Gb/s and have several different signals transmitting at such a rate through the optical fiber simultaneously (Bourouha et al., 2002). Due to advancements in technology however, the number of wavelengths will continue to increase (Wright et al., 2013). There are a few technological solutions which enable optical networks to meet the required bandwidth and flexibility for increased traffic demands. WDM was introduced to provide optical networks with additional capacity on existing optical fibers. Multiplexing is the process of combining several different wavelengths in a single optical fiber and then separating them at the receiving end by means of de-multiplexing. A light detector or receiver is then required for each of the de-multiplexed wavelengths in order to convert the signal back into useful information. The WDM technique allows for the better utilisation of bandwidth within an optical fiber and overcomes the optoelectronic bottleneck by performing routing in the network nodes (Barpanda

et al., 2009). Each wavelength of each fiber link then becomes a sub-channel that is independent of the other wavelengths (Fernando et al., 2013).

Dense Wavelength Division Multiplexing (DWDM) has provided the core network capacity required by network operators for the past 15 years to maintain the exponential growth in bandwidth demand. The bandwidth of an optical fiber has been divided into a choice of either 100, 50 or even 25 GHz fixed spaced channels providing high capacity transport (Chen et al., 2014). The channel spacing allows for up to 160 optical channels to be utilised. The fixed grids have allowed network operators to serve the traffic growth well by either increasing the speed of the transponders on each channel or by moving to a denser grid spacing as the traffic levels have increased (Wright et al., 2013). DWDM systems, when compared to that of WDM, have had to maintain a finer and more stable transmission wavelength due to the finer granularity of the grid spacing. Granularity refers to the size of the spectrum channel spacing (Jinno et al., 2009). A standard grid has been successful in allowing vendors to develop components to the same specifications. An evenly spaced grid allows for simpler wavelength control and manufacture of de/multiplexing components. Technological improvements have allowed transponders to increase transmission bit rates from 2.5 Gb/s per-wavelength to capacities of 10, 40 or even 100 Gb/s while still confining the signal to the 50 GHz channel grid spacing (Wright et al., 2013; Amaya et al., 2011).

## 2.3 Routing

This section introduces the RWA process, describing its application, presenting the importance of the WCC and further details rudimentary RWA methods.

### 2.3.1 Routing and Wavelength Assignment

The routing and wavelength allocation process establishes a path, a route and wavelength, in a network for a connection request. The problem of assigning the path is

referred to as the Routing and Wavelength Assignment (RWA) problem. The problem consists of two distinct parts, computing a route from the source to destination node pair and then assigning an available wavelength (Barpanda et al., 2010). The RWA process has the goal of fulfilling the connection request, minimising the blocking probability of future incoming requests and utilising available network resources in an efficient manner (Siddiqui et al., 2004; Bhanja et al., 2010). The following are three forms of traffic generation for connection requests in optical networks:

- Static traffic is when all of the connections requests are known in advance, remain in the network for a long period of time and are not released once they have been setup.
- Incremental traffic have the connection requests arrive sequentially and remain in the network indefinitely.
- Dynamic traffic is when all of the connection requests arrive sequentially, are handled and routed one at a time where each of the connection requests remain in the network for a finite amount of time.

All discussed literature, experimental results and findings hereafter will be in terms of the Dynamic traffic generation. The RWA process determines the route and wavelength to assign to an incoming connection request for a particular source and destination node pair. Separating the RWA problem into two distinct parts, consider the routing component. The routing process calculates the route along which the incoming connection request will travel in order to reach the destination node (Siddiqui et al., 2004; Lin et al., 2008; Binh, 2008). Typically, the shortest route is selected as it would make use of the least optical resources. In a wavelength routed WDM network a link would have a fixed number of wavelengths in accordance with the fixed grid. The second component of the RWA process selects an available wavelength along the route chosen above. The wavelength routed WDM network may have no wavelength conversion at the intermediary nodes, therefore the selected path (route and wavelength) would need to satisfy the WCC.

The WCC forces the connection request to maintain the same wavelength throughout the routing process which serves to avoid a costly optical-electrical conversion at the node level in order to alter a wavelength. In order to satisfy the WCC, the

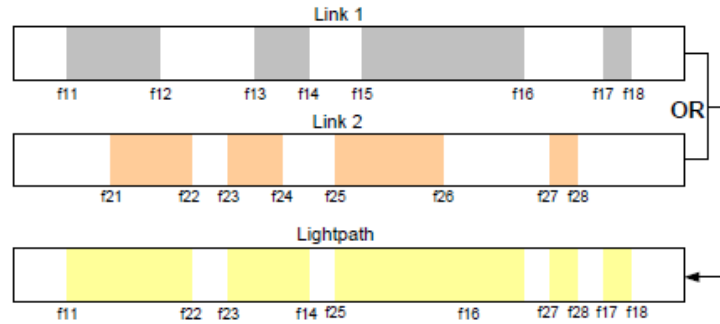


Figure 2.1: Available optical channels for a path composed of two links that satisfy the WCC (Shen and Yang, 2011).

path must be bound to a single wavelength in order to traverse all the nodes along the selected path as seen in Figure 2.1. Figure 2.1 is an illustration of the currently reserved wavelengths on two links (Link 1 and Link 2). In Figure 2.1, the currently reserved wavelengths are displayed in colour while currently available wavelengths are represented as white space. The illustration at the bottom of Figure 2.1 is a representation of the combined reserved (represented in colour) and unreserved (represented as white space) wavelengths on Link 1 and Link 2. Only the unreserved wavelengths (represented as white space) in the illustration at the bottom of Figure 2.1 satisfy the WCC for a path composed of the two links. The allocation of a route and wavelength for a connection request must conform to the WCC (Binh, 2008; Durn et al., 2012). With this in mind, it is necessary to align both the RWA of a connection request in an integrated manner.

### 2.3.2 Rudimentary Assignment Processes

The RWA problem is usually simplified and separated into two distinct processes, a routing or path assignment and the wavelength assignment. There are many different routing assignment approaches. The following are three basic approaches to the routing assignment process:

- Fixed routing is a straightforward approach to the routing assignment process as there is only a single fixed route to make use of between the source and destination node pair. An example of this approach is Shortest Path Routing (SPR) which makes use of the shortest path between any source and destination node pair. The shortest route for each source to node pair is calculated offline, typically using Dijkstras algorithm.
- The Fixed-Alternate routing approach makes use of multiple fixed routes between the source and destination node pair. As a result, each node in the network must maintain a routing table of candidates for routes from the source to each destination. The candidates are typically made up of the shortest routes between the source and destination node pair. Typically, the alternate route does not share any links with the first or shortest path in the routing table.
- Adaptive routing is an approach that selects routes dynamically based on the current availability of wavelength on each of the links within the network. This approach requires current data on all the links within the network. Any feasible route, from source to destination node pair, can be a candidate for the routing process. The choice of route is determined by the approach, shortest-cost path first or least congested path first.

The wavelength assignment process is required to select a feasible wavelength for a given route from source to destination node pair. The wavelength assignment process can be performed either after or during the routing assignment process. There is the possibility of multiple available wavelengths to select. If no wavelengths are



available a new route must be selected or the request is blocked. The following are four basic approaches to the wavelength assignment process:

- The First-Fit wavelength assignment approach selects the first available wavelength by searching through an indexed list of wavelengths. The approach iterates through the indexed list of wavelengths, considering the lower indexed wavelengths above those of the higher indexed wavelengths. This approach confines the existing connection within a small wavelength range, leaving a large number of wavelengths available for the longer routes.
- Random wavelength assignment is an approach which selects a wavelength from the set of available wavelengths on the source to destination node pair. This is performed by selecting at random one of the available wavelengths in the set, typically with a uniform probability. In a distributed scenario, Random wavelength assignment may outperform First-Fit as only limited and outdated information may be available.
- Most-Used wavelength assignment is a simple approach which determines the most used wavelength within the entire network. The approach then selects and assigns the most used wavelength to the incoming connection. The most used wavelength is selected in order to reduce the number of used wavelengths and promote maximum wavelength reuse in the network.
- The Least-Used wavelength assignment approach determines which is the least used wavelength within the entire network. The approach then selects and assigns the least used wavelength to the incoming connection. The least used wavelength is selected in order to evenly spread the load in the network across all the wavelengths.

A simple greedy algorithm for RWA is the combination of SPR with First-Fit wavelength assignment.

## 2.4 Optical Switching

This section introduces optical switching and different proposed optical switching techniques. A detailed description of OBS is presented followed by an introduction to optical switching reservation protocols.

### 2.4.1 Optical Switching Techniques

With an ever growing demand for more bandwidth in optical transport networks the telecommunication industry has been forced to upgrade its infrastructure and seek out new techniques to increase the capacity of optical transport networks (Imran and Aziz, 2014; Yao et al., 2000). Advances in WDM technology have dramatically increased the network capacity (Yao et al., 2000). Three optical switching techniques have been proposed to satisfy the requirements of current and future applications to satisfy the requirements of bandwidth-greedy application.

Optical networks primarily employ OCS as the current switching technique. In OCS networks, an all optical path between the source and destination node pair is established prior to the transmission of data in a static manner (Jue et al., 2009). The all optical path remains for the duration of transmission ensuring the full availability of the bandwidth. OCS is well suited for persistent high bandwidth traffic that does not vary much over time (Ngo et al., 2006). The bandwidth is inefficiently utilised as the resources are reserved when not in use, especially when carrying varying traffic over time (Jue et al., 2009). Internet traffic consists of a small number of large and long duration traffic flows and many small traffic flows (Hu et al., 2015). A requirement for the effective management and utilization of the network optical resources.

OPS and OBS techniques have been developed to address the bursty internet traffic (Hu et al., 2015). OPS is an optical switching technology developed to overcome the static and inefficient allocation of network resources by existing OCS networks (Agrawal et al., 2005). OPS transmits the packets through the all optical

network on a packet-per-packet basis. The packet headers are processed and converted from optical to electronic. Meanwhile, the packet payloads are optically buffered until such time that the desired link is available. Current optical buffer technology is not sufficient enough to buffer large amounts of packets for any extended period of time due to contention in the network leaving OPS as an excellent theoretical option for the future (Aguas et al., 2015).

The lack of feasible optical buffers and packet losses are the major limiting factors for OPS (Imran et al., 2016). Among the different proposed optical switching techniques, OBS is the most promising (Aguas et al., 2015). OBS is a technical compromise between OCS and OPS in a flexible yet feasible way as it does not require optical buffering or packet-level processing as is the case with OPS (Galdino et al., 2010). In OBS the bursts are transmitted in the optical domain throughout the network, this decreases the optical to electronic conversion and processing times (Aguas et al., 2015). This eliminates the need for buffers at the switching nodes by delaying the burst long enough for the Burst Control Packet (BCP) to be processed, which is sent prior to the burst (Hu et al., 2015). A major challenge for OBS is the reservation of optical resources, it is possible to ensure zero burst loss with two-way reservation (Imran et al., 2016). However, two-way reservation has the negative aspect of a comparatively long setup time.

### 2.4.2 Optical Burst Switching

OBS is an optical switching technique for transmitting bursts of traffic through the network only for the duration of the burst (Xu et al., 2001). The OBS optical switching paradigm is designed to achieve increased bandwidth flexibility with a lack of efficient optical buffers. In OBS, instead of converting and transmitting a single packet of data, the packets are aggregated into large chunks of data at the edge of the network and transmitted in the form of a burst (Papadimitriou et al., 2003; Galdino et al., 2010). The bursts of data are transmitted using a wavelength

channel and are switched through the core nodes of the network. These bursts are later disassembled at the destination node and its packets are delivered accordingly (Papadimitriou et al., 2003). Bursts of data are preceded by a BCP. The BCP for each burst is responsible for the resource reservation and is sent ahead of the data burst on a separate wavelength channel (Aydin et al., 2008). There is a delay between the BCP and the corresponding burst (Imran and Aziz, 2014). The delay allows the BCP to undergo optical to electronic and electronic to optical conversion at each intermediate node along the routing path of the burst (Chen et al., 2004). The intermediate nodes are then able to configure their switching matrix to direct the upcoming data burst to the available wavelength channel on the appropriate output link (Imran and Aziz, 2015). The burst is transmitted and switched without acknowledgement of resource reservations from the BCP (Rodrigues and Vaidya, 2009).

The BCP functions only to perform a set-up (reservation) request for optical resources, thereafter the source node transmits the burst (Imran and Aziz, 2014). Intermediate nodes perform the bandwidth reservation and switching immediately after receiving the BCP. As soon as the BCP is received by the switch, the switching elements are configured for the coming burst. Upon transmission of a data burst, the destination node transmits an acknowledgement to the source of the burst to acknowledge the successful or failed delivery thereof. The acknowledgement is the BCP Release Acknowledgement (BCP-RA) which is also responsible for deallocating optical resources. Until the intermediate node receives a BCP-RA, the switching elements will remain reserved (Kirci and Zaim, 2006). It is possible for multiple data bursts to contend at an intermediate node for the same bandwidths. Unresolved contention will lead to burst dropping and ultimately degrade network performance as bursts are switched all optically. In the case that the BCP is unable to reserve the required optical resources, the transmission is blocked, the node will create a BCP-RA in order to notify the source of the failure and to release the reserved optical resources. In the case that the BCP is able to reserve the optical resources and

the burst is successfully transmitted, the destination node will create a BCP-RA in order to notify the source of the success and to release the reserved optical resources.

### 2.4.3 Signalling Protocol

The two most popular signalling protocols for OBS are Just-In-Time (JIT) and Just-Enough-Time (JET). The two protocols differ in that JIT will immediately reserve optical resources and explicitly release them, while JET delays the reservation of resources and then implicitly releases them (Kirci and Zaim, 2006).

In JIT, as soon as the BCP has been received and processed by a node it will immediately configure the optical switches for the incoming burst. Optical resources are reserved prior to the actual arrival of the incoming burst as no offset time is used (Kirci and Zaim, 2006). This contributes to a less efficient use of resources as the wavelengths are reserved prior to the burst arrival time and as a result the wavelength cannot be utilized until the corresponding burst has been sent. The manner in which the switching elements are configured can lead to increased burst loss.

Unlike JIT, JET makes use of offset time information that is contained within the BCP. JET functions by sending a BCP to the destination node containing the relevant offset time that is processed at each subsequent node. The offset time allows for the delayed reservation of optical resources by only configuring the optical switches at the node right before the arrival time of the burst (Kirci and Zaim, 2006). JET provides a protocol which makes more efficient utilization of optical resources with the cost of a more complex method.

## 2.5 Flexible Spectrum

This section introduces the Flexible Spectrum technique, the drive toward spectrum efficient techniques, the resource reservation process for Flexible Spectrum and some associated obstacles (the SCC and Spectrum Fragmentation).

### 2.5.1 Flexible Spectrum Drivers

There is still plenty of space to fit a 10 Gb/s directly modulated signal within a 50 GHz channel (Lord, 2014). It is more challenging to fit transmissions greater than or equal to 100 Gb/s within the 50 GHz channel. The Fixed Grid optical networks were designed on the premise that all traffic demands would have the same spectrum requirements. In order to fit the 100 Gb/s signal within a 50 GHz channel spacing it is necessary to modulate the signal, which could then only require the use of 37.5 GHz (Muoz et al., 2013; Lord, 2014). The rigid Fixed Grid approach is not ideal for the spectrum requirements of the long-reach transmission and high speed data rates of 400 Gb/s or higher. Modulation of the 400 Gb/s transmission cannot be accommodated within a 50 GHz channel (Amaya et al., 2011; Gerstel et al., 2012). A solution would be to increase the channel spacing of the Fixed Grid as a modulated 400 Gb/s transmission would require 150 GHz of spectrum (Muoz et al., 2013). It is however possible to demultiplex the 400 Gb/s transmission into four separate 100 Gb/s signals which could be accommodated within the 50 GHz channel spacing (Muoz et al., 2013; Wright et al., 2013). This method is wasteful and inefficient in terms of spectral utilisation.

With the increase of transmission rates, a 50 GHz fixed grid spacing would no longer be able to support future traffic growth (Wright et al., 2013). An option would be to convert to a 100 GHz fixed grid spacing. As mentioned above, this would be wasteful in terms of traffic demands that make use of lower transmission rates. It could be more beneficial to utilise a fixed grid comprised of different sized spectrum slots for different speed transponders. This would require an understanding of when and where traffic demands would take place at the design level of the network. A less rigid approach to the transmission rate allocation could be advantageous with respect to network capacity and efficiency.

Traditional optical networks strictly follow the traditional ITU Fixed Grid for wavelength spacing (Shen and Yang, 2011). These grids have a coarse granularity

which ultimately leads to non-optimal spectrum utilization (Yumer et al., 2014). The demands of exponential traffic growth and increased dynamic traffic have forced the creation of flexible and adaptive networks. The Flexible Spectrum technology addresses the above mentioned concerns.

### 2.5.2 Flexible Spectrum Approach

A Flexi-Grid network provides additional flexibility in terms of spectrum assignment through the combination of two concepts, namely, the use of a finer wavelength granularity and the ability to concatenate adjacent wavelength slots together to form arbitrary sized spectrum channels (Yumer et al., 2014; Klinkowski et al., 2013). This approach allows for a finer match with respect to the required and provided spectrum allocation for a transmission (Wright et al., 2013). Flexi-Grid improves the spectral utilization as compared to traditional WDM and DWDM networks using a Fixed Grid (Wen et al., 2013). The Flexi-Grid implementation replaces the rigid frequency grid with a more flexible structure, organised into a much finer granularity grid (Manousakis and Ellinas, 2016). Each transmission allocation is assigned an appropriate number of concatenated slots to form the required spectrum allocation (Waldman et al., 2013; Capucho and Resendo, 2013; Klinkowski and Walkowiak, 2011). The key feature of Flexi-Grid is the manipulation of multiple contiguous sub-carrier wavelength slots, instead of independent wavelength channels. The Grid-Less (Flexible Spectrum) approach is a recent concept that does not follow the standard ITU Fixed Grid for wavelengths, as illustrated by Figure 2.2. In traditional WDM networks the granularity of the frequency spacing is typically coarse with frequency spacing ranges from 50 GHz and above. However, DWDM and Flexi-Grid networks will have a much finer frequency spacing granularity as small as 6.25 GHz (Wright et al., 2013). The Flexible Spectrum approach has no concept of a grid or frequency spacing, there is a continuous band of optical spectrum from which to use. Figure 2.2 illustrates the possible spectrum savings or improved spectral utilization between

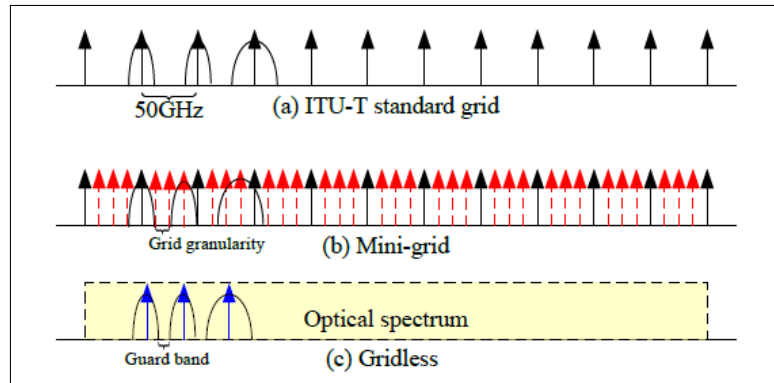


Figure 2.2: Frequency grid structures for Fixed, Flexi-Grid and Grid-Less (Flexible Spectrum) (Shen and Yang, 2011).

the three technologies. The ITU Fixed Grid structure is rigid in spectrum assignment and can allocate far more spectrum resources than is necessary. The Flexi-Grid (Mini-grid in Figure 2.2) approach makes use of a finer granularity grid which is able to more efficiently allocate spectrum resources and illustrates significant spectrum savings over the standard ITU Fixed Grid structure (Shen and Yang, 2011; Zhang et al., 2011; Amaya et al., 2011). The Flexible Spectrum (referred to as Grid-Less in Figure 2.2) approach provides a more elastic method of spectrum allocation, making it a possible candidate for increase spectrum efficiency (Shen and Yang, 2011). The flexibility gain can only be made through a combination of key optical components and subsystems. Tunable laser sources and Wavelength Selective Switches (WSS) with a tunable central wavelength are required to make use of transmission techniques which allow for variable bandwidth allocation for a demand (Shen and Yang, 2011; Zhang et al., 2011; Klinkowski et al., 2013). The objective of the routing and spectrum allocation processes are to minimise the blocking probability of incoming and future traffic demands while optimally utilising the available spectrum. The additional flexibility within the network, namely the Flex-Grid and Flexible Spectrum approaches, create a challenge in controlling and managing the spectral resources (Wright et al., 2013). The use of arbitrary bandwidth channels further compounds the network blocking probability and can limit the network capacity due to spectrum



fragmentation (Wright et al., 2013).

### 2.5.3 Routing and Spectrum Assignment

The Routing and Spectrum Assignment (RSA) process is analogous to the RWA process described in Section 2.3.1. RSA and RWA share a key similarity in first calculating the route for the source to destination node pair for an incoming connection request. In contrast with RWA, the RSA process is applied to a network that does not follow the standard ITU Fixed Grid. RSA is applied to a network with fine granularity for the spectrum grid (Flexi-Grid) or to a lack of grid altogether (Grid-Less). The second component of the RSA process would allocate a spectrum channel for the assigned route comprised of one or multiple frequency grid blocks for the Flexi-Grid network (Lord, 2014; Wright et al., 2013). Allocation of spectrum differs in the Grid-Less network, as an appropriate amount of bandwidth on a wavelength must be allocated in order to satisfy the incoming connection request (Takagi et al., 2011; Shen and Yang, 2011; Yin et al., 2013). RSA has a similar constraint to that of the WCC with respect to RWA, the RSA process is required to establish a path that occupies the same spectrum on all links along the source to destination node pair (Capucho and Resendo, 2013; Klinkowski et al., 2013). The above mentioned concept is referred to as the Spectrum Continuity Constraint (SCC) as seen in Figure 2.3 which would apply to both the Flexi-Grid and Grid-Less spectrum approaches. Figure 2.3 is an illustration of fulfilling five connection requests in a Flexi-Grid under the SCC and is referred to in the following text. The RSA process has allocated paths for four of the connection requests as illustrated by the multiple colours. Each of the paths have been allocated spectrum that satisfies the SCC. The fifth connection requests requires a total of three available contiguous frequency blocks between the source (node b) and destination (node d) node pair. The RSA process attempts to reserve the necessary spectrum along route  $b-c-d$  indicated with a light blue colour. However, only frequency slots  $0-1-2$  are available

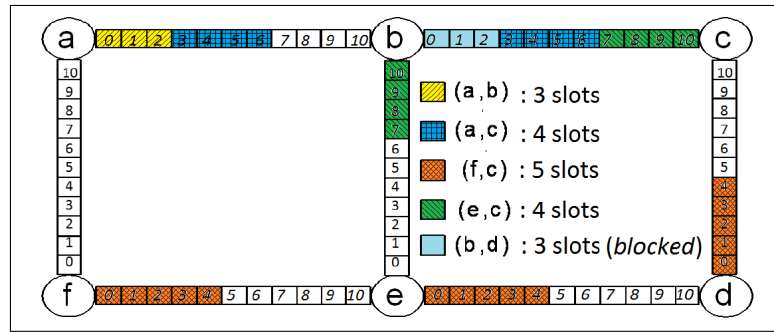


Figure 2.3: Spectrum Continuity of established paths(Capucho and Resendo, 2013).

on link  $bc$  which accommodates the necessary spectrum requirements. There are six frequency blocks available on link  $cd$ , however, the available frequency blocks 5-6-7-8-9-10 cannot be allocated to the connection request as they do not satisfy the SCC. Frequency blocks 0-1-2 on link  $cd$  satisfy the SCC, but are currently in use to satisfy an existing connection request and are therefore unavailable. If the RSA process attempted to reserve the necessary spectrum along route  $b-e-d$ , there would be sufficient frequency blocks available on link  $be$ . Frequency blocks 0-1-2-3-4 on link  $ed$  are currently in use and as a result only frequency blocks 5-6 would satisfy the SCC. Route  $b-e-d$  cannot satisfy the connection request as it does not provide sufficient contiguous spectrum to the destination node.

The only feasible route that can satisfy the SCC for the fifth connection request is along  $b-a-f-e-d$ . There are four frequency blocks 7-8-9-10 available along all the links which provide sufficient contiguous spectrum along route  $b-a-f-e-d$ . Although the above reservation would satisfy the connection request, it would not be ideal as it is optical resource intensive. The construction and destruction of dynamic connections creates the isolated and non-contiguous bandwidth within the network's available spectrum (Yin et al., 2013; Zhang et al., 2014). Integrating both the path calculation and spectrum allocation of connection requests within the RSA process is essential in reducing the fragmentation of available spectrum in the network. With this in mind, a less optical resource intensive solution could be achieved to satisfy the fifth connection request. It would be necessary to reprocess the third connection

request and reallocate the required spectrum. Frequency blocks *0-1-2-3-4* could be reallocated to *6-7-8-9-10*, still satisfying the connection requests. The reallocation of connection request three would allow the fifth connection request to be routed along *b-e-d* as frequency blocks *0-1-2-3-4-5* are available and satisfy the SCC.

#### 2.5.4 Spectrum Fragmentation

The transmission of a connection request from a source to destination node pair, requires that all the links along the route satisfy the SCC. This requirement is to avoid the costly electro-optical conversion at each of the nodes to change the wavelength of the transmission (Wright et al., 2013). Spectrum fragmentation is a side effect of dynamically altering spectrum allocations in a Flexi-Grid or Grid-Less environment. This fragmentation of the available spectrum bandwidth results in small spectral gaps that become unusable (Lord, 2014; Yin et al., 2013). The varied size of spectrum allocation for transmissions that exist in the Flexi-Grid and Grid-Less environments cause the spectrum to become isolated (Wen et al., 2013; Wright et al., 2013). The effect of spectrum fragmentation is illustrated in Figure 2.4. For example, a new connection request places a demand for 75 GHz of spectrum along route A to E. The RSA process allocates a path for the connection request. Inspection of the available spectrum along the allocated path reveals there is sufficient available spectrum to satisfy the requirements of the connection request. The available 75 GHz of spectrum is in the form of two non-contiguous spectrum blocks, 25 GHz and 50 GHz respectively. The RSA process is unable to allocate the path to the connection request as the available spectrum is fragmented.

Without prior knowledge of the order in which traffic demands will be requested, network operators are unable to predict how network traffic will grow and how spectrum will become fragmented. Future traffic demands are expected to be more dynamic. Network operators can use online approaches to reduce network fragmentation. A de-fragmentation scheme could be applied to all of the current connec-

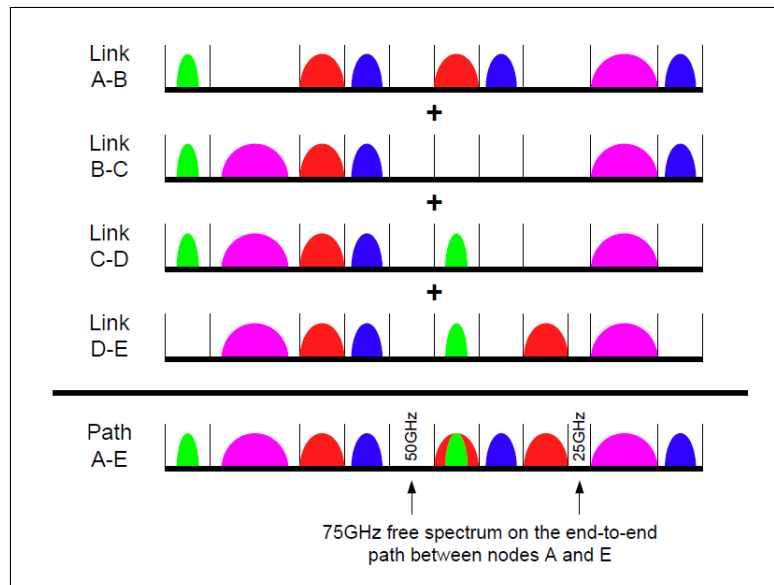


Figure 2.4: Available spectrum for a route between nodes A and E (Wright et al., 2013).

tions on the network while it is still operational. This scheme would attempt to re-route and re-allocate the spectrum for the current connection in order to reduce the amount of isolated spectrum. This de-fragmentation scheme is not ideal as it would disrupt the network and customers. An improved approach would manage the spectrum fragmentation of the network within the RSA process. Handling the spectrum fragmentation during the RSA process would improve spectral efficiency and reduce the traffic blocking probability. This approach would limit the need to de-fragment the network spectrum globally, thereby limiting the disruption to the network and customers. Figure 2.5 illustrates the effect and risk of untreated spectrum fragmentation over time within a network. Mismanagement of transmissions that are no longer required will leave spectral holes behind, causing the network to suffer from even greater spectrum fragmentation (Yin et al., 2013). It is possible that during a transmissions lifespan it may need to either increase or decrease its spectrum requirements. The use of bandwidth variable transponders allow a transmission demand to increase or decrease its spectrum requirement as the need arises

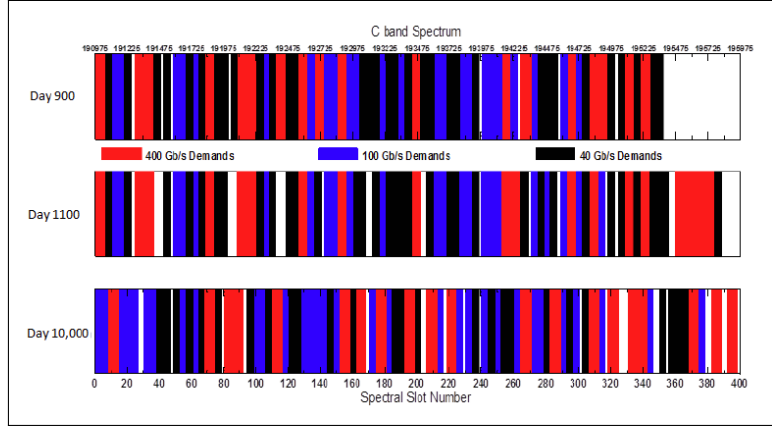


Figure 2.5: Spectrum fragmentation over a network's lifespan (Wright et al., 2013).

(Wright et al., 2013). The spectrum made available from one transmission that is no longer required may be used to increase the bandwidth of another, provided the available spectrum is not isolated and forms a contiguous band with the current transmission.

## 2.6 Physical Layer Impairments

PLIs cause transmission impairments in optical networks. The linear and non-linear effects which cause impairments are introduced in the following section. A transmission penalty equation used to model linear and non-linear effects is detailed in Section 2.6.2.

### 2.6.1 Linear and Non-Linear Effects

PLIs are comprised of linear and non-linear effects. These effects increasingly deteriorate the quality of transmissions with respect to an increase in transmission distance, bit-rates and various modulations. Optical fiber transmission are susceptible to degradation due to several physical phenomena. In Flexible Spectrum networks, transmissions with various modulations and bandwidths can share the same fiber link (Yan et al., 2015b).

Linear impairments are independent of the signal power and affect each of the wavelengths (optical channels) individually. Attenuation and dispersion are important linear effects that limit transmission systems. Attenuation is the deterioration of signal strength through the traversal of optical fiber. Different wavelengths propagate at different speeds within the optical fiber that results in interference that leads to transmission errors.

The simultaneous transmission of multiple wavelengths through optical fiber affect not only each optical channel individually but they also cause disturbance and interference between them in the form of non-linear effects. The effects of non-linear impairments become crucial as data transmission rates, different modulation formats, transmission lengths, number of multiplexed wavelengths and transmission intensities increase in addition to reduction in channel spacing. These linear and non-linear effects need to be effectively managed as they pose a serious risk within Flexible Spectrum networks. Network designers must be aware of these limitations and of the steps that can be taken to minimize the detrimental effects of these fiber non-linearities. To account for inter- and intra-channel interference in such networks, a realistic, yet tractable physical layer impairments (PLI) model is needed (Yan et al., 2015a). Thus, in today's optical networks it is imperative that appropriate care is taken to combat the crosstalk effect (Monoyios et al., 2016).

### 2.6.2 Transmission Penalty Equation

A novel part of this work, is that both linear and non-linear effects on the transmissions are taken into consideration. The transmissions are affected by attenuation over the fiber and non-linear effects incurred by other transmissions simultaneously traversing the fiber. The signal channels are either separated by fixed channel spacing (Fixed Grid) or flexible spacing in the case of Flexible Spectrum. Depending on the spacing, there arises crosstalk interferences between contiguous channels. The crosstalk is due to the non-linear effects as a result of the intensity dependence of

the refractive index of the fibre core (Agrawal, 2001). For multiple wavelengths, crosstalk is as a result of Cross-Phase Modulation leading to a non-linear phase change on channel 1 given by:

$$\phi_1 = \gamma L_{eff}(P_1 + P_2) \quad (2.1)$$

where  $\gamma$  is the non-linear coefficient due to the Kerr effect,  $L_{eff}$  is the effective length where non-linear effects accumulate with the length of the fibre and  $P_1$  and  $P_2$  are the powers of channel 1 and channel 2 respectively (Agrawal, 2001). The eventual outcome of crosstalk is that the signal receiver fails to distinguish closer wavelengths due to the incurred interference. With respect to a receiver sensitivity, the transmission penalty due to crosstalk can therefore be determined as the power difference in received signal power and the receiver sensitivity. Crosstalk depends on the signal bit-rate, channel spacing, received powers, length of the fibre and the band-pass filter bandwidth in the receiver (Agrawal, 2001). The crosstalk penalty can be quantified as the power ratio of the interfering signal that leaks into the desired channel to the signal channel power without crosstalk.

According to D.K. Boiyo (personal communication, April 27, 2015), the effects within the network and Flexible Spectrum environment can be replicated using a transmission penalty equation.

$$Penalty(dB) = AL + kL \sum_{i \in T_f \setminus \{s\}} \frac{B_s 10^{\frac{P_i}{10}}}{B_i 10^{\frac{P_s}{10}} (f_s - f_i)} \quad (2.2)$$

where constant  $k = 4.78$ ,  $A$  is the Line Attenuation in dB/km,  $L$  is equal to the length in km,  $T_f$  is the set of signals traversing the fibre link,  $B_s$  is the bit rate of the signal in Mb/s,  $B_i$  is the bit rate of the signal causing the interference in Mb/s,  $P_i$  is the intensity of the signal causing the interference in dBm,  $P_s$  is the intensity of the signal in dBm,  $(f_s - f_i)$  is the difference in central frequency of the signal and the signal causing the interference in GHz.

The penalty on the intensity of a transmission is due to the simultaneous traversal of other transmissions and is calculated using equation (2.2). The result calculated

by the sum of penalties due to the interfering transmissions and line attenuation is subtracted from the transmission intensity. The intensity of the transmission is compared to the sensitivity of the receiver at the receiving node. If the intensity of the transmission is lower than the sensitivity of the receiving node, the signal is considered lost. A transmission is successful if the intensity of the transmission is greater than or equal to the sensitivity of the receiving node.

## 2.7 Conclusion

This chapter discussed important background theory providing a basic understanding of Optical Networks. The general process of RWA was detailed, rudimentary RWA methods were provided and the importance of the WCC was illustrated relating to the RWA process. The current optical switching technique was discussed and new optical switching techniques were presented. OPS and OBS are able to make more efficient use of optical resources under bursty internet traffic. OBS is the more promising optical switching technique and was discussed in further detail. With the increase in internet traffic, there is a need for more efficient bandwidth usage. Flexible Spectrum is introduced as a candidate for more efficient usage of available bandwidth. However, more efficient bandwidth usage comes with a possible penalty in terms of Spectrum Fragmentation and PLIs.



# Chapter 3

## LITERATURE REVIEW

### 3.1 Introduction

This chapter introduces fundamental ideas for later development, mainly focusing on ACO. The fundamental principles of ACO and the application in the RWA context (Section 3.2) are examined. The application of ACO and associated techniques focused on OBS are presented in Section 3.2.4. Literature relating to ACO in the RWA context is probed in order to collate the previous problems context which are then taken into account in the present research. In particular, Ant Colony Routing and Wavelength Assignment (ACRWA) is selected as a benchmark algorithm because it follows a specific direction which the current research intends to pursue. ACRWA is presented and defined in detail in Section 3.2.5. The Upper Confidence Bound concept is then introduced and presented with respect to its application in choosing move branches, balancing exploration and exploitation of possible solutions are discussed in Section 3.3.

### 3.2 Ant Colony Optimisation

This section provides an introduction into ACO, the manner in which the ACO functions and describes a simple ACO algorithm. The application of ACO to the

RWA process, specifically in the context of OBS, is detailed and an existing ant-based algorithm is presented.

### 3.2.1 Introduction

ACO is a biologically inspired algorithm that is based on the social and foraging behaviour patterns of ants seeking an optimal path between their food source and colony (Dorigo and Di Caro, 1999). Individual ants are simple insects with a limited amount of memory whose behaviour appears to have a large random component. Ants are however able to execute complex tasks with significant consistency and reliability when acting together as a colony (Pedro et al., 2009). These tasks range from forming bridges to finding the shortest routes to a food source. These and many more complex tasks are achieved using co-operative behaviour (Garlick and Barr, 2002). Communication between individual ants is based on the use and deposition of pheromones. The pheromone serves as a means for indirect communication for cooperative behaviour. The trail pheromone, which is of particular importance, is used for marking paths on the ground. While travelling between a food source and the nest an ant will deposit pheromones on the ground (Triay and Cervello-Pastor, 2010). The deposition of pheromones forms a trail which is sensed by subsequent ants (Dorigo and Di Caro, 1999). These ants will probabilistically select paths with a stronger pheromone concentration and further reinforce it. After a period, the scenario allows the ants to converge to the best solution within a set of viable alternatives (Donato et al., 2012).

### 3.2.2 Ant Colony Optimisation Process

Figure 3.1 is an illustration of the imitated foraging process of ant colonies searching for the shortest path between the ant colony nest and food source. Initially, all of the ants are in the ant colony nest. Therefore, pheromone or pheromone trails do not currently exist in this environment. The ants search for food and begin the

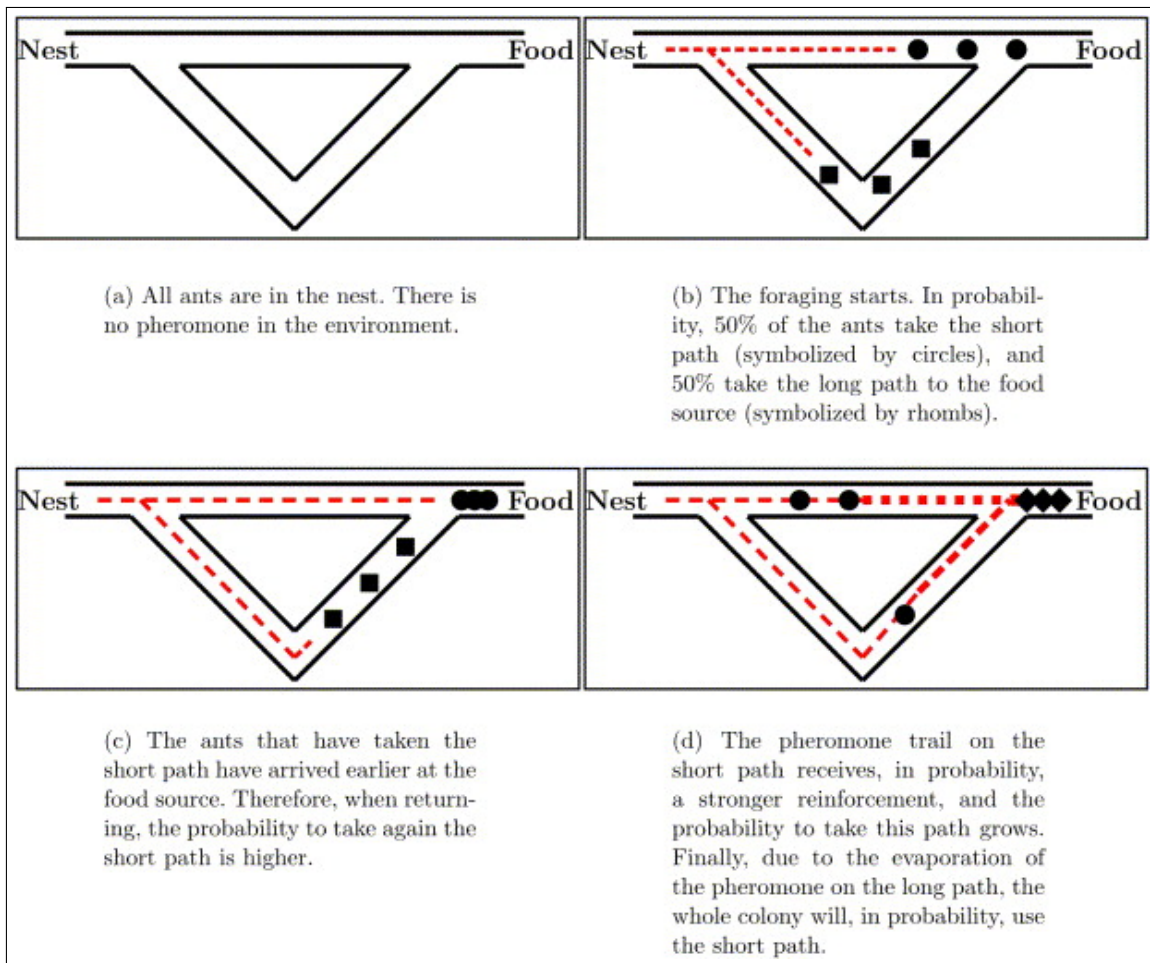


Figure 3.1: Shortest Path Finding capability of ant colonies (Blum, 2007).

foraging process. In this scenario, the ants are met with a branch consisting of two possible paths to explore. There are currently no pheromone or pheromone trails available for the ants to make use of at this branch. Ants probabilistically select a path based on the strength of its pheromone concentration. Both paths have zero pheromone concentration resulting in the selection of a random path. As a result, 50% of the ants will choose to take the shortest path represented as circles and the other 50% of ants choose to take the longest path to the food source represented as squares. The ants which had chosen to take the shortest path would arrive at the nest with the food prior to the ants which had taken the longest path. The length of a path influences the pheromone concentration thereof, because the ants will

reinforce the quicker path more than the longer one. Over time, the evaporation of pheromone along the long path will ensure that the shorter path has a higher pheromone concentration and as a result the ants will choose to use the shortest path.

### 3.2.3 Simple Ant Colony Optimisation Algorithm

ACO is based on the foraging behaviour of ants as previously mentioned above. The foraging behaviour of ants can and has been imitated. ACO has been applied to a large range of problems, ranging from the travelling salesman problem to routing in telecommunication networks and even the protein folding problem to name a few examples. The following is a simple framework comprised of some of the basic properties of ACO. The Simple Ant Colony Optimisation algorithm is the application of the ACO process on a network with the aim of finding the shortest path between two nodes (Dorigo and Stützle, 2001).

Each ant constructs a candidate solution to the shortest path problem between the source and destination node by applying the probability decision policy in order to decide which link to follow. Initially, each link is assigned an initial pheromone concentration of 1. When located at node  $i$  the ant  $k$  uses the pheromone trail  $\tau_{ij}$  to calculate the probability  $p_{ij}^k$  of choosing  $j$  as the next node:

$$p_{ij}^k = \frac{\tau_{ij}^\sigma}{\sum_{j \in \Omega_i^k} \tau_{ij}^\sigma} \quad (3.1)$$

Where the feasible neighbourhood  $\Omega_i^k$  of ant  $k$  located in node  $i$  contains all the nodes directly connected to node  $i$ , with the exception of the predecessor node  $i$ . The ants repeatedly hop from node to node using the decision policy until they have eventually reached the destination node. Ant  $k$  returning to the source node deposits an amount of pheromone  $\Delta\tau^k$  on each link  $ij$  it had visited.

$$\tau_{ij}(t) = \tau_{ij}(t) + \Delta\tau^k \quad (3.2)$$

Where  $\tau_{ij}$  is the amount of pheromones on link  $ij$ . By using this rule, forthcoming

ants will have a higher probability of using the same link in the future. The change in pheromone  $\Delta\tau^k$  is calculated based on the length  $L^k$  of the path constructed by ant  $k$  such that

$$\Delta\tau^k = \frac{1}{L^k} \quad (3.3)$$

The pheromone concentration on each link is also after each iteration in order to emulate pheromone evaporation.

$$\tau = (1 - \theta)\tau \quad (3.4)$$

Where  $\theta \in (0, 1]$  is a user specified value that determines the rate at which pheromones evaporate.

### 3.2.4 Ant Colony Optimisation applied to RWA

ACO algorithms have been extensively applied to solve routing problems within telecommunication networks (Ngo et al., 2006). Several ACO algorithms have been used for solving the RWA problem in WDM optical networks (Triay and Cervello-Pastor, 2010; Pedro et al., 2009; Donato et al., 2012). Many algorithms have also been applied to RWA in OBS (Donato et al., 2012; Triay and Cervello-Pastor, 2010; Pedro et al., 2009). ACO is of particular interest as it is able to run continuously, adapting to changes in the network state and traffic load in real time which provides a dynamic solution to the RWA problem. Applications of ant based algorithms in RWA have been previously explored and extensively applied to solve routing problems within telecommunication networks (Triay and Cervello-Pastor, 2010). As previously mentioned, ACO has been proposed for solving dynamic RWA (Garlick and Barr, 2002). The algorithm launches a number of ants from the source node to the destination node in search of paths for each incoming burst request. Each launched ant will report back a path that it has determined to be the best path based on length and congestion information. Once all of the launched ants have returned to their source, the algorithm will select the best path and fulfil the burst

request. The above mentioned process is not suitable for the OBS scenario as each incoming burst request will be delayed by the set-up procedure. This is too costly as the set-up procedure must wait for all the ants to return. However, ant based algorithms have been proposed for OBS (Ngo et al., 2006). This algorithm reduces the set-up delay for each incoming burst request by means of using a routing table to immediately determine a path. The ants in this approach are continuously launched throughout the network. This is done in order to update the routing tables, monitor the current network state, share gathered information as well as scoring paths based on the path length and number of available wavelengths. Ant-based algorithms have been further developed for OBS, specifically for a network with no buffers under the WCC (Pedro et al., 2009; Donato et al., 2012). A path for the incoming connection request is immediately determined from the routing table. The dominant path is selected for the specific source and destination node pair within the routing table and given a randomly selected wavelength at the source node (Pedro et al., 2009). However, in (Donato et al., 2012), the path is selected probabilistically at the source node with a wavelength assigned by First Fit at the source node and is thereafter selected based on the highest pheromone levels. Ant Colony Routing and Wavelength Assignment (ACRWA) is of particular interest as it utilises a globally distributed approach in which the ant colonies share information with one another as a solution to the RWA problem for dynamic WDM OBS networks with the WCC (Triay and Cervello-Pastor, 2010).

### **3.2.5 Ant Colony Routing and Wavelength Assignment**

ACRWA utilises a distributed approach in which the ant colonies share information among each other with the objective of improving the overall performance of the network. The ACRWA protocol is based on the Ant Colony System (ACS) protocol which was originally developed as a solution for resolving problems such as the Travelling Salesman Problem (TSP), but has been modified to solve the problem

of RWA on WCC optical networks (Triay and Cervello-Pastor, 2010). ACRWA make use of OBS and its convenient properties for their ACO solution in terms of representing the ant as the OBS BCP as it navigates its way to the destination (Triay and Cervello-Pastor, 2010). The ACRWA algorithm provides an interesting solution to the RWA process for a connection request. ACRWA selects the next node and wavelength based on the best product of the pheromone concentration of the output link, the wavelength and the desirability of using such an output link. The algorithm does not make use of random or First Fit wavelength assignment, but has rather linked the wavelength and path (if only for the initial hop and not from source to destination). Thereafter, at every hop, the ACRWA would repeat the process of selecting the next output link. The results obtained by this previous work are promising, making a suitable candidate for benchmark testing as the algorithm has been developed for OBS with the WCC and has demonstrated a link between wavelength and route to destination.

### 3.2.5.1 Initialisation

The ACRWA algorithm is comprised of two protocols, the initialisation protocol which is followed by the RWA process governing the specific behaviour of the ants. The initialisation protocol is responsible for initialising the parameter values and routing tables. This protocol is performed at each of the nodes within the network initialising the routing, pheromone tables and pheromone values. Pheromone values are assigned for every switching configuration of input link, output link and wavelength at a node. Table 3.1 is an example of an initialised pheromone table for a node with two links, in a network with four wavelengths. A routing protocol is used to generate a list of k-shortest routes to all the remaining nodes within the network with each route using a different output link. Each node,  $n$ , constructs a candidate list  $S_n^m$  of available neighbour nodes for every destination node  $m$  from the previously generated list of k-shortest routes. The list of k-shortest routes is

Table 3.1: ACRWA Pheromone Table (Triay and Cervello-Pastor, 2010)

		Output Link	
Input Link	Wave	Link1	Link 2
Link 1	1	$\tau_{1,1,1}$	$\tau_{1,2,1}$
	2	$\tau_{1,1,2}$	$\tau_{1,2,2}$
	3	$\tau_{1,1,3}$	$\tau_{1,2,3}$
	4	$\tau_{1,1,4}$	$\tau_{1,2,4}$
Link 2	1	$\tau_{2,1,1}$	$\tau_{2,2,1}$
	2	$\tau_{2,1,2}$	$\tau_{2,2,2}$
	3	$\tau_{2,1,3}$	$\tau_{2,2,3}$
	4	$\tau_{2,1,4}$	$\tau_{2,2,4}$

used to calculate the desirability values for each link  $j \in S_n^m$ :

$$\eta_{nmj} = \frac{1}{L_{nmj}} \quad (3.5)$$

where  $L_{nmj}$  is equal to the length of the shortest path between node  $n$  and destination node  $m$  using output link  $j$ . A list of wavelength candidates  $D_n^m$  is also initialised, equal to  $c_D$ , the total number of wavelengths available in the network.

### 3.2.5.2 Routing and Wavelength Assignment

The RWA protocol governs the specific behaviour of the ants once the initialisation process has been completed. This protocol is executed by the nodes within the network for each new transmission request. The objective of the algorithm is to select the most beneficial output link,  $u \in S_n^m$ , and wavelength,  $\lambda \in D_n^m$ , combination to assign the ant. This assignment is a greedy selection of the  $u$  and  $\lambda$  pair that has the greatest benefit calculated using the product of desirability of a certain output link and pheromone deposition described by the following equation:

$$(u, \lambda) = \underset{j \in S_n^m(t), k \in D_n^m(t)}{\operatorname{argmax}} \{ \tau_{ijk}(t) \eta_{nj}^\beta(t) \} \quad (3.6)$$



where  $u$  is the selected output link and  $\lambda$  the selected wavelength.  $\tau_{ijk}$  is the pheromone level stored at the node for input link  $i$  and output link  $j$  on wavelength  $k$  and where  $D_n^m$  is the set of existing wavelengths at node  $n$  that have been initialized for destination  $m$ .  $\beta$  is a constant used to emphasize the use of shorter paths.

### 3.2.5.3 State Transition Rule

The initial RWA performed on the ant at the source node,  $n$ , assigns a permanent wavelength to the ant, requiring only the selection of output links for further routing. The state transition rule is responsible for selecting the next hop (output link) in the ant routing process toward its destination. The transition rule selects the next node  $u$  (or output link) to switch by means of exploiting or exploring. Let  $r$  be a random number  $r \sim U(0, 1)$ . The user-specified parameter  $r_0 \in [0, 1]$  is used to balance between exploitation and exploration. In the case that  $r \leq r_0$ , the algorithm will exploit otherwise  $r > r_0$  and the algorithm will explore. If it is determined the ant must exploit, the algorithm will iterate through the output links  $j$  and select the output link with the greatest product of pheromone level  $\tau_{ijk}$  and output link desirability  $\eta_{nj}$  using the following equation:

$$u = \operatorname{argmax}_{j \in S_n^m(t)} \{ \tau_{ijk}(t) \eta_{nj}^\beta(t) \} \quad (3.7)$$

Otherwise, the ant will choose to explore by selecting an output link with each link being assigned a probability,  $P_{iuk}$ , based on  $\tau_{ijk}$  and  $\eta_{nj}$  as follows:

$$P_{iuk}(t) = \frac{\tau_{iuk}(t) \eta_{nu}^\beta(t)}{\sum_{j \in S_n^m} \tau_{ijk}(t) \eta_{nj}^\beta(t)} \quad (3.8)$$

The output link is selected based on an empirical distribution based on the assigned probabilities above.

### 3.2.5.4 Global Update

The global updating rule is performed by the feedback ants. The feedback ants backtracks the path of the ant and updates the pheromone trails using the global

update. All feedback ants are allowed to reinforce or weaken the pheromone concentrations. If the ant successfully reached its destination, the pheromone is updated as follows:

$$\tau_{ijk}(t+1) = (1 - \rho)\tau_{ijk}(t) + \rho\Delta\tau_{ijk} \quad (3.9)$$

Otherwise, if the ant did not successfully reach its destination:

$$\tau_{ijk}(t+1) = (1 - \rho)\tau_{ijk}(t) - \rho\Delta\tau_{ijk} \quad (3.10)$$

where  $\rho$  is a user-specified parameter for the pheromone evaporation coefficient. The amount of new pheromone deposited by the feedback ant depends on the length of the path followed by the feedback ant so far:

$$\Delta\tau_{ijk} = e^{-\omega\Delta l} \quad (3.11)$$

where  $\omega$  is the global decay constant (user specified parameter),  $\Delta l$  is the difference in length of the reverse path followed by the feedback ant so far and the length of the shortest path to the origin of that ant from the current node that processes it.

### 3.2.5.5 Local Update

The purpose of the local updating rule is to diversify the search space to include good local solutions. The routing protocol attempts to reserve the optical resources of output link  $j$  and wavelength  $k$  for the ant. If the reservation is successful, the ant is sent to the adjacent node on output link  $j$  and a positive pheromone update is performed on  $\tau_{ijk}$  according to the local update equation:

$$\tau_{ijk}(t+1) = \tau_{ijk}(t) + \alpha e^{-\phi\Delta l} \quad (3.12)$$

where  $\alpha$  is a user-specified value that controls the amount of emphasis placed on good local solutions and the parameter  $\phi$  is the local decay constant.

### 3.3 Upper Confidence Bound

The Monte Carlo Tree Search (MCTS) is often applied to game playing algorithms. The branches of the tree consist of all possible moves that can be made by the players. These trees are too large to be exhaustively searched (for all but the simplest games). Monte Carlo based algorithms randomly explore branches and then make a move based on the ratio of the random games that yielded a victory for the player. One of the most effective and widely applied variant of these algorithms is the UCT algorithm (Kocsis and Szepesvári, 2006). The key strength of UCT is that branches are not explored purely randomly. Rather, promising branches that are more likely to result in victory are explored in more detail driven by the combination of the UCB bandit algorithm with MCTS. The mechanism that is used to guide the search process is the UCB1 formula of Auer et al. (Auer et al., 2002). The UCB component controls which branch of the game tree should be examined more closely. The UCB1 formula was initially developed to solve the N-Armed Bandit problem (Katehakis and Veinott, 1987).

The N-Armed bandit problem is a decision making problem which refers to a gambler being faced with a series of possible slot machines. The gambler must determine which slot machines to play more often as to maximise winnings. The gambler must solve the dilemma of taking the best action of either exploiting the promising slot machines based on information of currently explored slot machines, or, to further explore the series of slot machines to gather more information at the cost of possibly selecting a sub-optimal action. The combination of the UCB algorithm for the N-Armed Bandit problem with the MCTS, balances the exploration of the game tree with the exploitation of promising branches.

In a bandit-problem, if the upper confidence bound of optimality of each arm is known, regret can be minimised. The upper confidence bound is a statistical measure of the highest confidence interval of an unknown distribution. Auer et al. (Auer et al., 2002) proposed a policy, named UCB1, that minimises this regret by

assigning a penalty to moves that have been played too often, thus providing an automatic means of selecting when to exploit good moves, and when exploration becomes favourable. UCB1 allows the regret to grow logarithmically over the span of  $c_T$  plays without a priori knowledge of the distribution of each arm. The arm with the highest UCB is played calculated using the following equation:

$$UCB(j) = \bar{\mu}_j + C \sqrt{\frac{2 \ln(c_T)}{c_j}} \quad (3.13)$$

where  $\bar{\mu}_j$  is the mean reward of arm  $j$ ,  $c_j$  is the total number of times arm  $j$  has been played, and  $c_T$  indicates the total number of plays so far. The two terms of equation (3.13) encourage exploitation and exploration respectively. The mean reward of the arm  $\bar{\mu}_j$  encourages UCB1 to play moves that have been demonstrated to be effective.  $\sqrt{\frac{2 \ln(c_T)}{c_j}}$  is a penalty term to encourage exploration of less visited branches by weighting branch cumulative payout values by the number of times that they have been played. An additional scaling term,  $C$ , is added in practice to the decaying penalty term to further control the exploration and exploration rates of the approach.

### 3.4 Conclusion

This chapter presented ACO illustrating and describing the basic process. A Simple Ant Colony Optimisation algorithm was introduced and detailed in order to indicate how the basic ACO process functions. Applications of the ACO algorithm were presented in the RWA context, starting with OCS and focusing on OBS application. In traditional ACO-based approaches the route and wavelength selection were treated separately, such that the route was often calculated on a hop for hop basis with either First-Fit or random wavelength assignment. Thereafter, ACRWA, a promising distributed ACO-based algorithm developed for OBS under the WCC was presented. The UCB1 formula applied to the N-Armed bandit problem is discussed. This formula essentially controls the exploitation and exploration of promis-

ing branches. The formula ensures that all branches are explored, but that more successful branches are selected more often. The application of UCB to the RWA process is discussed and detailed in the following chapter.

# Chapter 4

## PROPOSED APPROACHES

### 4.1 Introduction

A detailed description of the adaptation for the OBS reservation protocol in Flexible Spectrum is given in Section 4.2. Reasons for the adaptation of the OBS reservation protocol for Flexible Spectrum are provided. This chapter contains the principal contributions of this research, introduced and detailed in Section 4.3, the FSAC algorithm. Furthermore, Section 4.3 proposes a novel approach with 10 new pheromone calculations for the use of the route and wavelength combinations. Motivations for the original application of UCB to the RWA process is given (Section 4.4). The novel application of UCB in the RWA process is detailed in Section 4.4, the UCBRWA algorithm.

### 4.2 Impairment Adaptation for OBS

The OBS protocol used for our implementation is the JIT with explicit setup and explicit release (Kirci and Zaim, 2006). The JIT scheme immediately reserves the wavelength channel once the BCP has been processed. The BCP is used to reserve optical resources prior to the transmission of the burst. The BCP is received by the switch, the switching elements will configure for the incoming burst if the re-

sources are available. If not, the node will generate a BCP-RA to release the optical resources as until a node receives the BCP-RA the switches will remain in that configuration. BCP-RA is used only to acknowledge the positive delivery of the burst to its destination, whereas the BCP-FA for the negative delivery. This works well in the Fixed Grid case where the BCPs are transmitted within their own bandwidth and are not interfered with by the bursts. However, the Flexible Spectrum scenario makes use of the BCPs to test the feasibility of the particular bandwidth. In this scenario, the implementation cannot assume that the BCP always traverses the fibre successfully using the above mentioned OBS protocol, as it cannot be guaranteed when catering for optical impairments in Flexible Spectrum. If a BCP was lost during traversal, there is no measure in place to generate an acknowledgement to notify the network of the loss, to free up the optical resources reserved by the lost BCP and to notify the source of the transmission that the transmission was a failure. Ultimately, optical reservations would build-up due to the lost BCPs as BCP-RAs would not be generated to release the optical resources and would eventually lead to a complete network failure.

The Impairment Adapted OBS acknowledgement protocol, Algorithm 1, accounts for the loss of a BCP. The above mentioned protocol implements the BCP, the BCP-RA, the failure acknowledgement (BCP-FA) and the traversal acknowledgement (BCP-TA). Algorithm 1 makes use of the BCP-RA in order to release optical resources and to notify the source node of a burst failure. The BCP-FA is then generated to release optical resources and to notify the source node of a burst failure due to optical impairments in Flexible Spectrum or for a block in the case that the optical resources are already reserved. In the case that a BCP is lost, Algorithm 1 accounts for this by generating a BCP-TA. Once a BCP is sent from one node to an adjacent node, a timeout is created at the sending node. Upon successfully arriving at the adjacent node, a BCP-TA is generated to inform the sending node that the BCP has successfully traversed the fibre between the two nodes. The timeout is removed from the sending node once it has received the BCP-TA. In the event that

no BCP-TA is received within the timeout limit, the sending node will generate a BCP-FA to backtrack the path of the BCP in order to free the optical resources and notify the nodes of the failure. Algorithm 1 assumes that the acknowledgements will traverse the fibre successfully. The acknowledgements are sent using the same wavelength reserved for the burst transmission as the optical resource reservations are still maintained until their release by the BCP-RA or BCP-FA.

**Algorithm 1:** Impairment Adapted OBS for Flexible Spectrum

```

if  $|N| > 0$  then
  | Send(BCP-TA,  $N_{[i]}$ ,  $N_{[i-1]}$ )
if Burst Arrives then
  | Send(BCP-RA,  $N_{[i]}$ ,  $N_{[i-1]}$ )
else
  | if Reserved( $N_{[i]}$ ,  $N_{[i+1]}$ ) then
  | | Send(BCP-FA,  $N_{[i]}$ ,  $N_{[i-1]}$ )
  | else
  | | Reserve( $N_{[i]}$ ,  $N_{[i+1]}$ )
  | | Send(BCP,  $N_{[i]}$ ,  $N_{[i+1]}$ )
  | | Wait for BCP-TA or Timeout
  | | if Timeout then
  | | | if  $i == 0$  then
  | | | | Record Failure
  | | | else
  | | | | Send(BCP-FA,  $N_{[i]}$ ,  $N_{[i-1]}$ )
  | | | else if BCP-TA then
  | | | | Wait for BCP-FA or BCP-RA
  | | | | if BCP-FA then
  | | | | | if  $i == 0$  then
  | | | | | | Record Failure
  | | | | | else
  | | | | | | Send(BCP-FA,  $N_{[i]}$ ,  $N_{[i-1]}$ )
  | | | | | else if BCP-RA then
  | | | | | | if  $i == 0$  then
  | | | | | | | Record Success
  | | | | | | else
  | | | | | | | Send(BCP-RA,  $N_{[i]}$ ,  $N_{[i-1]}$ )
  | | | | | | Remove Reservation( $N_{[i]}$ ,  $N_{[i+1]}$ )

```



## 4.3 Flexible Spectrum Ant Colony Algorithm

In this section the FSAC algorithm is described in detail indicating its specific characteristics as opposed to previous application of ant based works. Pheromone Information is described in Section 4.3.2. The Pheromone Table for the FSAC algorithm is presented in Section 4.3.3. The initialisation procedure for the FSAC algorithm is discussed in Section 4.3.4. Section 4.3.5 describes the Routing and Wavelength Assignment process of the FSAC algorithm. Details of the Pheromone Calculation variations are discussed in Section 4.3.6.

### 4.3.1 Introduction

The FSAC algorithm treats the combination of a wavelength and a route to destination as a single routing tuple for an ant to utilize unlike traditional ACO-based works which separate the route and wavelength selection process. Unlike traditional ACO-based approaches where the route and wavelength were not joined, it appears that they did not exploit, let alone greedily exploit a successful path that the algorithm had discovered. The purpose of the FSAC algorithm is to find a path, route and wavelength combination, and to greedily exploit it. The method used was to join the route and wavelength which was traditionally treated separately into a single combination or routing tuple. The last section proposes the investigation of 10 different pheromone calculations for the use with the whole path, route and wavelength combination or routing tuple.

### 4.3.2 Pheromone Information

The pheromone concentrations are calculated according to two distinct sources of information. The first is the level of success, which is a measure of both the number of successes or failures a particular path and wavelength combination has. The values for the success or failure of a path is incremented by a value of 1. The greater the number of successes, the higher the pheromone deposition and vice versa.

The second source of information stems from the path length. The selection of short paths would imply less allocation of optical resources for a single transmission. There would thus be more resources available for other transmissions. Consequently, shorter paths can decrease the congestion level amongst different traffic flows. The shorter the path length, the higher the pheromone deposition for the given solution.

The desirability value,  $\eta_{nmi}$ , provides the heuristic information about the desirability of a path,  $\mathcal{N}_{nmi}$ , for the ant and takes a value inversely proportional to the distance of the path (Dorigo and Stützle, 2001).

$$\eta_{nmi} = \frac{1}{L_{nmi}} \quad (4.1)$$

Where  $L_{nmi}$  is equal to the length of the path from the source node  $n$  to the destination node  $m$ .

### 4.3.3 Pheromone Table

Each node,  $n$ , in the network has a pheromone table  $PT_n$ .  $PT_n$  contains a number of routing tuples  $\varepsilon_i$ . Each routing tuple,  $\varepsilon_i$ , is a tuple  $\langle \mathcal{N}_{nmi}, \lambda_i, \kappa_i, \chi_i, \tau_i, \eta_{nmi} \rangle$ . The tuple is composed of a route,  $\mathcal{N}_{nmi}$ , from node  $n$  to  $m$ , a wavelength,  $\lambda_i$ , the number of successes,  $\kappa_i$ , the number of failures,  $\chi_i$  and a pheromone value  $\tau_i$ . Table 4.1 gives an example of the pheromone table  $PT_A$  for node  $A$  with two links in a network running three wavelength channels. In the case of Flexible Spectrum, the pheromone table values for wavelengths would be the particular routing tuples channel spacing value. The number of nodes in the network is  $c_V$ , the number of wavelengths is  $c_W$  and parameter  $c_J$  limits the total number of routing tuples within the pheromone table of node  $n$ . Each destination is given an equal number of routing tuples,  $\frac{c_J}{c_V-1}$ .

### 4.3.4 FSAC Initialisation

The FSAC protocol is composed of two main algorithms, the initialization and routing algorithms. The initialization algorithm, Algorithm 2, is responsible for

Table 4.1: FSAC Pheromone Table for node  $A$ ,  $PT_A$ 

Route	Wave	Success	Fail	Pheromone
AB	1	59	0	$\tau_1$
ACB	2	2	33	$\tau_2$
AB	3	22	19	$\tau_3$
AC	1	16	4	$\tau_4$
ABC	2	103	7	$\tau_5$
AC	3	42	25	$\tau_J$

running the first stage of the protocol. This includes the generation of routing information, configuring the FSAC parameters, setting up the pheromone tables and managing traffic generation in the network.

$N$  represents the set of all network nodes. A local routing table is generated for each node  $n \in N$  in the network. The routing table is formed by calculating for every possible destination,  $\forall m \in (N \setminus \{n\})$ , a candidate list  $\mathcal{N}_{nm}$  of  $k$ -shortest routes from node  $n$ . The desirability values  $\eta_{nmi} \forall \mathcal{N}_{nmi} \in \mathcal{N}_{nm}$  are calculated by using these tables.

A pheromone table  $PT_n$  for each node  $n \in N$  is initialised. This process is performed by creating routing tuples,  $\varepsilon_i$  where  $i = 1, 2, \dots, c_J$ , for  $PT_n$ .  $PT_n$  is composed of  $c_J$  randomly generated routing tuples. Each routing tuple is composed of a destination node  $m$ , a randomly selected route from the candidate list  $\mathcal{N}_{nm}$  from node  $n$  to  $m$  for  $PT_{nm} \subset PT_n$  and the wavelength is generated from a random number within the valid wavelength range. Once all of these steps have been completed, the network nodes are ready to process data transmissions.

### 4.3.5 Routing and Wavelength Assignment

The RWA algorithm, Algorithm 3, is run by each of the nodes within the network for each new data transmission request. The objective of the algorithm is to calculate

**Algorithm 2:** Initialization Algorithm

```

Variables:  $N$ 
Initialize parameters:  $\alpha_1, \alpha_2, c_J, \beta, \psi$ 
foreach node  $n \in N$  do
  Initialize local routing tables
   $m \in (N \setminus \{n\})$ 
  foreach possible destination  $m$  do
    Initialize candidate route list  $\mathcal{N}_{nm}$ 
    Compute initial  $\eta_{nmi}$  using  $\mathcal{N}_{nmi}$ 
  end
  Initialize pheromone table  $PT_n$ 
end
while Data to transmit do
  Run RWA Algorithm
end

```

the best routing tuple for the transmission request. The routing component of the algorithm describes the specific behaviour followed by the ant, the BCP in Algorithm 1, on its task of searching for food, i.e. the destination node of the burst. Upon receiving a transmission request, the node runs the RWA process to select the route, wavelength combination  $\varepsilon_i \in PT_n$  with which to transmit. Once the ant has been assigned  $\mathcal{N}_{nmi}$  and  $\lambda_i$ , it will schedule and reserve the necessary resources for transmission. At every hop, the ant will select the particular output link defined within the assigned route to the destination node. During the routing process the ant may be unable to reserve the optical resources for its assigned route. In this case, the ant has been blocked which would initiate a negative feedback, BCP-FA in Algorithm 1, on the reverse path. However, an ant may be lost to impairments. This would generate a negative feedback along the reverse path originating from the

sending node which had not received the BCP-TA before the timeout had elapsed. Otherwise, the ant finally arrives at the destination and the burst has been successful initiating a positive feedback, BCP-RA in Algorithm 1. The algorithm terminates once the feedback ant, BCP-RA or BCP-FA, arrives at the source of the burst.

The chosen FSAC action rules have been developed to explicitly balance the exploitation, exploration and creation abilities of the algorithm in order to select a suitable routing tuple. At each node in the network, Algorithm 3 governs the process of routing each ant and assigning a route-wavelength combination to those ants which are newly generated. If a transmission is currently being sent from its source node, it must be assigned both a route and a wavelength. During the creation of a new ant, the computation of a random number  $r$  is used to decide whether the ant is going to exploit, explore or create a new routing tuple. An ant located at

**Algorithm 3:** Routing and Wavelength Assignment Algorithm

```

 $r \leftarrow \text{random}();$ 
if  $r < \alpha_1$  then
    Find  $\varepsilon_B \in PT_{nm}$  using equation (4.3)
    Return  $\lambda_B$  and  $\mathcal{N}_{nmB}$ 
else if  $r < (\alpha_1 + \alpha_2)$  then
    Select  $\varepsilon_i \in PT_{nm}$  with each element assigned a probability using equation
    (4.4)
    Return  $\lambda_i$  and  $\mathcal{N}_{nmi}$ 
else
    Create new routing tuple  $\varepsilon_\nu$ 
     $\lambda_\nu \leftarrow$  random value within the wavelength range
     $\mathcal{N}_{nm\nu} \leftarrow$  random path from  $\mathcal{N}_{nm}$ 
    Remove lowest performing  $\varepsilon_i \in PT_{nm}$ 
    Return  $\lambda_\nu$  and  $\mathcal{N}_{nm\nu}$ 

```

the source node  $n$  selects its route wavelength combination using the following rule:

$$P(r) = \begin{cases} \mathbf{Greedy} & \text{if } r < \alpha_1, \\ \mathbf{Explore} & \text{if } \alpha_1 < r < (\alpha_1 + \alpha_2), \\ \mathbf{Creation} & \text{if } r \geq (\alpha_1 + \alpha_2). \end{cases} \quad (4.2)$$

For **Greedy**, the objective is to calculate the best possible route wavelength combination,  $\varepsilon_B$ . The selection process makes use of  $PT_{nm}$ , the set of valid route wavelength combinations from source  $n$  to destination  $m$ , where the combination with the greatest value of the product between pheromone deposition and the desirability of using such a route using equation (4.3).

$$\varepsilon_B = \operatorname{argmax}_{\varepsilon_j \in PT_{nm}} \{\tau_j(t)\eta_j^\beta(t)\} \quad (4.3)$$

To **Explore**, a pseudo-random-proportional action rule is developed to explicitly balance exploration and exploitation abilities of the algorithm to look for a suitable routing tuple, i.e. initially providing each routing tuple an equal probability for selection using equation (4.4).  $P_i(t)$  is the probability of selecting the path from entry  $\varepsilon_i$  where :

$$P_i(t) = \frac{\tau_i(t)\eta_i^\beta(t)}{\sum_{\varepsilon_j \in PT_{nm}} \tau_j(t)\eta_j^\beta(t)} \quad (4.4)$$

If **Creation** is selected, it is determined that the algorithm must calculate a new routing tuple  $\varepsilon_\nu$ . During the creation of  $\varepsilon_\nu$ , a random wavelength,  $\lambda_\nu$ , is selected within the wavelength range and a route,  $\mathcal{N}_{nm\nu}$ , from source node  $n$  to destination node  $m$  is selected at random. This new routing tuple is given to the ant and added to the set of routing tuples located in the  $PT_{nm}$ . However, there is a set limit to the number of routing tuples contained within the  $PT$ . The routing tuple with the lowest pheromone value within the  $PT_{nm}$  set of routing tuples is removed and replaced with the newly created one. The limit ensures that low performing routing tuples do not linger on and decrease network performance. Restricting the removal of a low performing routing tuples to the same destination set as the newly created one, ensures that all destinations are given an equal allocation of routing tuples.

### 4.3.6 Calculation of Pheromones

The global updating rule is performed by the feedback ants, the BCP-RA. This BCP-RA contains the information regarding the success or failure (BCP-FA) of delivering the burst to the destination. The BCP-RA follows the reverse path followed by the forward ant, BCP. All of the feedback ants, BCP-RA or BCP-FA, are allowed to update the  $\kappa$  (the number of successes) and  $\chi$  (the number of failures). There is no universally accepted single opinion with respect to updating the routing tuple. The FSAC approach is significantly different from previous work so there is no guarantee that previous Global Update (GU) equations would be good. Ten Pheromone Calculation (PC) equations are suggested in the spirit of previously used equations to interpret the information contained within the pheromone table for the GU. All the experience, both recent and past, of the routing tuple is treated as having the same weighting.

#### 4.3.6.1 Pheromone Calculation GU-1

GU-1 calculates the pheromone value as the ratio of successful historic transmission to the total number of transmissions. Unity is added to the numerator and denominator to avoid dividing by zero initially and ensuring that an untested path has a high probability of being selected.

$$\tau_i(t) = \frac{\kappa_i(t) + 1}{\kappa_i(t) + \chi_i(t) + 1} \quad (\text{GU-1})$$

#### 4.3.6.2 Pheromone Calculation GU-2

GU-2 calculates the pheromone value as the number of successful historic transmissions. Unity is added to ensure that each path, even if it has failed several times, has an possibility of being selected.

$$\tau_i(t) = \kappa_i(t) + 1 \quad (\text{GU-2})$$

### 4.3.6.3 Pheromone Calculation GU-3

GU-3 calculates the pheromone value as the maximum value of either 1 or of the total number of successful historic transmissions subtracted by the total number of failed historic transmissions.

$$\tau_i(t) = \max(1, \kappa_i(t) - \chi_i(t)) \quad (\text{GU-3})$$

### 4.3.6.4 Pheromone Calculation GU-4

GU-4 calculates the pheromone value as the ratio of successful historic transmission to the number of unsuccessful historic transmissions. Unity is added to the numerator and denominator to avoid dividing by zero initially and ensuring that an untested path has a high probability of being selected.

$$\tau_i(t) = \frac{\kappa_i(t) + 1}{\chi_i(t) + 1} \quad (\text{GU-4})$$

### 4.3.6.5 Pheromone Calculation GU-5

GU-5 calculates the pheromone value as the ratio of successful historic transmission to the number of unsuccessful historic transmissions squared to punish failures severely. Unity is added to the numerator and denominator to avoid dividing by zero initially ensuring that an untested path has a high probability of being selected.

$$\tau_i(t) = \frac{\kappa_i(t) + 1}{(\chi_i(t) + 1)^2} \quad (\text{GU-5})$$

### 4.3.6.6 Pheromone Calculation GU-6

GU-6 provides a similar pheromone concentration value as is used by ACRWA. This technique calculates the difference of the sums of the exponential inverse of successful and unsuccessful path lengths. In other words, a short successful path will significantly increase the pheromone value (as opposed to an increase that is exponentially smaller from long successful paths), while unsuccessful paths will similarly decrease the pheromone levels.  $\beta$  is the short path emphasis and  $\Delta l$  is the difference



in length of the reverse path of the returning ant and the shortest path to the source node.

$$\tau_i(t) = \psi \left( \sum_{\kappa_i(t)} e^{-\beta \Delta l_i} - \sum_{\chi_i(t)} e^{-\beta \Delta l_i} \right) \quad (\text{GU-6})$$

#### 4.3.6.7 Pheromone Calculation GU-7

GU-7 calculates the pheromone level based on the success and failures. The number of successes or failures increase or decrease the pheromone value with equal weighting. The higher the number of success or failures, the less the effect on the difference in pheromone value. However, successful paths have a higher probability for selection and vice versa. Parameter  $\psi$  is a user-specified value.

$$\tau_i(t) = (1 - e^{-\psi \kappa_i(t)}) - (1 - e^{-\psi \chi_i(t)}) \quad (\text{GU-7})$$

#### 4.3.6.8 Pheromone Calculation GU-8

GU-8 assigns pheromone levels based on an exponentially decaying function of the failure over success ratio. Unity is once again added to numerator and denominator to avoid dividing by zero initially and ensuring that an untested path has a high probability of being selected. Paths for which the number of successes outnumbers the number of failures will thus be assigned larger pheromone values. Where  $\psi$  is a user-specified value.

$$\tau_i(t) = e^{-\psi \frac{\chi_i(t)+1}{\kappa_i(t)+1}} \quad (\text{GU-8})$$

#### 4.3.6.9 Pheromone Calculation GU-9

GU-9 assigns pheromone levels based on the overall success of the solution. Paths in which the number of success outweigh the number of failures will be assigned larger pheromone values. This ensures that the most successful paths are selected over mediocre performing ones. However, there is a limit placed on the minimum value that can be obtained by a poor performing path.

$$\tau_i(t) = e^{\psi(\max(1, \kappa_i(t) - \chi_i(t)))} \quad (\text{GU-9})$$

#### 4.3.6.10 Pheromone Calculation GU-10

GU-10 uses a similar approach to GU-1, however, the value of GU-1 is exponentially decayed so that poorly performing routes which have been used many times would contribute minimally to the pheromone values. Large pheromone values will only be possible if the number of successes is close to the total number of times that the path was used.

$$\tau_i(t) = e^{\psi \frac{\kappa_i(t)+1}{\kappa_i(t)+\chi_i(t)+1}} \quad (\text{GU-10})$$

## 4.4 Upper Confidence Bound Routing and Wavelength Assignment

The proposed algorithm, Upper Confidence Bound Routing and Wavelength Assignment (UCBRWA), describes a distributed ant-based protocol which treats the combination of a wavelength and a route to destination as a single routing tuple (or tuple) using the UCB formula for Trees. The Routing Table is described in Section 4.4.2. The initialisation procedure for the UCBRWA algorithm is discussed in Section 4.4.3. Section 4.4.4 describes the Routing and Wavelength Assignment process of the UCBRWA algorithm. Details of the Global Update are discussed in Section 4.4.5.

### 4.4.1 Introduction

Investigating the use of a tuple for the RWA problem was proposed. A tuple is comprised of a combination of a wavelength and a route from source to destination node pair. The tuple would also contain a record of the success and failure. The use of the tuples in the RWA problem would require the creation of tuples in order to include all the available wavelengths in the network, but also to include different possible routes from the source to destination node pair. The combination of all these possibilities would essentially create a huge tree comprised of all the tuples

from which to select for RWA. The RWA process would be required to search through the huge tree in order to find an appropriate tuple that would give the transmission request the highest probability of success. It would not be feasible for the RWA process to exhaustively search through the huge tree of tuples in order to find a good performing solution and also explore the tree in search thereof. The RWA process would need to balance the exploitation and exploration of tuples similar to that of ACO.

Each tuple in a set of all tuples would have its own reward distribution independent of all the other tuples within the tree. The selection of a tuple for the RWA process can be considered to be a bandit-problem. The RWA process would essentially need to select one of  $c_K$  possible tuples that would maximise the reward or likelihood of successful transmission through the network. The choice of the tuple can thus be seen as a separate decision problem. The reward of each tuple is not known initially. This exploitation-exploration scenario is a trade off between searching tuples discovered to have a higher reward and tuples that exhibit lower reward but could have been classified incorrectly. The UCB1 policy could balance the exploration of the tuple tree with the exploitation of promising tuple branches. Hybridising ACO with UCB1 will ensure that all paths are explored, but that more successful paths are selected more often.

#### 4.4.2 Routing Table

Each node,  $n$ , in the network has a routing table  $RT_n$ . The updating and assignment rules make use of the routing table. The routing table,  $RT$ , contains a number of routing tuples  $\varepsilon_i$ . Each routing tuple,  $\varepsilon_i$ , is a tuple  $\langle \mathcal{N}_{nmi}, \lambda_i, \kappa_i, \chi_i \rangle$ . A tuple is composed of a route  $\mathcal{N}_{nmi}$  from node  $n$  to  $m$ , wavelength  $\lambda_i$ , number of successes  $\kappa_i$  and number of failures  $\chi_i$ . Table 4.2 gives an example of the routing table for a node, A, with two links in a network running three wavelength channels.

Table 4.2: Routing Table

Route	Wave	Success	Fail
AB	1	59	0
ACB	2	2	33
AB	3	22	19
AC	1	16	4
ABC	2	103	7
AC	3	42	25

### 4.4.3 Initialisation

The UCBRWA protocol is composed of two main algorithms, the initialization and routing algorithms. The initialization protocol performs the same task as Algorithm 2 described in Section 4.3.4 with the exception of desirability value calculations. This process is performed by creating routing tuples and adding them to the routing table. The routing table  $RT_n$ , for node  $n$  is composed of a total of  $c_K$  randomly generated routing tuples. A total of  $\frac{c_K}{c_N-1}$  routing tuples are generated for each destination node  $m \in (N \setminus \{n\})$  where  $c_N$  is the total number of nodes in the network. Each routing tuple is composed of a destination node  $m$ , a randomly selected route from the candidate list  $\mathcal{N}_{nm}$  from node  $n$  to  $m$  and the wavelength is generated from a random number within the valid wavelength range. Once all of these steps have been completed, the network nodes are ready to process burst transmissions.

### 4.4.4 Routing and Wavelength Assignment

The RWA algorithm, Algorithm 4, is run by each of the nodes within the network for each new data transmission request. The objective of the algorithm is to calculate the best routing tuple for the transmission request. The routing tuple is selected by making use of the routing table at the source node. It is responsible for selecting a routing tuple, route and wavelength combination, for the burst routing process to the destination node. For exploitation and exploration, the objective is to calculate the best possible route wavelength combination  $\varepsilon_B$ . The selection process makes

**Algorithm 4:** Routing and Wavelength Assignment

```

r ← random();
if r <  $\alpha_1$  then
    Find  $\varepsilon_B \in RT_{nm}$  using (4.5)
    Return  $\lambda_B$  and  $\mathcal{N}_{nmB}$ 
else
    Create new routing tuple  $\varepsilon_\nu$ 
     $\lambda_\nu$  ← random value within the wavelength range
     $\mathcal{N}_{nm\nu}$  ← random path from  $\mathcal{N}_{nm}$ 
    Remove lowest performing  $\varepsilon_i \in RT_{nm}$ 
    Return  $\lambda_\nu$  and  $\mathcal{N}_{nm\nu}$ 

```

use of the  $RT_{nm}$  using equation (4.5).  $RT_{nm}$  is the set of valid route wavelength combinations to forward a burst, avoiding loops or ports without a feasible route from source  $n$  to destination  $m$ .

$$\varepsilon_B = \underset{\varepsilon_j \in RT_{nm}}{\operatorname{argmax}} \left\{ \frac{\kappa_j}{\kappa_j + \chi_j} + C \sqrt{\frac{2 \ln(\kappa_{nm} + \chi_{nm})}{\kappa_j}} \right\} \quad (4.5)$$

where  $C$  is a user-specified value for exploration and  $\frac{\kappa_j}{\kappa_j + \chi_j}$  is the mean reward for  $\varepsilon_j$ .  $\kappa_j$  is the number of successes for  $\varepsilon_j$ .  $\chi_j$  is the number of failures for  $\varepsilon_j$ .  $\kappa_{nm} = \sum_{\varepsilon_j \in RT_{nm}} \kappa_j$  is the total number of successes for all  $\varepsilon_j \in RT_{nm}$ .  $\chi_{nm} = \sum_{\varepsilon_j \in RT_{nm}} \chi_j$  is the total number of failures for all  $\varepsilon_j \in RT_{nm}$ .

If creation is selected, it is determined that the algorithm must calculate a new routing tuple  $\varepsilon_\nu$ . During the creation of  $\varepsilon_\nu$ , a random wavelength,  $\lambda_\nu$ , is selected within the wavelength range and a route,  $\mathcal{N}_{nm\nu}$ , from source node  $n$  to destination node  $m$  is selected at random. This new routing tuple is assigned to the burst and added to the set of routing tuples located in  $RT_{nm}$ . However, there is a set limit to the number of routing tuples contained within the  $RT$ . The routing tuple  $\varepsilon_j$  with the lowest mean reward,  $\frac{\kappa_j}{\kappa_j + \chi_j}$ , where  $\varepsilon_j \in RT_{nm}$  is removed and replaced with the newly created one. The limit ensures that low performing routing tuples do not

linger on and decrease network performance.

#### 4.4.5 Global Update

The routing tuples  $\varepsilon_i$  are updated in the same manner as the FSAC updating procedure detailed in Section 4.3.6. The BCP-RA or BCP-FA contains the information regarding the success or failure of the bursts delivery to the destination. The BCP-RA updates the  $\chi$  and  $\kappa$  values for the routing tuples within the routing table  $RT$ .  $\kappa_i$  is the count of the success of routing tuple  $\varepsilon_i$  and likewise  $\chi_i$  is a count of the failure of the routing tuple. The values for  $\chi_i$  and  $\kappa_i$  for routing tuple  $\varepsilon_i$  are increased in increments of 1.

### 4.5 Conclusion

The OBS reservation protocol was adapted to function in the Flexible Spectrum because the bursts could be lost due to PLIs. BCPs are transmitted in band in order to test the feasibility of a bandwidth channel in Flexible Spectrum. The adapted OBS reservation protocol further caters for the loss of BCPs.

The use of ACO-based algorithms is of particular interest as they have been extensively applied to solving static and dynamic RWA problems. Several ACO algorithms have been adapted for use in WDM optical networks, including OBS networks. This research aims to treat the RWA selection process unlike traditional ACO-based algorithms. The novel FSAC algorithm was developed to investigate the use of a route and wavelength combination from source to destination node as a single routing tuple for the RWA selection process. The application of the above mentioned routing tuples to the RWA process prompted the investigation of 10 new pheromone calculation equations. The pheromones needed to be updated with respect to the use of routing tuples as opposed to the traditional approach of updating for each link along the traversed route.

No known research has been conducted on the use of UCB in the RWA selection

process. Exploration into the use of routing tuples for the RWA process in an ACO-based approach inspired the novel UCBRWA algorithm. UCBRWA integrated the UCB1 policy to balance exploitation and exploration components for the selection of a routing tuple in the RWA process. The proposed hybridisation of ACO and the UCB1 policy provided an effective and novel approach to RWA.

# Chapter 5

## EVALUATION ON FIXED GRID

### 5.1 Introduction

In this chapter details of the evaluation process for the algorithms on a simulated traditional ITU Fixed Grid OBS network are discussed in Section 5.2. The evaluation is first performed on the novel FSAC algorithm, determining which of the 10 proposed pheromone calculations is the most successful. The best performing pheromone calculation is then used to represent the FSAC algorithm when compared to ACRWA, SPR and UCBRWA in simulation. The simulations results are gathered on a small (Section 5.3), medium (Section 5.4) and large (Section 5.5) network topology. These results are analysed and discussed with an overall summary of the chapter given in Section 5.7.

### 5.2 Experimental Procedure

This section details the performance measures (Section 5.2.1), network topologies (Section 5.2.2), algorithms used for comparison with the proposed approaches (Section 5.2.3) and the procedure (Section 5.2.4) followed during the evaluation process.



### 5.2.1 Performance Measures

This section discusses the series of experiments that will be conducted on the algorithms proposed in Chapter 4. This includes testing and comparing all of the proposed pheromone calculation equations against one another in terms of their overall performances and timewise behaviour. The best performing pheromone calculation will be selected to represent the FSAC routing algorithm. The proposed FSAC and UCBRWA routing algorithms will be tested and compared with ACRWA and SPR. The tests will compare the algorithms's overall performances and timewise behaviour. The tests will be implemented on three different network topologies. The Fixed Grid experiments simulated a traditional ITU Fixed Grid WDM OBS network without PLIs (no transmission penalty). In this scenario, the network topology had a set quantity of distinct wavelength channels for the RWA process. Each link in the network is only able to transmit bursts along the distinct wavelength channels. Only one burst could reserve and transmit along a particular wavelength channel, other burst requests attempting to reserve the wavelength channel would be blocked. In this scenario there is a limit placed on the number of available wavelengths channels for each network topology. The test simulations only gather information on the number of successful and unsuccessful (or blocked) burst transmissions.

### 5.2.2 Network Topologies

Three different network topologies are adopted in the simulations. A small test network topology composed of 6 nodes with 8 links in Figure 5.1, a medium test network topology of 11 nodes with 26 links in Figure 5.2 and a large test network topology of 14 nodes with 21 links in Figure 5.3 (Donato et al., 2012; Pedro et al., 2009; Triay and Cervello-Pastor, 2010). The purpose of the different network topologies is to evaluate the performance of the protocol in a simple network, a larger but more connected graph and also within a more complex scenario (NFSNET-14 topology in Figure 5.3). The small network topology illustrated in Figure 5.1 has 8 available

wavelengths on each of the links within the network. The medium network topology illustrated in Figure 5.2 has 12 available wavelengths on each of the links within the network. The large network topology illustrated in Figure 5.3 has 16 wavelengths on each of the links within the network. The values illustrated on all three of the Figures 6.1, 6.2 and 6.3 are unit-less ratios depicting link lengths.

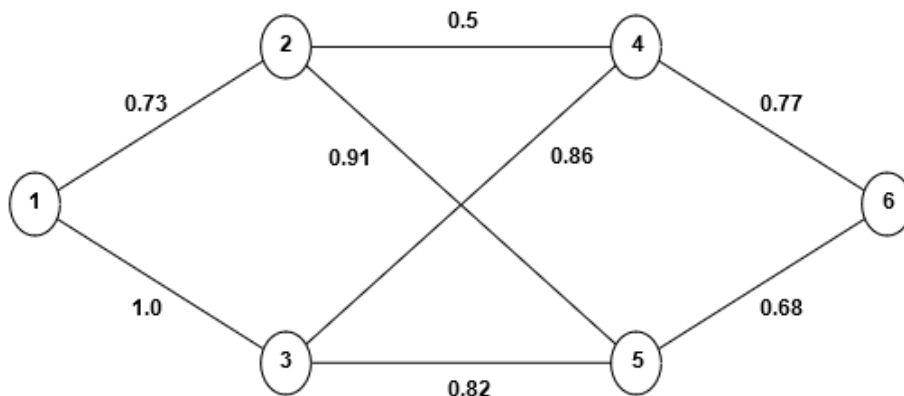


Figure 5.1: Small 6-Node network topology

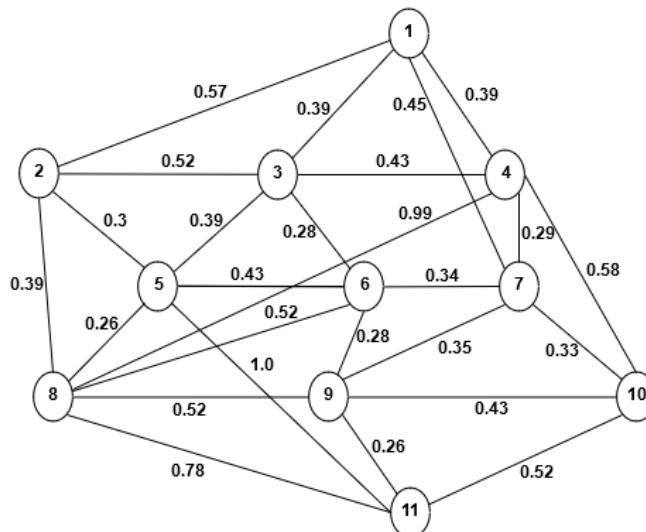


Figure 5.2: Medium 11-Node network topology

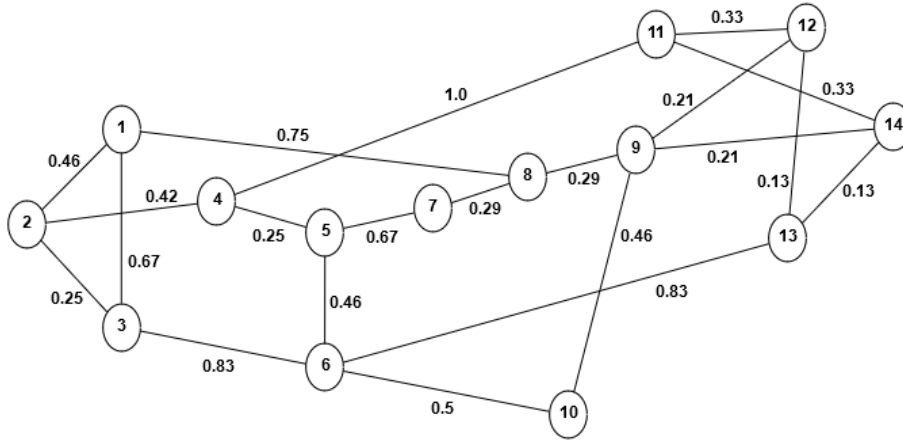


Figure 5.3: Large 14-Node network topology

### 5.2.3 Comparison Algorithms

The existing algorithm is an ant based routing algorithm, ACRWA (previously discussed in Section 3.2.5), and a simple but greedy, Shortest Path Routing (SPR) algorithm for comparison. The SPR algorithm computes the shortest path for each source to destination node pair. In the Fixed Grid simulation setup, SPR has been implemented to function by selecting the shortest path with the first available (First-Fit) wavelength for each incoming burst request at the source node. ACRWA has been implemented as discussed in Section 3.2.5 for the Fixed Grid setup simulation. Implementation in the Fixed Grid scenario was with the given number of wavelengths for the tested network with all the input, output link wavelength combinations initialised with a pheromone value of 1. The parameters for all the tested algorithms have been manually tuned through preliminary experiments. The selected parameters gave the highest performances measured in simulation. Parameters for ACRWA have been selected from Triay and Cervello-Pastor and manually tuned as above (Triay and Cervello-Pastor, 2010). The parameters of the UCBRWA protocol used throughout the simulations are as follows:  $\alpha_1 = 0.995$ ,  $C = 2.0$ ,  $c_K = 200$  for the small network topology,  $c_K = 400$  for the medium network topology and  $c_K = 700$  for the large network topology. The parameters of the ACRWA protocol

used throughout the simulations are as follows:  $\rho = 0.01$ ,  $\omega = 0.75$ ,  $\alpha = 0.001$ ,  $\phi = 0.75$ ,  $\beta = 2.0$ ,  $r_0 = 0.8$  for the small network topology,  $r_0 = 0.7$  for the medium network topology and  $r_0 = 0.8$  for the large network topology. The parameters of the FSAC protocol used throughout the simulations are as follows:  $\alpha_1 = 0.9$ ,  $\alpha_2 = 0.09$ ,  $\alpha_3 = 0.01$ ,  $\beta = 2.0$ ,  $\psi = 0.01$ ,  $c_J = 250$  for the small network topology,  $c_J = 400$  for the medium network topology and  $c_J = 500$  for the large network topology.

### 5.2.4 Procedure

Each of the simulations were tested under various network loads. The load placed on a network in simulation refers to the total number of new burst requests at each given timestep in the simulator. These simulations were repeated a total of 30 times and the results are averaged. Each simulation attempts to transmit  $5 \times 10^5$  bursts, including the initial learning phase. A total of  $5 \times 10^5$  bursts requests was chosen for simulation purposes through preliminary testing as an appropriate quantity. This quantity allowed the tested algorithms the opportunity to adapt (learning phase) and stabilise (peak performance) to a load in simulation. The source and destination nodes are randomly selected for each burst. Two values are measured throughout the duration of a simulation. The number of successful burst transmissions  $\kappa_T$  and the number of burst blocks  $\chi_T$ . The success ratio  $R$  used as a performance measure is calculated as follows:

$$R = \frac{\kappa_T}{\chi_T + \kappa_T} \quad (5.1)$$

The results gathered for the mean success ratio at various loads and the timewise behaviour for three specific loads will be graphed. The mean success ratios over 30 repeats of each pheromone calculation for various loads will be tabled along with a 95% confidence interval and the statistically significantly better mean success ratios are printed in bold. The best performing pheromone calculation in terms of overall performance at various loads and timewise behaviour at specific loads with the most number of statistically significant results will be selected to represent the FSAC

algorithm when compared to ACRWA, SPR and UCBRWA. The gathered results for FSAC, UCBRWA, ACRWA and SPR for the mean success ratio at various loads and timewise behaviour for the specific loads will be graphed. The mean success ratios over 30 repeats of each of the algorithms for various loads will be tabled along with a 95% confidence interval and the statistically significantly better mean success ratios are printed in bold. The outcomes of Mann-Whitney U tests for each of the tested algorithms against all the other algorithms for being greater than each other is used to determine which algorithm has the statistically significant results. The purpose of measuring the timewise behaviour of the algorithms in terms of low, medium and high loads is to gauge the value obtained for the mean success ratio. Plotting the timewise behaviour allows for the identification of whether the algorithm improves, degrades or remains constant in performance. The above mentioned comparisons will be performed on each network topology.

## 5.3 Small Topology Results

The results of the experiments described in the Section 5.2 are now presented. The experiments were conducted in simulation on the small network topology shown in Figure 5.1. The FSAC algorithm is represented by pheromone calculation 4 in the sections that follow for the small network topology.

### 5.3.1 Comparison of FSAC Pheromone Calculations

This section details the results gathered for all of the FSAC pheromone calculations and compares the equations against one another.

#### 5.3.1.1 Relative Performance of Pheromone Calculations

Figure 5.4 illustrates the performance of each of the pheromone calculations for the various loads placed on the small network. The pheromone calculations appear to

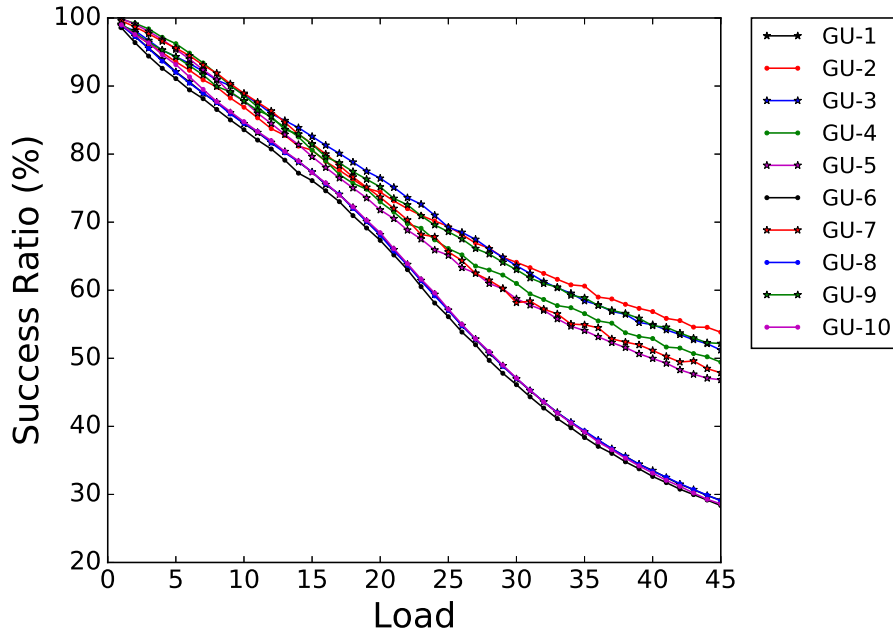


Figure 5.4: Burst Success Ratio for FSAC PCs on the small network topology with 8 wavelengths.

split up into 2 distinct groups. A lower performing group comprised of pheromone calculation 3, 6, 8 and 10. A higher performing group comprised of the remaining pheromone calculations, with some performing well initially relative to others then decreasing in performance at the higher loads and vice versa. Interestingly, the pheromone calculations within each group illustrate almost identical performance trend lines. All of the pheromone calculations begin with similar success ratio values at the initial low load placed on the network topology. In Figure 5.4, from a load of 5, pheromone calculations 1, 6, 8 and 10 begin to diverge from the remaining pheromone calculations. Pheromone calculations 1, 6, 8 and 10 begin to significantly diverge from the other pheromone calculations at a load of 15 placed on the network topology. A comparison of pheromone calculation 2 with 6, the best and worst performing of all the tested pheromone calculations on the small network topology is discussed below. At a load of 5 placed on the network the performance difference is 3.22%, whereas at a load of 25 placed on the network the difference in

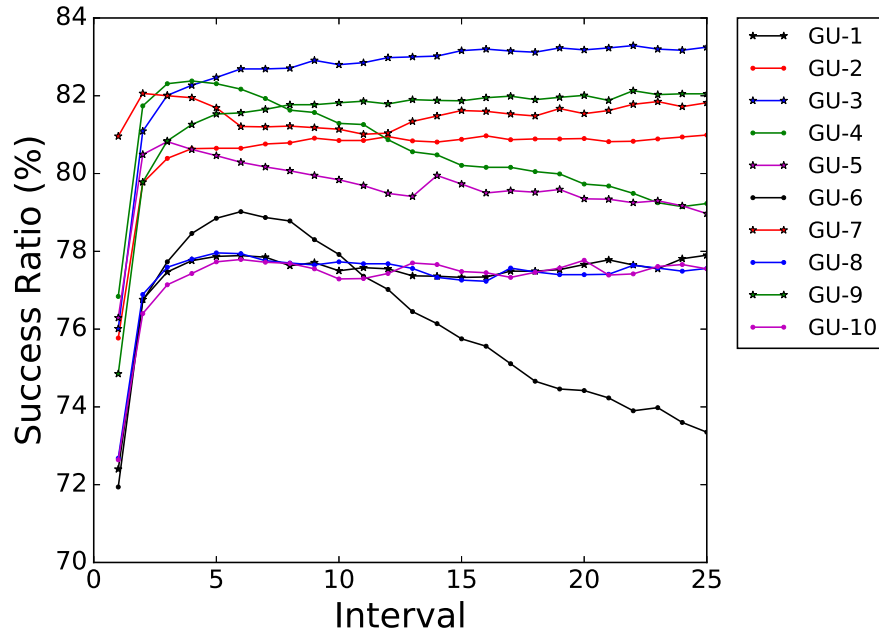


Figure 5.5: Burst Success Ratio for FSAC PCs over time at a load of 15.

performance has increased to 13.26%. Thereafter, at the highest load of 45 placed on the network there is a notable performance difference of 25.47% when comparing the two pheromone calculations. There is a substantial difference in performance between the best and worst performing pheromone calculations on the small network topology.

### 5.3.1.2 Timewise Performance of Pheromone Calculations

Figures 5.5, 5.6 and 5.7 are illustrations of the pheromone calculation variations of the FSAC algorithm adapting to a specific network load over the duration of a simulation. Figure 5.5 is an illustration of the pheromone calculation variation adapting to a load of 15 placed on the network. Under this low load, there is a predominant performance success ratio pattern for the pheromone calculations. Namely, the starting and ending performance values are different with the latter at a higher value than the initial starting point. The algorithms have an initial jump in

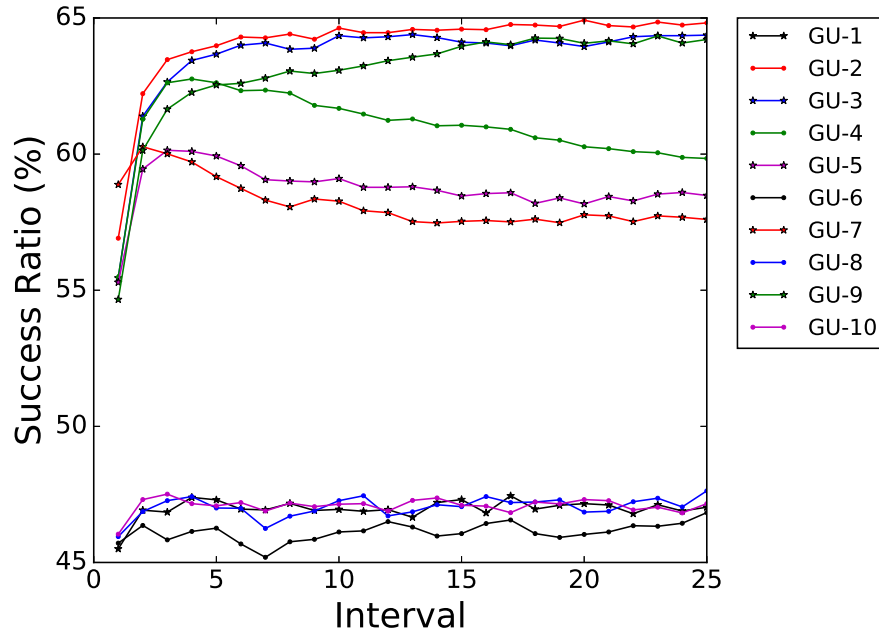


Figure 5.6: Burst Success Ratio for FSAC PCs over time at a load of 30.

performance which stabilizes swiftly with the exception of pheromone calculations 4, 5 and 6 which decrease in performance after the initial spike. Pheromone calculations 6 and 7 differ the most from the other performance trend lines displayed. Pheromone calculation 6 has a gradual taper in the initial performance jump that does not stabilize, but rather decreases in performance over the duration of the simulation. Pheromone calculation 7 does not differ as much in that it has a smaller initial jump in performance as compared to the other pheromone calculations.

Figure 5.6 is an illustration of the pheromone calculation variations adapting to a load of 30 placed on the network. Under a medium load placed on the network, the performance trends of the pheromone calculations are similar but are however squashed when compared to the low load with the exception of pheromone calculation 6 exhibiting a completely different trend. Pheromone calculations 1, 6, 8 and 10 exhibit stable performance trends for the duration of the simulation with no real overall increase in performance at any point throughout the simulation period. Pheromone calculations 2, 3, 4, 5 and 9 display an initial spike in performance that



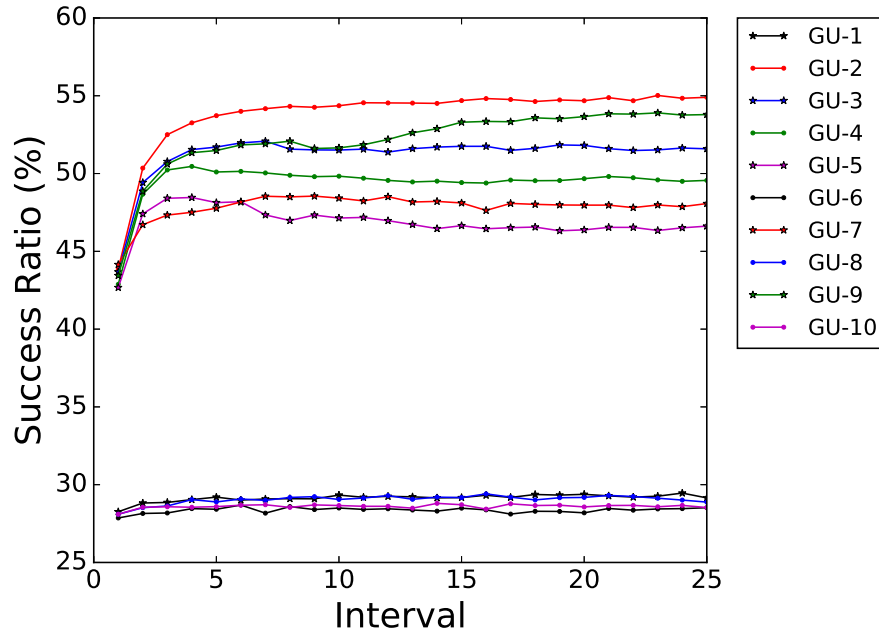


Figure 5.7: Burst Success Ratio for FSAC PCs over time at a load of 45.

stabilizes quickly. Pheromone calculations 4 and 5 differ from above in that their performance at the end of the simulation is lower than that of their peak after the initial spike. Similarly, pheromone calculation 7 has a decaying performance after the spike.

Figure 5.7 is an illustration of the pheromone calculation variation adapting to a load of 45 placed on the network. At the maximum tested load of 45, the FSAC pheromone calculation performance trend lines appear much smoother and flatter for the period of the simulation. The most significant differences in the performance trend lines are the initial performance spikes for pheromone calculations. The pheromone calculations 2, 3, 4, 5, 7 and 9 exhibit the classic trend of an initial spike into stable performance for the duration of the simulation. However, pheromone calculation 2 displays a higher spike in performance compared to the other pheromone calculations, while pheromone calculations 1, 6, 8 and 10 illustrate flat and stable performance trend lines for the entire duration of the simulation.

Table 5.1: Overall performance of the FSAC PCs on the small network topology with 8 wavelengths.

Pheromone Calculation	Number of Statistically Significant Results	Overall Average Performance
GU-1	0	61.81
GU-2	18	72.98
GU-3	15	73.26
GU-4	6	71.58
GU-5	1	70.06
GU-6	0	60.87
GU-7	5	71.00
GU-8	0	61.79
GU-9	0	72.71
GU-10	0	61.89

### 5.3.1.3 Overall Performance of Pheromone Calculations

The performance of the pheromone calculations under specific loads over the duration of the simulations as seen in Figures 5.5, 5.6 and 5.7 are in line with that of the overall performances of the pheromone calculations displayed in Figure 5.4. In the small network topology, pheromone calculations 1, 6, 8 and 10 performed significantly lower as compared to the other pheromone calculations illustrated in Figure 5.4. Inspection of Table 5.1 further illustrates this where pheromone calculations 1, 6, 8 and 10 have the lowest overall average performances (approximately 10% lower than the rest of the pheromone calculations). Pheromone calculation 2 has the most number of significant results, tallying 18 out of 45 with the second highest overall average performance of 72.98%. Pheromone calculation 3 has the second highest number of significant results (15 out of 45) and the highest overall average performance of 73.26%. Pheromone calculations 7 and 5 both have a number of significant results, while pheromone calculation 9 has less but illustrates a higher overall average performance of 72.71%.

### 5.3.2 Comparison Against Existing Algorithms

This section details the results gathered for the FSAC, UCBRWA, ACRWA and SPR algorithms. The algorithms are compared against one another in terms of the gathered results.

#### 5.3.2.1 Relative Performance Comparison

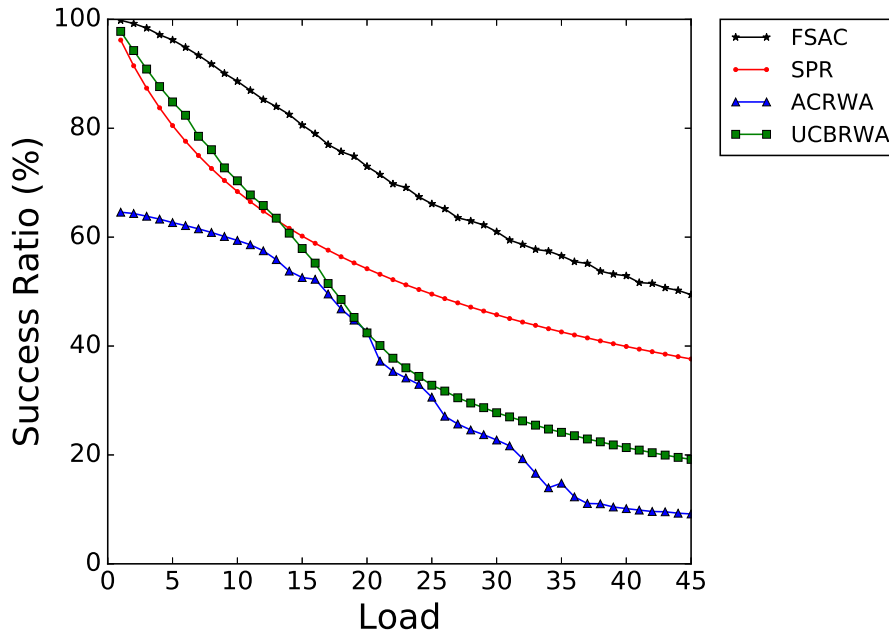


Figure 5.8: Burst Success Ratio on the small network topology with 8 wavelengths.

Figure 5.8 illustrates a comparison of the success ratio performances of FSAC and UCBRWA with the ACRWA and SPR as a function of the various loads placed on the small network topology. A clear differentiation is observed regarding the performances of each of the algorithms with the exception of the loads between 10 and 25. The performances of UCBRWA and SPR converge at an approximate load of 10 and diverge at a load of 15. Thereafter, the performances of UCBRWA and ACRWA converge from a load of 15 and diverge at a load of 25. ACRWA reduces the gap in performance with SPR at the initial loads placed on the network up to

Table 5.2: Success ratio and 95% confidence interval at a specific load on the small network topology with 8 wavelengths.

Load	FSAC	SPR	ACRWA	UCBRWA
5	<b>96.22 ± 0.15</b>	80.49 ± 0.02	62.67 ± 0.08	84.83 ± 0.40
10	<b>88.62 ± 0.36</b>	68.38 ± 0.03	59.40 ± 0.06	70.35 ± 0.39
15	<b>80.58 ± 0.47</b>	60.19 ± 0.03	52.58 ± 0.66	57.91 ± 0.31
20	<b>72.98 ± 0.78</b>	54.20 ± 0.02	42.63 ± 0.69	42.41 ± 0.27
25	<b>66.12 ± 0.56</b>	49.54 ± 0.02	30.61 ± 0.67	32.80 ± 0.14
30	<b>60.99 ± 0.62</b>	45.75 ± 0.02	22.74 ± 0.43	27.75 ± 0.09
35	<b>56.56 ± 0.48</b>	42.59 ± 0.02	14.81 ± 1.41	24.15 ± 0.08
40	<b>52.90 ± 0.47</b>	39.92 ± 0.02	10.14 ± 0.16	21.35 ± 0.05
45	<b>49.43 ± 0.50</b>	37.62 ± 0.02	9.16 ± 0.13	19.18 ± 0.05

Table 5.3: Overall Algorithm performance on the small network topology with 8 wavelengths.

Algorithm	Number of Statistically Significant Results	Overall Average Performance
FSAC	45	71.58
SPR	0	55.79
ACRWA	0	36.00
UCBRWA	0	45.84

approximately a load of 20, but never performs better than SPR in this scenario. The FSAC algorithm performed the best throughout the loads tested on the network in this scenario. SPR performed well throughout the simulation, with UCBRWA performing better up until a load of 13 placed on the network.

### 5.3.2.2 Timewise Performance Comparison

Figures 5.9, 5.10 and 5.11 are illustrations of all the tested algorithms adapting to a specific network load over the duration of a simulation. Figure 5.9 is an illustration of all the tested algorithms adapting to a load of 15 placed on the network. Under this low load, all the tested algorithms present distinctive performance trend line patterns over the duration of the simulation. SPR has a remarkably flat and stable performance for the duration of the simulation. ACRWA displays a slight initial

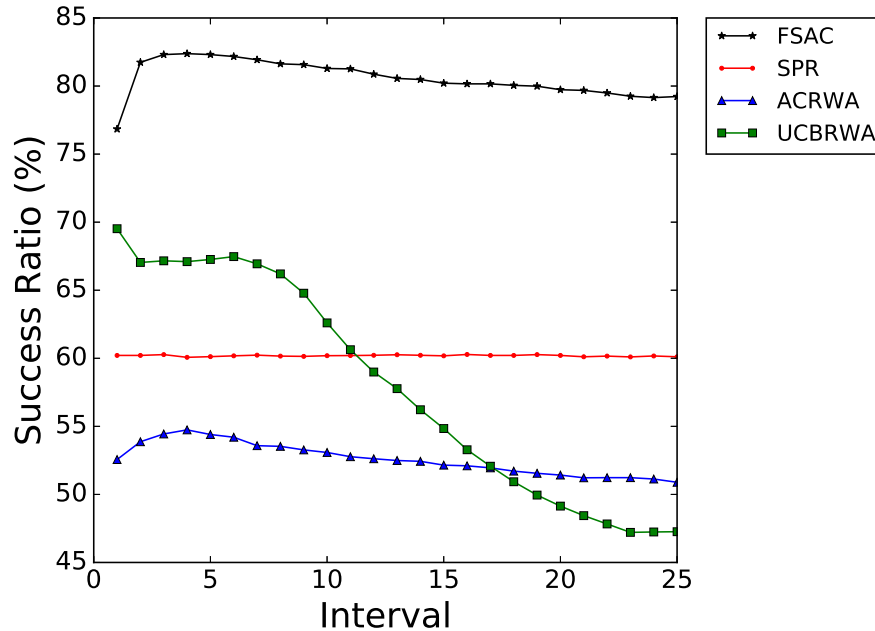


Figure 5.9: Burst Success Ratio over time at a load of 15.

increase in performance which stabilizes into a gradual decline for the remainder of the simulation. FSAC has an initial spike in performance, thereafter the algorithm displays stable performance with a gradual decline. UCBRWA initially performs well but steadily declines in performance until it stabilizes with the lowest performance.

Figure 5.10 is an illustration of all the tested algorithms adapting to a load of 30 placed on the network. Under this medium load, all the tested algorithms present performance trend line patterns which in the case of FSAC and SPR are similar to those seen previously in Figure 5.9. However, UCBRWA and ACRWA demonstrate significantly different performance trend lines as compared to those illustrated for the lower load placed on the network in Figure 5.9. FSAC illustrates a distinctive pattern of an initial increase in performance which stabilizes into a slight decline. SPR displays a uniquely flat trend line demonstrating a stable performance for the duration of the simulation. UCBRWA and ACRWA plummet initially but stabilize into no noticeable increase in performance for the remainder of the simulation. FSAC is the only algorithm which effectively increased in performance between the

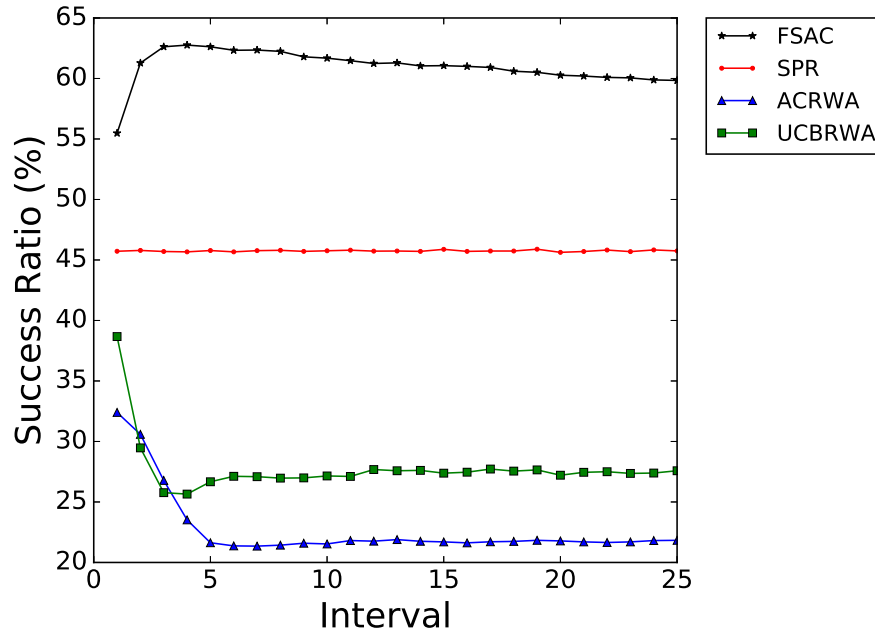


Figure 5.10: Burst Success Ratio over time at a load of 30.

beginning and end of the simulation period. UCBRWA and ACRWA essentially decrease in performance over the simulation period with the exception of SPR which remains constant throughout.

Figure 5.11 is an illustration of all the tested algorithms adapting to a load of 45 placed on the network. Under this high load, all the tested algorithms present performance trend line patterns which are more stable than those seen in Figure 5.9 and 5.10. UCBRWA displays a slight initial decrease in performance which stabilizes and remains constant for the duration of the simulation period. ACRWA has a significant decrease in performance initially which stabilizes and remains constant for the duration of the simulation period. SPR remains constant for the duration of the simulation period as seen previously for the other loads placed on the network. FSAC displays its characteristic performance trend line of an initial increase in performance which stabilizes for the remainder of the simulation period.

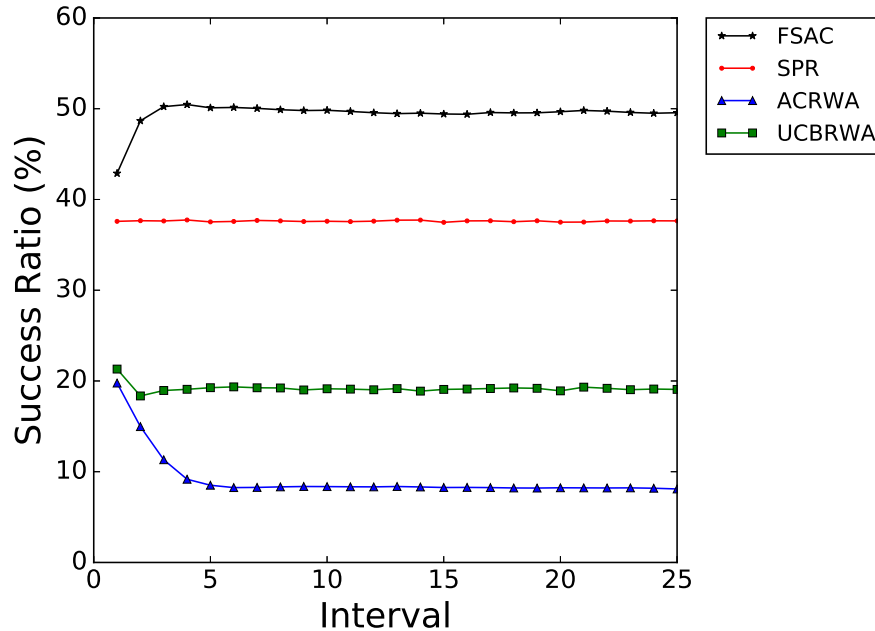


Figure 5.11: Burst Success Ratio for FSAC PCs over time at a load of 45.

### 5.3.2.3 Overall Performance Analysis

The mean success ratios over 30 repeats for each of the algorithms are reported along with the 95% confidence interval in Table 5.2. The outcomes of Mann-Whitney U tests comparing the algorithms against one another are included with results that are statistically significantly better printed in bold. At a load of 10, FSAC is approximately 17.35% more successful than UCBRWA, 19.67% more successful than SPR and 29.95% more successful than ACRWA. At a load of 20, FSAC is approximately 19.57% more successful than SPR, 29.59% more successful than UCBRWA and 30.08% more successful than ACRWA. At a load of 30, FSAC is approximately 15.80% more successful than SPR, 33.55% more successful than UCBRWA and 38.51% more successful than ACRWA. At a load of 40, FSAC is approximately 12.98% more successful than SPR, 31.55% more successful than UCBRWA and 42.76% more successful than ACRWA.

Under all the tested loads placed on the small network topology, the FSAC

algorithm performed significantly better than the other tested algorithms. The FSAC algorithm demonstrated the most significant results for all of the tested loads according to the Mann-Whitney U tests performed on all of the algorithms as seen in Table 5.3. Furthermore, in Table 5.3 the overall average performances can be seen. The FSAC algorithm had an overall average performance of 71.58%. On average, the FSAC algorithm performed approximately 15.79% higher than SPR, 25.74% higher than UCBRWA and 35.58% higher than ACRWA.

## 5.4 Medium Topology Results

The results of the experiments described in the Section 5.2 are now presented. The experiments were conducted in simulation on the medium network topology in Figure 5.2. The FSAC algorithm is represented by pheromone calculation 4 in the sections that follow for the medium network topology.

### 5.4.1 Comparison of FSAC Pheromone Calculations

This section details the results gathered for all of the FSAC pheromone calculations and compares the equations against one another.

#### 5.4.1.1 Relative Performance of Pheromone Calculations

Figure 5.12 displays the performance for each of the pheromone calculations for the various loads placed on the medium network. As seen before in Figure 5.4, the performance of the pheromone calculations are divided into two distinct groups, a lower and higher performing group. The lower performing group comprises of the pheromone calculations 2, 3 and 9. These pheromone calculations start with the same performance as the other pheromone calculations at the initial low load placed on the network, but decrease in performance at a higher rate than the other pheromone calculations. At a load of 1 placed on the network, all of the pheromone



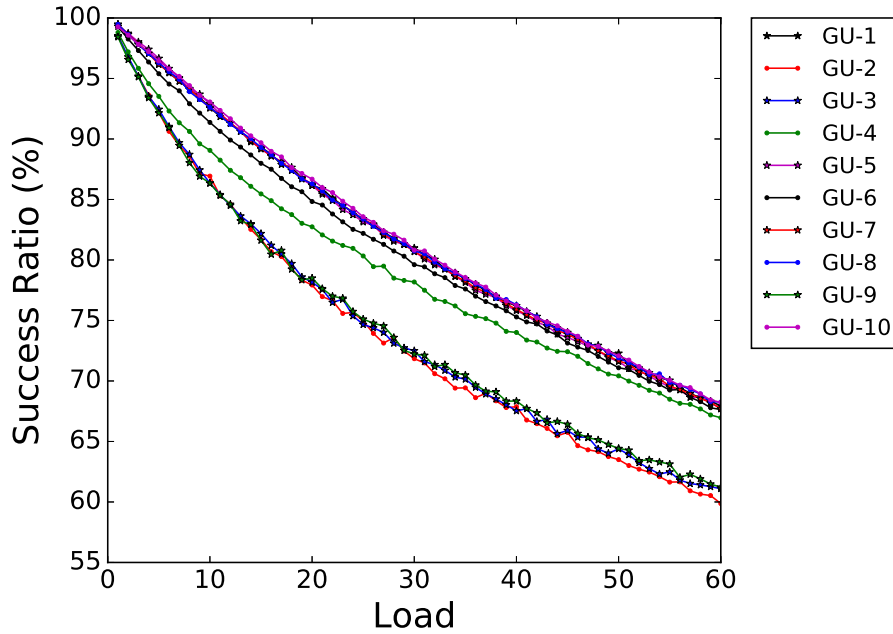


Figure 5.12: Burst Success Ratio for FSAC PCs on the medium network topology with 12 wavelengths.

calculations have similar performances but immediately thereafter begin to diverge into the two groups. Pheromone calculation 4 displays a similar trend line to those of the lower performing group at the lower loads placed on the network and only comes close the higher groups performance at the higher loads placed on the network. The higher performing group comprises of pheromone calculations 1, 5, 6, 7, 8 and 10 with pheromone calculation 4 displaying a somewhat individual performance. From a load of 5 placed on the network, pheromone calculation 4 begins to diverge from the lower performing group towards the higher performing one. Comparing pheromone calculation 2 with 10, pheromone calculation 10 performing the best on the network and pheromone calculation 2 is the lowest performing of all. With a load of 15 placed on the network, the performance difference is 8.00%, whereas at a load of 30 the difference in performance is 8.98%. Thereafter, at a load of 45 and up to a load of 60, the difference in performance between the two pheromone calculations is 8.36%.

Table 5.4: Overall performance of the FSAC PCs on the medium network topology with 12 wavelengths.

Pheromone Calculation	Number of Statistically Significant Results	Overall Average Performance
GU-1	5	81.65
GU-2	0	73.95
GU-3	0	74.32
GU-4	0	79.09
GU-5	6	81.49
GU-6	0	80.74
GU-7	1	81.54
GU-8	5	81.66
GU-9	0	74.49
GU-10	43	81.85

#### 5.4.1.2 Timewise Performance of Pheromone Calculations

Figures 5.13, 5.14 and 5.15 are illustrations of the FSAC algorithms pheromone calculation variations adapting to a specific network load over the duration of a simulation. Figure 5.13 is an illustration of the pheromone calculation variation adapting to a load of 20 placed on the network. When a load of less than 20 is placed on the network, there is a predominant performance trend for the period of the simulation with the exceptions of pheromone calculations 6 and 9. This predominant pattern is described as having an initial spike in performance where the pheromone calculations end with a higher success ratio value than that which they started with. The pheromone calculations 1, 2, 3, 4, 5, 7, 8 and 10 display an initial spike in performance at the start of the simulation which quickly stabilizes for the remainder of the simulation period. In the case of pheromone calculations 6, the difference is that it does not stabilize after the initial spike in performance but rather gradually decreases in performance for the remainder of the simulation period. Pheromone calculation 9 differs from the rest of the pheromone calculations with a lack of the initial performance spike at the start of the simulation period and remains stable for the entire duration.

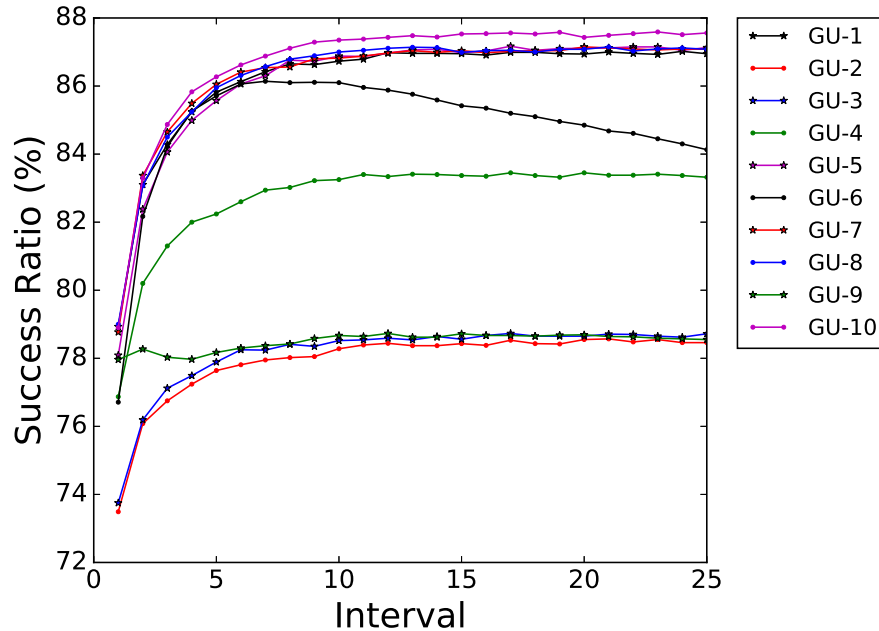


Figure 5.13: Burst Success Ratio for FSAC PCs over time at a load of 20.

Figure 5.14 is an illustration of the pheromone calculation variation adapting to a load of 40 placed on the network. Under the medium load of 40 placed on the network, the pheromone calculation performance trend lines are remarkably similar to those illustrated in Figure 5.13, but do however have higher or more accentuated initial performance spikes which take longer to stabilize. Pheromone calculation 9 exhibits a different performance trend line to what was previously seen under the lower load as in this case the pheromone calculation displays an initial spike in performance which gradually stabilizes. With the exception of pheromone calculation 9, the rest of the pheromone calculations exhibit identical trend lines to those seen under the lower load placed on the network.

Figure 5.15 is an illustration of the pheromone calculation variation adapting to a load of 60 placed on the network. At the maximum tested load of 60 placed on the network, the pheromone calculation trend lines appear to be more closely spaced than previously seen in Figures 5.13 and 5.14 but still exhibit identical trend lines. Above holds true with the exception of pheromone calculations 2 and 3 which

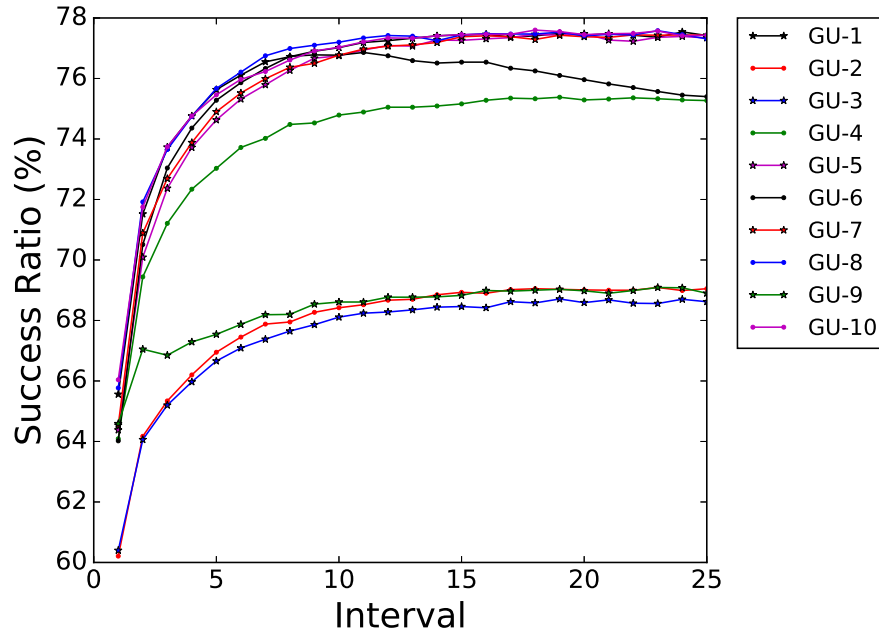


Figure 5.14: Burst Success Ratio for FSAC PCs over time at a load of 40.

under the highest tested load have separated in performance more so than previously seen. Pheromone calculations 4 and 6 are now comparatively closer to the higher performing pheromone calculations than they have been compared to Figure 5.13 and 5.14.

#### 5.4.1.3 Overall Performance of Pheromone Calculations

The pheromone calculation performances under the specific loads over the duration of the simulations as seen in Figure 5.13, 5.14 and 5.15 do fall in line with that of the overall performances displayed in Figure 5.12. In the medium network topology, pheromone calculations 2, 3 and 9 performed significantly lower with an overall average performance approximately 7% lower as compared to the other pheromone calculations illustrated in Figure 5.12. Pheromone calculation 4 was an outlier performing between the lower and higher performing pheromone calculations, but closer to the higher performing group with an overall average performance of 79.09%.

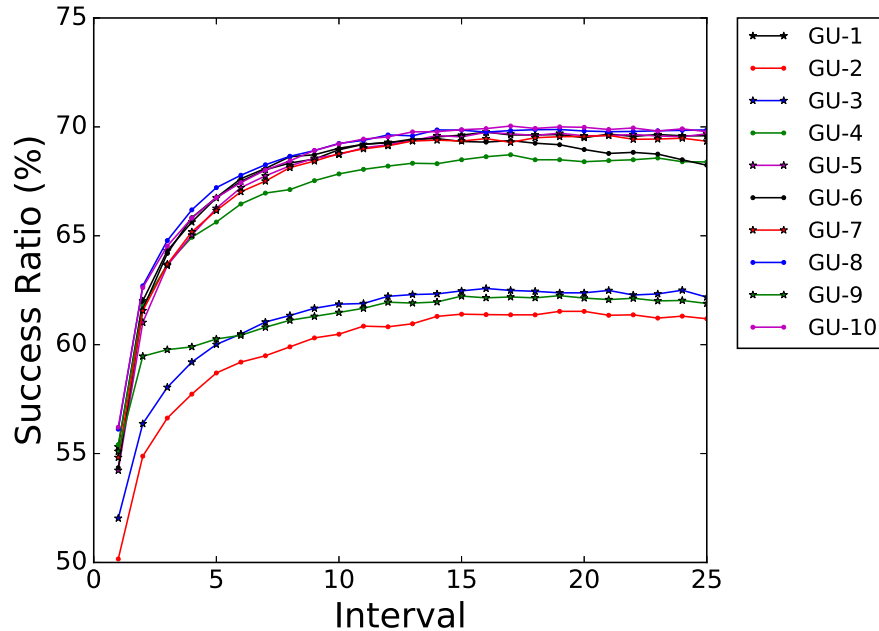


Figure 5.15: Burst Success Ratio for FSAC PCs over time at a load of 60.

Pheromone calculations 1 and 8 have the same number of significant results each, namely 5 out of 60 with averages of 81.65% and 81.66% respectively. Similarly, pheromone calculation 5 has a total of 6 out of 60 significant results with an average of 81.49% being lower than the above mentioned pheromone calculations. However, the most successful pheromone calculation is number 10 with 43 out of 60 significant results and an overall average performance of 81.85%.

#### 5.4.2 Comparison Against Existing Algorithms

This section details the results gathered for the FSAC, UCBRWA, ACRWA and SPR algorithms. The algorithms are compared against one another in terms of the gathered results.

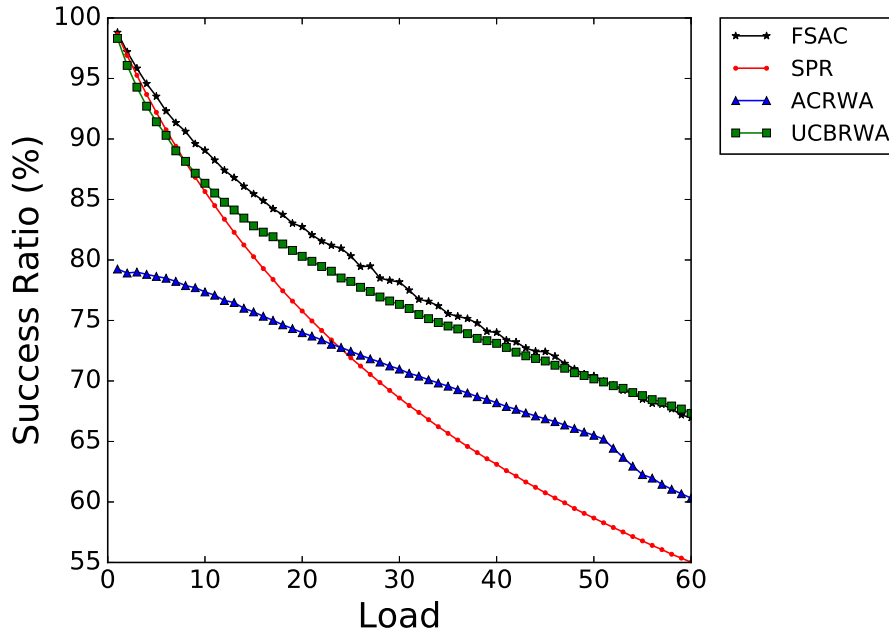


Figure 5.16: Burst Success Ratio on the medium network topology with 12 wavelengths.

#### 5.4.2.1 Relative Performance Comparison

Figure 5.16 illustrates a comparison of the success ratio performances of FSAC and UCBRWA with ACRWA and SPR as a function of the various loads placed on the medium network topology. The success ratio performances on the medium network topology are noticeably higher than this obtained on the small network topology. This is as a result of the medium network topology having more links and wavelengths with which to transmit bursts within the network. In this scenario there is no clear a difference in performance between FSAC and UCBRWA as the algorithms perform similarly. The FSAC algorithm performs the best out of the tested algorithms up to a load of approximately 50 placed on the network. Thereafter, UCBRWA marginally performs better than FSAC for the remainder of the tested loads. FSAC, SPR and UCBRWA initially are similar in performance up to a load of 5. UCBRWA and SPR achieve almost identical results up to a load of 10 placed

Table 5.5: Success ratio and 95% confidence interval at a specific load on the medium network topology with 12 wavelengths.

Load	FSAC	SPR	ACRWA	UCBRWA
5	<b>93.52 ± 0.24</b>	92.20 ± 0.02	78.64 ± 0.12	91.42 ± 0.11
10	<b>89.06 ± 0.28</b>	85.65 ± 0.02	77.36 ± 0.07	86.34 ± 0.14
15	<b>85.46 ± 0.25</b>	80.27 ± 0.02	75.71 ± 0.06	82.82 ± 0.12
20	<b>82.74 ± 0.33</b>	75.78 ± 0.02	73.99 ± 0.06	80.30 ± 0.11
25	<b>80.33 ± 0.42</b>	71.91 ± 0.02	72.45 ± 0.06	78.23 ± 0.12
30	<b>78.18 ± 0.37</b>	68.59 ± 0.02	70.98 ± 0.05	76.33 ± 0.11
35	<b>75.56 ± 0.34</b>	65.67 ± 0.02	69.57 ± 0.05	74.54 ± 0.10
40	<b>74.01 ± 0.37</b>	63.11 ± 0.02	68.20 ± 0.05	73.11 ± 0.09
45	<b>72.42 ± 0.32</b>	60.76 ± 0.02	66.87 ± 0.04	71.65 ± 0.08
50	<b>70.42 ± 0.36</b>	58.67 ± 0.02	65.51 ± 0.06	70.17 ± 0.08
55	68.49 ± 0.26	56.78 ± 0.03	62.26 ± 0.17	<b>68.79 ± 0.09</b>
60	66.96 ± 0.34	55.02 ± 0.03	60.32 ± 0.07	<b>67.32 ± 0.08</b>

Table 5.6: Overall Algorithm performance on the medium network topology with 12 wavelengths.

Algorithm	Number of Statistically Significant Results	Overall Average Performance
FSAC	53	79.09
SPR	0	70.99
ACRWA	0	70.80
UCBRWA	7	77.77

on the network whereupon they diverge and UCBRWA has a higher performance. ACRWA performs the lowest up until approximately when a load of 25 is placed on the network, thereafter ACRWA overtakes SPR and performs higher for the remainder of the tested loads on the network. ACRWA demonstrates a stable performance trend line up until when a load of 50 is placed on the network, thereafter the algorithm displays significant decrease in performance.

#### 5.4.2.2 Timewise Performance Comparison

Figures 5.17, 5.18 and 5.19 are illustrations of all the tested algorithms adapting to a specific network load over the duration of a simulation. Figure 5.17 is an illustration

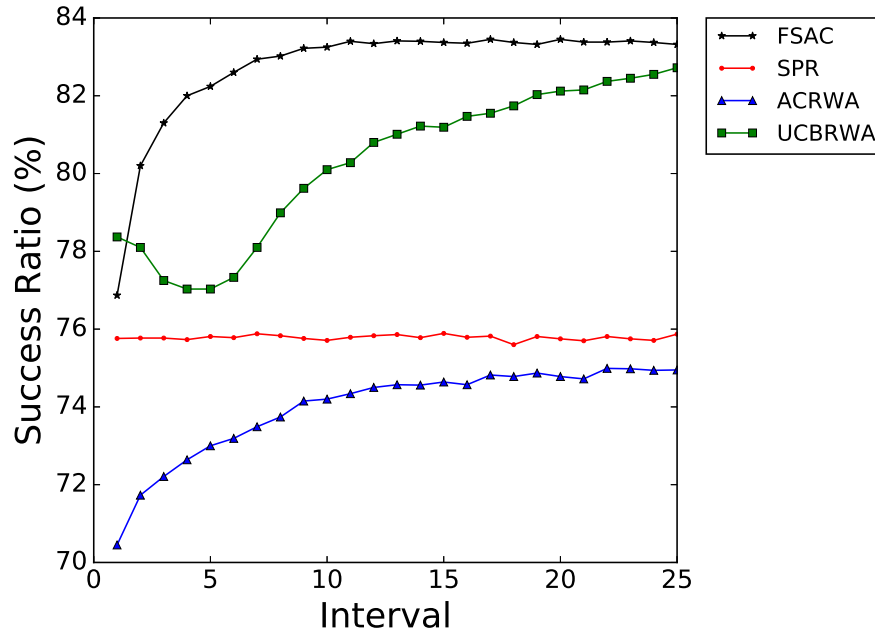


Figure 5.17: Burst Success Ratio over time at a load of 20.

of all the tested algorithms adapting to a load of 20 placed on the network. Under this low load, all the tested algorithms present distinctive performance trend line patterns over the duration of the simulation. As seen previously in the small network topology, SPR demonstrates a stable performance trend line for the duration of the simulation period. FSAC performs well, with a substantial initial increase in performance which stabilizes halfway through and remains constant for the duration of the simulation period. ACRWA illustrates a steady increase in performance which stabilizes towards the end of the simulation period. UCBRWA demonstrates a unique trend line which has an initial decrease in performance that levels out into a substantial increase in performance that continues for the remainder for the simulation period.

Figure 5.18 is an illustration of all the tested algorithms adapting to a load of 40 placed on the network. Under this medium load, all the tested algorithms present performance trend line patterns identical to those seen in Figure 5.17. SPR has a performance trend line which remains constant and stable for the duration of the



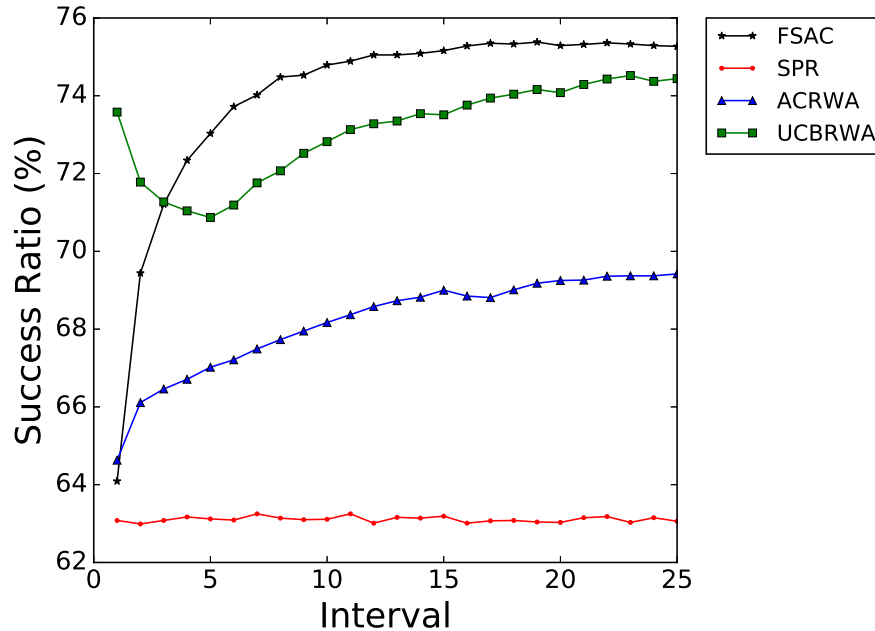


Figure 5.18: Burst Success Ratio over time at a load of 40.

simulation period. However, SPR performs lower than the rest of the algorithms under this load unlike previously noted in Figure 5.17. ACRWA demonstrates a linear increase in performance for the first two thirds of the simulation period, stabilizing for the remainder of the simulation. FSAC has a large initial increase in performance which stabilizes approximately halfway through the simulation period. UCBRWA displays a very similar trend line to that seen in Figure 5.17 with the exception of a more substantial initial decrease.

Figure 5.19 is an illustration of all the tested algorithms adapting to a load of 60 placed on the network. Under this high load, all the tested algorithms present performance trend line patterns which are similar to those previously seen in Figure 5.17 and 5.18 for FSAC and SPR. SPR displayed a consistent and stable performance throughout the duration of the simulation period. The FSAC algorithm displayed the typical performance trend line which was noted previously when lower loads were placed on the network. The performance trend line exhibited a substantial initial increase in performance which peaked approximately halfway through the simula-

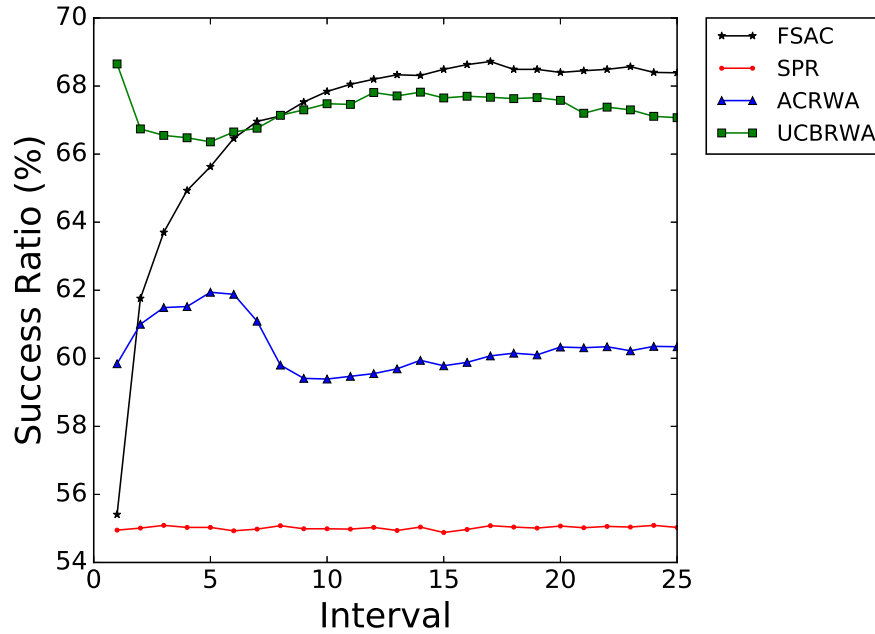


Figure 5.19: Burst Success Ratio over time at a load of 60.

tion period. Thereafter, FSAC stabilizes and provides a constant performance for the remainder of the simulation period. UCBRWA and ACRWA present different performance trend lines to those previously seen at the lower tested loads on the network. ACRWA presents a significantly different performance trend line that has an initial snaking “hump” in performance. ACRWA stabilizes after the “hump” to its initial performance for the remainder of the simulation period. UCBRWA illustrates a performance trend line that no longer has as an accentuated increase in performance after the initial decrease as previously seen at the lower tested loads placed on the network. Approximately halfway through the duration of the simulation period UCBRWA is stable and remains constant thereafter.

#### 5.4.2.3 Overall Performance Analysis

The mean success ratios over 30 repeats of each of the algorithms are reported along with the 95% confidence interval in Table 5.5. The outcomes of Mann-Whitney U

tests comparing the algorithms against one another are included with results that are statistically significantly better printed in bold. At a load of 15, FSAC is approximately 2.64% more successful than UCBRWA, 5.19% more successful than SPR and 9.75% more successful than ACRWA. At a load of 30, FSAC is approximately 1.85% more successful than UCBRWA, 7.20% more successful than ACRWA and 9.59% more successful than SPR. At a load of 45, FSAC is approximately 0.77% more successful than UCBRWA, 5.55% more successful than ACRWA and 11.66% more successful than SPR. At a load of 60, UCBRWA is approximately 0.36% more successful than FSAC, 7.00% more successful than SPR and 12.30% more successful than ACRWA. Under most of the tested loads, 0 to approximately 50, placed on the medium network topology, the FSAC algorithm performed significantly better than the other tested algorithms with the exception of the UCBRWA algorithm which at the higher tested loads, approximately 50 to 60, placed on the network performed marginally better than the FSAC algorithm. The FSAC algorithm demonstrated the most number of significant results for all the tested loads according the Mann-Whitney U tests performed on all the algorithms as seen in Table 5.6. The FSAC algorithm obtained a total number of 53 out of 60 significant results, whereas UCBRWA was able to obtain a total number of 7 out of 60 significant results. The overall average performances of the algorithms are displayed in Table 5.6. FSAC has the highest overall average performance among the tested algorithms with a value of 79.09%. UCBRWA follows FSAC closely with an overall average performance of 77.77%. On average the FSAC algorithm performed approximately 1.32% higher than UCBRWA, 8.10% higher than SPR and 8.29% higher than ACRWA on this network topology.

## 5.5 Large Topology Results

The results of the experiments described in the Section 5.2 are now presented. The experiments were conducted in simulation on the large network topology in Figure

5.3. The FSAC algorithm is represented by pheromone calculation 4 in the sections that follow for the large network topology.

### 5.5.1 Comparison of FSAC Pheromone Calculations

This section details the results gathered for all of the FSAC pheromone calculations and compares the equations against one another.

#### 5.5.1.1 Relative Performance of Pheromone Calculations

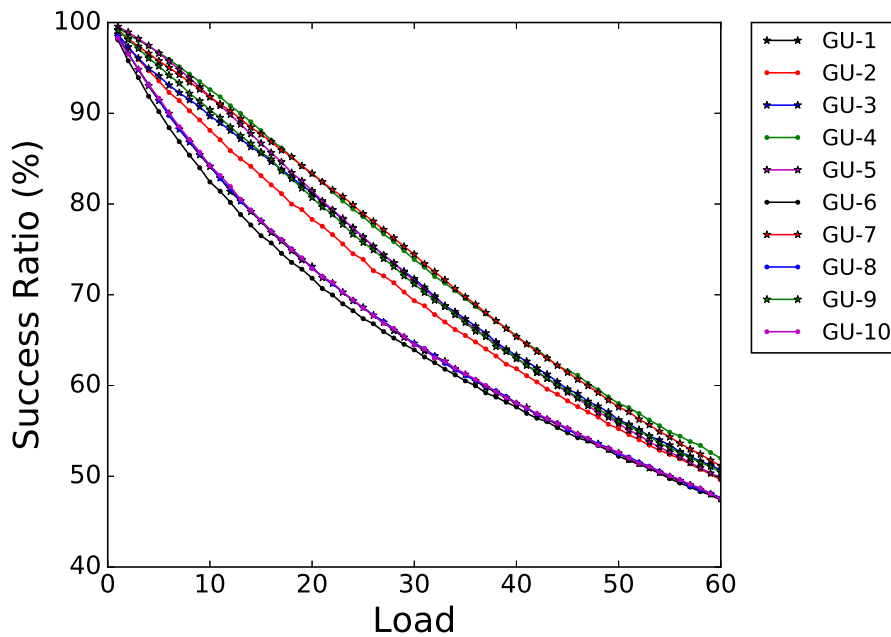


Figure 5.20: Burst Success Ratio for FSAC PCs on the large network topology with 16 wavelengths.

Figure 5.20 illustrates the performance of each of the pheromone calculations for the various loads placed on the large network. In Figure 5.20, the performance of the pheromone calculations is divided into two groups with one outlier. A higher performing group, the lower performing outlier and the low performing group. The low performing group is comprised of pheromone calculations 1, 6, 8 and 10 with

Table 5.7: Overall performance of the FSAC PCs on the large network topology with 16 wavelengths.

Pheromone Calculation	Number of Statistically Significant Results	Overall Average Performance
GU-1	0	67.05
GU-2	0	70.75
GU-3	0	72.38
GU-4	36	74.51
GU-5	4	72.68
GU-6	0	66.27
GU-7	20	74.28
GU-8	0	67.11
GU-9	0	72.31
GU-10	0	67.13

pheromone calculation 6 being the worst. As previously seen in Figure 5.4 and 5.12, the pheromone calculations all have similar performances. Immediately after a load of 1, the pheromone calculations split in two groups. When a load of 5 is placed on the network, pheromone calculation 2 which displays a similar trend line to the better performing group begins to diverge performing slightly under par. Comparing pheromone calculation 4 with 6, pheromone calculation 4 is the best performing and pheromone calculation 6 the worst performing. At a load of 15 being placed on the network the performance difference is 11.58%, whereas at a load of 30 the difference in performance is 9.96%. Thereafter, with a load of 45 placed on the network the difference in performance is 6.82% while at the highest load placed on the network the difference in performance of the two pheromone calculations is 4.61%. Unlike the performances on the previous network topologies in Figure 5.1 and 5.9, the lower and higher performing pheromone calculations do not increase in performance difference under higher loads but rather begin to slowly converge.

### 5.5.1.2 Timewise Performance of Pheromone Calculations

Figures 5.21, 5.22 and 5.23 are illustrations of the FSAC algorithms pheromone calculation variations adapting to a specific network load over the duration of a

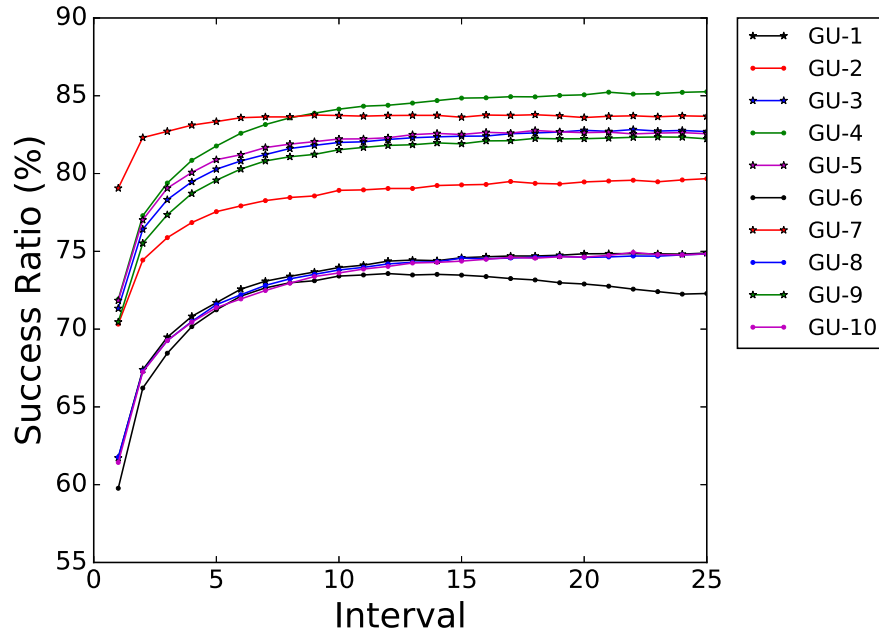


Figure 5.21: Burst Success Ratio for FSAC PCs over time at a load of 20.

simulation. Figure 5.21 is an illustration of the pheromone calculation variation adapting to a load of 20 placed on the network. Under a load of 20 placed on the network, as previously seen in Figure 5.13 there is a predominant performance trend for the period of the simulation with the exception of pheromone calculations 6 and 7. As mentioned previously, the predominant pattern is described as having an initial spike in performance where the pheromone calculations end with a higher success ratio value than that which they started with. All of the pheromone calculations display an initial spike in performance at the start of the simulation which quickly stabilizes for the remainder of the simulation period with the exception of pheromone calculation 6. Pheromone calculation 6 differs from the rest of the pheromone calculations in that it does not stabilize after the initial performance spike, but rather decreases in performance for the remainder of the simulation period. Pheromone calculation 7 has a slight difference compared to the rest of the pheromone calculations in that it has a smaller initial performance spike, remaining stable thereafter.

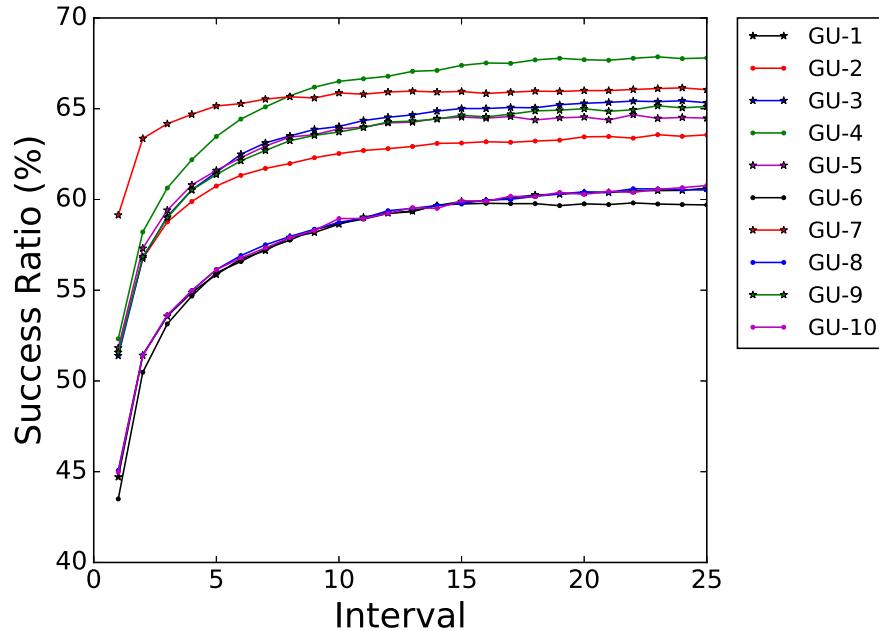


Figure 5.22: Burst Success Ratio for FSAC PCs over time at a load of 40.

Figure 5.22 is an illustration of the pheromone calculation variation adapting to a load of 40 placed on the network. Under a medium load of 40, the pheromone calculation trend lines are identical to that of those observed in Figure 5.21 on the lower load of 20 placed on the network. All of the pheromone calculations display an extended initial performance spike which takes longer to stabilize. Pheromone calculation 6 no longer decreases in performance over the period of the simulation, but remains stable after the initial performance spike.

Figure 5.23 is an illustration of the pheromone calculation variation adapting to a load of 60 placed on the network. Under the maximum tested load of 60, the pheromone calculation trend lines appear more compacted when compared to Figure 5.21 and 5.22 but they still exhibit the same trends. Pheromone calculations 1, 6, 8 and 10 are comparatively closer in performance to the rest of the global equations. The performance gap between the groups has somewhat diminished under the higher load placed on the network. Pheromone calculation 7 no longer has the second highest performance in Figure 5.23 as compared to Figure 5.21 and 5.22.

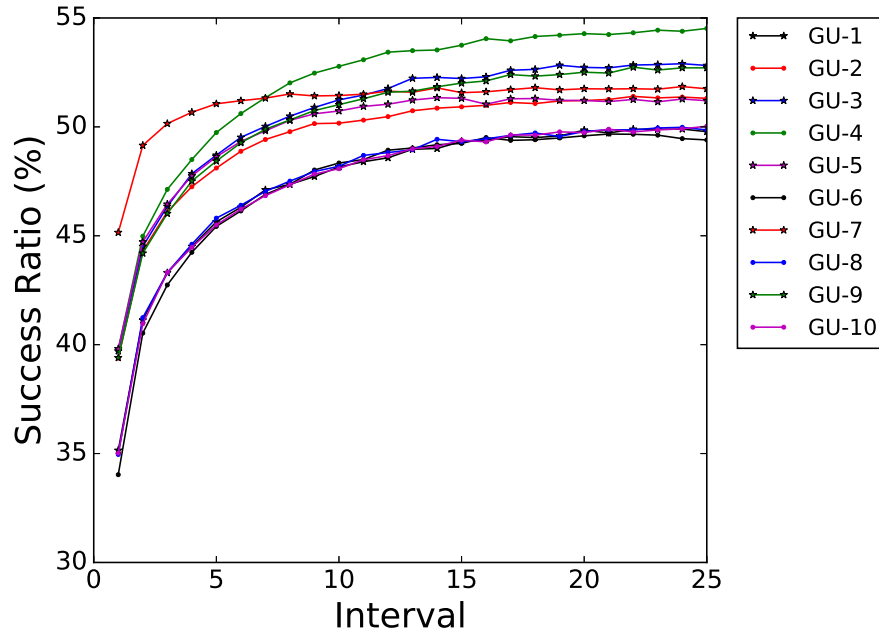


Figure 5.23: Burst Success Ratio for FSAC PCs over time at a load of 60.

It has the smallest initial performance spike compared to the rest of the pheromone calculations. The performance of pheromone calculation 6 remains stable after the initial performance spike as in Figure 5.22, but not in Figure 5.20.

### 5.5.1.3 Overall Performance of Pheromone Calculations

The performance of the pheromone calculations under specific loads over the duration of the simulations as seen in Figure 5.21, 5.22 and 5.23 correspond with that of the overall performances of the pheromone calculations displayed in Figure 5.20. In the large network topology, pheromone calculations 1, 6, 8 and 10 performed significantly lower as compared to the others illustrated in Figure 5.20. Inspection of Table 5.7 further illustrates the performance differences where pheromone calculations 1, 6, 8 and 10 have the lowest overall average performances of approximately 5% to 7% lower than the rest of the pheromone calculations. Pheromone calculation 4 has the most number of significant results (36 out of 60) and the highest overall



average performance of 74.51%. The next best performance is that of pheromone calculation 7 with a total number of 20 significant results and an overall average performance of 74.28%. Pheromone calculation 4 and 7 both had a large number of significant results and performed very similarly overall. Pheromone calculation 5 had 4 significant results and an overall average performance of 72.68%.

## 5.5.2 Comparison Against Existing Algorithms

This section details the results gathered for the FSAC, UCBRWA, ACRWA and SPR algorithms. The algorithms are compared against one another in terms of the gathered results.

### 5.5.2.1 Relative Performance Comparison

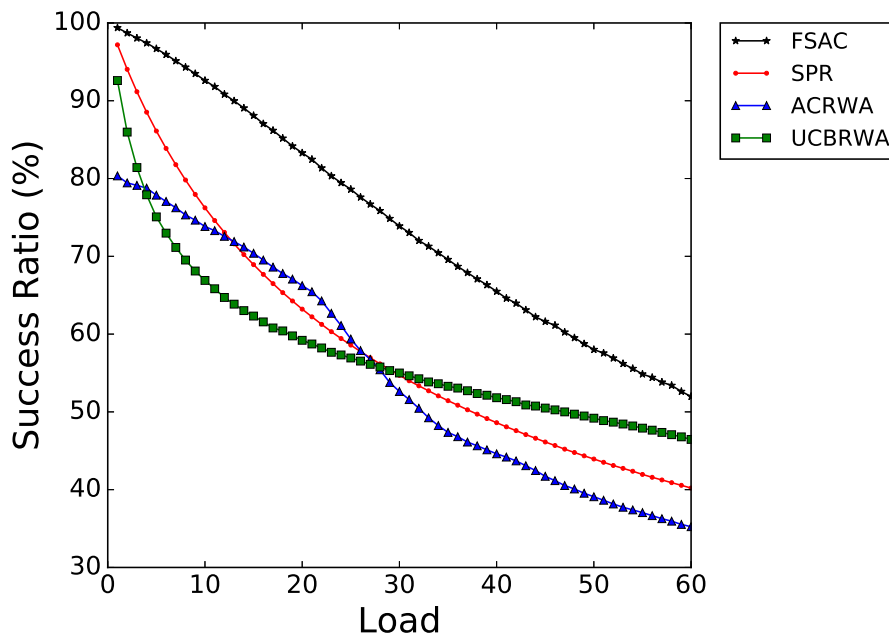


Figure 5.24: Burst Success Ratio on the large network topology with 16 wavelengths.

Figure 5.24 illustrates a comparison of the success ratio performances of FSAC and UCBRWA with ACRWA and SPR as a function of the various loads placed on

Table 5.8: Success ratio and 95% confidence interval at a specific load on the large network topology with 16 wavelengths.

Load	FSAC	SPR	ACRWA	UCBRWA
5	<b>96.69 ± 0.04</b>	86.11 ± 0.02	77.86 ± 0.15	75.07 ± 0.11
10	<b>92.60 ± 0.07</b>	76.23 ± 0.02	73.83 ± 0.15	66.90 ± 0.11
15	<b>88.09 ± 0.07</b>	68.93 ± 0.02	70.39 ± 0.09	62.32 ± 0.08
20	<b>83.29 ± 0.13</b>	63.21 ± 0.02	66.23 ± 0.09	59.20 ± 0.07
25	<b>78.61 ± 0.11</b>	58.59 ± 0.03	59.37 ± 0.29	56.93 ± 0.08
30	<b>73.89 ± 0.13</b>	54.70 ± 0.03	52.62 ± 0.21	55.00 ± 0.07
35	<b>69.58 ± 0.14</b>	51.44 ± 0.02	47.36 ± 0.13	53.29 ± 0.05
40	<b>65.48 ± 0.16</b>	48.61 ± 0.02	44.61 ± 0.05	51.82 ± 0.05
45	<b>61.61 ± 0.14</b>	46.13 ± 0.02	41.72 ± 0.22	50.49 ± 0.05
50	<b>58.01 ± 0.18</b>	43.94 ± 0.02	39.09 ± 0.09	49.19 ± 0.03
55	<b>54.86 ± 0.13</b>	41.96 ± 0.02	37.05 ± 0.07	47.91 ± 0.03
60	<b>51.98 ± 0.14</b>	40.21 ± 0.02	35.24 ± 0.05	46.46 ± 0.05

Table 5.9: Overall Algorithm performance on the large network topology with 16 wavelengths.

Algorithm	Number of Statistically Significant Results	Overall Average Performance
FSAC	60	74.51
SPR	0	58.58
ACRWA	0	55.33
UCBRWA	0	57.73

the large network topology. Notably, the success ratio performances in the large network topology are lower than that of the medium network topology. This is because the larger network has more nodes and wavelengths per link but is a less connected topology. In this scenario there is a clear differentiate in performance between FSAC and the other tested algorithms. The FSAC algorithm has the best performance under all the tested loads on the network. UCBRWA, ACRWA and SPR takes turns performing better than one another under the tested loads on the network. Initially, up to a load of 5 was placed on the network, UCBRWA performs better than ACRWA. Thereafter, between a load of approximately 5 to 30, ACRWA has a higher performance than that of UCBRWA. When a load between 15 and 25

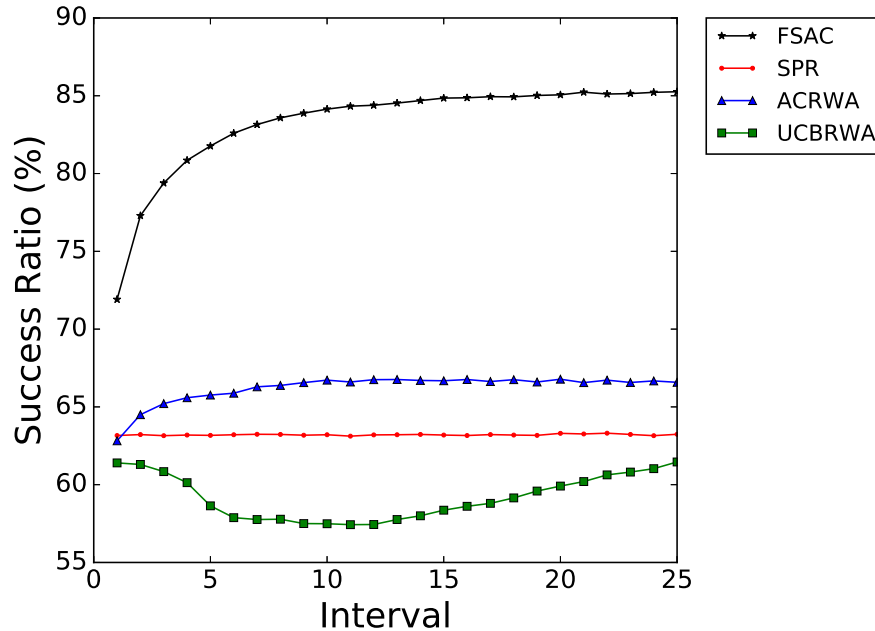


Figure 5.25: Burst Success Ratio over time at a load of 20.

was placed on the network, ACRWA has a higher performance than SPR. This is as a result of ACRWA having an increased drop in performance between a load of 20 and 30 where it begins to stabilize. With an approximate load of 30 placed on the network, UCBRWA performs higher than ACRWA and SPR for the remainder of the tested loads approaching the performance of the FSAC algorithm.

### 5.5.2.2 Timewise Performance Comparison

Figures 5.25, 5.26 and 5.27 are illustrations of all the tested algorithms adapting to a specific network load over the duration of a simulation. Figure 5.25 is an illustration of all the tested algorithms adapting to when a load of 20 placed on the network. Under this low load, all the tested algorithms present distinctive performance trend line patterns over the duration of the simulation. SPR demonstrates a stable performance trend line for the duration of the simulation period. FSAC, however, has a substantial increase in performance which stabilizes at approximately two thirds into

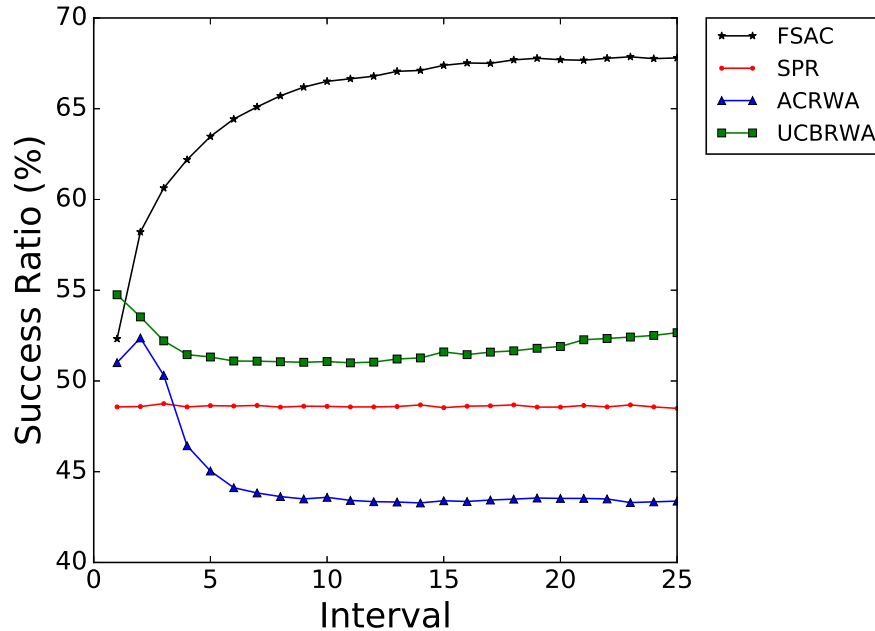


Figure 5.26: Burst Success Ratio over time at a load of 40.

the simulation period. ACRWA has an initial performance lower than that of SPR, however, ACRWA then has a spike in performance to a higher success ratio than that of SPR. Approximately halfway through the simulation period, ACRWA displays a steady and stable performance. UCBRWA illustrates an interesting performance trend line which initially decreases in performance where it plateaus approximately one third into the simulation period. Thereafter, UCBRWA steadily increases in performance for the remainder of the simulation period nearing the performance of SPR at the end.

Figure 5.26 is an illustration of all the tested algorithms adapting to a load of 40 placed on the network. Under this medium load, all the tested algorithms presented performance trend line patterns which in the case of FSAC and SPR are identical to those seen previously in Figure 5.25 with UCBRWA displaying a similar trend line. As previously seen in Figure 5.25, UCBRWA's trend line initially decreases and then stabilizes into a steady increase in performance for the remainder of the simulation period. However, ACRWA demonstrates a significantly different trend

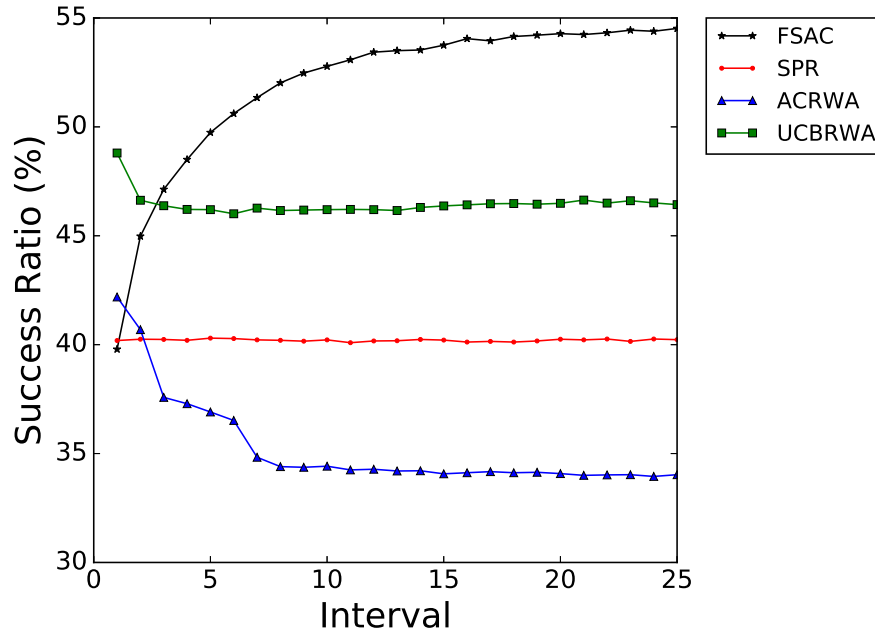


Figure 5.27: Burst Success Ratio over time at a load of 60.

line to that seen previously in Figure 5.25 with ACRWA having a higher performance than that of SPR at the start of the simulation and then has the lowest performance at the end of the simulation period. ACRWA no longer increases in performance at the beginning of the simulation period. It has an initial spike which decreases substantially and stabilizes after approximately one third of the simulation period. FSAC demonstrates a distinctively large increase in performance over the first half of the simulation period thereafter it stabilizes and remain constant for the remainder of the simulation period.

Figure 5.27 is an illustration of all the tested algorithms adapting to a load of 60 placed on the network. Under this high load, all the tested algorithms present performance trend line patterns which are identical to those seen in Figure 5.25 and 5.26 for FSAC and SPR. SPR has a consistent performance trend line for the simulation period. Whereas FSAC illustrates its typical performance trend line which has a substantial increase in performance for the first half of the simulation period, thereafter FSAC stabilizing and remaining constant for the remainder of the

simulation period. UCBRWA and ACRWA demonstrate similar performance trend lines to those seen previously in Figure 5.26. UCBRWA has a similar performance trend line with the exception of having no discernible increase in performance after stabilizing for the remainder of the simulation period. ACRWA presents a slightly different performance trend line as there is no initial performance increase or spike and the decrease in performance is no longer smooth but rather step-like. However, the ACRWA does demonstrate a stable performance for the remainder of the simulation period.

### 5.5.2.3 Overall Performance Analysis

The mean success ratios over 30 repeats of each of the algorithms are reported along with the 95% confidence interval in Table 5.8. The outcomes of Mann-Whitney U tests comparing the algorithms against one another are included with results that are statistically significantly better printed in bold. At a load of 15, FSAC is approximately 17.70% more successful than ACRWA, 19.16% more successful than SPR and 25.77% more successful than UCBRWA. At a load of 30, FSAC is approximately 18.89% more successful than UCBRWA, 19.19% more successful than SPR and 21.27% more successful than ACRWA. At a load of 45, FSAC is approximately 11.12% more successful than UCBRWA, 15.48% more successful than SPR and 19.89% more successful than ACRWA. At a load of 60, FSAC is approximately 5.52% more successful than UCBRWA, 11.77% more successful than SPR and 16.74% more successful than ACRWA.

Under all the tested loads placed on the small network topology, the FSAC algorithm performed significantly better than the other tested algorithms. The FSAC algorithm demonstrated the most significant results for all of the tested loads according to the Mann-Whitney U tests performed on all of the algorithms as seen in Table 5.9. The FSAC algorithm had an overall average performance of 74.51% and on average performed approximately 15.93% higher than SPR, 16.78% higher than UCBRWA and 19.18% higher than ACRWA on this network topology.

## 5.6 Umbrella Analysis

Table 5.10: Overall Pheromone Calculation performance on all the tested network topologies.

Pheromone Calculation	Number of Statistically Significant Results	Overall Average Performance
GU-1	5	70.17
GU-2	18	72.56
GU-3	15	73.32
GU-4	42	75.06
GU-5	11	74.74
GU-6	0	69.30
GU-7	26	75.61
GU-8	5	70.19
GU-9	0	73.17
GU-10	43	70.29

Table 5.11: Overall Algorithm performance on all the tested network topologies.

Algorithm	Number of Statistically Significant Results	Overall Average Performance
FSAC	158	75.06
SPR	0	61.79
ACRWA	0	54.04
UCBRWA	7	60.45

The overall pheromone calculation performance on all the tested network topologies is displayed in Table 5.10, including the total number of statistically significant results obtained for each of the pheromone calculations gathered from the results given in Appendix A. Similarly, the overall algorithm performance on all the tested network topologies is provided in Table 5.11 which includes the total number of statistically significant results obtained for each of the tested algorithms gathered from the results given in Appendix C.

For the FSAC algorithm, the pheromone calculations with the most number of statistically significant results is 10 (43 out of 135), 4 (42 out of 135) and then 7 (26 out of 135). However, the pheromone calculations with the highest overall av-

erage performances are 7 (75.61%), 4 (75.06%) and then 5 (74.74%). Pheromone calculation 10 only achieved statistically significant results on the medium network topology, performing poorly on the small and large network topologies. Pheromone calculations 5 and 7 accumulated statistically significant results on all of the network topologies, while pheromone calculation 4 only obtained statistically significant results on the small and large network topologies. Notably, pheromone calculation 7 has the third most number of statistically significant results but has the highest overall average of all the tested pheromone calculations. Pheromone calculation 4 has the second highest number of statistically significant results and the second highest overall average performance. The most promising pheromone calculation are 4 and 7. Overall, pheromone calculation 7 performed the best out of the other tested pheromone calculations considered in this work, with pheromone calculation 4 performing almost identically.

In the small network topology, FSAC displayed the best performance compared to SPR, ACRWA and UCBRWA for all the tested loads. UCBRWA performed better than ACRWA under low and high loads. Under a medium load placed on the network, they performed similarly. In the medium network topology, FSAC had the best performance for all but the highest tested loads placed on the network. UCBRWA performed better than FSAC at the highest load. Notably, it performed significantly better than SPR and ACRWA for all the tested loads. In the large network topology, FSAC outperformed the other tested algorithms for all the loads placed on the network. Under low loads, ACRWA performed better than UCBRWA. However, UCBRWA faired better than ACRWA under high loads.

## 5.7 Conclusion

This chapter applied the proposed algorithms on a simulated traditional Fixed Grid WDM network. The proposed algorithms used entire path (wavelength and route tuple) selection from the source to destination node pair. The use of different



pheromone updating equations, pheromone calculations, were investigated for the FSAC algorithm. The use of UCB for path (wavelength and route tuple) selection was investigated in the UCBRWA algorithm. FSAC, ACRWA, SPR and UCBRWA were evaluated on three separate network topologies, each with a limited number of available wavelength channels for wavelength assignment.

The FSAC algorithm displayed the inclination to initially explore routing tuples and thereafter exploit the successful routing tuples for the remainder of the simulations. UCBRWA displayed the same tendency, initially exploring routing tuples and exploiting the successful solutions thereafter. The FSAC algorithm accumulated the most number of statistically significant results (158 out of 165) and achieved the highest overall average performance. FSAC performed significantly better than all of the tested algorithms considered in this work. UCBRWA performed better than ACRWA and was also able to outperform FSAC at the highest tested loads on the medium topology. The FSAC algorithm displayed the adaptability needed for the OBS environment on a traditional Fixed Grid WDM network. Compared to ACRWA, UCBRWA displayed similar and improved performance throughout most of the test network topologies.

# Chapter 6

## EVALUATION ON FLEXIBLE SPECTRUM AND IMPAIRMENTS

### 6.1 Introduction

This chapter details the evaluation process for the proposed algorithms on a simulated Flexible Spectrum OBS network with PLIs, discussed in Section 6.2. The evaluation is first performed on the novel FSAC algorithm, determining which of the 10 proposed pheromone calculations is the most successful. The best performing pheromone calculation is then used to represent the FSAC algorithm when compared to ACRWA, SPR and UCBRWA in simulation. The simulation results are gathered on a small (Section 6.3), medium (6.4) and large (6.5) network topology. These results are analysed and discussed with an overall summary of the chapter given in Section 6.7.

## 6.2 Experimental Procedure

This section details the performance measures (Section 6.2.1), network topologies (Section 6.2.2), algorithms used for comparison with the proposed approaches (Section 6.2.3) and the procedure (Section 6.2.4) followed during the evaluation process.

### 6.2.1 Performance Measures

This section discusses the series of experiments that will be conducted on the algorithms proposed in Chapter 4. This includes testing and comparing all of the proposed pheromone calculation equations against one another in terms of their overall performances and timewise behaviour. The best performing pheromone calculation will be selected to represent the FSAC routing algorithm for each network scenario. The proposed FSAC and UCBRWA routing algorithms will be tested and compared with ACRWA and SPR. The tests will compare the algorithms overall performances and timewise behaviour. The Flexible Spectrum experiments simulated a Flexible Spectrum OBS network with PLIs. The PLIs are modelled using equation 2.2 to simulate the Flexible Spectrum environment with the parameters presented in Section 2.6.2 and the network link lengths (in km) illustrated on the associated network topologies illustrated in Section 6.2.2. The transmission penalty associated to the PLIs is calculated using the difference in wavelength channel spacing (in GHz) between all the bursts simultaneously traversing the network links. In this scenario, the network topologies are given a distinct bandwidth range from which to select the wavelength channel spacings in the RWA process. Each link in the network is only able to transmit bursts within the distinct bandwidth channel spacing range. Only one burst can reserve and transmit along a particular wavelength channel spacing. Other burst requests attempting to reserve the wavelength channel spacing would be blocked. In the Flexible Spectrum scenario, the number of burst successes that occur within the PLIs are used to measure performance.

## 6.2.2 Network Topologies

Three different network topologies are adopted in the simulations. A small test network topology composed of 6 nodes with 8 links in Figure 6.1, a medium test network topology of 11 nodes with 26 links in Figure 6.2 and a large test network topology of 14 nodes with 21 links in Figure 6.3 (Donato et al., 2012; Pedro et al., 2009; Triay and Cervello-Pastor, 2010). The purpose of the different network topologies is to evaluate the performance of the protocol on a simple network, a larger but more connected graph and also within a more complex scenario (NFSNET-14 topology in Figure 6.3). The values illustrated on all three of the Figures 6.1, 6.2 and 6.3 are the distances in km.

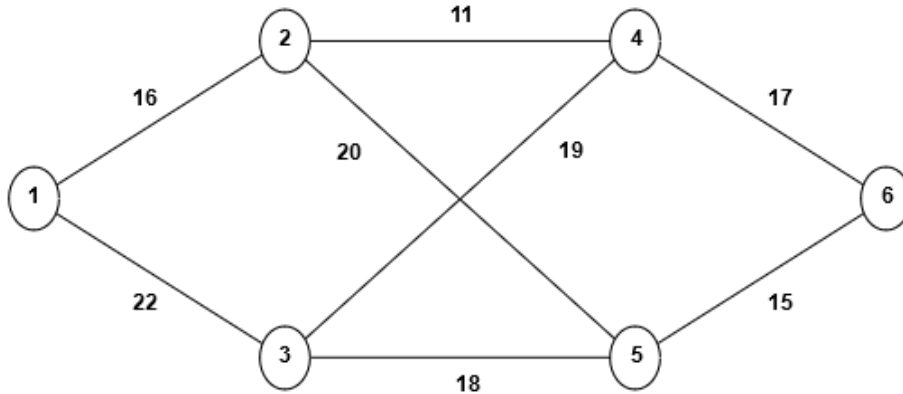


Figure 6.1: Small 6-Node network topology

In the Flexible Spectrum the network links no longer have a set of pre-defined wavelengths in order to simulate a dynamic Flexible Spectrum environment. Each of the protocols were allowed to select a suitable wavelength channel spacing within a specified wavelength channel range, [1200,1400] in GHz. A Line Attenuation,  $A$ , of 0.2 dB/km was used. The transmission intensity,  $P$ , of each burst is 18.0 dBm and the minimum receiving intensity is 0.0 dBm. The transmission bit-rate is 1024 Mb/s. The above mentioned values were used in equation (2.2). The measure of

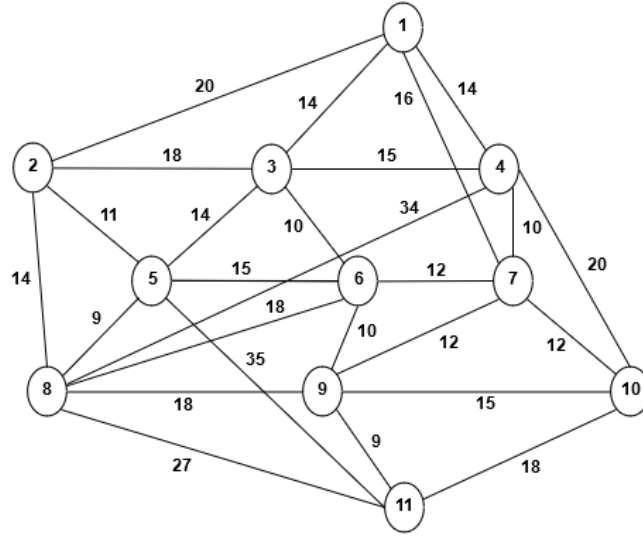


Figure 6.2: Medium 11-Node network topology

performance for the algorithms are based on the successful transmission of bursts throughout the network.

### 6.2.3 Comparison Algorithms

The existing algorithm is an ant based routing algorithm, ACRWA, previously discussed in Section 3.2.5 and a greedy, but simple, Shortest Path Routing (SPR) algorithm for comparison. The SPR algorithm computes the shortest path for each source to destination node pair. In the Flexible Spectrum scenario, SPR has been adapted and implemented to select the shortest path with Random wavelength assignment. The selected random wavelength is generated from within the specific wavelength range. ACRWA has been implemented as discussed in Section 3.2.5 for the Flexible Spectrum scenario is an adapted setup such that all the input, output link wavelength combinations are generated by means of using a wavelength selected within a specific wavelength range and distribute to each node with a pheromone value initialised to a value of 1. The 1000 selected wavelength channel spacing values were evenly distributed within the specific wavelength channel range.

The parameters for all the tested algorithms have been manually tuned through

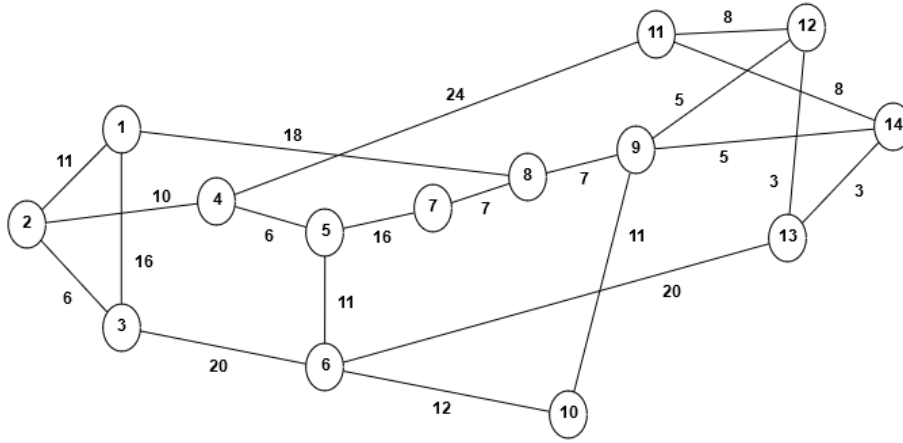


Figure 6.3: Large 14-Node network topology

preliminary experiments. The selected parameters gave the highest performances measured in simulation. Parameters for ACRWA have been selected from Triay and Cervello-Pastor and manually tuned as above (Triay and Cervello-Pastor, 2010). The parameters of the UCBRWA protocol used throughout the simulations are as follows:  $\alpha_1 = 0.995$ ,  $C = 2.0$ ,  $c_K = 200$  for the small network topology,  $c_K = 400$  for the medium network topology and  $c_K = 500$  for the large network topology. The parameters of the FSAC protocol used throughout the simulations are as follows:  $\alpha_1 = 0.9$ ,  $\alpha_2 = 0.09$ ,  $\alpha_3 = 0.01$ ,  $\beta = 2.0$ ,  $\psi = 0.01$ ,  $c_J = 250$  for the small network topology,  $c_J = 400$  for the medium network topology and  $c_J = 400$  for the large network topology. The parameters of the ACRWA protocol used throughout the simulations are as follows:  $r_0 = 0.8$ ,  $\rho = 0.01$ ,  $\omega = 0.75$ ,  $\alpha = 0.001$ ,  $\phi = 0.75$ ,  $\beta = 2.0$ ,  $r_0 = 0.8$  for the small network topology,  $r_0 = 0.9$  for the medium network topology and  $r_0 = 0.9$  for the large network topology.

### 6.2.4 Procedure

Each of the simulations were tested under various network loads. The load placed on a network in simulation refers to the total number of new burst requests at each given timestep in the simulator. These simulations were repeated a total of 30 times

and the results are averaged. Each simulation attempts to transmit  $5 \times 10^5$  bursts, including the initial learning phase. A total of  $5 \times 10^5$  bursts requests was chosen for simulation purposes through preliminary testing as an appropriate quantity. This quantity allowed the tested algorithms the opportunity to adapt (learning phase) and stabilise (peak performance) to a load in simulation. The source and destination nodes are randomly selected for each burst. Two values are measured throughout the duration of a simulation. The number of successful burst transmissions  $\kappa_T$ .  $\chi_T$  is the sum of failed burst transmissions (due to linear and non-linear effects) and burst blocks. The success ratio  $R$  used as a performance measure is calculated as follows:

$$R = \frac{\kappa_T}{\chi_T + \kappa_T} \quad (6.1)$$

The results gathered for the mean success ratio at various loads and the timewise behaviour for three specific loads will be graphed. The mean success ratios over 30 repeats of each pheromone calculation for various loads will be tabled along with a 95% confidence interval and the statistically significantly better mean success ratios are printed in bold. The best performing pheromone calculation in terms of overall performance at various loads and timewise behaviour at specific loads with the most number of statistically significant results will be selected to represent the FSAC algorithm when compared to ACRWA, SPR and UCBRWA. The gathered results for FSAC, UCBRWA, ACRWA and SPR for the mean success ratio at various loads and timewise behaviour for the specific loads will be graphed. The mean success ratios over 30 repeats of each of the algorithms for various loads will be tabled along with a 95% confidence interval and the statistically significantly better mean success ratios are printed in bold. The outcomes of Mann-Whitney U tests for each of the tested algorithms against all the other algorithms for being greater than each other is used to determine which algorithm has the statistically significant results. The purpose of measuring the timewise behaviour of the algorithms in terms of low, medium and high loads is to gauge the value obtained for the mean success ratio. Plotting the timewise behaviour allows for the identification of whether the algorithm improves,

degrades or remains constant in performance. The above mentioned comparisons will be performed on each network topology.

## 6.3 Small Topology Results

The results of the experiments described in the Section 6.2 are now presented. The experiments were conducted in simulation on the small network topology in Figure 6.1. The FSAC algorithm is represented by pheromone calculation 4 in the sections that follow for the small network topology.

### 6.3.1 Comparison of FSAC Pheromone Calculations

This section details the results gathered for all of the FSAC pheromone calculations and compares the equations against one another.

#### 6.3.1.1 Relative Performance of Pheromone Calculations

Table 6.1: Overall performance of the FSAC PCs on the small network topology.

Pheromone Calculation	Number of Statistically Significant Results	Overall Average Performance
GU-1	0	35.60
GU-2	11	42.88
GU-3	1	42.65
GU-4	16	41.89
GU-5	0	40.61
GU-6	0	39.00
GU-7	0	38.71
GU-8	0	39.41
GU-9	17	42.71
GU-10	0	42.35

Figure 6.4 is an illustration of the performance of each of the pheromone calculations for the various loads placed on the small network. In Figure 6.4 the pheromone calculations remain tightly grouped up to a load of 20 placed on the network with



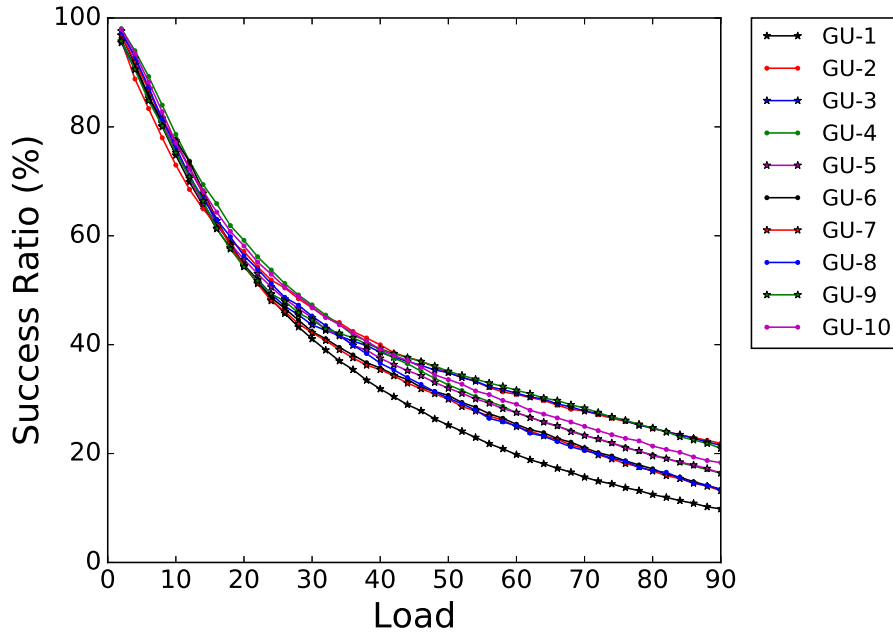


Figure 6.4: Burst Success Ratio for FSAC PCs on the small network topology.

all pheromone calculations having similar performances. Thereafter, the pheromone calculations begin to diverge from one another. The pheromone calculations are roughly divided into 2 groups where the first group performs well initially up to a load of 40, while members from the second group performs better thereafter. In particular, at a load of 30 pheromone calculation 1 starts a notable decline in performance for the remainder of the simulated loads and performs poorly with an overall average performance of 35.60%. Comparing pheromone calculation 1 with 9, pheromone calculation 9 performs the best on the network while pheromone calculation 1 has the worst performance. At a load of 30 placed on the network the performance difference is 3.44%, whereas under a load of 60 placed on the network the difference in performance has increased to 11.83%. At the highest load of 90 placed on the network the difference in performance remains constant at 11.14%.

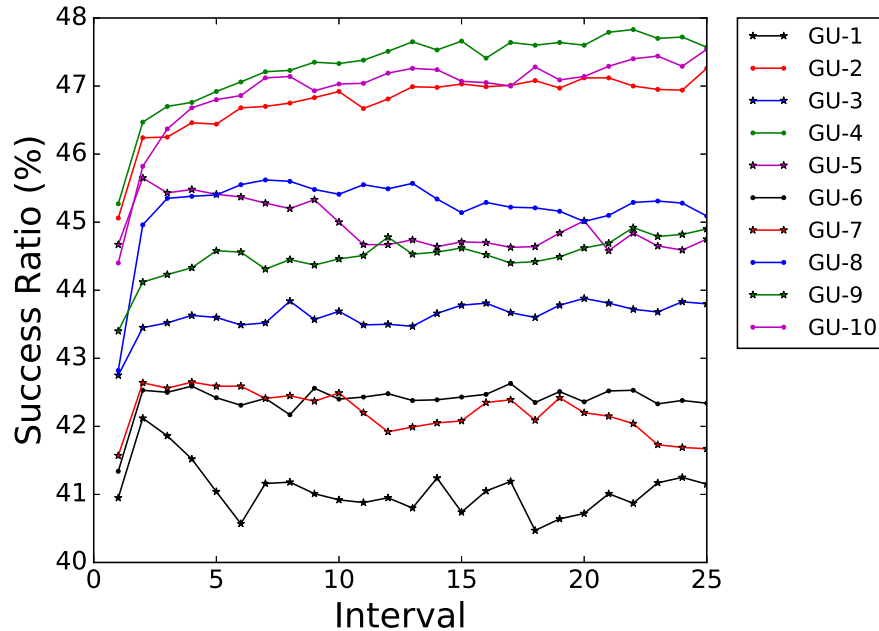


Figure 6.5: Burst Success Ratio for FSAC PCs over time at a load of 30.

### 6.3.1.2 Timewise Performance of Pheromone Calculations

Figures 6.5, 6.6 and 6.7 are illustrations of the pheromone calculation variations for the FSAC algorithm adapting to a specific network load over the duration of a simulation. Figure 6.5 is an illustration of the pheromone calculation variation adapting to a load of 30 placed on the network. The trend lines appear “jumpy”, but this is due to a much lower success ratio range than that of the previously illustrated learning graphs for the Fixed Grid scenario. Under this low load placed on the network, the predominant pattern for the pheromone calculations is no longer as pronounced as seen before in the Fixed Grid scenario. The pheromone calculations 4, 8 and 10 do demonstrate the expected trend line form as seen previously. They display an initial jump in performance which stabilizes for the remainder of the simulation. Pheromone calculations 1, 5 and 7 initially increase in performance with a performance spike, but do not stabilize and decrease in performance for the remainder of the simulation. Pheromone calculations 2, 3, 6 and 9 display similar

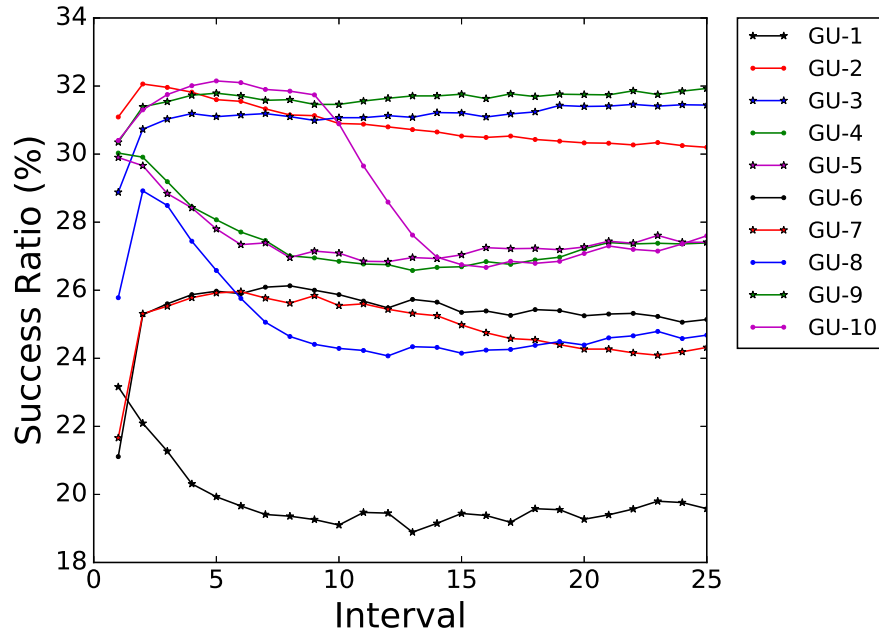


Figure 6.6: Burst Success Ratio for FSAC PCs over time at a load of 60.

trend lines. Initially they have a performance spike that flattens immediately which differs from the predominant pattern. The trend lines are similar to those previously seen for pheromone calculation 7 in the Fixed Grid scenario.

Figure 6.6 is an illustration of the pheromone calculation variation adapting to a load of 60 placed on the network. Under the medium load placed on the network, the performance trend of the pheromone calculations is vastly different to those previously seen at the lower load placed on the network and in the Fixed Grid scenario. Pheromone calculations 3, 6, 7 and 9 illustrate the classic performance trend line with an initial performance spike stabilizing thereafter. Pheromone calculation 10 differs the most as compared to all of the pheromone calculations previous performance trend lines. This pheromone calculation displays a small initial performance spike which stabilizes quickly. Immediately thereafter, at around interval 10, the pheromone calculation drastically drops in performance from approximately 32% to 27%. By interval 15 the pheromone calculation remains constant for the duration of the simulation period. Pheromone calculations 1, 2, 4, 5 and 8 all have a perfor-

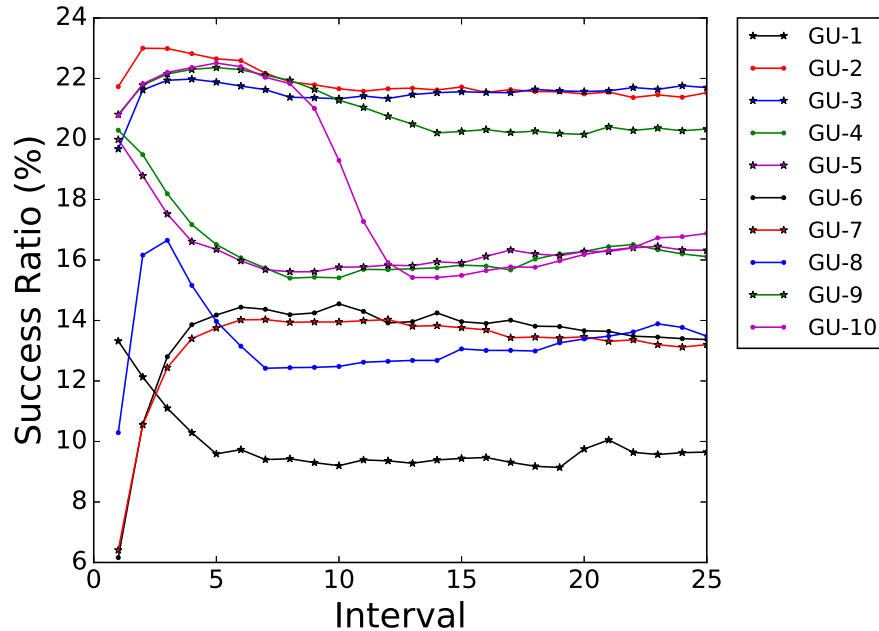


Figure 6.7: Burst Success Ratio for FSAC PCs over time at a load of 90.

mance trend line that steadily decrease in performance that is ultimately lower at completion of the simulation than at the start. Pheromone calculations 2 and 8 do however differ from the aforementioned pheromone calculations in that they each display a small initial performance spike.

Figure 6.7 is an illustration of the pheromone calculation variation adapting to a load of 90 placed on the network. At the maximum tested load of 90 placed on the network, the pheromone calculation trend lines appear to display the same trends as previously seen at the medium load, but do however have larger and more accentuated curves than previously seen. Pheromone calculation 10 has a more drastic decrease in performance, whereas pheromone calculation 8 has a larger initial performance spike which drops off just as rapidly. Pheromone calculations 4 and 5 exhibit identical performance trend lines as previously seen with the exception of a larger decrease in performance. The classic performance trend line as seen in the Fixed Grid scenario are displayed with pheromone calculations 6 and 7.

### 6.3.1.3 Overall Performance of Pheromone Calculations

The performance of the pheromone calculations under the specific loads over the duration of the simulations as seen in Figures 6.5, 6.6 and 6.7 are in line with that of the overall performances of the pheromone calculations displayed in Figure 6.5. In the small network topology, pheromone calculation 1 performed poorly in comparison to all the other pheromone calculations illustrated in Figure 6.5. Inspection of Table 6.1 illustrates which pheromone calculations had the most number of significant results and overall average performances. Pheromone calculation 4 performed well with a large number of significant results, namely 16 out of 45 and an overall average performance of 41.89%. However, pheromone calculation 2 had a lower number of significant results, 11 out of 45 but had a higher overall average performance of 42.88%. This is in line with what was seen in Figures 6.5, 6.6 and 6.7. Pheromone calculation 9 has the most number of significant results, 17 out of 45 and the second highest overall average performance of 42.71%.

## 6.3.2 Comparison Against Existing Algorithms

This section details the results gathered for the FSAC, UCBRWA, ACRWA and SPR algorithms. The algorithms are compared against one another in terms of the gathered results.

### 6.3.2.1 Relative Performance Comparison

Figure 6.8 illustrates a comparison of the success ratio performances of FSAC and UCBRWA with ACRWA and SPR as a function of the various loads placed on the small network topology. There is a clear differentiation between ACRWA and the other algorithms which display similarly shaped performance trend lines to one another for all the loads tested on the small network topology. ACRWA displays a lower decrease in performance with respect to an increase in the tested load as compared to the other algorithms. UCBRWA has a higher performance than ACRWA

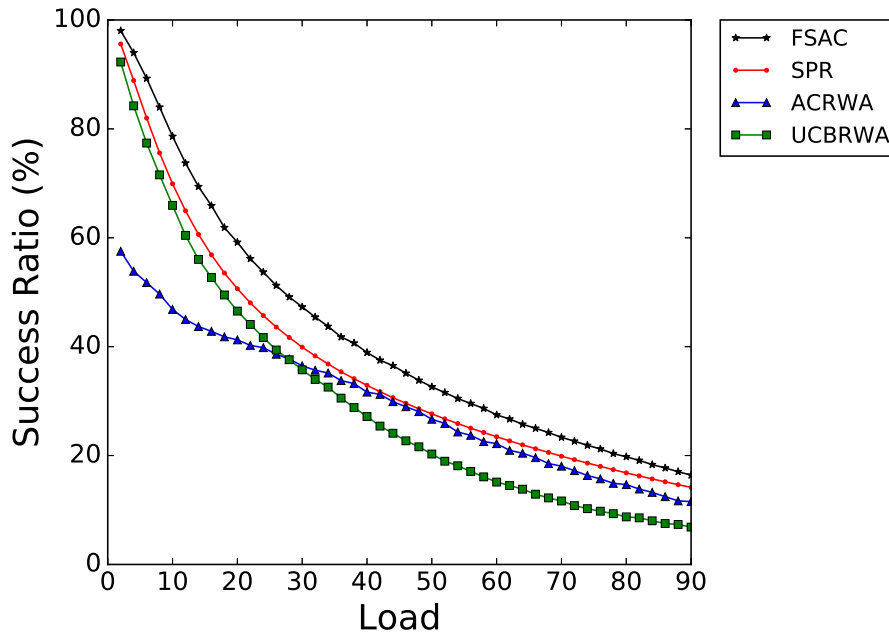


Figure 6.8: Burst Success Ratio on the small network topology.

until approximately a load of 25 is placed on the network. ACRWA levels out of the decrease under the loads of approximately 10 to 40 placed on the network where ACRWA displays very similar performance to SPR from a load of approximately 35 for the remainder of all the tested loads. FSAC remains the highest performing algorithm with SPR nearing a similar performance under the highest tested loads placed on the network.

### 6.3.2.2 Timewise Performance Comparison

Figures 6.9, 6.10 and 6.11 are illustrations of all the tested algorithms adapting to a specific network load over the duration of a simulation. Figure 6.9 is an illustration of all the tested algorithms adapting to a load of 30 placed on the network. Under this low load, all the tested algorithms present distinctive performance trend line patterns over the duration of the simulation. ACRWA displays an initial increase in performance which stabilizes into a gradual decline for the remainder of the

Table 6.2: Success ratio and 95% confidence interval at a specific load on the small network topology.

Load	FSAC	SPR	ACRWA	UCBRWA
10	<b>78.62 ± 0.34</b>	69.91 ± 0.03	46.84 ± 0.55	65.95 ± 0.13
20	<b>59.17 ± 0.40</b>	50.64 ± 0.02	41.25 ± 0.33	46.53 ± 0.12
30	<b>47.30 ± 0.32</b>	39.91 ± 0.03	36.48 ± 0.56	35.75 ± 0.26
40	<b>38.93 ± 0.33</b>	32.90 ± 0.03	31.65 ± 0.58	27.17 ± 0.31
50	<b>32.62 ± 0.24</b>	27.66 ± 0.03	26.67 ± 0.56	20.28 ± 0.29
60	<b>27.47 ± 0.30</b>	23.45 ± 0.02	22.19 ± 0.67	15.13 ± 0.25
70	<b>23.35 ± 0.19</b>	19.88 ± 0.02	18.05 ± 0.59	11.66 ± 0.25
80	<b>19.78 ± 0.16</b>	16.82 ± 0.01	14.67 ± 0.62	8.74 ± 0.23
90	<b>16.40 ± 0.19</b>	14.16 ± 0.02	11.54 ± 0.40	6.86 ± 0.20

Table 6.3: Overall Algorithm performance on the small network topology.

Algorithm	Number of Statistically Significant Results	Overall Average Performance
FSAC	45	41.89
SPR	0	36.47
ACRWA	0	29.76
UCBRWA	0	30.22

simulation period. SPR has a remarkably flat and stable performance trend line for the duration of the simulation. UCBRWA has an initial performance spike which decreases in steps until halfway through the simulation period where it remains in an increase and decrease oscillation for the remainder of the simulation period. The FSAC algorithm illustrates a performance trend line which has a small initial performances spike which tapers into a stable increase for the remainder of the simulation period.

Figure 6.10 is an illustration of all the tested algorithms adapting to a load of 60 placed on the network. Under this medium load, all the tested algorithms present performance trend line patterns which are different to those seen previously at the lower tested load placed on the network with the exception of SPR. SPR as previously seen displays a flat and stable performance for the entire simulation period. FSAC has a distinctive performance trend line which decreases under the

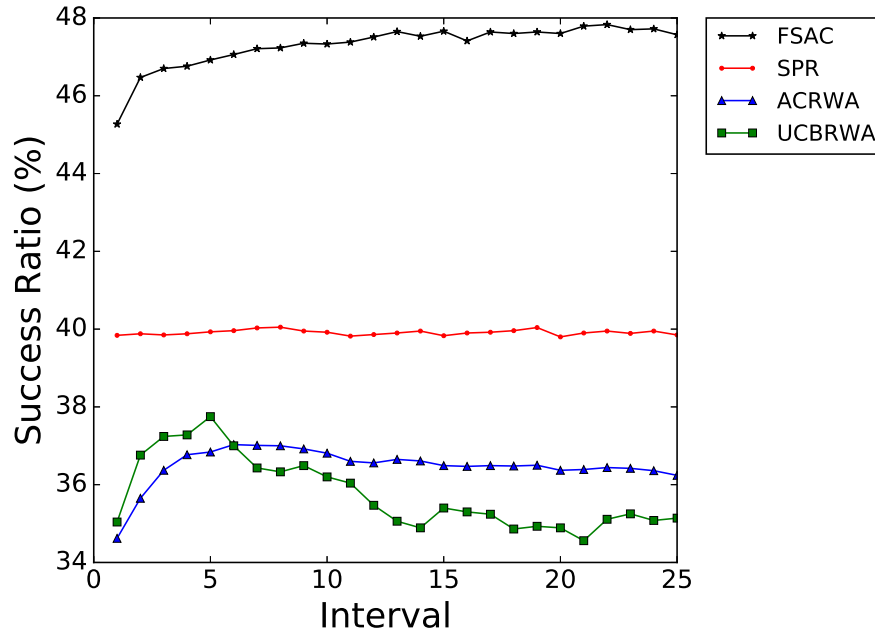


Figure 6.9: Burst Success Ratio over time at a load of 30.

increased load but stabilizes halfway through the simulation and increase slightly for the remainder of the simulation period. UCBRWA has a performance trend line which steadily decreases at a marginal rate over the duration of the simulation period. ACRWA displays a unique performance trend line which initially increases, then decreases and stabilizes halfway through the simulation and remains constant for the remainder of the simulation period.

Figure 6.11 is an illustration of all the tested algorithms adapting to a load of 90 placed on the network. Under this high load, all the tested algorithms present performance trend line patterns which are no longer increasing in performance over the duration of the simulation period but are rather decreasing and the stabilizing with the exception of SPR and UCBRWA. SPR as previously seen at the lower tested loads placed on the network remains steady and constant in performance. FSAC starts the simulation with a high performance which decreases substantially initially, thereafter, FSAC stabilises and increases slightly by the completion of the simulation period. ACRWA has a performance trend line which resembles a squashed



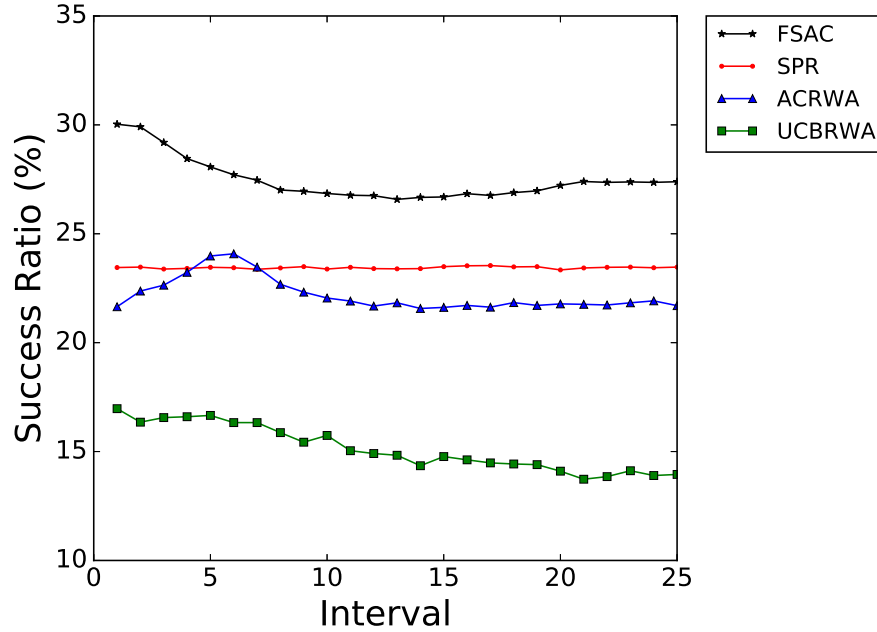


Figure 6.10: Burst Success Ratio over time at a load of 60.

version of that previously seen at the lower tested loads. ACRWA decreases slightly over the first third of the simulation period and thereafter remains stable for the remainder of the simulation. UCBRWA displays a performance trend line which decreases steadily over the duration of the simulation period.

### 6.3.2.3 Overall Performance Analysis

The mean success ratios over 30 repeats of each of the algorithms are reported along with the 95% confidence interval in Table 6.2. The outcomes of Mann-Whitney U tests comparing the algorithms against one another are included with results that are statistically significantly better printed in bold. At a load of 20, FSAC is approximately 8.53% more successful than SPR, 12.64% more successful than UCBRWA and 17.92% more successful than ACRWA. At a load of 40, FSAC is approximately 6.03% more successful than SPR, 7.28% more successful than ACRWA and 11.76% more successful than UCBRWA. At a load of 60, FSAC is approximately 4.02%

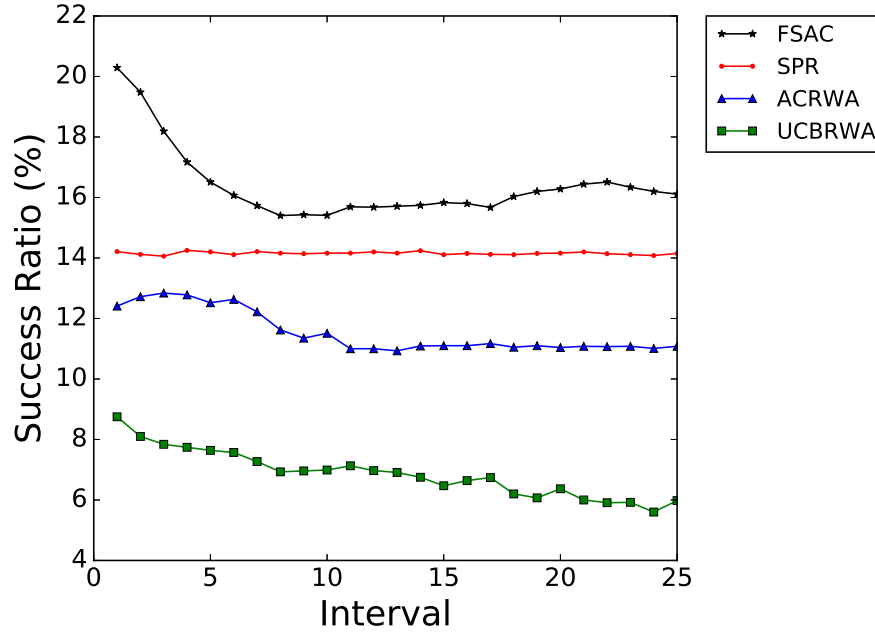


Figure 6.11: Burst Success Ratio over time at a load of 90.

more successful than SPR, 5.28% more successful than ACRWA and 12.34% more successful than UCBRWA. At a load of 80, FSAC is approximately 2.96% more successful than SPR, 5.11% more successful than ACRWA and 11.04% more successful than UCBRWA. Under all the tested loads placed on the small network topology, the FSAC algorithm performed significantly better than the other tested algorithms. The FSAC algorithm demonstrated the most significant results for all of the tested loads according to the Mann-Whitney U tests performed on all of the algorithms as seen in Table 6.3. Furthermore, in 6.3 the overall average performances can be seen. The FSAC algorithm had an overall average performance of 41.89%. Therefore, on average the FSAC algorithm performed approximately 5.42% higher than SPR, 11.67% higher than UCBRWA and 12.13% higher than ACRWA on this network topology.

## 6.4 Medium Topology Results

The results of the experiments described in the Section 6.2 are now presented. The experiments were conducted in simulation on the medium network topology in Figure 6.2. The FSAC algorithm is represented by pheromone calculation 4 in the sections that follow for the medium network topology.

### 6.4.1 Comparison of FSAC Pheromone Calculations

This section details the results gathered for all of the FSAC pheromone calculations and compares the equations against one another.

#### 6.4.1.1 Relative Performance of Pheromone Calculations

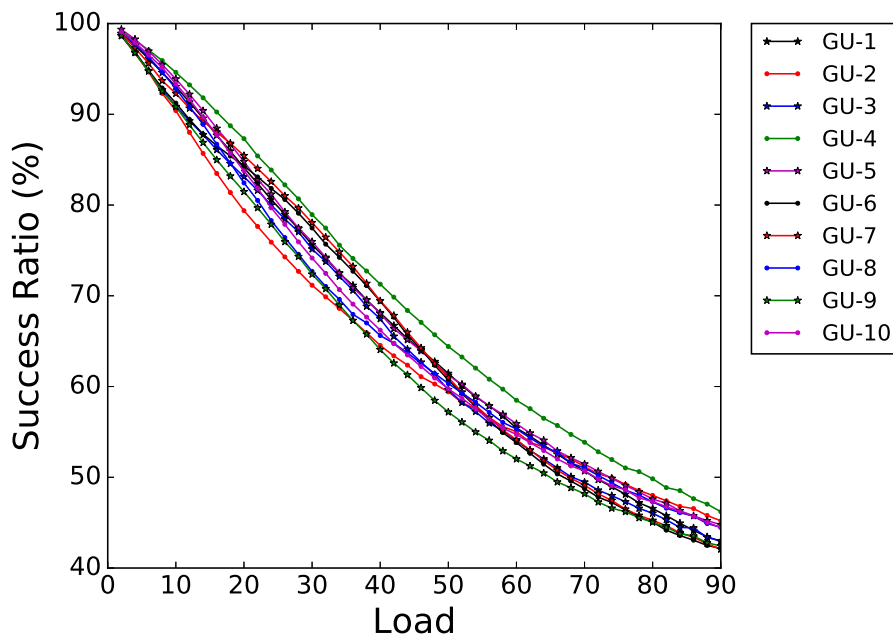


Figure 6.12: Burst Success Ratio for FSAC PCs on the medium network topology.

Figure 6.12 is an illustration of the performance of each of the pheromone calculations for the various loads placed on the medium network. In Figure 6.12 the

Table 6.4: Overall performance of the FSAC PCs on the medium network topology.

Pheromone Calculation	Number of Statistically Significant Results	Overall Average Performance
GU-1	0	66.74
GU-2	0	65.09
GU-3	0	65.69
GU-4	43	69.58
GU-5	2	67.28
GU-6	0	66.14
GU-7	0	66.62
GU-8	0	66.02
GU-9	0	64.03
GU-10	0	66.26

pheromone calculations all remain bundled together up to when a load of 15 is placed on the network, thereafter the pheromone calculations diverge. The pheromone calculations remain spread out until when a load of approximately 50 is placed on the network, where upon the pheromone calculations converge together and remain relatively tightly bundled for the remainder of the simulated loads. From visual inspection, it is clear that from a load of 10 placed on the network pheromone calculation 4 performs better than the rest of the pheromone calculations with an overall average performance that is 2.3% higher than the next best pheromone calculation. Comparing pheromone calculation 4 with 9, pheromone calculation 4 performed the best and pheromone calculation 9 performed the worst. When a load of 30 is placed on the network, the performance difference is 6.56%. Whereas under a load of 60 placed on the network the difference in performance is 6.48%. At the highest load of 90 placed on the network the difference in performance is 3.78%.

#### 6.4.1.2 Timewise Performance of Pheromone Calculations

Figures 6.13, 6.14 and 6.15 are illustrations of the FSAC algorithms pheromone calculation variations adapting to a specific network load over the duration of a simulation. Figure 6.13 is an illustration of the pheromone calculation variation adapting to a load of 30 placed on the network. The pheromone calculation per-

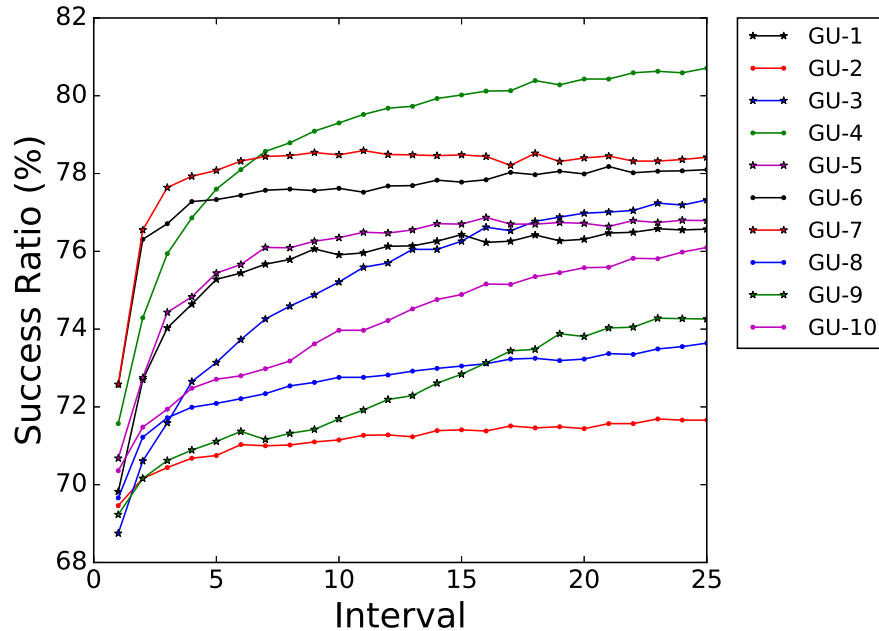


Figure 6.13: Burst Success Ratio for FSAC PCs over time at a load of 30.

formance trend lines in Figure 6.13 are much smoother than those illustrated for the small network topology. All the pheromone calculation performance trend lines demonstrate an overall performance increase at the end of the simulation as compared to that at the start of the simulation. Pheromone calculation 9 and 10 display very similar performance trend lines that steadily increase in performance throughout the simulation period with no initial performance spike. Pheromone calculation 2 and 8 have fairly flat performance trend lines, with pheromone calculation 8 having a slightly more pronounced initial performance spike. Pheromone calculations 1, 5, 6 and 7 display the classic trend line with the initial performance spike which stabilizes for the remainder of the simulation period. Pheromone calculations 3 and 4 demonstrate very similar trend lines, with pheromone calculation 4 displaying a more pronounced increase in performance to finish with the highest performance.

Figure 6.14 is an illustration of the pheromone calculation variation adapting to a load of 60 placed on the network. Under the medium load placed on the network, the performance trend lines of the pheromone calculations are somewhat different to

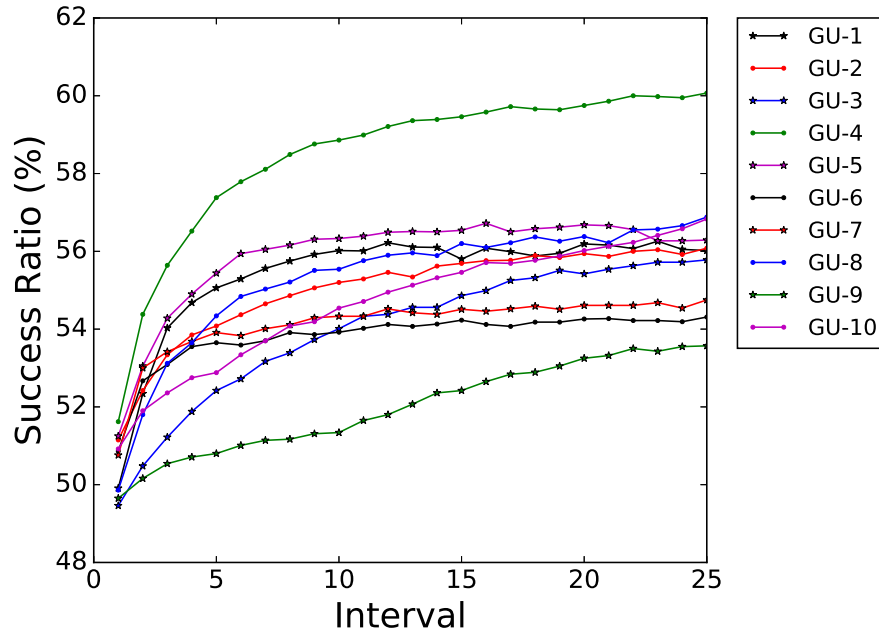


Figure 6.14: Burst Success Ratio for FSAC PCs over time at a load of 60.

the low loads previously displayed on the network with their performance trend lines more closely distributed. The pheromone calculations display a much gentler initial performance spike than what was seen previously with all the pheromone calculations displaying similar trend line shapes. All the pheromone calculations increased in performance from the start of the simulation to the end period. Pheromone calculation 4 distinguishes itself from the rest of the pheromone calculations performing much better and mimicking its previous performance curve.

Figure 6.15 is an illustration of the pheromone calculation variation adapting to a load of 90 placed on the network. When the maximum tested load of 90 is placed on the network, the pheromone calculation trend lines appear to be very similar to those seen at the medium load, but do however appear to be less smooth with more variation in performances. Pheromone calculation 2 increased in performance compared to that on the medium load where it attains the second highest success ratio over the simulation period. The performance trend line of pheromone calculation 10 displayed a steady increase in performance for the entire simulation period.

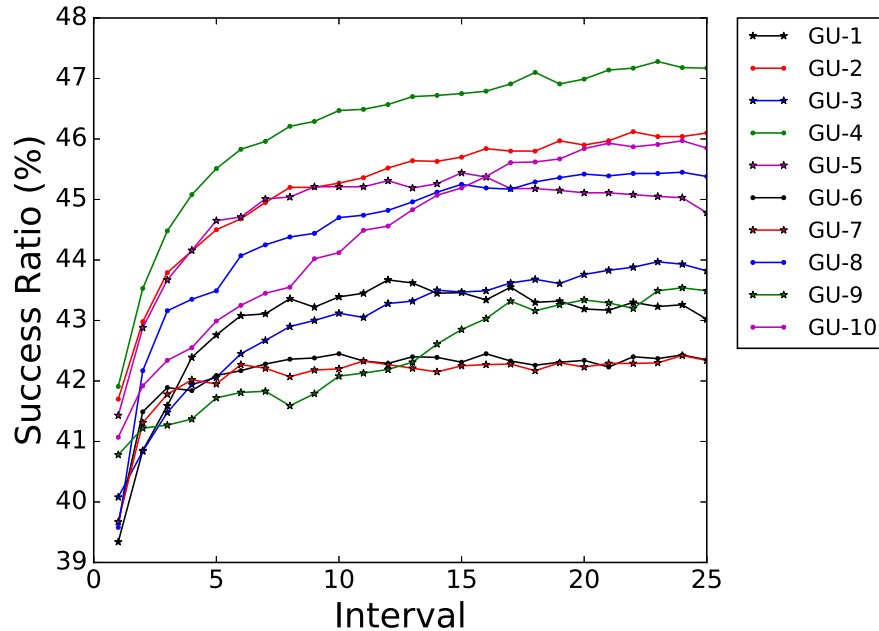


Figure 6.15: Burst Success Ratio for FSAC PCs over time at a load of 90.

### 6.4.1.3 Overall Performance of Pheromone Calculations

The performance of the pheromone calculations under the specific loads over the duration of the simulations as seen in Figures 6.13, 6.14 and 6.15 are in line with that of the overall performances of the pheromone calculations displayed in Figure 6.12. In the small network topology, pheromone calculation 9 performed poorly in comparison to all the other pheromone calculations illustrated in Figure 6.12 with an overall average performance of 64.03%. Inspection of Table 6.4 illustrates which pheromone calculations had the most number of significant results and overall average performances. Pheromone calculation 4 performed the best with most number of significant results, 43 out of 45 and an overall average performance of 69.58%. The next best was pheromone calculation 5 with the second most number of significant results, 2 out of 45 and an overall average performance of 67.28%. This is in line with what was seen in Figures 6.13, 6.14 and 6.15 where pheromone calculation 4 consistently performed the best.

## 6.4.2 Comparison Against Existing Algorithms

This section details the results gathered for the FSAC, UCBRWA, ACRWA and SPR algorithms. The algorithms are compared against one another in terms of the gathered results.

### 6.4.2.1 Relative Performance Comparison

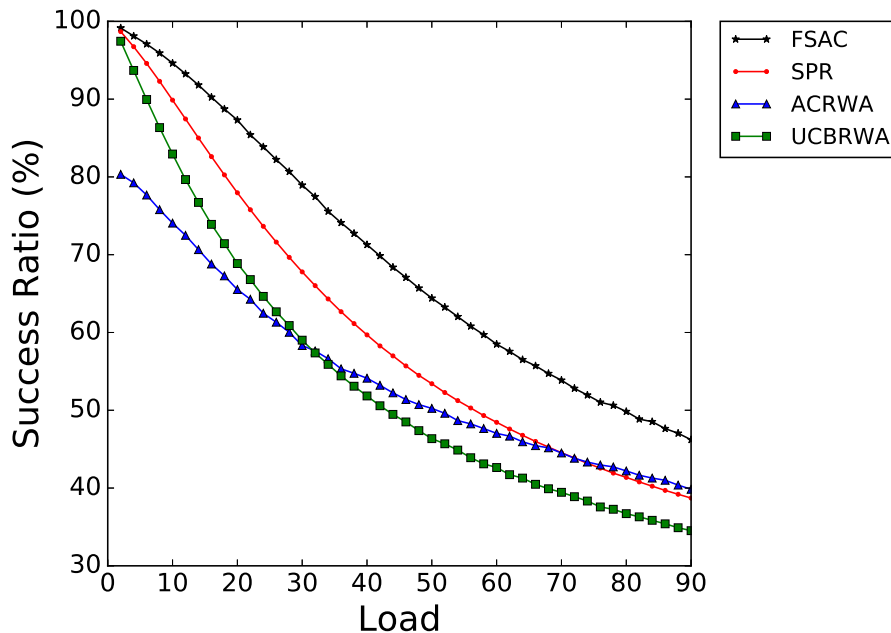


Figure 6.16: Burst Success Ratio on the medium network topology.

Figure 6.16 illustrates a comparison of the success ratio performances of FSAC and UCBRWA with ACRWA and SPR as a function of the various loads placed on the small network topology. The success ratio performances on the medium network topology are noticeably higher than that obtained on the small network topology. This is as a result of the medium network topology having more links and as a result more bandwidth with which to transmit bursts within the network. The FSAC algorithm performs the best out of all the tested algorithms under all the tested loads placed on the network. FSAC, SPR and UCBRWA illustrate similarly



Table 6.5: Success ratio and 95% confidence interval at a specific load on the medium network topology.

Load	FSAC	SPR	ACRWA	UCBRWA
10	<b>94.62 ± 0.07</b>	89.87 ± 0.02	74.06 ± 0.25	82.94 ± 0.07
20	<b>87.31 ± 0.12</b>	77.96 ± 0.03	65.52 ± 0.34	68.86 ± 0.11
30	<b>78.94 ± 0.21</b>	67.79 ± 0.03	58.32 ± 0.33	59.01 ± 0.12
40	<b>71.28 ± 0.20</b>	59.69 ± 0.03	54.12 ± 0.37	51.84 ± 0.14
50	<b>64.41 ± 0.15</b>	53.41 ± 0.02	50.24 ± 0.43	46.35 ± 0.12
60	<b>58.49 ± 0.20</b>	48.45 ± 0.03	47.03 ± 0.36	42.64 ± 0.19
70	<b>53.86 ± 0.18</b>	44.54 ± 0.03	44.51 ± 0.22	39.45 ± 0.16
80	<b>49.83 ± 0.20</b>	41.37 ± 0.02	42.20 ± 0.29	36.71 ± 0.17
90	<b>46.21 ± 0.18</b>	38.71 ± 0.03	39.84 ± 0.35	34.52 ± 0.19

Table 6.6: Overall Algorithm performance on the medium network topology.

Algorithm	Number of Statistically Significant Results	Overall Average Performance
FSAC	45	69.58
SPR	0	60.67
ACRWA	0	54.73
UCBRWA	0	54.19

shaped performance trend lines for all the tested loads placed on the network. FSAC, SPR and UCBRWA initially perform similarly under the lowest tested load and soon diverge thereafter. While UCBRWA has a higher performance than that of ACRWA up until a load of approximately 30 is placed on the network, thereafter, ACRWA has a higher performance for the remainder of the simulation period. Until a load of approximately 70 is placed on the network, SPR has a higher performance than that of ACRWA. Thereafter, ACRWA performs marginally better than SPR for the remainder of the tested loads placed on the network.

#### 6.4.2.2 Timewise Performance Comparison

Figures 6.17, 6.18 and 6.19 are illustrations of all the tested algorithms adapting to a specific network load over the duration of a simulation. Figure 6.17 is an illustration of all the tested algorithms adapting to a load of 30 placed on the network.

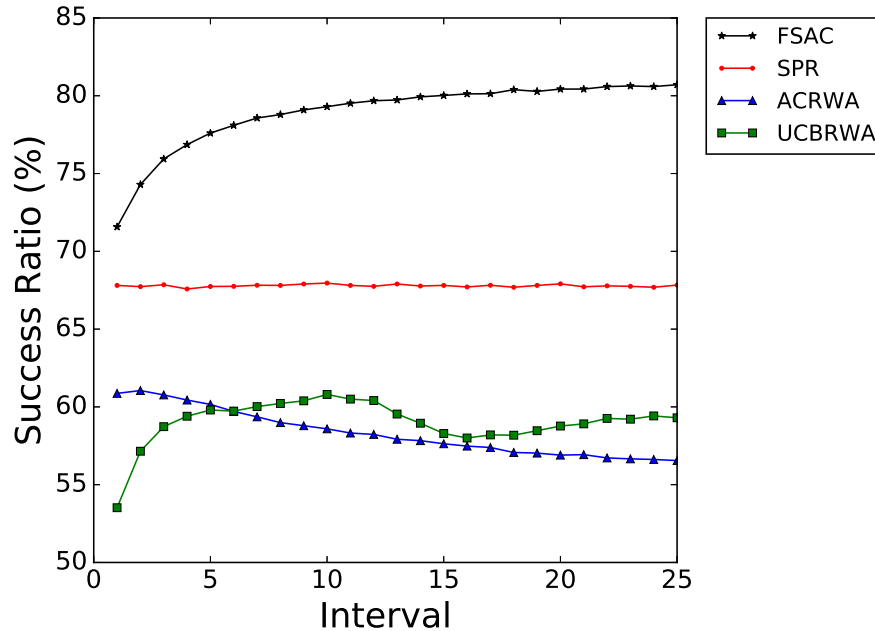


Figure 6.17: Burst Success Ratio over time at a load of 30.

Under this low load, all the tested algorithms present distinctive performance trend line patterns over the duration of the simulation. SPR displays a performance trend line that is steady and stable for the duration of the simulation period. ACRWA illustrates a steady decline in performance for the duration of the simulation period, finishing with a lower success ratio performance than achieved at the start of the simulation. UCBRWA has a unique performance trend line which initially increases in performance until approximately halfway through the simulation. Thereafter, UCBRWA decreases marginally and regains the lost performance with a slight performance increase for the remainder of the simulation period. FSAC demonstrates a performance trend line which has a smooth and steady increase in performance for the duration of the simulation period.

Figure 6.18 is an illustration of all the tested algorithms adapting to a load of 60 placed on the network. Under this medium load, all the tested algorithms present performance trend line patterns which are identical to those previously seen in Figure 6.17 for FSAC and SPR. UCBRWA demonstrated a similar performance trend

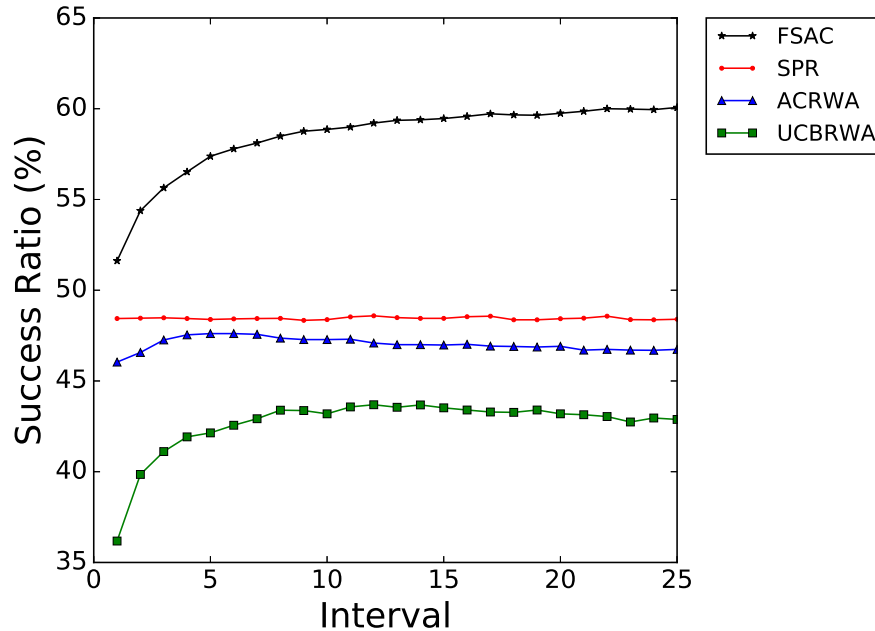


Figure 6.18: Burst Success Ratio over time at a load of 60.

line to that seen previously in Figure 6.17, however, UCBRWA has a performance trend line which is smoother and remains stable for the duration of the simulation period. SPR has a steady and stable performance trend line for the duration of the simulation. FSAC once again illustrates a performance trend line which has a significant initial increase in performance that stabilizes with a slight increase for the remainder of the simulation period. ACRWA has a performance trend line which differs to that previously seen at the lower tested load on the network, where it displays a slight initial increase that stabilizes and remains constant for the remainder of the simulation.

Figure 6.19 is an illustration of all the tested algorithms adapting to a load of 90 placed on the network. Under this high load, all the tested algorithms present performance trend line patterns which are almost identical to those seen in Figure 6.18. The tested algorithms display only minor differences in performance trend lines to the those previously seen at the lower tested loads placed on the network. The FSAC performance trend line displays an initial increase which is not as large as

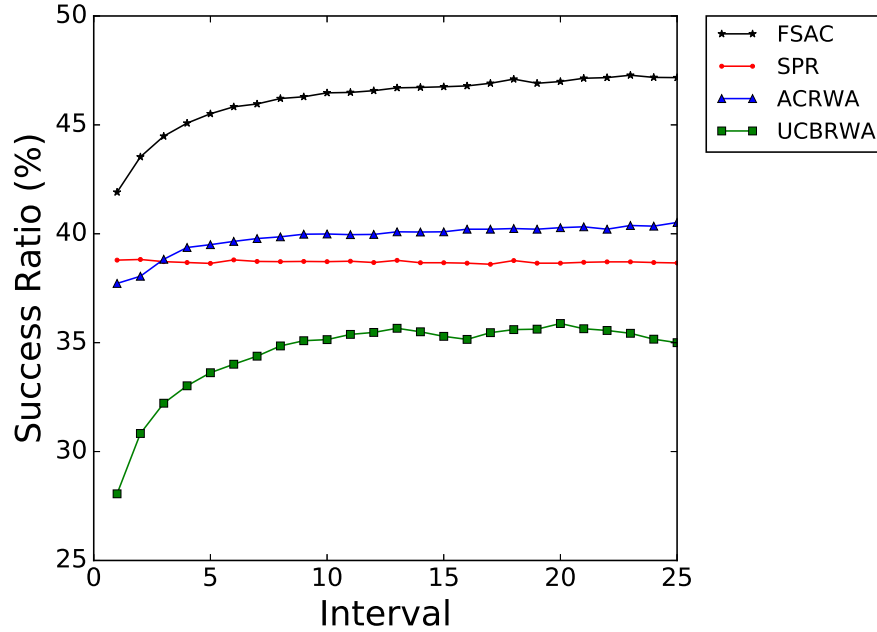


Figure 6.19: Burst Success Ratio over time at a load of 90.

previously seen at the lower tested loads. It stabilizes and remains constant for the remainder of the simulation. SPR displays a steady and stable performance trend line for the simulation, while ACRWA has a slight initial increase in performance that stabilizes and remains constant for the remainder of the simulation period. UCBRWA has the most notable initial increase in performance, much larger than the other tested algorithms and begins to stabilize approximately halfway through the simulation period remaining consistent thereafter.

#### 6.4.2.3 Overall Performance Analysis

The mean success ratios over 30 repeats of each of the algorithms are reported along with the 95% confidence interval in Table 6.5. The outcomes of Mann-Whitney U tests comparing the algorithms against one another are included with results that are statistically significantly better printed in bold. At a load of 20, FSAC is approximately 9.35% more successful than SPR, 18.45% more successful than UCBRWA

and 21.79% more successful than ACRWA. At a load of 40, FSAC is approximately 11.59% more successful than SPR, 17.16% more successful than ACRWA and 19.44% more successful than UCBRWA. At a load of 60, FSAC is approximately 10.04% more successful than SPR, 11.46% more successful than ACRWA and 15.85% more successful than UCBRWA. At a load of 80, FSAC is approximately 7.63% more successful than ACRWA, 8.46% more successful than SPR and 13.12% more successful than UCBRWA. Under all the tested loads placed on the small network topology, the FSAC algorithm performed significantly better than the other tested algorithms. The FSAC algorithm demonstrated the most significant results for all of the tested loads according to the Mann-Whitney U tests performed on all of the algorithms as seen in Table 6.5. Furthermore, in Table 6.6 the overall average performances can be seen, indicating that the FSAC algorithm had an overall average performance of 69.58%. On average the FSAC algorithm performed approximately 8.91% higher than SPR, 14.85% higher than ACRWA and 15.39% higher than UCBRWA on this network topology.

## 6.5 Large Topology Results

The results of the experiments described in the Section 6.2 are now presented. The experiments were conducted in simulation on the large network topology in Figure 6.3. The FSAC algorithm is represented by pheromone calculation 4 in the sections that follow for the large network topology.

### 6.5.1 Comparison of FSAC Pheromone Calculations

This section details the results gathered for all of the FSAC pheromone calculations and compares the equations against one another.

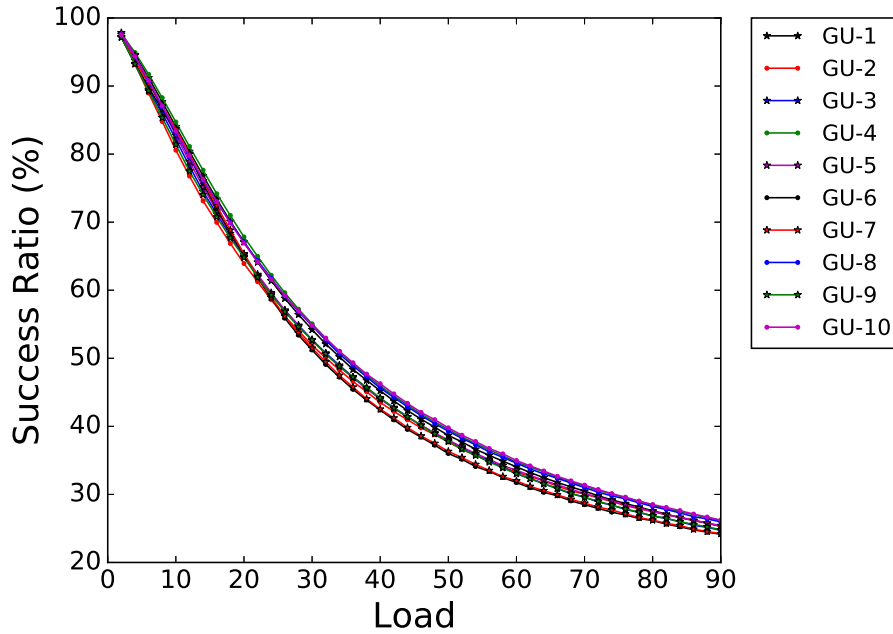


Figure 6.20: Burst Success Ratio for FSAC PCs on the large network topology.

### 6.5.1.1 Relative Performance of Pheromone Calculations

Figure 6.20 displays the performance for each of the pheromone calculations for the various loads placed on the large network. The pheromone calculations performance trend lines are all tightly bundled together for all the tested loads placed on the network. They all share identically shaped trend lines for the large network. Interestingly, pheromone calculations 1, 4, 8 and 10 remain the best performing pheromone calculations for all the tested loads placed on the network. For the first third of the tested loads placed on the network, pheromone calculation 4 is the most significant. Thereafter, pheromone calculation 10 is the most significant performer for the remainder of the simulated loads placed on the network. Comparing pheromone calculation 6 with 10, pheromone calculation 10 performed the best on the network while pheromone calculation 6 was the worst performing. At a load of 30 placed on the network the performance difference is 3.62%, whereas under a load of 60 the difference in performance is 3.24%. At the highest load of 90 placed on

Table 6.7: Overall performance of the FSAC PCs on the large network topology.

Pheromone Calculation	Number of Statistically Significant Results	Overall Average Performance
GU-1	0	48.41
GU-2	0	46.98
GU-3	0	47.22
GU-4	15	49.17
GU-5	1	47.60
GU-6	0	46.38
GU-7	0	46.62
GU-8	0	48.73
GU-9	0	47.12
GU-10	29	49.01

the network the difference in performance is 2.09%.

### 6.5.1.2 Timewise Performance of Pheromone Calculations

Figures 6.21, 6.22 and 6.23 are illustrations of the pheromone calculation variations for the FSAC algorithm adapting to a specific network load over the duration of a simulation. Figure 6.21 is an illustration of the pheromone calculation variation adapting to a load of 30. Under this low load placed on the network, pheromone calculations 1, 4, 8, and 10 display the classical performance success ratio trend line previously seen. These pheromone calculations have the initial performance spike and stabilize into a gentle increase in performance for the duration of the simulation period. Pheromone calculation 2 and 5 differ from the rest of the pheromone calculations in that they stabilize into a flat performance success ratio and do not seem to increase over the simulation period. Pheromone calculation 3, 6, 7 and 9 share similar performance trend lines shapes. These pheromone calculations have a gentle initial spike in performance which stabilizes into a gentle increase in performance for the remainder of the simulation period.

Figure 6.22 is an illustration of the pheromone calculation variation adapting to a load of 60 placed on the network. Under this medium load, the performance trend lines of the pheromone calculations share a similar shape to when compared to those

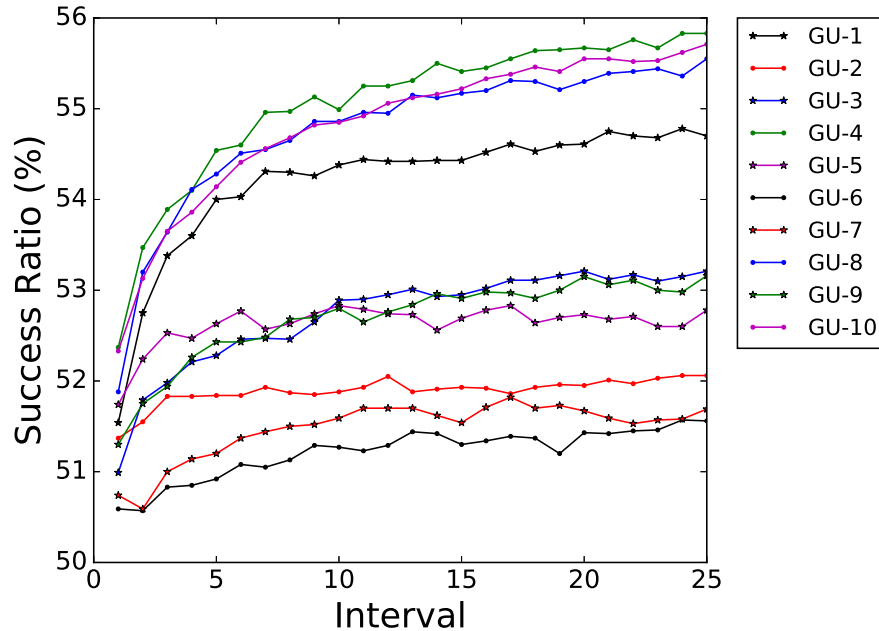


Figure 6.21: Burst Success Ratio for FSAC PCs over time at a load of 30.

on the low load with three exceptions. Pheromone calculation 10 now has a better performance than that of pheromone calculation 4, which is a direct contrast to what was seen at the low load. Pheromone calculation 2 and 5 have also improved in performance but still have the same performance trend line shape as seen at the low load. All of the pheromone calculations seem to have increase in performance at a much lower rate at the medium load than what was seen at the low load placed on the network.

Figure 6.23 is an illustration of the pheromone calculation variation adapting to a load of 90 placed on the network. At the maximum tested load of 90, the pheromone calculation trend lines appear to have bundled into 4 groups with identical trend line shapes. The worst performing group comprises of pheromone calculation 6 and 7 which have a slight performance increase until halfway where they stabilize for the remainder the simulation period. The second worst performing group is comprised of pheromone calculation 3 and 9 which have trend lines similarly shaped to those of pheromone calculation 6 and 7. Pheromone calculation 1, 2 and 5 make up



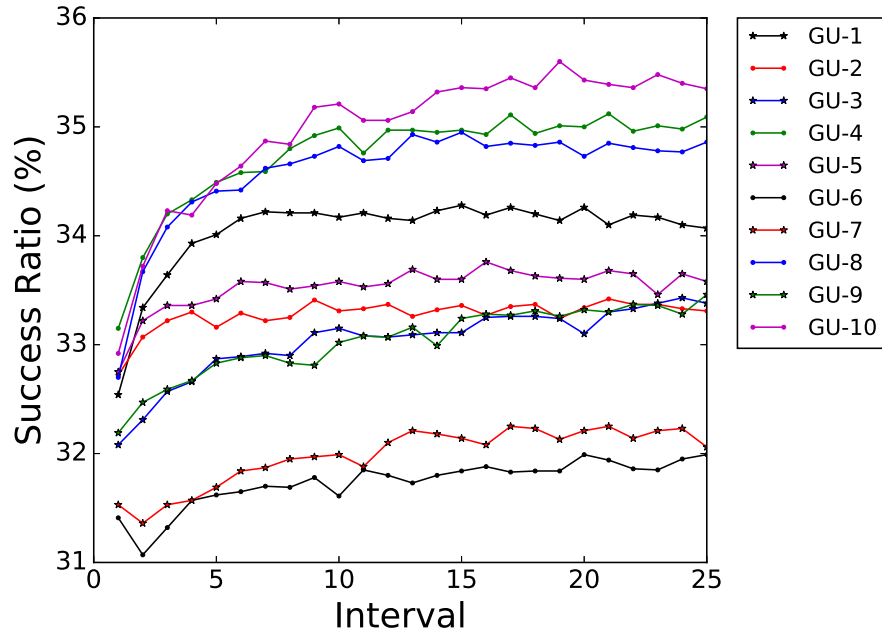


Figure 6.22: Burst Success Ratio for FSAC PCs over time at a load of 60.

the second best performing group of pheromone calculations which share a similar performance trend line. The best performing pheromone calculations are 4, 8 and 10 as previously seen at the medium and low load placed on the network. These updates displayed the same performance trend lines at the low, medium and high loads placed on the network.

### 6.5.1.3 Overall Performance of Pheromone Calculations

The performance of the pheromone calculations under specific loads over the duration of the simulations as seen in Figures 6.21, 6.22 and 6.23 are in line with that of the overall performances of the pheromone calculations illustrated in Figure 6.20. In the large network topology, pheromone calculations 2, 6 and 7 performed the worst compared to the other pheromone calculations illustrated in Figure 6.20. Table 6.7 illustrates that pheromone calculations 2, 6 and 7 performed the worst as they had the lowest overall average performances compared to the other pheromone

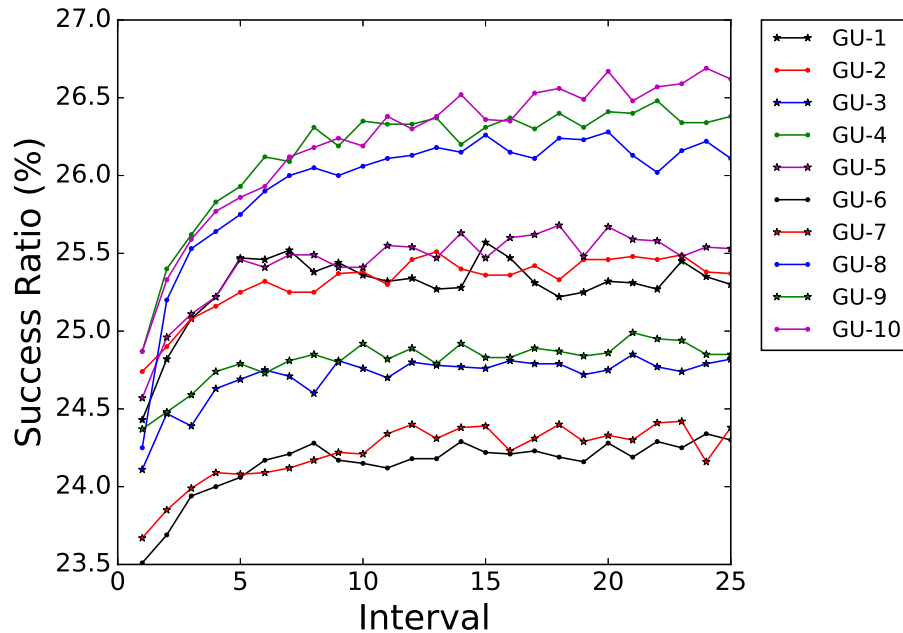


Figure 6.23: Burst Success Ratio for FSAC PCs over time at a load of 90.

calculations. Pheromone calculation 10 has the most number of significant results, namely 29 out of 45 and the second highest overall average performance of 49.01%. Pheromone calculation 4 has the second highest number of significant results, 15 out of 45 with the highest overall average performance of 49.17%. Pheromone calculation 4 and 10 both performed similarly from inspection of Table 6.7 and Figure 6.20.

### 6.5.2 Comparison Against Existing Algorithms

This section details the results gathered for the FSAC, UCBRWA, ACRWA and SPR algorithms. The algorithms are compared against one another in terms of the gathered results.

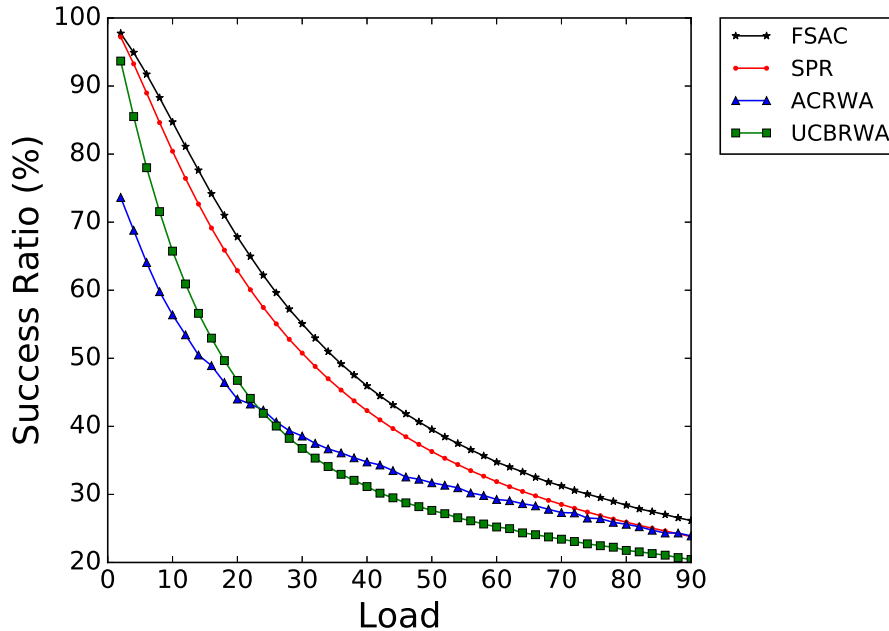


Figure 6.24: Burst Success Ratio on the large network topology.

### 6.5.2.1 Relative Performance Comparison

Figure 6.24 illustrates a comparison of the success ratio performances of FSAC and UCBRWA with ACRWA and SPR as a function of the various loads placed on the small network topology. Notably, the success ratio performances in the large network topology are lower than that of the medium network topology. This is due to that fact that the larger network has more nodes but is a less connected topology and as a result thereof has less available bandwidth with which to transmit bursts within the network. The FSAC algorithm is able to perform the best out of all the tested algorithms under all the tested loads placed on the network. SPR has a very similarly shaped performance trend line when compared to FSAC but has a lower performance for all the tested loads. UCBRWA initially has a higher performance than that of ACRWA up until when a load of approximately 25 is placed on the network, thereafter, ACRWA has a higher performance for the remainder of the simulation period. At the higher loads placed on the network, ACRWA nears

Table 6.8: Success ratio and 95% confidence interval at a specific load on the large network topology.

Load	FSAC	SPR	ACRWA	UCBRWA
10	<b>84.71 ± 0.06</b>	80.42 ± 0.02	56.38 ± 0.29	65.74 ± 0.10
20	<b>67.83 ± 0.05</b>	62.88 ± 0.03	44.01 ± 0.55	46.75 ± 0.07
30	<b>55.06 ± 0.07</b>	50.76 ± 0.03	38.57 ± 0.38	36.76 ± 0.13
40	<b>45.93 ± 0.09</b>	42.31 ± 0.03	34.77 ± 0.41	31.15 ± 0.11
50	<b>39.54 ± 0.09</b>	36.30 ± 0.02	31.71 ± 0.38	27.65 ± 0.09
60	<b>34.75 ± 0.09</b>	31.88 ± 0.02	29.26 ± 0.23	25.21 ± 0.13
70	<b>31.24 ± 0.07</b>	28.53 ± 0.02	27.33 ± 0.22	23.42 ± 0.07
80	<b>28.42 ± 0.07</b>	25.92 ± 0.02	25.61 ± 0.18	21.77 ± 0.10
90	<b>26.16 ± 0.10</b>	23.81 ± 0.02	23.90 ± 0.31	20.44 ± 0.08

Table 6.9: Overall Algorithm performance on the large network topology.

Algorithm	Number of Statistically Significant Results	Overall Average Performance
FSAC	45	49.17
SPR	0	45.82
ACRWA	0	36.94
UCBRWA	0	36.47

the performance of SPR. When a load of approximately 75 placed on the network, ACRWA illustrates an almost identical performance to that of SPR for the remainder of all the tested loads placed on the network.

### 6.5.2.2 Timewise Performance Comparison

Figures 6.25, 6.26 and 6.27 are illustrations of all the tested algorithms adapting to a specific network load over the duration of a simulation. Figure 6.25 is an illustration of all the tested algorithms adapting to a load of 30 placed on the network. Under this low load, all the tested algorithms present distinctive performance trend line patterns over the duration of the simulation. SPR illustrates a stable performance trend line for the duration of the simulation period. UCBRWA presents an interesting performance trend line which appears to be “snaking” or rather fluctuating over the duration of the simulation period. UCBRWA decreases slightly, stabilizing into

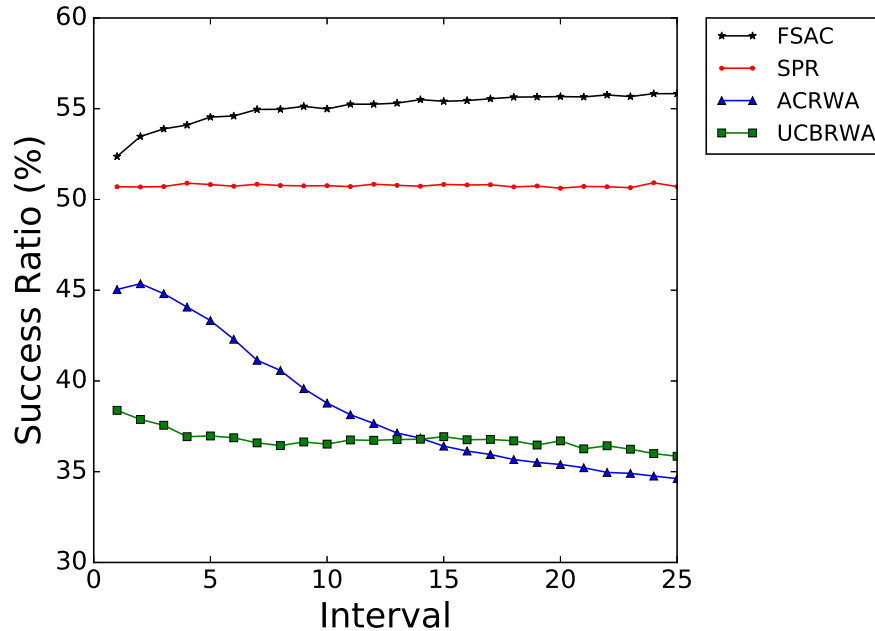


Figure 6.25: Burst Success Ratio over time at a load of 30.

an initial subtle increase which decreases towards the end of the simulation period. ACRWA displays a higher initial success ratio with its performance trend line which decreases significantly over the duration of the simulation period until its performance trend line is below that of UCBRWA where it stabilizes at the end of the simulation period. FSAC has a smooth performance trend line which is squashed when compared to those illustrated by the other tested network topologies. The FSAC performance trend line increases at a marginal rate over the duration of the simulation period.

Figure 6.26 is an illustration of all the tested algorithms adapting to a load of 60 placed on the network. Under this medium load, all the tested algorithms present performance trend line patterns somewhat different to those seen at the previously tested lower load. All of the performance trend lines are not as smooth as those previously seen at the lower tested load placed on the network. SPR provides a performance trend line that is stable for the duration of the simulation period with two minor fluctuations. ACRWA illustrates an initial increase in performance which

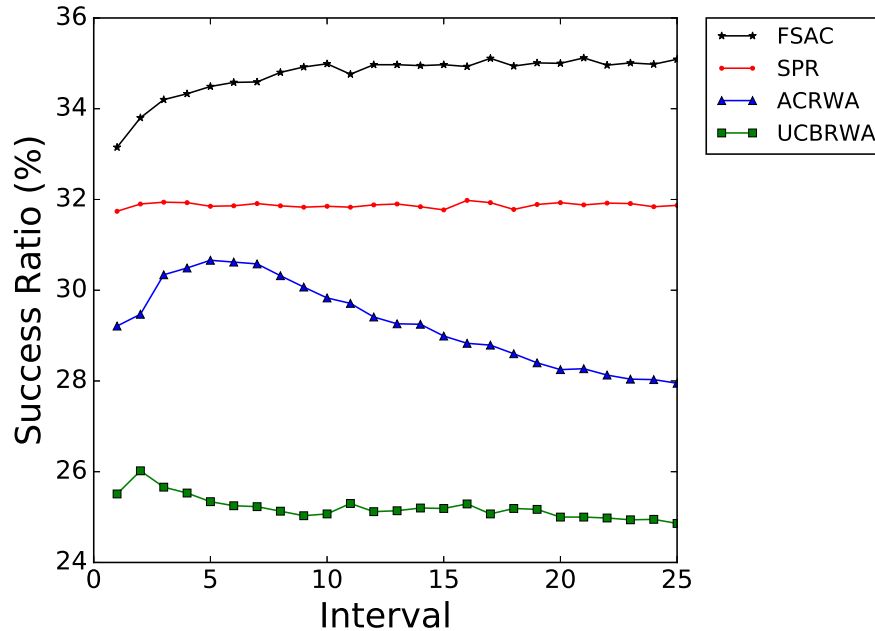


Figure 6.26: Burst Success Ratio over time at a load of 60.

quickly plateaus and stabilizes into a decrease for the remainder of the simulation period, ending with a success ratio lower than which it had initially started with. UCBRWA has a small initial performance increase that is short lived. Thereafter, UCBRWA slowly decreases in performance until approximately halfway through the simulation period where it almost stabilizes and fluctuates slightly. FSAC illustrates a performance trend line which is not as smooth and stable as previously seen at the lower tested load. The FSAC performance trend line has an initial increase, thereafter, FSAC stabilizes into a marginal increase for the remainder of the simulation period.

Figure 6.27 is an illustration of all the tested algorithms adapting to when a load of 90 is placed on the network. Under this high load, all the tested algorithms present performance trend line patterns which are different to those previously seen in Figures 6.25 and 6.26. The algorithms performance trend lines illustrated in Figure 6.24 end the simulation period with a success ratio higher than what was started, with the exception of SPR. All of the algorithms performance trend lines

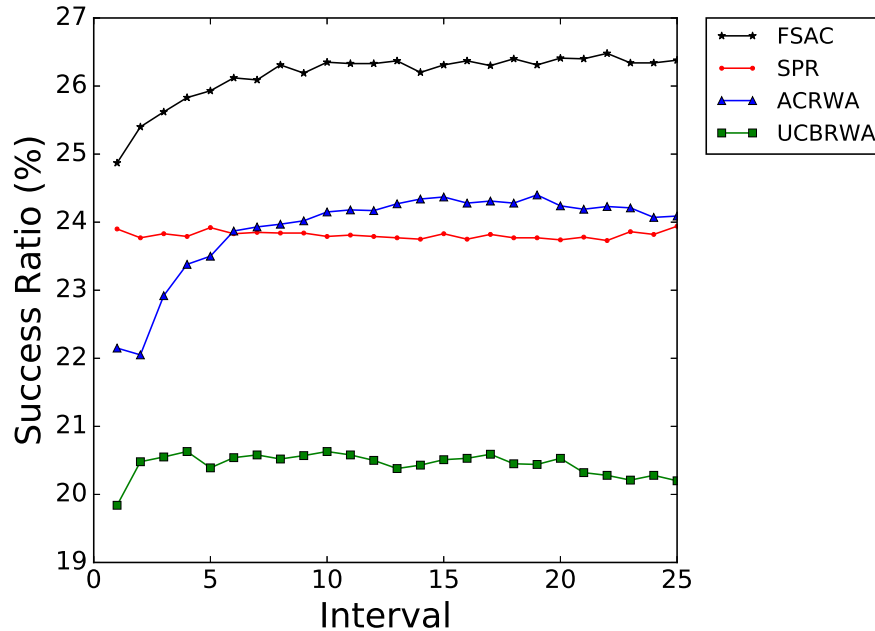


Figure 6.27: Burst Success Ratio over time at a load of 90.

are not as smooth as those previously seen and have minor fluctuations. SPR has a performance trend line which fluctuates somewhat, SPR decreases slightly over the first half of the simulation period and increase to the initial value it had over the second half. UCBRWA illustrates a small initial performance spike which stabilizes immediately, fluctuating marginally for the remainder of the simulation period. FSAC displays a performance trend line which is not as smooth as previously seen at the lower tested loads placed on the network in Figure 6.25 and 6.26. Whereas ACRWA has a performance trend line that has a large initial performance spike in the first third of the simulation period. ACRWA then stabilizes above SPR in performance in the second third of simulation period, decreasing slightly at the end of the simulation period to near SPR performance.

### 6.5.2.3 Overall Performance Analysis

The mean success ratios over 30 repeats of each of the algorithms are reported along with the 95% confidence interval in Table 6.8. The outcomes of Mann-Whitney U tests comparing the algorithms against one another are included with results that are statistically significantly better printed in bold. At a load of 20, FSAC is approximately 4.95% more successful than SPR, 21.08% more successful than UCBRWA and 23.82% more successful than ACRWA. At a load of 40, FSAC is approximately 3.62% more successful than SPR, 11.16% more successful than ACRWA and 14.78% more successful than UCBRWA. At a load of 60, FSAC is approximately 2.87% more successful than SPR, 5.49% more successful than ACRWA and 9.54% more successful than UCBRWA. At a load of 80, FSAC is approximately 2.50% more successful than SPR, 2.81% more successful than ACRWA and 6.65% more successful than UCBRWA. Under all the tested loads placed on the small network topology, the FSAC algorithm performed significantly better than the other tested algorithms. The FSAC algorithm demonstrated the most significant results for all of the tested loads according to the Mann-Whitney U tests performed on all of the algorithms as seen in Table 6.9. In Table 6.9 the overall average performances can be seen, with the FSAC algorithm having an overall average performance of 49.17%. Therefore, on average the FSAC algorithm performed approximately 3.35% higher than SPR, 12.23% higher than ACRWA and 12.70% higher than UCBRWA on this network topology.

## 6.6 Umbrella Analysis

The overall pheromone calculation performance on all the tested network topologies is displayed in Table 6.10, including the total number of statistically significant results obtained for each of the pheromone calculations gathered from the results given in Appendix B. Similarly, the overall algorithm performance on all the tested network topologies is provided in Table 6.11 which includes the total number of



Table 6.10: Overall Pheromone Calculation performance on all the tested network topologies.

Pheromone Calculation	Number of Statistically Significant Results	Overall Average Performance
GU-1	0	50.25
GU-2	11	51.65
GU-3	1	51.85
GU-4	74	53.55
GU-5	3	51.83
GU-6	0	50.50
GU-7	0	50.65
GU-8	0	51.39
GU-9	17	51.29
GU-10	29	52.54

Table 6.11: Overall Algorithm performance on all the tested network topologies.

Algorithm	Number of Statistically Significant Results	Overall Average Performance
FSAC	135	53.55
SPR	0	47.65
ACRWA	0	40.48
UCBRWA	0	40.29

statistically significant results obtained for each of the tested algorithms gathered from the results given in Appendix D.

For the FSAC algorithm, the pheromone calculations with the most number of statistically significant results is 4 (74 out of 135), 10 (29 out of 135) and then 9 (17 out of 135). However, the pheromone calculations with the highest overall average performances are 4 (53.55%), 10 (52.54%) and then 3 (51.85%). Pheromone calculation 10 accumulated the statistically significant results on the large topology only, but did perform well throughout. Pheromone calculation 9 performed well and accrued the statistically significant results on the small network topology. Pheromone calculation 3 was able to achieve a single statistically significant result on the small network topology, but did perform well on average throughout. Pheromone calculation 4 outperformed the other tested pheromone calculations considered in this

work, achieving the most number of statistically significant results and highest overall average performing near best on all the network topologies.

In the small network topology, FSAC displayed the highest performance for all the tested loads. SPR performed better than ACRWA and UCBRWA for all the tested loads. SPR neared FSAC's performance only at the highest load, while UCBRWA performed better than ACRWA only under low loads placed on the network. In the medium network topology, FSAC had the best performance throughout all the tested loads. UCBRWA performed better than ACRWA from low to medium loads, thereafter, ACRWA overtook UCBRWA and SPR under high loads. In the large network topology, FSAC outperformed the tested algorithms for all loads. Notably, UCBRWA performed better than ACRWA under low loads. Under medium and high loads, ACRWA performed better than UCBRWA. ACRWA matched the performance of SPR at the highest loads placed on the network.

## 6.7 Conclusion

This chapter applied the proposed algorithms on a simulated Flexible Spectrum environment where transmissions underwent linear and non-linear impairments. Under these effects, burst transmissions could be lost during traversal of the network. The algorithms were evaluated on three separate network topologies, including the use of the impairment model defined by equation (2.2) in Section 2.6.

FSAC achieved all of the statistically significant results and had the highest overall average. FSAC performed the best out of all the tested algorithms. Notably, SPR performed remarkably well considering the algorithm's simplicity. UCBRWA was the worst performing algorithm in Flexible Spectrum. The FSAC algorithm displayed the adaptability needed for OBS and the Flexible Spectrum environment.

# Chapter 7

## CONCLUSION

### 7.1 Introduction

This research developed and tested two different ACO-based approaches for RWA in an OBS network. Two test scenarios represented a traditional ITU Fixed Grid network scenario without PLIs and a Flexible Spectrum network scenario with a model for PLIs. The gathered results and research outcomes are discussed in Section 7.2. The major contributions of this research is detailed in Section 7.3 and the identified limitations are addressed in Section 7.4. Possible future development of this research is discussed in Section 7.5 and an overall summary of this work is provided in Section 7.6.

### 7.2 Overview of Results and Outcomes of Research Objectives

Research objectives were used to focus the scope of this study (Section 1.4). Each of the research objectives are discussed as follows:

**Improve on current algorithms for OBS networks.**

Traditional ACO-based approaches do not greedily exploit successful solutions discovered during the RWA process. This research explored the use of routing tuples, the tight coupling of a wavelength and route from source to destination node pair. Two novel ACO-based approaches were proposed which investigated the use of routing tuples for the RWA process, FSAC and UCBRWA. The FSAC approach proposed and investigated the use of new pheromone calculation equations for use with the routing tuples. Further investigation of the routing tuple developed the novel UCBRWA approach which uses the UCB1 policy to balance the exploration and exploitation of routing tuple selection in the RWA process.

**Provide for Flexible Spectrum in developed approaches.**

Flexible Spectrum is an interesting network technique that is presented and explored in Section 2.5. The use of Flexible Spectrum requires the consideration of PLIs in the form on linear and non-linear effects. In the traditional ITU Fixed Grid network the BCPs are transmitted within their own bandwidth and are not interfered with by the bursts. However, in the Flexible Spectrum scenario the BCPs are used to test the feasibility of the particular bandwidth. In this scenario, the implementation cannot assume that the BCP always traverses the fibre successfully as it cannot be guaranteed when catering for PLIs in Flexible Spectrum. The impairments necessitated the adaptation of the OBS protocol, presented in Section 4.2, to provide for Flexible Spectrum.

**Consider PLIs in Flexible Spectrum.**

It is important to consider and address the PLIs associated with Flexible Spectrum. In order to provide a realistic simulation of Flexible Spectrum a PLIs model

is needed. PLIs are discussed in Section 2.6 which details an equation (2.2) to model the associated transmission penalty. The above mentioned model was used in Chapter 6 to simulate the Flexible Spectrum technique with PLIs using the OBS protocol presented in Section 4.2.

### **Evaluate and refine the proposed ACO-based approaches.**

The proposed ACO-based approaches were tested in simulation on current (traditional ITU Fixed Grid network in Chapter 5) and future (Flexible Spectrum in Chapter 6) network technologies, which included the simulation of PLIs. The two novel ACO-based approaches were tested in simulation with and against SPR and ACRWA for benchmarking purposes. The simulations measured the overall performance and the performance over the duration of each simulation. This allowed for the comparison of the algorithm performances, but also the learning and adaptability of each of the algorithms. The simulations included the use of three different network topologies. The FSAC algorithm had the best performance in all the simulations, traditional ITU Fixed Grid and Flexible Spectrum, using pheromone calculation 4 which performed the best overall. UCBRWA provided a competitive performance in the traditional ITU Fixed Grid network, but performed poorly in the Flexible Spectrum scenario.

## **7.3 Contributions**

The simulation of the OBS technique on current (traditional ITU Fixed Grid) and future (Flexible Spectrum) networks was explored. Chapter 5 details the evaluations performed on the traditional ITU Fixed Grid scenario. The simulation of Flexible Spectrum with the associated PLIs are represented in Chapter 6. The use of Flexible Spectrum and the associated PLIs risk the loss of transmissions as well as the resource reservation BCPs. Therefore, the OBS reservation protocol was adapted

to cater for these impairments and the loss of BCPs detailed in Section 4.2.

The RWA process would typically be separated into two parts, routing and then wavelength assignment. The routing assignment process initially selects an available link between two nodes along a path toward the destination of the transmission request. Thereafter, an available wavelength is selected for that link and assigned to the transmission request for the remainder of its traversal within the network under the WCC. The routing assignment process continues until the transmission request reaches the intended destination, is blocked or lost during traversal. Investigation of the use of a route and wavelength combination, from source to destination node pair, for the RWA process was proposed for ACO-based approaches discussed in Chapter 4. The routing tuple for the RWA process is the tight coupling of a route and wavelength in combination. The tight coupling of the route and wavelength combination is intended to promote the greedy exploitation of successful paths for transmission requests. The routing tuple provided a successful approach to the RWA process in an OBS network under the WCC with respect to the novel proposed approaches, FSAC and UCBRWA.

The application of the above mentioned routing tuples to the RWA process of an ACO-based approach prompted the investigation of new pheromone calculation equations presented in Section 4.3.6. The pheromones needed to be updated with respect to the use of routing tuples as opposed to the traditional approach of updating for each link along the traversed route. Ten pheromone calculations were proposed for investigation with the routing tuples. Two pheromone calculation equations, pheromone calculation 4 and 7, performed significantly better than the other proposed equations. Pheromone calculation 7 had the best overall performance on the traditional ITU Fixed Grid OBS WDM network scenario, closely followed by pheromone calculation 4. Pheromone calculation 4 had the best overall performance on the Flexible Spectrum OBS network under PLIs. Over both network scenarios, pheromone calculation 4 was the most successful of all the investigated pheromone calculations.

Further exploration into the use of routing tuples for the RWA process in an ACO-based approach inspired the novel UCBRWA algorithm presented in Section 4.4. UCBRWA integrated the UCB1 policy to balance exploitation and exploration components of the selection of a routing tuple in the RWA process. Routing tuples represented a route and wavelength combination containing a tally of the success and failures thereof. Each of the routing tuples would have its own reward distribution independent of all the other routing tuples. The selection of routing tuples in the RWA process was likened to the bandit-problem. In order to balance the exploitation-exploration of the routing tuples in a similar manner to ACO, the proposed approach explored the use of the UCB1 policy. The proposed hybridisation of ACO and the UCB1 policy provided an effective and novel approach to RWA in a traditional ITU Fixed Grid WDM network.

The proposed ACO-based approaches presented in Chapter 4 were compared with ACRWA and SPR in Chapter 5 and Chapter 6. The SPR algorithm, presented in Section 2.3, was combined with First-Fit wavelength assignment in the traditional ITU Fixed Grid network and Random wavelength assignment in Flexible Spectrum network scenario. ACRWA, an existing ant-based algorithm is detailed in Section 3.2.5. The above mentioned algorithms provided a benchmark with which to compare the proposed approaches. The FSAC algorithm outperformed all the other tested algorithms using pheromone calculation 4 in both the traditional ITU Fixed Grid and Flexible Spectrum scenarios. FSAC performed better than UCBRWA in the Flexible Spectrum scenario, however, UCBRWA had a higher performance under the highest loads placed on the medium network topology in the traditional ITU Fixed Grid network scenario. UCBRWA performed the worst in the Flexible Spectrum scenario.

Lastly, ACRWA and SPR were used as benchmark algorithms in this research. ACRWA and SPR were investigated in a new problem domain represented by Flexible Spectrum in Chapter 6. Section 6.2 detailed the adaptations to ACRWA and SPR for use in Flexible Spectrum. The above mentioned algorithms were tested on

three different network topologies in the Flexible Spectrum scenario. The simple SPR demonstrated a consistently competitive performance with respect to FSAC under all loads tested on the networks. While the overall performance of ACRWA was not as high as SPR, it did perform well at high loads placed on the networks.

## 7.4 Limitations

The proposed ACO-based approaches were tested in a simulator which cannot be considered to perfectly simulate or replicate a real world scenario. The model used to simulate the PLIs, equation (2.2), was made use of in order to provide a more accurate representation of the Flexible Spectrum environment and does not perfectly model transmission impairments. Although there are many network topologies, the testing scenarios were limited to the use of three network topologies, ranging from 6 to 14 nodes and 8 to 26 links. The bursty traffic generated for the simulator does not perfectly represent real world traffic as it was generated with a strictly random approach. Each new transmission request in the simulator was created by randomly selecting the source and destination nodes from the network topology. As a result, there was no bias toward shorter or longer length transmission requests as could be the case in a real world scenario.

## 7.5 Recommendation for Future Investigation

Aspects of the novel proposed ACO-based approaches could be investigated further. The methods used could be varied in order to identify possible improvements in both the proposed algorithms and simulator. For example, the current traffic model in the simulator could be adapted to provide a variety of alternate traffic models to account for different network state changes.

The testing performed on the proposed algorithms in simulation was completed using static parameters. Future investigation could include the use of dynamic



parameters that could appropriately change to suite the network state. In general, a dynamic approach to the parameter controlling the number of routing tuples could be investigated for both of the proposed ACO-based approaches. For example, the use of a dynamic parameter values could vary the exploration rate of the proposed algorithms depending on the current network state. The parameters could be altered to increase the rate at which bad performing routing tuples are removed to encourage exploration when current routes are failing and replace them with new routing tuples. This could also include adaptively altering the exploration rate in order to decrease the removal of routing tuples which may yet prove to have good performances as there is no need for exploration with respect to the current network state.

Furthermore, more network topologies could be explored to evaluate the proposed approaches under different scenarios. Evaluation of the proposed algorithms on larger and differently shaped network topologies could be beneficial. It would be beneficial to implement and evaluate the proposed algorithms in a real world scenario or network when the technology is more developed.

Currently, the proposed algorithms have been developed to provide a decentralised approach to the RWA process. This approach restricts the global network state awareness of the algorithm, this factor could limit the overall success thereof. With this in mind, the possibility of hybridising the proposed approaches to combine both the centralised and decentralised aspects could provide a fragmentation aware algorithm that could adjust both the local and global routing tuple sets in order to improve overall spectrum efficiency.

## 7.6 Summary

This research explored the creation of ACO-based approaches for RWA in OBS networks, using both current and future networks. The traditional ACO-based approaches did not effectively greedily exploit successful solutions in the RWA process, the use of routing tuples in the RWA process demonstrated to be very effective.

This research investigated the use of a routing tuple, a route and wavelength combination from source to destination node pair, for the RWA process of the proposed novel ACO-based approaches discussed in Chapter 4. The routing tuple is the tight coupling of a wavelength with a route as a routing tuple for the RWA process. The tight coupling of the route and wavelength combination was intended to promote the greedy exploitation of successful paths for transmission requests. This research developed two novel ACO-based approaches, namely FSAC and UCBRWA. The FSAC approach proposed and investigated the use of new pheromone calculation equations for the use with routing tuples in the RWA process. Further investigation of the routing tuple lead to the development of UCBRWA which makes use of the UCB1 policy to balance the exploitation and exploration in the RWA process.

The two novel approaches were tested in simulation with and against SPR and ACRWA. The simulations included the use of three different network topologies. This work simulated the OBS technique on current (traditional ITU Fixed Grid network in Chapter 5) and future (Flexible Spectrum in Chapter 6) network technologies, which included the simulation of PLIs. The two novel proposed ACO-based approaches performed well, both displaying the adaptability needed for OBS in the traditional ITU Fixed Grid scenario. FSAC outperformed all the tested algorithms using pheromone calculation 4 which performed the best overall. UCBRWA provided a competitive performance in the traditional ITU Fixed Grid network, but performed poorly in the Flexible Spectrum scenario. FSAC performed the best in the Flexible Spectrum scenario, notably, the simple SPR algorithm delivered a competitive performance.

# Bibliography

- Agrawal, A., El-Bawab, T. S., and Sofman, L. B. (2005). Comparative Account of Bandwidth Efficiency in Optical Burst Switching and Optical Circuit Switching Networks. *Photonic Network Communications*, 9(3):297–309.
- Agrawal, G. P. (2001). *Nonlinear Fiber Optics*. Optics and Photonics. Academic Press, 3 edition.
- Aguas, E., Caldern, J., and Puerto, G. (2015). Failure Modeling in a WDM Optical Burst Switched Network. In *2015 Workshop on Engineering Applications - International Congress on Engineering (WEA)*, pages 1–7.
- Amar, D., Le Rouzic, E., Brochier, N., Bonetto, E., and Lepers, C. (2014). Traffic Forecast Impact on Spectrum Fragmentation in Gridless Optical Networks. In *2014 The European Conference on Optical Communication (ECOC)*, pages 1–3.
- Amaya, N., Irfan, M., Zervas, G., Baniyas, K., Garrich, M., Henning, I., Simeonidou, D., Zhou, Y. R., Lord, A., Smith, K., Rancano, V. J. F., Liu, S., Petropoulos, P., and Richardson, D. J. (2011). Gridless Optical Networking Field Trial: Flexible Spectrum Switching, Defragmentation and Transport of 10G/40G/100G/555G over 620-km Field Fiber. In *2011 37th European Conference and Exhibition on Optical Communication*, pages 1–3.
- Auer, P., Cesa-Bianchi, N., and Fischer, P. (2002). Finite-time Analysis of the Multiarmed Bandit Problem. *Machine Learning*, 47(2):235–256.

- Aydin, M. A., Atmaca, T., Zaim, H., Turna, O. C., and Nguyen, V. H. (2008). Performance Study of OBS Reservation Protocols. In *2008 Fourth Advanced International Conference on Telecommunications*, pages 428–433.
- Barpanda, R. S., Turuk, A. K., and Sahoo, B. (2009). A New Cost Function to Solve RWA Problem in Wavelength Routed Optical Network Using Genetic Algorithms. In *2009 World Congress on Nature Biologically Inspired Computing (NaBIC)*, pages 1297–1302.
- Barpanda, R. S., Turuk, A. K., and Sahoo, B. (2010). Soft Computing Techniques to Solve the RWA Problem in WDM Optical Networks with ILP. In *CAMIST , International Conference on Challenges and Applications of Mathematics in Sciences and Technology*, pages 47–57.
- Barpanda, R. S., Turuk, A. K., and Sahoo, B. (2014). A Review of Optical Burst Switching in Wavelength Division Multiplexing Networks. In *2014 International Conference on Information Technology*, pages 142–147.
- Bhanja, U., Mahapatra, S., and Roy, R. (2010). A Novel Solution to the Dynamic Routing and Wavelength Assignment Problem in Transparent Optical Networks. *IJCNC Journal 2010, International Journal of Computer Networks and Communications 2.2 (2010)*, 2(2):119–130.
- Binh, L. N. (2008). Routing and Wavelength Assignment in GMPLS-based 10 Gb/s Ethernet Long Haul Optical Networks With and Without Linear Dispersion Constraints. *International Journal of Communications, Network and System Sciences*, 1(2):154–67.
- Blum, C. (2007). Ant Colony Optimization: Introduction and Hybridizations. In *7th International Conference on Hybrid Intelligent Systems (HIS 2007)*, pages 24–29.
- Bourouha, M. A., Batatineh, M., and Guizani, M. (2002). Advances in Optical

- Switching and Networking: Past, Present, and Future. In *Proceedings IEEE SoutheastCon 2002*, pages 405–413.
- Capucho, J. H. L. and Resendo, L. C. (2013). ILP Model and Effective Genetic Algorithm for Routing and Spectrum Allocation in Elastic Optical Networks. In *2013 SBMO/IEEE MTT-S International Microwave Optoelectronics Conference (IMOC)*, pages 1–5.
- Chen, C., Chen, X., Zhang, M., Ma, S., Shao, Y., Li, S., Suleiman, M. S., and Zhu, Z. (2014). Demonstrations of Efficient Online Spectrum Defragmentation in Software-Defined Elastic Optical Networks. *Journal of Lightwave Technology*, 32(24):4701–4711.
- Chen, Y., Qiao, C., and Yu, X. (2004). Optical Burst Switching: a New Area in Optical Networking Research. *IEEE Network*, 18(3):16–23.
- Chino, M., Miyazaki, T., Oki, E., Okamoto, S., and Yamanaka, N. (2016). Adaptive Elastic Spectrum Allocation Based on Traffic Fluctuation Estimate in Flexible OFDM-Based Optical Networks. In *2016 IEEE 17th International Conference on High Performance Switching and Routing (HPSR)*, pages 81–86.
- Coulibaly, Y., Latiff, M. S. A., Umaru, A. M., and Garcia, N. M. (2015). QoS Performance Analysis of Non-Slotted and Slotted Optical Burst Switched Networks. In *2015 IEEE 12th Malaysia International Conference on Communications (MICC)*, pages 153–156.
- Donato, E. A., Júnior, J. C., Vieira, A., and Patel, A. (2012). A Proposal of Dynamic RWA Using Ant Colony in Optical Burst Switched Networks. In *ICN 2012, The Eleventh International Conference on Networks*, pages 246–252.
- Dorigo, M. and Di Caro, G. (1999). Ant Colony Optimization: A New Meta-Heuristic. In *Proceedings of the 1999 Congress on Evolutionary Computation-CEC99*, volume 2, pages 1470–1477.

- Dorigo, M. and Stützle, T. (2001). An Experimental Study of the Simple Ant Colony Optimization Algorithm. In *EC 2001 WSES International Conference on Evolutionary Computation*, pages 253–258.
- Durn, R. J., de Miguel, I., Merayo, N., Fernández, P., Aguado, J. C., Bahillo, A., de la Rosa, R., and Alonso, A. (2012). *Genetic Algorithms for Semi-Static Wavelength-Routed Optical Networks*, chapter 16, pages 317–342. InTech.
- Fernando, L., Frana, A., De Carvalho, S. V., and Rodrigues, R. C. M. (2013). Markov Decision Model for Spectrum Allocation in Elastic Optical Network Links. In *XLVSBPO , Simpósio Brasileiro de Pesquisa Operacional*.
- Galdino, L., Neto, J. M., Costa, J., Durand, F. R., Moschim, E., and Bonani, L. H. (2010). Performance Evolution of Optical Code Conversion Architectures in Hybrid WDM/OCDM OBS Network. In *2010 Sixth Advanced International Conference on Telecommunications*, pages 535–541.
- Garlick, R. M. and Barr, R. S. (2002). *Dynamic Wavelength Routing in WDM Networks via Ant Colony Optimization*, pages 250–255. Springer, Berlin, Heidelberg.
- Gerstel, O., Jinno, M., Lord, A., and Yoo, S. J. B. (2012). Elastic Optical Networking: A New Dawn for the Optical Layer? *IEEE Communications Magazine*, 50(2):12–20.
- Hu, H., Ji, H., Pu, M., Galili, M., Yvind, K., and Oxenlwe, L. K. (2015). 160-Gb/s Silicon All-Optical Packet Switch for Buffer-Less Optical Burst Switching. *Journal of Lightwave Technology*, 33(4):843–848.
- Imran, M. and Aziz, K. (2014). Quality of Service in Hybrid Optical Switching. In *2014 12th International Conference on Frontiers of Information Technology*, pages 7–10.

- Imran, M. and Aziz, K. (2015). Performance Evaluation of Hybrid Optical Switching With Quality of Service. In *2015 26th Irish Signals and Systems Conference (ISSC)*, pages 1–6.
- Imran, M., Collier, M., Landais, P., and Katrinis, K. (2016). Software-Defined Optical Burst Switching for HPC and Cloud Computing Data Centers. *IEEE/OSA Journal of Optical Communications and Networking*, 8(8):610–620.
- Jinno, M., Takara, H., Kozicki, B., Tsukishima, Y., Sone, Y., and Matsuoka, S. (2009). Spectrum-Efficient and Scalable Elastic Optical Path Network: Architecture, Benefits, and Enabling Technologies. *IEEE Communications Magazine*, 47(11):66–73.
- Johannisson, P. and Agrell, E. (2014). Modeling of Nonlinear Signal Distortion in Fiber-Optic Networks. *Journal of Lightwave Technology*, 32(23):4544–4552.
- Jue, J. P., Yang, W. H., Kim, Y. C., and Zhang, Q. (2009). Optical Packet and Burst Switched Networks: A Review. *IET Communications*, 3(3):334–352.
- Katehakis, M. N. and Veinott, A. F. (1987). The Multi-Armed Bandit Problem: Decomposition and Computation. *Mathematics of Operations Research*, 12(2):262–268.
- Kirci, P. and Zaim, A. H. (2006). Just-In-Time, Just-Enough-Time and Horizon Signalling Protocols on Optical Burst Switches. *Optica Applicata*, 36(1):111–123.
- Klinkowski, M., Ruiz, M., Velasco, L., Careglio, D., Lopez, V., and Comellas, J. (2013). Elastic Spectrum Allocation for Time-Varying Traffic in FlexGrid Optical Networks. *IEEE Journal on Selected Areas in Communications*, 31(1):26–38.
- Klinkowski, M. and Walkowiak, K. (2011). Routing and Spectrum Assignment in Spectrum Sliced Elastic Optical Path Network. *IEEE Communications Letters*, 15(8):884–886.

- Kocsis, L. and Szepesvári, C. (2006). *Bandit Based Monte-Carlo Planning*, pages 282–293. Springer, Berlin, Heidelberg.
- Lin, H. C., Wang, S. W., and Hung, M. L. (2008). Finding Routing Paths for Alternate Routing in All-Optical WDM Networks. *Journal of Lightwave Technology*, 26(11):1432–1444.
- Lord, A. (2014). Core Networks in the Flexgrid Era. In *2014 The European Conference on Optical Communication (ECOC)*, pages 1–3.
- Manousakis, K. and Ellinas, G. (2016). Crosstalk-Aware Routing and Spectrum Assignment in Flexible Grid Networks. In *2016 IEEE Symposium on Computers and Communication (ISCC)*, pages 696–701.
- Monoyios, D., Manousakis, K., Christodoulou, C., Hadjiantonis, A., Vlachos, K., and Ellinas, G. (2016). Indirect Crosstalk-Aware Routing and Wavelength Assignment in Transparent Optical Networks with the use of Genetic Algorithms. In *2016 18th International Conference on Transparent Optical Networks (ICTON)*, pages 1–4.
- Muoz, R., Lpez, V., Casellas, R., De Dios, . G., Cugini, F., Sambo, N., D’Errico, A., Gerstel, O., King, D., Lpez-Buedo, S., Layec, P., Cimmino, A., Martnez, R., and Morro, R. (2013). IDEALIST Control and Service Management Solutions for Dynamic and Adaptive Flexi-Grid DWDM networks. In *2013 Future Network Mobile Summit*, pages 1–10.
- Ngo, S. H., Jiang, X., and Horiguchi, S. (2006). An Ant-Based Approach for Dynamic RWA in Optical WDM Networks. *Photonic Network Communications*, 11(1):39–48.
- Papadimitriou, G. I., Papazoglou, C., and Pomportsis, A. S. (2003). Optical Switching: Switch Fabrics, Techniques, and Architectures. *Journal of Lightwave Technology*, 21(2):384–405.



- Pedro, J., Pires, J., and Carvalho, J. P. (2009). Distributed Routing Path Optimization for OBS Networks Based on Ant Colony Optimization. In *GLOBECOM 2009 - 2009 IEEE Global Telecommunications Conference*, pages 1–7.
- Rodrigues, J. J. P. C. and Vaidya, B. (2009). Evaluation of Resource Reservation Protocols for IP over OBS networks. In *2009 11th International Conference on Transparent Optical Networks*, pages 1–4.
- Shen, G. and Yang, Q. (2011). From Coarse Grid to Mini-Grid to Gridless: How much can Gridless Help Contentionless? In *2011 Optical Fiber Communication Conference and Exposition and the National Fiber Optic Engineers Conference*, pages 1–3.
- Siddiqui, S., Wu, J., Mouftah, H. T., and Savoie, M. (2004). A Dynamic K-Routing Algorithm in Wavelength-Routed Optical Networks. In *Canadian Conference on Electrical and Computer Engineering 2004*, pages 555–558.
- Takagi, T., Hasegawa, H., Sato, K., Sone, Y., Kozicki, B., Hirano, A., and Jinno, M. (2011). Dynamic Routing and Frequency Slot Assignment for Elastic Optical Path Networks that Adopt Distance Adaptive Modulation. In *2011 Optical Fiber Communication Conference and Exposition and the National Fiber Optic Engineers Conference*, pages 1–3.
- Triay, J. and Cervello-Pastor, C. (2009). An Ant-Based Algorithm for Distributed RWA in Optical Burst Switching. In *2009 11th International Conference on Transparent Optical Networks*, pages 1–4.
- Triay, J. and Cervello-Pastor, C. (2010). An Ant-Based Algorithm for Distributed Routing and Wavelength Assignment in Dynamic Optical Networks. *IEEE Journal on Selected Areas in Communications*, 28(4):542–552.
- Waldman, H., Almeida, R. C., Assis, K. D. R., and Bortoletto, R. C. (2013).

- Spectrum-Sliced Elastic Optical Networking. In *2013 15th International Conference on Transparent Optical Networks (ICTON)*, pages 1–4.
- Wen, K., Cai, X., Yin, Y., Geisler, D. J., Proietti, R., Scott, R. P., Fontaine, N. K., and Yoo, S. J. B. (2013). Adaptive Spectrum Control and Management in Elastic Optical Networks. *IEEE Journal on Selected Areas in Communications*, 31(1):39–48.
- Wright, P., Lord, A., and Velasco, L. (2013). The Network Capacity Benefits of Flexgrid. In *2013 17th International Conference on Optical Networking Design and Modeling (ONDM)*, pages 7–12.
- Xu, L., Perros, H. G., and Rouskas, G. (2001). Techniques for Optical Packet Switching and Optical Burst Switching. *IEEE Communications Magazine*, 39(1):136–142.
- Yan, L., Agrell, E., and Wymeersch, H. (2015a). Resource Allocation for Flexible-Grid Nonlinear Fiber-Optic Networks. In *2015 Optical Fiber Communications Conference and Exhibition (OFC)*, pages 1–3.
- Yan, L., Agrell, E., Wymeersch, H., Johannisson, P., Di Taranto, R., and Brandt-Pearce, M. (2015b). Link-Level Resource Allocation for Flexible-Grid Nonlinear Fiber-Optic Communication Systems. *IEEE Photonics Technology Letters*, 27(12):1250–1253.
- Yao, S., Mukherjee, B., and Dixit, S. (2000). Advances in Photonic Packet Switching: An Overview. *IEEE Communications Magazine*, 38(2):84–94.
- Yin, Y., Zhang, M., Zhu, Z., and Yoo, S. J. B. (2013). Fragmentation-Aware Routing, Modulation and Spectrum Assignment Algorithms in Elastic Optical Networks. In *2013 Optical Fiber Communication Conference and Exposition and the National Fiber Optic Engineers Conference (OFC/NFOEC)*, pages 1–3.

- Yumer, R., Akar, N., and Karasan, E. (2014). Class-Based First-Fit Spectrum Allocation with Fragmentation Avoidance for Dynamic Flexgrid Optical Networks. *Optical Switching and Networking*, 15:44–52.
- Zhang, M., You, C., Jiang, H., and Zhu, Z. (2014). Dynamic and Adaptive Bandwidth Defragmentation in Spectrum-Sliced Elastic Optical Networks With Time-Varying Traffic. *Journal of Lightwave Technology*, 32(5):1014–1023.
- Zhang, Y., Zheng, X., Li, Q., Hua, N., Li, Y., and Zhang, H. (2011). Traffic Grooming in Spectrum-Elastic Optical Path Networks. In *2011 Optical Fiber Communication Conference and Exposition and the National Fiber Optic Engineers Conference*, pages 1–3.

# Appendix A

## Appendix FSAC Fixed Grid Dataset

Table A.1: Fixed Grid dataset of the Success ratio for FSAC PCs on the small network topology.

Load	GU-1	GU-2	GU-3	GU-4	GU-5	GU-6	GU-7	GU-8	GU-9	GU-10
1	98.99 ± 0.07	98.88 ± 0.12	98.84 ± 0.12	99.82 ± 0.02	<b>99.90 ± 0.01</b>	98.57 ± 0.09	99.58 ± 0.03	98.93 ± 0.08	99.09 ± 0.14	99.01 ± 0.11
2	97.31 ± 0.12	97.60 ± 0.17	98.13 ± 0.16	<b>99.22 ± 0.06</b>	99.09 ± 0.06	96.38 ± 0.22	98.70 ± 0.07	97.28 ± 0.13	97.82 ± 0.18	97.56 ± 0.20
3	95.57 ± 0.14	96.27 ± 0.28	96.70 ± 0.23	<b>98.40 ± 0.10</b>	98.03 ± 0.08	94.40 ± 0.25	97.69 ± 0.10	95.52 ± 0.15	96.43 ± 0.28	96.35 ± 0.20
4	93.90 ± 0.18	94.92 ± 0.23	95.27 ± 0.33	<b>97.16 ± 0.19</b>	96.84 ± 0.11	92.60 ± 0.32	96.58 ± 0.14	93.66 ± 0.16	95.28 ± 0.26	94.61 ± 0.22
5	92.10 ± 0.19	93.56 ± 0.39	94.31 ± 0.35	<b>96.22 ± 0.15</b>	95.40 ± 0.14	91.09 ± 0.32	95.59 ± 0.16	92.04 ± 0.15	94.31 ± 0.25	93.15 ± 0.22
6	90.58 ± 0.14	92.32 ± 0.45	93.33 ± 0.29	<b>94.84 ± 0.27</b>	93.97 ± 0.16	89.43 ± 0.31	94.45 ± 0.15	90.43 ± 0.18	92.99 ± 0.38	91.35 ± 0.30
7	88.95 ± 0.19	90.91 ± 0.37	92.16 ± 0.35	<b>93.39 ± 0.27</b>	92.38 ± 0.20	88.14 ± 0.27	93.09 ± 0.21	88.96 ± 0.16	91.63 ± 0.42	89.51 ± 0.23
8	87.61 ± 0.17	89.85 ± 0.39	90.88 ± 0.32	91.79 ± 0.22	90.98 ± 0.20	86.56 ± 0.35	<b>91.89 ± 0.20</b>	87.57 ± 0.17	89.94 ± 0.43	87.73 ± 0.20
9	86.07 ± 0.20	88.24 ± 0.57	90.04 ± 0.32	90.07 ± 0.40	89.00 ± 0.27	85.02 ± 0.43	<b>90.33 ± 0.23</b>	85.89 ± 0.18	89.15 ± 0.33	86.23 ± 0.16
10	84.47 ± 0.16	86.89 ± 0.39	88.72 ± 0.34	88.62 ± 0.36	87.80 ± 0.26	83.58 ± 0.33	<b>88.93 ± 0.30</b>	84.50 ± 0.14	87.79 ± 0.43	84.76 ± 0.16
11	83.17 ± 0.16	85.33 ± 0.48	87.48 ± 0.39	86.94 ± 0.59	86.02 ± 0.30	82.06 ± 0.26	<b>87.63 ± 0.28</b>	83.33 ± 0.14	86.42 ± 0.47	83.31 ± 0.15
12	81.72 ± 0.15	83.74 ± 0.43	85.94 ± 0.46	85.26 ± 0.47	84.49 ± 0.28	80.75 ± 0.36	<b>86.33 ± 0.29</b>	81.64 ± 0.14	85.55 ± 0.39	81.97 ± 0.19
13	80.37 ± 0.17	82.75 ± 0.48	<b>84.93 ± 0.43</b>	83.97 ± 0.53	82.89 ± 0.30	79.11 ± 0.46	84.67 ± 0.38	80.19 ± 0.16	83.60 ± 0.50	80.39 ± 0.17
14	78.84 ± 0.15	81.17 ± 0.49	<b>83.88 ± 0.35</b>	82.52 ± 0.46	81.39 ± 0.33	77.20 ± 0.42	82.93 ± 0.29	78.90 ± 0.13	82.94 ± 0.49	79.00 ± 0.09
15	77.37 ± 0.13	80.58 ± 0.41	<b>82.59 ± 0.46</b>	80.58 ± 0.47	79.63 ± 0.42	76.10 ± 0.41	81.51 ± 0.35	77.36 ± 0.13	81.44 ± 0.47	77.29 ± 0.16
16	75.52 ± 0.16	78.92 ± 0.50	<b>81.30 ± 0.34</b>	79.00 ± 0.64	78.03 ± 0.29	74.61 ± 0.30	80.01 ± 0.32	75.62 ± 0.12	79.59 ± 0.47	75.77 ± 0.15
17	74.09 ± 0.17	77.63 ± 0.40	<b>80.09 ± 0.31</b>	77.00 ± 0.63	76.49 ± 0.37	73.01 ± 0.36	78.33 ± 0.34	74.08 ± 0.14	78.70 ± 0.33	73.97 ± 0.15
18	72.15 ± 0.14	76.29 ± 0.43	<b>78.82 ± 0.46</b>	75.71 ± 0.62	75.02 ± 0.45	70.96 ± 0.38	76.63 ± 0.55	72.02 ± 0.19	77.43 ± 0.43	72.25 ± 0.11
19	70.11 ± 0.17	74.98 ± 0.47	<b>77.48 ± 0.45</b>	74.84 ± 0.56	73.56 ± 0.40	69.14 ± 0.33	75.13 ± 0.41	70.12 ± 0.17	76.30 ± 0.53	70.29 ± 0.19
20	68.16 ± 0.14	74.42 ± 0.39	<b>76.45 ± 0.38</b>	72.98 ± 0.78	71.80 ± 0.40	67.33 ± 0.24	73.65 ± 0.40	68.08 ± 0.19	75.18 ± 0.37	68.44 ± 0.16
21	65.95 ± 0.14	73.12 ± 0.38	<b>75.11 ± 0.44</b>	71.49 ± 0.55	70.52 ± 0.36	65.18 ± 0.34	72.02 ± 0.44	65.76 ± 0.17	73.49 ± 0.47	66.10 ± 0.13
22	63.78 ± 0.15	71.99 ± 0.40	<b>73.59 ± 0.40</b>	69.77 ± 0.52	68.83 ± 0.51	63.02 ± 0.27	70.32 ± 0.56	63.69 ± 0.17	72.54 ± 0.46	63.89 ± 0.12
23	61.43 ± 0.14	70.98 ± 0.54	<b>72.63 ± 0.52</b>	69.10 ± 0.67	67.52 ± 0.41	60.52 ± 0.32	68.19 ± 0.60	61.39 ± 0.15	70.93 ± 0.41	61.63 ± 0.13
24	59.39 ± 0.14	70.18 ± 0.40	<b>71.01 ± 0.49</b>	67.40 ± 0.59	65.91 ± 0.40	58.12 ± 0.35	67.85 ± 0.51	59.17 ± 0.17	69.59 ± 0.38	59.59 ± 0.12
25	57.07 ± 0.12	<b>69.37 ± 0.43</b>	69.25 ± 0.46	66.12 ± 0.56	65.13 ± 0.39	56.11 ± 0.25	65.63 ± 0.52	57.05 ± 0.16	68.59 ± 0.45	57.23 ± 0.13
26	54.81 ± 0.18	68.18 ± 0.44	<b>68.50 ± 0.38</b>	65.19 ± 0.70	63.31 ± 0.46	53.85 ± 0.17	64.36 ± 0.42	54.77 ± 0.15	67.52 ± 0.48	54.99 ± 0.13
27	52.82 ± 0.17	66.92 ± 0.44	<b>67.47 ± 0.37</b>	63.55 ± 0.60	62.50 ± 0.45	51.99 ± 0.17	62.47 ± 0.70	52.81 ± 0.14	66.12 ± 0.39	52.87 ± 0.10
28	50.75 ± 0.11	<b>66.16 ± 0.40</b>	66.08 ± 0.52	62.97 ± 0.52	60.99 ± 0.39	49.70 ± 0.18	61.46 ± 0.66	50.91 ± 0.11	65.32 ± 0.45	50.98 ± 0.14
29	48.90 ± 0.15	64.84 ± 0.40	<b>64.83 ± 0.46</b>	62.23 ± 0.55	60.21 ± 0.44	47.80 ± 0.14	60.26 ± 0.63	48.82 ± 0.12	64.10 ± 0.37	48.99 ± 0.11
30	46.98 ± 0.13	<b>64.10 ± 0.48</b>	63.60 ± 0.43	60.99 ± 0.62	58.74 ± 0.41	46.12 ± 0.12	58.17 ± 0.64	47.04 ± 0.13	63.01 ± 0.44	47.09 ± 0.11
31	45.25 ± 0.11	<b>63.31 ± 0.35</b>	62.46 ± 0.48	59.46 ± 0.59	57.82 ± 0.33	44.34 ± 0.13	58.39 ± 0.50	45.31 ± 0.10	61.80 ± 0.39	45.29 ± 0.10
32	43.60 ± 0.11	<b>62.47 ± 0.33</b>	61.27 ± 0.50	58.64 ± 0.55	57.05 ± 0.39	42.69 ± 0.09	57.22 ± 0.64	43.62 ± 0.11	60.98 ± 0.42	43.58 ± 0.10
33	42.03 ± 0.10	<b>61.60 ± 0.37</b>	60.35 ± 0.51	57.74 ± 0.47	55.79 ± 0.41	41.14 ± 0.11	56.52 ± 0.61	42.01 ± 0.10	60.45 ± 0.27	41.95 ± 0.09
34	40.59 ± 0.10	<b>60.79 ± 0.38</b>	59.55 ± 0.39	57.43 ± 0.65	54.72 ± 0.40	39.79 ± 0.10	55.03 ± 0.63	40.64 ± 0.11	59.26 ± 0.33	40.51 ± 0.07
35	39.19 ± 0.10	<b>60.61 ± 0.46</b>	58.43 ± 0.43	56.56 ± 0.48	54.06 ± 0.46	38.36 ± 0.12	54.92 ± 0.50	39.34 ± 0.11	58.88 ± 0.46	39.17 ± 0.08

Continued on Next Page...

Table A.1 – Continued

Load	GU-1	GU-2	GU-3	GU-4	GU-5	GU-6	GU-7	GU-8	GU-9	GU-10
36	37.95 ± 0.09	<b>58.99 ± 0.34</b>	57.85 ± 0.32	55.49 ± 0.57	53.16 ± 0.44	37.06 ± 0.09	54.48 ± 0.37	38.01 ± 0.12	57.76 ± 0.42	37.72 ± 0.07
37	36.71 ± 0.08	<b>58.72 ± 0.40</b>	56.89 ± 0.43	55.16 ± 0.49	52.31 ± 0.42	36.03 ± 0.09	52.85 ± 0.37	36.72 ± 0.12	57.04 ± 0.33	36.56 ± 0.09
38	35.58 ± 0.10	<b>57.93 ± 0.38</b>	56.47 ± 0.34	53.75 ± 0.54	51.57 ± 0.50	34.79 ± 0.08	52.38 ± 0.54	35.54 ± 0.10	56.58 ± 0.31	35.32 ± 0.08
39	34.44 ± 0.07	<b>57.33 ± 0.36</b>	55.26 ± 0.44	53.20 ± 0.64	50.66 ± 0.37	33.76 ± 0.09	51.97 ± 0.52	34.44 ± 0.13	55.86 ± 0.34	34.19 ± 0.08
40	33.51 ± 0.09	<b>56.86 ± 0.36</b>	54.94 ± 0.41	52.90 ± 0.47	49.96 ± 0.38	32.64 ± 0.09	51.14 ± 0.41	33.41 ± 0.11	54.78 ± 0.39	33.13 ± 0.09
41	32.48 ± 0.08	<b>55.86 ± 0.40</b>	54.17 ± 0.34	51.65 ± 0.56	49.27 ± 0.38	31.73 ± 0.07	50.27 ± 0.61	32.54 ± 0.09	54.56 ± 0.29	32.07 ± 0.08
42	31.50 ± 0.08	<b>55.54 ± 0.44</b>	53.49 ± 0.29	51.50 ± 0.43	48.30 ± 0.31	30.77 ± 0.08	49.45 ± 0.53	31.57 ± 0.08	53.71 ± 0.34	31.19 ± 0.07
43	30.70 ± 0.09	<b>54.58 ± 0.35</b>	52.72 ± 0.35	50.69 ± 0.43	47.66 ± 0.32	29.97 ± 0.08	49.60 ± 0.47	30.72 ± 0.11	52.97 ± 0.38	30.21 ± 0.08
44	29.83 ± 0.08	<b>54.55 ± 0.37</b>	52.14 ± 0.44	50.22 ± 0.57	47.08 ± 0.33	29.17 ± 0.08	48.49 ± 0.38	29.90 ± 0.11	52.29 ± 0.39	29.28 ± 0.07
45	29.15 ± 0.07	<b>53.83 ± 0.41</b>	51.21 ± 0.36	49.43 ± 0.50	46.84 ± 0.27	28.36 ± 0.06	47.86 ± 0.43	29.05 ± 0.08	52.17 ± 0.30	28.61 ± 0.06

Table A.2: Fixed Grid dataset of the Success ratio for FSAC PCs on the medium network topology.

Load	GU-1	GU-2	GU-3	GU-4	GU-5	GU-6	GU-7	GU-8	GU-9	GU-10
1	99.46 ± 0.02	98.57 ± 0.10	98.53 ± 0.09	98.80 ± 0.06	99.31 ± 0.02	99.26 ± 0.03	<b>99.48 ± 0.02</b>	99.47 ± 0.02	98.43 ± 0.09	99.27 ± 0.04
2	98.64 ± 0.05	96.70 ± 0.17	96.78 ± 0.15	97.20 ± 0.14	<b>98.73 ± 0.04</b>	98.26 ± 0.06	98.64 ± 0.06	98.63 ± 0.05	96.56 ± 0.14	98.58 ± 0.05
3	97.81 ± 0.06	95.19 ± 0.21	95.19 ± 0.20	95.84 ± 0.17	<b>98.02 ± 0.07</b>	97.31 ± 0.10	97.88 ± 0.06	97.80 ± 0.08	95.13 ± 0.19	97.81 ± 0.09
4	97.07 ± 0.09	93.63 ± 0.32	93.52 ± 0.30	94.57 ± 0.28	<b>97.41 ± 0.08</b>	96.36 ± 0.13	97.07 ± 0.09	97.06 ± 0.11	93.40 ± 0.28	97.22 ± 0.11
5	96.25 ± 0.09	92.18 ± 0.31	92.45 ± 0.30	93.52 ± 0.24	<b>96.66 ± 0.10</b>	95.39 ± 0.13	96.16 ± 0.13	96.29 ± 0.10	92.15 ± 0.31	96.45 ± 0.10
6	95.46 ± 0.15	90.63 ± 0.27	91.03 ± 0.37	92.31 ± 0.19	<b>95.82 ± 0.13</b>	94.54 ± 0.15	95.53 ± 0.13	95.56 ± 0.09	90.93 ± 0.39	95.79 ± 0.13
7	94.78 ± 0.14	89.45 ± 0.41	89.69 ± 0.46	91.34 ± 0.30	95.04 ± 0.13	93.98 ± 0.15	94.78 ± 0.10	94.93 ± 0.11	89.46 ± 0.43	<b>95.16 ± 0.14</b>
8	94.09 ± 0.14	88.58 ± 0.36	88.72 ± 0.37	90.62 ± 0.29	94.17 ± 0.15	92.91 ± 0.17	94.13 ± 0.15	93.91 ± 0.14	88.03 ± 0.43	<b>94.41 ± 0.14</b>
9	93.44 ± 0.13	87.13 ± 0.51	87.44 ± 0.37	89.60 ± 0.39	<b>93.7 ± 0.11</b>	92.14 ± 0.21	93.36 ± 0.18	93.26 ± 0.15	86.92 ± 0.52	93.60 ± 0.18
10	92.60 ± 0.11	86.93 ± 0.44	86.36 ± 0.45	89.06 ± 0.28	92.89 ± 0.17	91.37 ± 0.17	92.55 ± 0.16	92.61 ± 0.18	86.34 ± 0.46	<b>93.06 ± 0.15</b>
11	91.85 ± 0.18	85.30 ± 0.41	85.40 ± 0.53	88.25 ± 0.33	92.08 ± 0.15	90.63 ± 0.19	92.06 ± 0.14	91.95 ± 0.15	85.34 ± 0.51	<b>92.36 ± 0.18</b>
12	91.29 ± 0.18	84.62 ± 0.42	84.50 ± 0.55	87.41 ± 0.35	91.34 ± 0.17	89.91 ± 0.14	91.33 ± 0.19	91.21 ± 0.14	84.60 ± 0.48	<b>91.67 ± 0.21</b>
13	90.67 ± 0.16	83.52 ± 0.35	83.63 ± 0.41	86.80 ± 0.31	90.62 ± 0.16	89.33 ± 0.16	90.63 ± 0.13	90.61 ± 0.13	83.23 ± 0.45	<b>90.90 ± 0.21</b>
14	89.76 ± 0.16	82.53 ± 0.54	82.99 ± 0.53	86.09 ± 0.40	89.82 ± 0.16	88.68 ± 0.19	89.85 ± 0.23	90.02 ± 0.16	82.92 ± 0.57	<b>90.26 ± 0.20</b>
15	89.32 ± 0.17	81.69 ± 0.39	82.18 ± 0.54	85.46 ± 0.25	89.19 ± 0.13	87.99 ± 0.24	89.18 ± 0.17	89.30 ± 0.18	81.63 ± 0.64	<b>89.69 ± 0.19</b>
16	88.74 ± 0.19	80.69 ± 0.60	81.21 ± 0.55	84.90 ± 0.34	88.58 ± 0.16	87.50 ± 0.23	88.62 ± 0.16	88.69 ± 0.17	80.47 ± 0.46	<b>88.98 ± 0.22</b>
17	87.89 ± 0.18	80.28 ± 0.54	80.49 ± 0.47	84.23 ± 0.34	88.13 ± 0.16	86.74 ± 0.22	88.10 ± 0.17	87.99 ± 0.16	80.79 ± 0.45	<b>88.52 ± 0.21</b>
18	<b>87.65 ± 0.14</b>	79.29 ± 0.48	79.70 ± 0.46	83.75 ± 0.40	87.40 ± 0.19	86.05 ± 0.18	87.43 ± 0.20	87.41 ± 0.17	79.24 ± 0.52	87.64 ± 0.23
19	86.77 ± 0.16	78.33 ± 0.52	78.59 ± 0.42	83.03 ± 0.31	86.69 ± 0.24	85.64 ± 0.21	86.77 ± 0.19	86.70 ± 0.14	78.35 ± 0.50	<b>87.15 ± 0.21</b>
20	86.17 ± 0.19	77.93 ± 0.48	78.16 ± 0.43	82.74 ± 0.33	86.16 ± 0.19	84.83 ± 0.33	86.28 ± 0.20	86.30 ± 0.22	78.50 ± 0.53	<b>86.68 ± 0.22</b>
21	85.87 ± 0.23	76.97 ± 0.57	77.57 ± 0.44	82.07 ± 0.35	85.44 ± 0.23	84.54 ± 0.21	85.56 ± 0.19	85.69 ± 0.25	77.63 ± 0.38	<b>85.98 ± 0.21</b>
22	85.11 ± 0.18	76.63 ± 0.49	76.49 ± 0.57	81.56 ± 0.33	84.91 ± 0.22	83.80 ± 0.24	84.99 ± 0.19	84.95 ± 0.15	77.00 ± 0.50	<b>85.57 ± 0.23</b>
23	84.50 ± 0.17	75.58 ± 0.51	76.75 ± 0.53	81.20 ± 0.33	84.17 ± 0.21	83.15 ± 0.24	84.47 ± 0.21	84.51 ± 0.18	76.84 ± 0.51	<b>84.86 ± 0.17</b>
24	83.97 ± 0.16	75.66 ± 0.45	75.38 ± 0.56	80.96 ± 0.30	83.74 ± 0.16	82.53 ± 0.24	83.95 ± 0.22	83.91 ± 0.18	75.74 ± 0.54	<b>84.27 ± 0.21</b>
25	83.25 ± 0.20	74.97 ± 0.53	74.67 ± 0.44	80.33 ± 0.42	83.14 ± 0.16	82.20 ± 0.28	83.41 ± 0.17	83.38 ± 0.23	75.11 ± 0.55	<b>83.57 ± 0.16</b>
26	82.96 ± 0.19	73.93 ± 0.51	74.39 ± 0.54	79.45 ± 0.35	82.85 ± 0.13	81.71 ± 0.24	82.89 ± 0.25	82.79 ± 0.23	74.77 ± 0.48	<b>83.11 ± 0.19</b>
27	82.29 ± 0.19	73.13 ± 0.41	74.01 ± 0.53	79.49 ± 0.33	82.04 ± 0.21	81.29 ± 0.26	82.11 ± 0.22	82.27 ± 0.21	74.55 ± 0.48	<b>82.41 ± 0.20</b>
28	81.80 ± 0.20	73.59 ± 0.48	73.12 ± 0.49	78.50 ± 0.31	81.55 ± 0.17	80.74 ± 0.22	81.65 ± 0.20	81.73 ± 0.20	73.59 ± 0.52	<b>82.13 ± 0.19</b>
29	81.32 ± 0.20	72.47 ± 0.55	72.73 ± 0.41	78.31 ± 0.33	81.27 ± 0.24	80.31 ± 0.26	81.31 ± 0.19	81.36 ± 0.20	72.53 ± 0.63	<b>81.64 ± 0.22</b>
30	<b>80.99 ± 0.17</b>	71.84 ± 0.55	72.50 ± 0.63	78.18 ± 0.37	80.73 ± 0.19	79.61 ± 0.22	80.68 ± 0.27	80.74 ± 0.21	72.22 ± 0.42	80.82 ± 0.25
31	80.46 ± 0.22	71.49 ± 0.54	71.59 ± 0.43	77.50 ± 0.37	80.08 ± 0.23	79.43 ± 0.25	80.23 ± 0.14	80.51 ± 0.22	72.12 ± 0.50	<b>80.75 ± 0.24</b>
32	80.05 ± 0.20	70.60 ± 0.52	71.35 ± 0.52	76.75 ± 0.44	79.59 ± 0.19	78.86 ± 0.19	79.71 ± 0.17	79.82 ± 0.19	71.19 ± 0.47	<b>80.07 ± 0.23</b>
33	79.26 ± 0.20	70.18 ± 0.53	70.88 ± 0.46	76.57 ± 0.39	79.26 ± 0.16	78.54 ± 0.30	79.26 ± 0.15	79.27 ± 0.26	71.35 ± 0.48	<b>79.57 ± 0.20</b>
34	78.94 ± 0.17	69.41 ± 0.71	70.32 ± 0.42	76.20 ± 0.32	78.63 ± 0.15	77.89 ± 0.27	78.68 ± 0.25	78.92 ± 0.22	70.67 ± 0.48	<b>79.02 ± 0.26</b>
35	78.43 ± 0.21	69.43 ± 0.50	70.15 ± 0.40	75.56 ± 0.34	78.15 ± 0.16	77.60 ± 0.22	78.25 ± 0.20	78.47 ± 0.22	70.49 ± 0.52	<b>78.55 ± 0.23</b>

Continued on Next Page...

Table A.2 – Continued

Load	GU-1	GU-2	GU-3	GU-4	GU-5	GU-6	GU-7	GU-8	GU-9	GU-10
36	78.00 ± 0.22	68.62 ± 0.48	69.48 ± 0.61	75.34 ± 0.42	77.49 ± 0.19	77.01 ± 0.25	77.68 ± 0.23	78.01 ± 0.15	69.66 ± 0.56	<b>78.10 ± 0.21</b>
37	77.44 ± 0.21	68.98 ± 0.43	68.92 ± 0.57	75.15 ± 0.35	77.17 ± 0.17	76.56 ± 0.20	77.34 ± 0.22	77.56 ± 0.24	69.15 ± 0.48	<b>77.76 ± 0.22</b>
38	77.00 ± 0.19	68.36 ± 0.42	68.51 ± 0.54	74.78 ± 0.39	76.89 ± 0.21	76.20 ± 0.24	76.93 ± 0.23	76.84 ± 0.25	69.10 ± 0.56	<b>77.10 ± 0.20</b>
39	76.51 ± 0.17	67.80 ± 0.51	68.03 ± 0.49	74.10 ± 0.34	76.24 ± 0.24	75.80 ± 0.22	76.39 ± 0.21	<b>76.73 ± 0.18</b>	68.33 ± 0.53	76.61 ± 0.22
40	76.22 ± 0.19	67.87 ± 0.50	67.53 ± 0.45	74.01 ± 0.37	75.81 ± 0.23	75.29 ± 0.22	75.91 ± 0.21	<b>76.30 ± 0.19</b>	68.34 ± 0.61	76.25 ± 0.19
41	75.74 ± 0.22	66.77 ± 0.51	67.71 ± 0.48	73.38 ± 0.34	75.41 ± 0.22	74.88 ± 0.24	75.47 ± 0.15	75.78 ± 0.21	67.72 ± 0.44	<b>75.80 ± 0.20</b>
42	<b>75.33 ± 0.24</b>	66.47 ± 0.57	66.65 ± 0.47	73.22 ± 0.31	74.85 ± 0.21	74.71 ± 0.22	75.03 ± 0.22	75.31 ± 0.14	67.36 ± 0.50	75.21 ± 0.23
43	74.76 ± 0.20	66.08 ± 0.55	66.82 ± 0.49	72.72 ± 0.43	74.55 ± 0.21	74.13 ± 0.29	74.76 ± 0.29	74.69 ± 0.22	66.54 ± 0.46	<b>74.88 ± 0.19</b>
44	74.37 ± 0.17	65.47 ± 0.43	65.64 ± 0.50	72.45 ± 0.31	73.88 ± 0.19	73.8 ± 0.23	74.18 ± 0.19	74.32 ± 0.20	66.65 ± 0.45	<b>74.56 ± 0.21</b>
45	74.01 ± 0.21	65.75 ± 0.35	65.91 ± 0.38	72.42 ± 0.32	73.60 ± 0.23	73.13 ± 0.19	73.86 ± 0.23	74.00 ± 0.23	66.42 ± 0.52	<b>74.11 ± 0.18</b>
46	73.51 ± 0.20	64.65 ± 0.57	65.36 ± 0.49	72.04 ± 0.30	73.26 ± 0.20	72.80 ± 0.24	73.43 ± 0.16	73.68 ± 0.17	65.66 ± 0.40	<b>73.70 ± 0.23</b>
47	73.01 ± 0.20	64.31 ± 0.54	65.36 ± 0.54	71.44 ± 0.30	72.89 ± 0.22	72.52 ± 0.23	73.04 ± 0.24	<b>73.07 ± 0.18</b>	65.31 ± 0.48	72.97 ± 0.21
48	<b>72.94 ± 0.22</b>	64.16 ± 0.44	64.38 ± 0.37	71.00 ± 0.35	72.50 ± 0.16	72.03 ± 0.19	72.49 ± 0.23	72.85 ± 0.25	65.13 ± 0.50	72.87 ± 0.22
49	72.33 ± 0.20	63.75 ± 0.46	64.02 ± 0.42	70.57 ± 0.26	71.93 ± 0.17	71.56 ± 0.22	72.06 ± 0.24	72.34 ± 0.17	64.75 ± 0.42	<b>72.46 ± 0.23</b>
50	<b>72.29 ± 0.21</b>	63.5 ± 0.57	64.39 ± 0.53	70.42 ± 0.36	71.61 ± 0.25	71.09 ± 0.24	71.65 ± 0.26	71.90 ± 0.17	64.42 ± 0.50	72.08 ± 0.20
51	71.38 ± 0.22	63.01 ± 0.53	63.90 ± 0.45	69.99 ± 0.30	71.04 ± 0.22	70.94 ± 0.17	71.40 ± 0.20	71.5 ± 0.17	64.28 ± 0.39	<b>71.73 ± 0.24</b>
52	71.06 ± 0.20	62.71 ± 0.35	63.24 ± 0.50	69.64 ± 0.28	70.84 ± 0.24	70.46 ± 0.22	70.75 ± 0.18	71.13 ± 0.22	63.41 ± 0.40	<b>71.20 ± 0.22</b>
53	70.68 ± 0.24	62.47 ± 0.60	62.75 ± 0.50	69.23 ± 0.32	70.40 ± 0.20	69.98 ± 0.20	70.52 ± 0.22	70.53 ± 0.21	63.48 ± 0.47	<b>70.74 ± 0.18</b>
54	70.26 ± 0.22	62.09 ± 0.54	62.31 ± 0.45	69.00 ± 0.31	69.93 ± 0.20	69.70 ± 0.18	70.16 ± 0.21	<b>70.59 ± 0.19</b>	63.30 ± 0.53	70.34 ± 0.26
55	70.06 ± 0.21	61.64 ± 0.48	62.48 ± 0.44	68.49 ± 0.26	69.50 ± 0.23	69.25 ± 0.30	69.59 ± 0.21	69.87 ± 0.20	63.13 ± 0.48	<b>70.06 ± 0.19</b>
56	69.45 ± 0.28	61.66 ± 0.40	61.81 ± 0.48	68.15 ± 0.33	69.26 ± 0.29	69.29 ± 0.21	69.28 ± 0.19	69.65 ± 0.21	62.03 ± 0.45	<b>69.64 ± 0.21</b>
57	68.98 ± 0.23	60.92 ± 0.54	61.52 ± 0.51	68.07 ± 0.31	68.65 ± 0.25	68.65 ± 0.29	68.94 ± 0.28	69.30 ± 0.20	62.29 ± 0.48	<b>69.45 ± 0.25</b>
58	68.59 ± 0.21	60.65 ± 0.50	61.41 ± 0.46	67.69 ± 0.41	68.66 ± 0.22	68.29 ± 0.19	68.54 ± 0.23	68.93 ± 0.25	61.91 ± 0.40	<b>68.94 ± 0.20</b>
59	68.32 ± 0.24	60.53 ± 0.52	61.26 ± 0.45	67.19 ± 0.34	68.16 ± 0.19	67.79 ± 0.22	68.24 ± 0.19	68.29 ± 0.23	61.48 ± 0.41	<b>68.43 ± 0.23</b>
60	67.95 ± 0.24	59.87 ± 0.57	61.10 ± 0.45	66.96 ± 0.34	67.76 ± 0.24	67.63 ± 0.27	67.69 ± 0.23	<b>68.26 ± 0.21</b>	61.22 ± 0.46	68.23 ± 0.26



Table A.3: Fixed Grid dataset of the Success ratio for FSAC PCs on the large network topology.

Load	GU-1	GU-2	GU-3	GU-4	GU-5	GU-6	GU-7	GU-8	GU-9	GU-10
1	98.47 ± 0.03	98.69 ± 0.05	98.70 ± 0.04	99.38 ± 0.02	<b>99.56 ± 0.01</b>	98.08 ± 0.05	99.18 ± 0.02	98.54 ± 0.03	99.12 ± 0.04	98.27 ± 0.04
2	96.61 ± 0.06	97.24 ± 0.11	97.31 ± 0.07	98.71 ± 0.03	<b>98.93 ± 0.02</b>	95.79 ± 0.07	98.23 ± 0.04	96.58 ± 0.06	98.11 ± 0.08	96.51 ± 0.07
3	94.81 ± 0.10	95.95 ± 0.12	96.07 ± 0.13	98.05 ± 0.04	<b>98.21 ± 0.02</b>	93.93 ± 0.11	97.37 ± 0.05	94.82 ± 0.07	97.14 ± 0.07	94.89 ± 0.08
4	93.03 ± 0.12	94.71 ± 0.14	94.93 ± 0.11	97.42 ± 0.03	<b>97.46 ± 0.03</b>	91.87 ± 0.12	96.59 ± 0.04	93.18 ± 0.08	96.08 ± 0.08	93.11 ± 0.10
5	91.39 ± 0.12	93.57 ± 0.17	94.11 ± 0.14	<b>96.69 ± 0.04</b>	96.61 ± 0.04	90.18 ± 0.13	95.77 ± 0.09	91.47 ± 0.12	95.20 ± 0.11	91.67 ± 0.13
6	89.97 ± 0.10	92.29 ± 0.14	93.09 ± 0.14	<b>95.94 ± 0.05</b>	95.75 ± 0.04	88.41 ± 0.18	95.03 ± 0.06	89.73 ± 0.11	94.19 ± 0.11	90.03 ± 0.13
7	88.25 ± 0.13	91.40 ± 0.21	92.26 ± 0.13	<b>95.12 ± 0.04</b>	94.83 ± 0.05	86.87 ± 0.17	94.26 ± 0.08	88.28 ± 0.14	93.32 ± 0.13	88.52 ± 0.16
8	86.82 ± 0.14	90.27 ± 0.17	91.48 ± 0.13	<b>94.31 ± 0.07</b>	93.89 ± 0.05	85.38 ± 0.13	93.44 ± 0.09	86.88 ± 0.12	92.18 ± 0.16	87.10 ± 0.10
9	85.42 ± 0.13	89.26 ± 0.28	90.72 ± 0.13	<b>93.48 ± 0.08</b>	92.89 ± 0.06	83.99 ± 0.20	92.65 ± 0.08	85.55 ± 0.13	91.35 ± 0.14	85.72 ± 0.20
10	84.14 ± 0.13	88.12 ± 0.18	89.70 ± 0.12	<b>92.60 ± 0.07</b>	91.83 ± 0.07	82.43 ± 0.19	91.79 ± 0.07	84.22 ± 0.15	90.38 ± 0.14	84.24 ± 0.13
11	82.87 ± 0.13	87.08 ± 0.23	88.95 ± 0.17	<b>91.81 ± 0.07</b>	90.86 ± 0.08	81.41 ± 0.17	91.01 ± 0.10	82.80 ± 0.12	89.51 ± 0.14	83.14 ± 0.17
12	81.37 ± 0.14	85.88 ± 0.21	88.10 ± 0.12	<b>90.83 ± 0.09</b>	89.85 ± 0.06	80.18 ± 0.18	90.26 ± 0.08	81.69 ± 0.14	88.48 ± 0.15	81.93 ± 0.21
13	80.33 ± 0.15	84.99 ± 0.22	87.19 ± 0.16	<b>89.98 ± 0.08</b>	88.79 ± 0.07	78.84 ± 0.20	89.38 ± 0.07	80.28 ± 0.16	87.53 ± 0.15	80.52 ± 0.19
14	79.16 ± 0.16	84.16 ± 0.21	86.30 ± 0.14	<b>89.06 ± 0.10</b>	87.74 ± 0.08	77.69 ± 0.20	88.46 ± 0.10	79.31 ± 0.11	86.67 ± 0.11	79.32 ± 0.19
15	78.08 ± 0.14	83.12 ± 0.24	85.61 ± 0.13	<b>88.09 ± 0.07</b>	86.69 ± 0.07	76.51 ± 0.17	87.70 ± 0.11	78.19 ± 0.17	85.71 ± 0.14	78.15 ± 0.18
16	76.86 ± 0.22	82.11 ± 0.27	84.67 ± 0.15	<b>87.04 ± 0.13</b>	85.66 ± 0.08	75.71 ± 0.18	86.85 ± 0.12	77.03 ± 0.17	84.93 ± 0.14	77.01 ± 0.13
17	75.93 ± 0.16	81.15 ± 0.18	83.81 ± 0.16	<b>86.18 ± 0.10</b>	84.64 ± 0.09	74.56 ± 0.16	85.94 ± 0.11	76.06 ± 0.17	83.65 ± 0.13	76.06 ± 0.15
18	74.85 ± 0.15	79.99 ± 0.23	82.94 ± 0.17	85.18 ± 0.09	83.45 ± 0.11	73.57 ± 0.21	<b>85.20 ± 0.08</b>	75.06 ± 0.16	82.78 ± 0.16	74.97 ± 0.18
19	73.84 ± 0.16	79.39 ± 0.23	82.05 ± 0.15	84.17 ± 0.12	82.54 ± 0.10	72.82 ± 0.20	<b>84.20 ± 0.11</b>	74.04 ± 0.18	81.75 ± 0.13	74.05 ± 0.16
20	73.11 ± 0.14	78.30 ± 0.24	81.26 ± 0.14	83.29 ± 0.13	81.46 ± 0.11	71.83 ± 0.16	<b>83.38 ± 0.10</b>	72.96 ± 0.21	80.73 ± 0.14	72.88 ± 0.18
21	71.88 ± 0.16	77.55 ± 0.22	80.16 ± 0.14	<b>82.46 ± 0.13</b>	80.34 ± 0.12	70.69 ± 0.21	82.44 ± 0.11	72.02 ± 0.14	79.67 ± 0.19	71.98 ± 0.18
22	71.26 ± 0.18	76.62 ± 0.18	79.32 ± 0.14	81.35 ± 0.11	79.37 ± 0.11	69.98 ± 0.25	<b>81.57 ± 0.12</b>	71.19 ± 0.20	78.89 ± 0.17	71.36 ± 0.18
23	70.28 ± 0.16	75.60 ± 0.20	78.27 ± 0.16	80.33 ± 0.10	78.41 ± 0.09	69.00 ± 0.15	<b>80.82 ± 0.09</b>	70.30 ± 0.16	77.77 ± 0.16	70.27 ± 0.18
24	69.33 ± 0.17	74.52 ± 0.20	77.40 ± 0.19	79.45 ± 0.13	77.33 ± 0.09	68.24 ± 0.22	<b>79.90 ± 0.08</b>	69.40 ± 0.14	76.68 ± 0.17	69.43 ± 0.17
25	68.60 ± 0.17	73.89 ± 0.18	76.35 ± 0.15	78.61 ± 0.11	76.36 ± 0.07	67.36 ± 0.14	<b>78.91 ± 0.11</b>	68.57 ± 0.19	75.77 ± 0.19	68.54 ± 0.16
26	67.74 ± 0.20	72.65 ± 0.19	75.32 ± 0.15	77.60 ± 0.11	75.33 ± 0.10	66.80 ± 0.14	<b>78.09 ± 0.13</b>	67.76 ± 0.17	74.95 ± 0.18	67.71 ± 0.19
27	66.97 ± 0.13	72.08 ± 0.22	74.38 ± 0.18	76.70 ± 0.15	74.35 ± 0.11	65.94 ± 0.16	<b>77.17 ± 0.12</b>	67.07 ± 0.18	73.98 ± 0.19	66.87 ± 0.18
28	66.06 ± 0.17	71.32 ± 0.23	73.49 ± 0.18	75.86 ± 0.11	73.51 ± 0.13	65.23 ± 0.18	<b>76.25 ± 0.10</b>	66.26 ± 0.17	73.11 ± 0.13	66.26 ± 0.19
29	65.31 ± 0.16	70.30 ± 0.18	72.58 ± 0.18	74.85 ± 0.13	72.47 ± 0.12	64.54 ± 0.17	<b>75.31 ± 0.13</b>	65.39 ± 0.17	72.08 ± 0.17	65.39 ± 0.20
30	64.64 ± 0.18	69.34 ± 0.29	71.75 ± 0.14	73.89 ± 0.13	71.54 ± 0.12	63.93 ± 0.14	<b>74.45 ± 0.13</b>	64.67 ± 0.17	71.19 ± 0.14	64.50 ± 0.18
31	63.81 ± 0.15	68.78 ± 0.22	70.82 ± 0.17	73.04 ± 0.12	70.60 ± 0.12	63.14 ± 0.17	<b>73.40 ± 0.12</b>	64.07 ± 0.15	70.25 ± 0.22	64.03 ± 0.16
32	63.25 ± 0.17	67.81 ± 0.24	69.85 ± 0.15	72.02 ± 0.13	69.70 ± 0.11	62.52 ± 0.17	<b>72.54 ± 0.10</b>	63.28 ± 0.13	69.40 ± 0.16	63.05 ± 0.15
33	62.67 ± 0.16	67.00 ± 0.25	68.80 ± 0.17	71.28 ± 0.13	68.74 ± 0.11	61.80 ± 0.18	<b>71.62 ± 0.12</b>	62.42 ± 0.13	68.71 ± 0.14	62.66 ± 0.15
34	61.82 ± 0.15	66.16 ± 0.23	68.13 ± 0.14	70.44 ± 0.13	67.92 ± 0.08	61.18 ± 0.16	<b>70.67 ± 0.11</b>	61.77 ± 0.20	67.80 ± 0.18	61.90 ± 0.17
35	61.21 ± 0.20	65.51 ± 0.22	67.33 ± 0.18	69.58 ± 0.14	67.03 ± 0.12	60.51 ± 0.12	<b>69.77 ± 0.10</b>	61.12 ± 0.15	66.93 ± 0.20	61.30 ± 0.18

Continued on Next Page...

Table A.3 – Continued

Load	GU-1	GU-2	GU-3	GU-4	GU-5	GU-6	GU-7	GU-8	GU-9	GU-10
36	60.51 ± 0.16	64.80 ± 0.19	66.53 ± 0.15	68.69 ± 0.14	66.23 ± 0.09	59.97 ± 0.15	<b>68.94 ± 0.09</b>	60.58 ± 0.16	65.98 ± 0.16	60.67 ± 0.16
37	59.78 ± 0.11	64.03 ± 0.21	65.78 ± 0.17	67.89 ± 0.14	65.39 ± 0.10	59.19 ± 0.18	<b>68.03 ± 0.10</b>	59.91 ± 0.14	65.42 ± 0.14	60.00 ± 0.15
38	59.25 ± 0.14	63.25 ± 0.17	64.79 ± 0.18	67.08 ± 0.11	64.61 ± 0.14	58.73 ± 0.16	<b>67.13 ± 0.10</b>	59.42 ± 0.16	64.30 ± 0.15	59.31 ± 0.18
39	58.64 ± 0.17	62.35 ± 0.23	64.00 ± 0.15	<b>66.32 ± 0.13</b>	63.77 ± 0.14	58.16 ± 0.15	66.29 ± 0.10	58.80 ± 0.17	63.80 ± 0.15	58.65 ± 0.16
40	57.99 ± 0.17	61.85 ± 0.22	63.30 ± 0.21	<b>65.48 ± 0.16</b>	62.95 ± 0.11	57.64 ± 0.17	65.37 ± 0.12	58.07 ± 0.15	63.02 ± 0.18	58.06 ± 0.15
41	57.58 ± 0.14	61.08 ± 0.18	62.67 ± 0.17	<b>64.60 ± 0.13</b>	62.29 ± 0.10	56.93 ± 0.15	64.57 ± 0.10	57.45 ± 0.14	62.21 ± 0.16	57.53 ± 0.13
42	56.77 ± 0.17	60.39 ± 0.17	61.91 ± 0.14	<b>63.96 ± 0.15</b>	61.42 ± 0.15	56.40 ± 0.15	63.75 ± 0.11	56.84 ± 0.18	61.57 ± 0.19	56.92 ± 0.14
43	56.26 ± 0.15	59.60 ± 0.24	61.23 ± 0.13	<b>63.10 ± 0.14</b>	60.79 ± 0.12	56.01 ± 0.14	63.01 ± 0.12	56.30 ± 0.14	60.81 ± 0.16	56.35 ± 0.17
44	55.74 ± 0.16	59.04 ± 0.21	60.41 ± 0.20	<b>62.21 ± 0.16</b>	59.96 ± 0.14	55.35 ± 0.12	62.22 ± 0.09	55.86 ± 0.13	60.06 ± 0.18	55.81 ± 0.14
45	55.20 ± 0.14	58.31 ± 0.18	59.60 ± 0.15	<b>61.61 ± 0.14</b>	59.25 ± 0.13	54.79 ± 0.14	61.45 ± 0.09	55.13 ± 0.16	59.38 ± 0.15	55.31 ± 0.14
46	54.58 ± 0.16	57.67 ± 0.17	59.10 ± 0.18	<b>61.13 ± 0.14</b>	58.60 ± 0.10	54.24 ± 0.13	60.68 ± 0.11	54.61 ± 0.15	58.69 ± 0.22	54.68 ± 0.16
47	54.01 ± 0.16	57.08 ± 0.22	58.25 ± 0.16	<b>60.25 ± 0.13</b>	57.78 ± 0.12	53.88 ± 0.12	59.97 ± 0.09	54.14 ± 0.13	58.04 ± 0.21	54.19 ± 0.15
48	53.58 ± 0.16	56.53 ± 0.19	57.71 ± 0.14	<b>59.52 ± 0.15</b>	57.04 ± 0.16	53.38 ± 0.12	59.23 ± 0.09	53.60 ± 0.16	57.39 ± 0.16	53.45 ± 0.18
49	52.99 ± 0.17	55.73 ± 0.21	57.07 ± 0.14	<b>58.75 ± 0.18</b>	56.51 ± 0.14	52.85 ± 0.14	58.40 ± 0.10	53.12 ± 0.13	56.73 ± 0.15	53.08 ± 0.16
50	52.55 ± 0.15	55.24 ± 0.18	56.21 ± 0.17	<b>58.01 ± 0.18</b>	55.80 ± 0.11	52.20 ± 0.13	57.63 ± 0.10	52.45 ± 0.19	55.99 ± 0.18	52.64 ± 0.14
51	51.87 ± 0.14	54.59 ± 0.19	55.72 ± 0.20	<b>57.56 ± 0.19</b>	55.07 ± 0.13	51.74 ± 0.13	57.10 ± 0.10	52.12 ± 0.15	55.58 ± 0.15	52.00 ± 0.18
52	51.42 ± 0.15	54.02 ± 0.22	55.13 ± 0.12	<b>56.91 ± 0.13</b>	54.55 ± 0.13	51.31 ± 0.14	56.28 ± 0.11	51.55 ± 0.13	54.96 ± 0.17	51.43 ± 0.15
53	50.91 ± 0.13	53.42 ± 0.18	54.44 ± 0.14	<b>56.20 ± 0.16</b>	53.78 ± 0.12	50.87 ± 0.11	55.67 ± 0.10	51.11 ± 0.14	54.43 ± 0.16	51.06 ± 0.17
54	50.44 ± 0.14	52.86 ± 0.15	53.99 ± 0.21	<b>55.57 ± 0.14</b>	53.23 ± 0.13	50.32 ± 0.13	54.93 ± 0.10	50.56 ± 0.13	53.66 ± 0.22	50.48 ± 0.14
55	49.94 ± 0.14	52.40 ± 0.19	53.43 ± 0.18	<b>54.86 ± 0.13</b>	52.64 ± 0.15	49.74 ± 0.14	54.32 ± 0.11	50.05 ± 0.13	53.15 ± 0.15	50.03 ± 0.16
56	49.50 ± 0.13	51.93 ± 0.12	52.70 ± 0.18	<b>54.42 ± 0.13</b>	52.13 ± 0.09	49.25 ± 0.18	53.63 ± 0.12	49.61 ± 0.15	52.59 ± 0.21	49.62 ± 0.13
57	49.03 ± 0.16	51.37 ± 0.18	52.20 ± 0.13	<b>53.82 ± 0.15</b>	51.50 ± 0.14	48.80 ± 0.13	52.98 ± 0.10	48.89 ± 0.16	52.07 ± 0.21	49.12 ± 0.14
58	48.52 ± 0.15	50.76 ± 0.18	51.64 ± 0.16	<b>53.40 ± 0.12</b>	50.93 ± 0.12	48.31 ± 0.14	52.43 ± 0.13	48.52 ± 0.13	51.50 ± 0.19	48.69 ± 0.16
59	48.05 ± 0.11	50.25 ± 0.16	51.24 ± 0.20	<b>52.62 ± 0.09</b>	50.34 ± 0.14	47.94 ± 0.11	51.76 ± 0.10	48.14 ± 0.14	51.07 ± 0.17	48.08 ± 0.15
60	47.52 ± 0.15	49.58 ± 0.18	50.67 ± 0.17	<b>51.98 ± 0.14</b>	49.86 ± 0.12	47.37 ± 0.14	51.15 ± 0.09	47.61 ± 0.14	50.42 ± 0.18	47.52 ± 0.15

## Appendix B

# Appendix FSAC Flexible Spectrum Dataset

Table B.1: Flexible Spectrum dataset of the Success ratio for FSAC PCs on the small network topology.

Load	GU-1	GU-2	GU-3	GU-4	GU-5	GU-6	GU-7	GU-8	GU-9	GU-10
2	96.82 ± 0.04	95.80 ± 0.26	95.45 ± 0.22	<b>98.03 ± 0.05</b>	97.62 ± 0.04	95.88 ± 0.20	96.86 ± 0.09	97.40 ± 0.10	95.75 ± 0.23	97.93 ± 0.07
4	91.53 ± 0.07	88.79 ± 0.49	90.55 ± 0.27	<b>93.98 ± 0.15</b>	92.57 ± 0.11	90.87 ± 0.25	91.96 ± 0.16	92.83 ± 0.15	90.56 ± 0.32	93.55 ± 0.16
6	85.71 ± 0.08	83.36 ± 0.52	85.28 ± 0.34	<b>89.27 ± 0.20</b>	87.05 ± 0.11	85.65 ± 0.32	86.79 ± 0.15	87.27 ± 0.19	84.80 ± 0.30	88.25 ± 0.22
8	80.02 ± 0.09	77.99 ± 0.41	80.89 ± 0.41	<b>83.99 ± 0.31</b>	80.66 ± 0.29	80.85 ± 0.33	81.57 ± 0.25	81.37 ± 0.25	80.19 ± 0.24	82.77 ± 0.23
10	74.79 ± 0.11	72.98 ± 0.48	77.42 ± 0.38	<b>78.62 ± 0.34</b>	75.73 ± 0.26	77.58 ± 0.31	77.08 ± 0.30	76.29 ± 0.27	75.26 ± 0.41	77.10 ± 0.40
12	69.88 ± 0.13	68.51 ± 0.30	72.27 ± 0.43	<b>73.72 ± 0.35</b>	70.54 ± 0.37	73.58 ± 0.35	72.56 ± 0.35	70.98 ± 0.30	70.88 ± 0.35	72.30 ± 0.35
14	65.53 ± 0.14	64.94 ± 0.46	67.79 ± 0.50	<b>69.40 ± 0.38</b>	65.88 ± 0.42	68.25 ± 0.39	67.76 ± 0.39	66.82 ± 0.40	66.37 ± 0.38	68.24 ± 0.33
16	61.27 ± 0.11	61.87 ± 0.45	62.06 ± 0.60	<b>65.89 ± 0.33</b>	62.20 ± 0.33	62.99 ± 0.44	62.74 ± 0.38	62.95 ± 0.34	61.36 ± 0.41	64.34 ± 0.40
18	57.81 ± 0.12	59.07 ± 0.46	58.67 ± 0.49	<b>61.87 ± 0.48</b>	58.56 ± 0.35	58.31 ± 0.35	58.17 ± 0.38	59.83 ± 0.38	57.57 ± 0.36	60.81 ± 0.39
20	54.35 ± 0.15	57.13 ± 0.31	54.61 ± 0.37	<b>59.17 ± 0.40</b>	55.64 ± 0.39	54.63 ± 0.40	54.52 ± 0.32	56.32 ± 0.51	54.30 ± 0.47	58.13 ± 0.48
22	51.34 ± 0.15	54.29 ± 0.49	52.01 ± 0.42	<b>56.15 ± 0.35</b>	53.03 ± 0.37	51.66 ± 0.29	51.19 ± 0.45	53.87 ± 0.41	51.70 ± 0.45	55.18 ± 0.41
24	48.33 ± 0.21	51.86 ± 0.40	49.27 ± 0.47	<b>53.70 ± 0.44</b>	50.58 ± 0.31	48.66 ± 0.37	48.05 ± 0.41	51.21 ± 0.38	49.35 ± 0.43	52.93 ± 0.39
26	45.74 ± 0.18	50.42 ± 0.42	47.06 ± 0.45	<b>51.23 ± 0.34</b>	48.37 ± 0.37	46.63 ± 0.37	46.09 ± 0.43	48.69 ± 0.56	47.95 ± 0.31	50.59 ± 0.44
28	43.25 ± 0.19	48.43 ± 0.44	45.47 ± 0.31	<b>49.13 ± 0.34</b>	46.63 ± 0.31	44.50 ± 0.30	43.85 ± 0.44	47.25 ± 0.48	45.84 ± 0.35	48.83 ± 0.38
30	41.06 ± 0.17	46.77 ± 0.31	43.62 ± 0.42	<b>47.30 ± 0.32</b>	44.94 ± 0.35	42.39 ± 0.40	42.21 ± 0.37	45.23 ± 0.32	44.50 ± 0.36	46.94 ± 0.41
32	39.01 ± 0.17	44.99 ± 0.33	42.64 ± 0.40	<b>45.43 ± 0.30</b>	42.75 ± 0.35	41.08 ± 0.36	40.77 ± 0.29	43.49 ± 0.36	42.95 ± 0.42	45.05 ± 0.46
34	37.01 ± 0.18	<b>44.07 ± 0.38</b>	41.61 ± 0.38	43.72 ± 0.36	41.78 ± 0.28	39.49 ± 0.39	39.07 ± 0.31	41.66 ± 0.45	42.09 ± 0.36	43.67 ± 0.26
36	35.42 ± 0.14	<b>42.43 ± 0.31</b>	40.66 ± 0.37	41.78 ± 0.25	39.89 ± 0.25	38.11 ± 0.36	37.58 ± 0.34	39.92 ± 0.36	41.26 ± 0.28	42.15 ± 0.38
38	33.47 ± 0.23	<b>41.23 ± 0.26</b>	39.84 ± 0.30	40.66 ± 0.27	38.99 ± 0.31	36.68 ± 0.24	36.24 ± 0.41	38.37 ± 0.42	40.12 ± 0.39	40.60 ± 0.29
40	31.87 ± 0.15	<b>39.97 ± 0.34</b>	38.62 ± 0.38	38.93 ± 0.33	37.50 ± 0.26	35.73 ± 0.36	35.41 ± 0.33	36.59 ± 0.35	39.27 ± 0.35	39.16 ± 0.25
42	30.45 ± 0.17	<b>38.53 ± 0.39</b>	37.69 ± 0.33	37.52 ± 0.36	36.34 ± 0.27	34.49 ± 0.36	34.28 ± 0.36	35.36 ± 0.36	38.37 ± 0.29	38.01 ± 0.30
44	28.98 ± 0.16	<b>37.68 ± 0.28</b>	36.95 ± 0.33	36.51 ± 0.37	35.23 ± 0.25	33.59 ± 0.36	32.94 ± 0.31	33.96 ± 0.46	37.63 ± 0.30	37.11 ± 0.32
46	27.85 ± 0.15	<b>36.98 ± 0.31</b>	36.20 ± 0.34	35.12 ± 0.30	34.29 ± 0.25	32.16 ± 0.29	31.89 ± 0.26	32.70 ± 0.36	36.90 ± 0.26	35.89 ± 0.26
48	26.37 ± 0.17	35.87 ± 0.36	35.35 ± 0.26	33.83 ± 0.32	33.07 ± 0.28	31.40 ± 0.33	30.98 ± 0.25	31.36 ± 0.41	<b>36.09 ± 0.27</b>	34.46 ± 0.27
50	25.22 ± 0.16	34.83 ± 0.33	34.86 ± 0.28	32.62 ± 0.24	32.00 ± 0.32	30.69 ± 0.27	29.99 ± 0.27	30.18 ± 0.42	<b>35.10 ± 0.33</b>	33.59 ± 0.23
52	24.09 ± 0.17	34.00 ± 0.27	33.98 ± 0.27	31.57 ± 0.27	31.06 ± 0.27	29.38 ± 0.34	28.65 ± 0.34	29.14 ± 0.37	<b>34.37 ± 0.26</b>	32.74 ± 0.25
54	22.95 ± 0.14	33.24 ± 0.29	33.29 ± 0.41	30.48 ± 0.25	30.03 ± 0.26	28.51 ± 0.38	27.81 ± 0.30	27.97 ± 0.37	<b>33.65 ± 0.31</b>	31.50 ± 0.23
56	21.80 ± 0.17	32.11 ± 0.29	32.29 ± 0.29	29.56 ± 0.27	29.26 ± 0.22	27.31 ± 0.23	26.89 ± 0.34	26.47 ± 0.53	<b>32.96 ± 0.28</b>	30.83 ± 0.27
58	20.87 ± 0.14	31.33 ± 0.32	31.73 ± 0.23	28.66 ± 0.20	28.25 ± 0.26	26.48 ± 0.23	26.14 ± 0.26	25.82 ± 0.45	<b>32.33 ± 0.20</b>	29.75 ± 0.26
60	19.80 ± 0.14	30.87 ± 0.27	31.11 ± 0.26	27.47 ± 0.30	27.54 ± 0.25	25.38 ± 0.23	24.93 ± 0.30	25.10 ± 0.38	<b>31.63 ± 0.30</b>	29.06 ± 0.24
62	18.87 ± 0.18	30.30 ± 0.29	30.39 ± 0.28	26.71 ± 0.21	26.60 ± 0.26	24.38 ± 0.17	24.12 ± 0.29	23.75 ± 0.50	<b>30.99 ± 0.27</b>	27.95 ± 0.28
64	18.13 ± 0.12	29.76 ± 0.22	30.01 ± 0.30	25.75 ± 0.19	25.79 ± 0.27	23.83 ± 0.24	23.25 ± 0.24	23.20 ± 0.43	<b>30.20 ± 0.18</b>	27.25 ± 0.23
66	17.30 ± 0.13	28.89 ± 0.23	29.11 ± 0.31	25.01 ± 0.22	25.10 ± 0.28	22.74 ± 0.30	22.59 ± 0.30	22.20 ± 0.35	<b>29.73 ± 0.24</b>	26.54 ± 0.24
68	16.57 ± 0.17	28.13 ± 0.25	28.57 ± 0.26	24.22 ± 0.26	24.02 ± 0.19	22.09 ± 0.18	21.60 ± 0.24	21.25 ± 0.36	<b>28.97 ± 0.22</b>	25.79 ± 0.19
70	15.66 ± 0.13	27.82 ± 0.22	27.81 ± 0.29	23.35 ± 0.19	23.30 ± 0.23	21.06 ± 0.19	20.87 ± 0.21	20.56 ± 0.44	<b>28.34 ± 0.22</b>	25.00 ± 0.23

Continued on Next Page...

Table B.1 – Continued

Load	GU-1	GU-2	GU-3	GU-4	GU-5	GU-6	GU-7	GU-8	GU-9	GU-10
72	14.94 ± 0.12	27.15 ± 0.21	27.35 ± 0.20	22.64 ± 0.22	22.69 ± 0.24	20.16 ± 0.25	19.75 ± 0.29	19.92 ± 0.31	<b>27.54 ± 0.20</b>	24.21 ± 0.15
74	14.43 ± 0.10	26.49 ± 0.24	26.73 ± 0.28	21.88 ± 0.25	21.96 ± 0.17	19.55 ± 0.29	19.01 ± 0.19	19.15 ± 0.40	<b>26.68 ± 0.22</b>	23.46 ± 0.18
76	13.73 ± 0.16	25.89 ± 0.21	26.05 ± 0.23	21.22 ± 0.19	21.02 ± 0.22	18.67 ± 0.22	18.15 ± 0.24	18.61 ± 0.30	<b>26.10 ± 0.22</b>	22.79 ± 0.25
78	13.19 ± 0.12	25.32 ± 0.23	25.19 ± 0.25	20.36 ± 0.22	20.52 ± 0.16	17.90 ± 0.18	17.57 ± 0.23	17.44 ± 0.37	<b>25.38 ± 0.23</b>	22.32 ± 0.25
80	12.47 ± 0.13	24.55 ± 0.21	24.73 ± 0.24	19.78 ± 0.16	19.56 ± 0.18	17.20 ± 0.19	16.79 ± 0.23	16.86 ± 0.34	<b>24.68 ± 0.24</b>	21.37 ± 0.21
82	11.95 ± 0.10	<b>24.10 ± 0.18</b>	23.94 ± 0.22	19.11 ± 0.22	19.09 ± 0.17	16.13 ± 0.22	15.94 ± 0.25	16.56 ± 0.27	24.00 ± 0.21	20.76 ± 0.18
84	11.36 ± 0.08	23.43 ± 0.25	<b>23.48 ± 0.21</b>	18.34 ± 0.21	18.43 ± 0.15	15.66 ± 0.24	15.41 ± 0.26	15.51 ± 0.34	23.09 ± 0.23	20.23 ± 0.22
86	10.86 ± 0.11	<b>22.93 ± 0.20</b>	22.80 ± 0.25	17.72 ± 0.20	17.90 ± 0.18	14.83 ± 0.22	14.56 ± 0.17	14.57 ± 0.28	22.50 ± 0.18	19.38 ± 0.22
88	10.22 ± 0.10	<b>22.44 ± 0.25</b>	22.11 ± 0.24	17.04 ± 0.18	17.25 ± 0.18	14.15 ± 0.21	14.00 ± 0.16	14.17 ± 0.39	21.87 ± 0.24	18.73 ± 0.16
90	9.83 ± 0.11	<b>21.87 ± 0.18</b>	21.53 ± 0.20	16.40 ± 0.19	16.40 ± 0.19	13.46 ± 0.20	13.18 ± 0.18	13.31 ± 0.37	20.97 ± 0.22	18.33 ± 0.16

Table B.2: Flexible Spectrum dataset of the Success ratio for FSAC PCs on the medium network topology.

Load	GU-1	GU-2	GU-3	GU-4	GU-5	GU-6	GU-7	GU-8	GU-9	GU-10
2	98.92 ± 0.01	98.64 ± 0.05	98.64 ± 0.04	99.15 ± 0.03	<b>99.35 ± 0.01</b>	98.70 ± 0.04	98.88 ± 0.02	98.99 ± 0.02	98.67 ± 0.04	99.07 ± 0.02
4	97.57 ± 0.02	96.72 ± 0.07	96.84 ± 0.09	98.11 ± 0.04	<b>98.27 ± 0.02</b>	96.85 ± 0.09	97.30 ± 0.05	97.75 ± 0.04	96.77 ± 0.08	97.91 ± 0.04
6	96.12 ± 0.02	94.67 ± 0.11	94.81 ± 0.11	<b>97.08 ± 0.05</b>	96.96 ± 0.04	94.82 ± 0.12	95.61 ± 0.07	96.31 ± 0.04	94.75 ± 0.14	96.55 ± 0.05
8	94.60 ± 0.05	92.30 ± 0.17	92.70 ± 0.17	<b>95.92 ± 0.04</b>	95.47 ± 0.06	92.89 ± 0.13	93.70 ± 0.08	94.63 ± 0.07	92.54 ± 0.14	95.13 ± 0.05
10	93.04 ± 0.04	90.40 ± 0.14	90.86 ± 0.16	<b>94.62 ± 0.07</b>	93.89 ± 0.05	91.23 ± 0.16	92.29 ± 0.09	92.84 ± 0.08	90.83 ± 0.14	93.33 ± 0.07
12	91.34 ± 0.06	88.01 ± 0.16	89.28 ± 0.16	<b>93.24 ± 0.08</b>	92.20 ± 0.08	89.43 ± 0.15	90.67 ± 0.09	90.83 ± 0.10	88.83 ± 0.15	91.63 ± 0.07
14	89.55 ± 0.05	85.69 ± 0.21	87.74 ± 0.17	<b>91.81 ± 0.07</b>	90.39 ± 0.07	87.81 ± 0.15	89.23 ± 0.11	88.89 ± 0.07	86.88 ± 0.16	89.68 ± 0.10
16	87.69 ± 0.08	83.48 ± 0.20	86.09 ± 0.15	<b>90.25 ± 0.11</b>	88.45 ± 0.10	86.54 ± 0.18	88.04 ± 0.11	86.71 ± 0.10	84.98 ± 0.15	87.74 ± 0.13
18	85.95 ± 0.07	81.38 ± 0.22	84.56 ± 0.18	<b>88.73 ± 0.11</b>	86.69 ± 0.08	85.40 ± 0.23	86.80 ± 0.10	84.62 ± 0.09	83.19 ± 0.18	85.70 ± 0.12
20	84.11 ± 0.07	79.38 ± 0.27	83.12 ± 0.17	<b>87.31 ± 0.12</b>	84.79 ± 0.13	84.31 ± 0.17	85.44 ± 0.13	82.44 ± 0.12	81.47 ± 0.14	83.77 ± 0.11
22	82.37 ± 0.09	77.64 ± 0.21	81.62 ± 0.20	<b>85.41 ± 0.12</b>	82.81 ± 0.12	83.10 ± 0.18	84.02 ± 0.10	80.51 ± 0.08	79.69 ± 0.21	81.86 ± 0.12
24	80.61 ± 0.09	75.91 ± 0.29	80.00 ± 0.16	<b>83.86 ± 0.15</b>	81.19 ± 0.13	81.83 ± 0.17	82.58 ± 0.14	78.29 ± 0.14	77.87 ± 0.20	79.69 ± 0.15
26	78.98 ± 0.10	74.28 ± 0.26	78.45 ± 0.15	<b>82.22 ± 0.15</b>	79.24 ± 0.14	80.61 ± 0.18	81.01 ± 0.13	76.42 ± 0.14	75.95 ± 0.18	77.87 ± 0.16
28	77.39 ± 0.11	72.69 ± 0.30	77.04 ± 0.16	<b>80.68 ± 0.16</b>	77.47 ± 0.15	79.10 ± 0.17	79.67 ± 0.10	74.57 ± 0.10	74.32 ± 0.14	75.94 ± 0.13
30	75.62 ± 0.11	71.16 ± 0.27	75.15 ± 0.28	<b>78.94 ± 0.21</b>	75.96 ± 0.11	77.47 ± 0.21	78.05 ± 0.15	72.69 ± 0.13	72.38 ± 0.20	74.16 ± 0.20
32	74.12 ± 0.09	69.88 ± 0.29	73.77 ± 0.19	<b>77.46 ± 0.17</b>	74.24 ± 0.14	75.69 ± 0.23	76.45 ± 0.18	71.03 ± 0.15	70.77 ± 0.23	72.47 ± 0.13
34	72.48 ± 0.10	68.61 ± 0.27	72.14 ± 0.18	<b>75.58 ± 0.17</b>	72.53 ± 0.14	74.24 ± 0.22	74.82 ± 0.16	69.61 ± 0.16	68.98 ± 0.19	70.68 ± 0.18
36	71.14 ± 0.11	67.27 ± 0.31	70.61 ± 0.20	<b>74.11 ± 0.16</b>	70.89 ± 0.15	72.71 ± 0.11	73.22 ± 0.14	67.95 ± 0.14	67.28 ± 0.17	69.08 ± 0.19
38	69.55 ± 0.10	65.93 ± 0.29	68.84 ± 0.24	<b>72.73 ± 0.16</b>	69.52 ± 0.17	71.12 ± 0.16	71.36 ± 0.18	67.01 ± 0.14	65.77 ± 0.18	67.65 ± 0.19
40	68.12 ± 0.12	64.53 ± 0.25	67.46 ± 0.20	<b>71.28 ± 0.20</b>	68.04 ± 0.13	69.39 ± 0.19	69.44 ± 0.19	65.62 ± 0.19	64.06 ± 0.17	66.21 ± 0.19
42	66.72 ± 0.16	63.38 ± 0.24	65.54 ± 0.22	<b>69.85 ± 0.17</b>	66.38 ± 0.14	67.64 ± 0.20	67.82 ± 0.18	64.76 ± 0.17	62.58 ± 0.19	64.74 ± 0.21
44	65.26 ± 0.12	62.36 ± 0.29	64.11 ± 0.26	<b>68.38 ± 0.17</b>	65.15 ± 0.15	65.67 ± 0.18	65.97 ± 0.20	63.70 ± 0.17	61.29 ± 0.14	63.48 ± 0.16
46	64.04 ± 0.08	61.08 ± 0.22	62.68 ± 0.19	<b>67.07 ± 0.20</b>	63.92 ± 0.18	64.11 ± 0.19	64.25 ± 0.16	62.56 ± 0.18	59.86 ± 0.18	62.21 ± 0.19
48	62.75 ± 0.14	60.28 ± 0.18	61.31 ± 0.22	<b>65.70 ± 0.17</b>	62.57 ± 0.13	62.34 ± 0.25	62.54 ± 0.16	61.44 ± 0.22	58.46 ± 0.18	60.94 ± 0.18
50	61.44 ± 0.11	59.42 ± 0.25	59.65 ± 0.18	<b>64.41 ± 0.15</b>	61.23 ± 0.15	60.72 ± 0.21	60.99 ± 0.18	60.32 ± 0.19	57.19 ± 0.16	59.74 ± 0.20
52	60.10 ± 0.12	58.22 ± 0.20	58.25 ± 0.26	<b>63.25 ± 0.19</b>	60.24 ± 0.14	59.23 ± 0.17	59.39 ± 0.18	59.29 ± 0.17	56.08 ± 0.22	58.71 ± 0.20
54	58.87 ± 0.12	57.53 ± 0.26	57.23 ± 0.20	<b>62.03 ± 0.22</b>	58.94 ± 0.16	57.80 ± 0.21	57.91 ± 0.19	58.26 ± 0.22	54.99 ± 0.15	57.57 ± 0.20
56	57.87 ± 0.10	56.59 ± 0.21	55.97 ± 0.20	<b>60.81 ± 0.17</b>	57.86 ± 0.19	56.28 ± 0.18	56.57 ± 0.19	57.15 ± 0.17	54.06 ± 0.21	56.38 ± 0.21
58	56.75 ± 0.15	55.58 ± 0.26	55.15 ± 0.24	<b>59.71 ± 0.19</b>	56.93 ± 0.22	54.92 ± 0.22	55.21 ± 0.16	56.04 ± 0.23	52.90 ± 0.19	55.43 ± 0.23
60	55.42 ± 0.14	55.03 ± 0.24	54.01 ± 0.22	<b>58.49 ± 0.20</b>	55.90 ± 0.19	53.82 ± 0.22	54.14 ± 0.19	55.32 ± 0.16	52.01 ± 0.22	54.71 ± 0.21
62	54.52 ± 0.13	53.85 ± 0.25	52.95 ± 0.29	<b>57.56 ± 0.15</b>	54.87 ± 0.18	52.64 ± 0.17	53.00 ± 0.18	54.34 ± 0.16	51.24 ± 0.18	53.82 ± 0.21
64	53.54 ± 0.14	53.33 ± 0.19	52.02 ± 0.17	<b>56.50 ± 0.25</b>	54.07 ± 0.16	51.45 ± 0.20	51.86 ± 0.26	53.38 ± 0.19	50.46 ± 0.21	52.95 ± 0.19
66	52.55 ± 0.14	52.66 ± 0.23	51.04 ± 0.29	<b>55.71 ± 0.16</b>	52.90 ± 0.20	50.37 ± 0.25	50.78 ± 0.20	52.73 ± 0.19	49.48 ± 0.27	52.02 ± 0.18
68	51.57 ± 0.12	52.04 ± 0.16	50.06 ± 0.23	<b>54.72 ± 0.16</b>	52.14 ± 0.18	49.58 ± 0.19	49.89 ± 0.16	51.57 ± 0.21	48.84 ± 0.19	51.25 ± 0.21
70	50.69 ± 0.15	51.16 ± 0.23	49.47 ± 0.22	<b>53.86 ± 0.18</b>	51.46 ± 0.13	48.75 ± 0.25	49.12 ± 0.23	51.02 ± 0.20	48.18 ± 0.21	50.71 ± 0.18

Continued on Next Page...

Table B.2 – Continued

Load	GU-1	GU-2	GU-3	GU-4	GU-5	GU-6	GU-7	GU-8	GU-9	GU-10
72	49.73 ± 0.13	50.37 ± 0.24	48.58 ± 0.23	<b>52.81 ± 0.20</b>	50.64 ± 0.18	47.80 ± 0.23	48.18 ± 0.19	50.21 ± 0.22	47.27 ± 0.18	49.81 ± 0.19
74	48.96 ± 0.15	49.96 ± 0.27	47.97 ± 0.23	<b>51.95 ± 0.24</b>	49.88 ± 0.14	47.23 ± 0.19	47.44 ± 0.17	49.39 ± 0.19	46.59 ± 0.22	49.07 ± 0.21
76	48.12 ± 0.18	49.21 ± 0.21	47.30 ± 0.22	<b>51.03 ± 0.18</b>	49.10 ± 0.17	46.42 ± 0.21	46.49 ± 0.20	48.58 ± 0.20	46.20 ± 0.18	48.62 ± 0.17
78	47.18 ± 0.17	48.55 ± 0.29	46.58 ± 0.18	<b>50.62 ± 0.14</b>	48.38 ± 0.19	45.60 ± 0.21	45.80 ± 0.15	48.04 ± 0.27	45.53 ± 0.21	47.73 ± 0.23
80	46.55 ± 0.14	48.00 ± 0.20	46.03 ± 0.27	<b>49.83 ± 0.20</b>	47.60 ± 0.22	45.06 ± 0.18	45.25 ± 0.22	47.28 ± 0.16	45.05 ± 0.17	47.31 ± 0.17
82	45.77 ± 0.14	47.41 ± 0.22	45.31 ± 0.18	<b>48.86 ± 0.22</b>	47.13 ± 0.25	44.17 ± 0.16	44.66 ± 0.18	46.60 ± 0.19	44.49 ± 0.17	46.76 ± 0.21
84	44.94 ± 0.16	46.79 ± 0.18	44.47 ± 0.23	<b>48.53 ± 0.17</b>	46.31 ± 0.16	43.58 ± 0.16	43.88 ± 0.21	46.10 ± 0.16	43.78 ± 0.19	46.24 ± 0.18
86	44.15 ± 0.17	46.55 ± 0.14	44.42 ± 0.23	<b>47.64 ± 0.18</b>	45.75 ± 0.19	43.07 ± 0.23	43.39 ± 0.15	45.72 ± 0.20	43.53 ± 0.15	45.69 ± 0.19
88	43.44 ± 0.19	45.79 ± 0.16	43.37 ± 0.18	<b>47.04 ± 0.19</b>	45.22 ± 0.20	42.49 ± 0.22	42.67 ± 0.18	44.90 ± 0.18	42.78 ± 0.19	45.03 ± 0.18
90	42.94 ± 0.15	45.20 ± 0.21	42.99 ± 0.12	<b>46.21 ± 0.18</b>	44.78 ± 0.18	42.15 ± 0.21	42.07 ± 0.17	44.49 ± 0.23	42.43 ± 0.18	44.45 ± 0.14

Table B.3: Flexible Spectrum dataset of the Success ratio for FSAC PCs on the large network topology.

Load	GU-1	GU-2	GU-3	GU-4	GU-5	GU-6	GU-7	GU-8	GU-9	GU-10
2	97.61 ± 0.01	97.14 ± 0.05	97.16 ± 0.05	97.74 ± 0.02	<b>97.84 ± 0.01</b>	97.15 ± 0.04	97.28 ± 0.04	97.52 ± 0.02	97.18 ± 0.05	97.54 ± 0.02
4	94.62 ± 0.03	93.18 ± 0.08	93.29 ± 0.07	<b>94.92 ± 0.03</b>	94.48 ± 0.02	93.41 ± 0.08	93.75 ± 0.05	94.27 ± 0.03	93.23 ± 0.06	94.37 ± 0.04
6	91.21 ± 0.03	88.97 ± 0.10	89.47 ± 0.10	<b>91.73 ± 0.04</b>	90.68 ± 0.03	89.78 ± 0.11	90.33 ± 0.06	90.70 ± 0.04	89.28 ± 0.09	90.80 ± 0.04
8	87.69 ± 0.04	84.79 ± 0.11	86.01 ± 0.09	<b>88.28 ± 0.05</b>	86.69 ± 0.03	86.51 ± 0.10	87.06 ± 0.06	86.90 ± 0.05	85.36 ± 0.08	87.10 ± 0.06
10	84.01 ± 0.04	80.58 ± 0.13	82.17 ± 0.11	<b>84.71 ± 0.06</b>	82.77 ± 0.04	83.23 ± 0.13	83.70 ± 0.06	83.19 ± 0.05	81.41 ± 0.10	83.38 ± 0.05
12	80.39 ± 0.05	76.77 ± 0.16	78.24 ± 0.12	<b>81.11 ± 0.05</b>	78.93 ± 0.04	79.62 ± 0.13	80.01 ± 0.08	79.56 ± 0.06	77.50 ± 0.10	79.76 ± 0.06
14	76.80 ± 0.06	73.12 ± 0.16	74.50 ± 0.10	<b>77.63 ± 0.06</b>	75.19 ± 0.04	75.66 ± 0.10	76.06 ± 0.07	76.14 ± 0.06	74.04 ± 0.11	76.27 ± 0.07
16	73.38 ± 0.04	69.97 ± 0.14	71.22 ± 0.12	<b>74.17 ± 0.06</b>	71.64 ± 0.04	71.98 ± 0.09	72.39 ± 0.07	73.02 ± 0.09	70.76 ± 0.10	73.02 ± 0.06
18	70.12 ± 0.06	66.87 ± 0.12	68.01 ± 0.10	<b>70.98 ± 0.08</b>	68.31 ± 0.06	68.40 ± 0.08	68.83 ± 0.08	69.96 ± 0.06	67.67 ± 0.11	69.85 ± 0.06
20	67.08 ± 0.05	63.92 ± 0.17	65.00 ± 0.09	<b>67.83 ± 0.05</b>	65.22 ± 0.06	65.22 ± 0.09	65.36 ± 0.07	67.06 ± 0.06	64.81 ± 0.10	66.93 ± 0.06
22	64.12 ± 0.06	61.24 ± 0.13	62.17 ± 0.09	<b>64.98 ± 0.05</b>	62.32 ± 0.05	61.84 ± 0.08	62.03 ± 0.07	64.35 ± 0.07	61.92 ± 0.07	64.17 ± 0.05
24	61.39 ± 0.05	58.60 ± 0.13	59.46 ± 0.09	<b>62.20 ± 0.08</b>	59.63 ± 0.05	58.82 ± 0.10	58.96 ± 0.10	61.75 ± 0.06	59.29 ± 0.11	61.61 ± 0.06
26	58.80 ± 0.06	56.13 ± 0.13	57.06 ± 0.10	<b>59.62 ± 0.07</b>	57.05 ± 0.06	55.89 ± 0.09	56.19 ± 0.06	59.16 ± 0.06	56.86 ± 0.09	59.22 ± 0.06
28	56.42 ± 0.06	54.07 ± 0.14	54.85 ± 0.12	<b>57.22 ± 0.06</b>	54.78 ± 0.05	53.40 ± 0.10	53.71 ± 0.08	56.86 ± 0.08	54.62 ± 0.08	56.97 ± 0.07
30	54.21 ± 0.04	51.89 ± 0.14	52.73 ± 0.09	<b>55.06 ± 0.07</b>	52.63 ± 0.05	51.22 ± 0.11	51.48 ± 0.09	54.78 ± 0.08	52.69 ± 0.08	54.84 ± 0.07
32	52.11 ± 0.05	50.07 ± 0.12	50.77 ± 0.10	<b>52.96 ± 0.07</b>	50.63 ± 0.05	49.09 ± 0.07	49.47 ± 0.08	52.66 ± 0.08	50.67 ± 0.08	52.92 ± 0.08
34	50.22 ± 0.04	48.29 ± 0.15	48.98 ± 0.09	50.99 ± 0.09	48.77 ± 0.06	47.23 ± 0.12	47.49 ± 0.09	50.65 ± 0.06	48.85 ± 0.08	<b>51.05 ± 0.08</b>
36	48.37 ± 0.05	46.59 ± 0.12	47.25 ± 0.09	49.17 ± 0.07	47.13 ± 0.05	45.43 ± 0.09	45.77 ± 0.09	48.90 ± 0.08	47.25 ± 0.09	<b>49.34 ± 0.05</b>
38	46.77 ± 0.05	45.07 ± 0.10	45.65 ± 0.09	47.54 ± 0.07	45.51 ± 0.08	43.86 ± 0.10	44.04 ± 0.08	47.27 ± 0.07	45.71 ± 0.07	<b>47.68 ± 0.08</b>
40	45.23 ± 0.05	43.51 ± 0.13	43.99 ± 0.10	45.93 ± 0.09	44.05 ± 0.06	42.40 ± 0.09	42.53 ± 0.07	45.63 ± 0.09	44.20 ± 0.09	<b>46.26 ± 0.05</b>
42	43.74 ± 0.05	42.19 ± 0.13	42.78 ± 0.09	44.48 ± 0.09	42.63 ± 0.07	40.95 ± 0.11	41.23 ± 0.07	44.24 ± 0.07	42.68 ± 0.08	<b>44.77 ± 0.07</b>
44	42.32 ± 0.04	40.96 ± 0.14	41.40 ± 0.08	43.14 ± 0.08	41.38 ± 0.07	39.55 ± 0.10	39.81 ± 0.06	42.88 ± 0.07	41.41 ± 0.10	<b>43.38 ± 0.09</b>
46	41.06 ± 0.06	39.77 ± 0.15	40.14 ± 0.09	41.83 ± 0.08	40.16 ± 0.07	38.41 ± 0.10	38.59 ± 0.08	41.58 ± 0.08	40.14 ± 0.09	<b>42.05 ± 0.09</b>
48	39.87 ± 0.06	38.78 ± 0.12	38.95 ± 0.08	40.66 ± 0.11	39.04 ± 0.05	37.23 ± 0.10	37.50 ± 0.07	40.40 ± 0.07	38.90 ± 0.10	<b>40.98 ± 0.08</b>
50	38.67 ± 0.06	37.70 ± 0.12	37.84 ± 0.09	39.54 ± 0.09	37.99 ± 0.06	36.01 ± 0.09	36.31 ± 0.07	39.29 ± 0.08	37.80 ± 0.09	<b>39.78 ± 0.07</b>
52	37.71 ± 0.05	36.61 ± 0.12	36.84 ± 0.07	38.45 ± 0.09	36.96 ± 0.07	35.16 ± 0.09	35.41 ± 0.08	38.23 ± 0.09	36.66 ± 0.08	<b>38.70 ± 0.07</b>
54	36.64 ± 0.05	35.72 ± 0.09	35.77 ± 0.09	37.48 ± 0.10	36.01 ± 0.07	34.09 ± 0.09	34.40 ± 0.10	37.29 ± 0.06	35.75 ± 0.10	<b>37.77 ± 0.08</b>
56	35.74 ± 0.07	34.93 ± 0.11	34.90 ± 0.08	36.55 ± 0.07	35.13 ± 0.07	33.38 ± 0.09	33.51 ± 0.11	36.26 ± 0.07	34.75 ± 0.10	<b>36.75 ± 0.10</b>
58	34.89 ± 0.05	34.01 ± 0.11	33.93 ± 0.10	35.67 ± 0.07	34.25 ± 0.08	32.48 ± 0.11	32.62 ± 0.08	35.44 ± 0.07	33.91 ± 0.09	<b>35.96 ± 0.06</b>
60	34.05 ± 0.06	33.28 ± 0.13	33.04 ± 0.13	34.75 ± 0.09	33.53 ± 0.06	31.74 ± 0.10	31.99 ± 0.08	34.59 ± 0.07	33.04 ± 0.08	<b>34.98 ± 0.09</b>
62	33.22 ± 0.06	32.66 ± 0.11	32.36 ± 0.08	34.02 ± 0.07	32.80 ± 0.07	30.99 ± 0.10	31.18 ± 0.09	33.75 ± 0.07	32.29 ± 0.08	<b>34.19 ± 0.08</b>
64	32.46 ± 0.05	31.96 ± 0.11	31.58 ± 0.07	33.31 ± 0.07	32.07 ± 0.08	30.31 ± 0.08	30.55 ± 0.09	33.01 ± 0.08	31.55 ± 0.07	<b>33.44 ± 0.07</b>
66	31.76 ± 0.05	31.22 ± 0.12	30.83 ± 0.07	32.51 ± 0.06	31.41 ± 0.07	29.80 ± 0.09	29.94 ± 0.06	32.37 ± 0.08	30.91 ± 0.09	<b>32.66 ± 0.09</b>
68	31.11 ± 0.04	30.53 ± 0.11	30.11 ± 0.11	31.82 ± 0.09	30.76 ± 0.07	29.05 ± 0.09	29.28 ± 0.08	31.67 ± 0.08	30.18 ± 0.10	<b>31.99 ± 0.07</b>
70	30.48 ± 0.05	30.02 ± 0.11	29.59 ± 0.09	31.24 ± 0.07	30.13 ± 0.07	28.49 ± 0.09	28.71 ± 0.06	31.00 ± 0.07	29.57 ± 0.09	<b>31.36 ± 0.07</b>

Continued on Next Page...



Table B.3 – Continued

Load	GU-1	GU-2	GU-3	GU-4	GU-5	GU-6	GU-7	GU-8	GU-9	GU-10
72	29.80 ± 0.04	29.50 ± 0.12	28.90 ± 0.11	30.59 ± 0.09	29.57 ± 0.07	27.94 ± 0.09	28.13 ± 0.08	30.33 ± 0.09	28.98 ± 0.11	<b>30.72 ± 0.08</b>
74	29.20 ± 0.06	28.95 ± 0.10	28.41 ± 0.09	30.05 ± 0.08	29.04 ± 0.07	27.39 ± 0.09	27.71 ± 0.10	29.78 ± 0.08	28.41 ± 0.08	<b>30.11 ± 0.08</b>
76	28.66 ± 0.06	28.36 ± 0.08	27.80 ± 0.09	29.51 ± 0.09	28.46 ± 0.09	26.97 ± 0.10	27.13 ± 0.08	29.34 ± 0.08	27.88 ± 0.07	<b>29.59 ± 0.07</b>
78	28.14 ± 0.05	27.88 ± 0.11	27.34 ± 0.11	28.97 ± 0.08	27.99 ± 0.08	26.46 ± 0.08	26.61 ± 0.09	28.76 ± 0.08	27.38 ± 0.09	<b>29.02 ± 0.07</b>
80	27.60 ± 0.07	27.47 ± 0.10	26.81 ± 0.11	28.42 ± 0.07	27.51 ± 0.08	26.15 ± 0.10	26.22 ± 0.08	28.23 ± 0.09	26.87 ± 0.08	<b>28.51 ± 0.09</b>
82	27.11 ± 0.04	27.00 ± 0.12	26.46 ± 0.10	27.87 ± 0.09	27.01 ± 0.08	25.63 ± 0.10	25.75 ± 0.08	27.77 ± 0.07	26.49 ± 0.07	<b>28.08 ± 0.07</b>
84	26.56 ± 0.05	26.65 ± 0.09	25.98 ± 0.10	27.47 ± 0.08	26.65 ± 0.07	25.24 ± 0.10	25.43 ± 0.09	27.28 ± 0.08	25.99 ± 0.08	<b>27.62 ± 0.08</b>
86	26.17 ± 0.04	26.20 ± 0.09	25.46 ± 0.11	27.03 ± 0.09	26.20 ± 0.08	24.80 ± 0.11	24.89 ± 0.08	26.73 ± 0.07	25.59 ± 0.09	<b>27.11 ± 0.07</b>
88	25.77 ± 0.06	25.79 ± 0.11	25.16 ± 0.08	26.56 ± 0.08	25.77 ± 0.08	24.45 ± 0.10	24.55 ± 0.09	26.39 ± 0.08	25.23 ± 0.06	<b>26.67 ± 0.07</b>
90	25.29 ± 0.05	25.32 ± 0.14	24.71 ± 0.09	26.16 ± 0.10	25.44 ± 0.09	24.14 ± 0.09	24.22 ± 0.08	25.96 ± 0.07	24.81 ± 0.09	<b>26.23 ± 0.09</b>

# Appendix C

## Appendix Fixed Grid Comparison Dataset

Table C.1: Fixed Grid dataset of the Success ratio for all the tested algorithms on the small network topology.

Load	FSAC	SPR	ACRWA	UCBRWA
1	<b>99.82 ± 0.02</b>	96.19 ± 0.01	64.58 ± 0.13	97.79 ± 0.09
2	<b>99.22 ± 0.06</b>	91.47 ± 0.01	64.34 ± 0.09	94.27 ± 0.17
3	<b>98.40 ± 0.10</b>	87.36 ± 0.01	63.84 ± 0.12	90.87 ± 0.34
4	<b>97.16 ± 0.19</b>	83.75 ± 0.02	63.31 ± 0.10	87.65 ± 0.36
5	<b>96.22 ± 0.15</b>	80.49 ± 0.02	62.67 ± 0.08	84.83 ± 0.40
6	<b>94.84 ± 0.27</b>	77.61 ± 0.02	62.12 ± 0.09	82.38 ± 0.47
7	<b>93.39 ± 0.27</b>	74.99 ± 0.02	61.53 ± 0.05	78.52 ± 0.39
8	<b>91.79 ± 0.22</b>	72.61 ± 0.02	60.86 ± 0.06	76.06 ± 0.46
9	<b>90.07 ± 0.40</b>	70.40 ± 0.02	60.12 ± 0.06	72.72 ± 0.45
10	<b>88.62 ± 0.36</b>	68.38 ± 0.03	59.40 ± 0.06	70.35 ± 0.39
11	<b>86.94 ± 0.59</b>	66.51 ± 0.02	58.60 ± 0.05	67.75 ± 0.24
12	<b>85.26 ± 0.47</b>	64.77 ± 0.03	57.50 ± 0.08	65.81 ± 0.35
13	<b>83.97 ± 0.53</b>	63.17 ± 0.02	55.87 ± 0.35	63.48 ± 0.41
14	<b>82.52 ± 0.46</b>	61.62 ± 0.02	53.76 ± 0.58	60.73 ± 0.39
15	<b>80.58 ± 0.47</b>	60.19 ± 0.03	52.58 ± 0.66	57.91 ± 0.31
16	<b>79.00 ± 0.64</b>	58.87 ± 0.02	52.26 ± 0.55	55.23 ± 0.40
17	<b>77.00 ± 0.63</b>	57.61 ± 0.02	49.56 ± 0.74	51.48 ± 0.36
18	<b>75.71 ± 0.62</b>	56.40 ± 0.02	46.82 ± 0.40	48.55 ± 0.30
19	<b>74.84 ± 0.56</b>	55.27 ± 0.03	44.76 ± 0.61	45.25 ± 0.30
20	<b>72.98 ± 0.78</b>	54.20 ± 0.02	42.63 ± 0.69	42.41 ± 0.27
21	<b>71.49 ± 0.55</b>	53.18 ± 0.02	37.22 ± 0.80	40.09 ± 0.29
22	<b>69.77 ± 0.52</b>	52.19 ± 0.03	35.35 ± 0.49	37.76 ± 0.19
23	<b>69.10 ± 0.67</b>	51.24 ± 0.02	34.14 ± 0.16	36.00 ± 0.15
24	<b>67.40 ± 0.59</b>	50.38 ± 0.03	32.96 ± 0.45	34.42 ± 0.16
25	<b>66.12 ± 0.56</b>	49.54 ± 0.02	30.61 ± 0.67	32.80 ± 0.14
26	<b>65.19 ± 0.70</b>	48.71 ± 0.02	27.11 ± 0.36	31.73 ± 0.15
27	<b>63.55 ± 0.60</b>	47.93 ± 0.02	25.68 ± 0.21	30.50 ± 0.13

Continued on Next Page...

Table C.1 – Continued

Load	FSAC	SPR	ACRWA	UCBRWA
28	<b>62.97 ± 0.52</b>	47.15 ± 0.02	24.59 ± 0.11	29.54 ± 0.15
29	<b>62.23 ± 0.55</b>	46.43 ± 0.02	23.72 ± 0.10	28.68 ± 0.11
30	<b>60.99 ± 0.62</b>	45.75 ± 0.02	22.74 ± 0.43	27.75 ± 0.09
31	<b>59.46 ± 0.59</b>	45.05 ± 0.03	21.67 ± 0.73	26.99 ± 0.10
32	<b>58.64 ± 0.55</b>	44.40 ± 0.02	19.31 ± 1.37	26.25 ± 0.07
33	<b>57.74 ± 0.47</b>	43.80 ± 0.02	16.63 ± 1.51	25.47 ± 0.07
34	<b>57.43 ± 0.65</b>	43.18 ± 0.02	13.97 ± 1.26	24.75 ± 0.07
35	<b>56.56 ± 0.48</b>	42.59 ± 0.02	14.81 ± 1.41	24.15 ± 0.08
36	<b>55.49 ± 0.57</b>	42.03 ± 0.02	12.30 ± 0.84	23.53 ± 0.07
37	<b>55.16 ± 0.49</b>	41.49 ± 0.03	11.08 ± 0.10	22.93 ± 0.07
38	<b>53.75 ± 0.54</b>	40.94 ± 0.02	11.03 ± 0.53	22.41 ± 0.06
39	<b>53.20 ± 0.64</b>	40.42 ± 0.02	10.44 ± 0.14	21.84 ± 0.05
40	<b>52.90 ± 0.47</b>	39.92 ± 0.02	10.14 ± 0.16	21.35 ± 0.05
41	<b>51.65 ± 0.56</b>	39.43 ± 0.02	9.87 ± 0.16	20.89 ± 0.06
42	<b>51.50 ± 0.43</b>	38.96 ± 0.02	9.61 ± 0.12	20.41 ± 0.05
43	<b>50.69 ± 0.43</b>	38.51 ± 0.02	9.56 ± 0.14	19.97 ± 0.05
44	<b>50.22 ± 0.57</b>	38.05 ± 0.02	9.30 ± 0.13	19.55 ± 0.05
45	<b>49.43 ± 0.50</b>	37.62 ± 0.02	9.16 ± 0.13	19.18 ± 0.05

Table C.2: Fixed Grid dataset of the Success ratio for all the tested algorithms on the medium network topology.

Load	FSAC	SPR	ACRWA	UCBRWA
1	<b>98.80 ± 0.06</b>	98.63 ± 0.01	79.25 ± 0.12	98.31 ± 0.04
2	<b>97.20 ± 0.14</b>	96.90 ± 0.01	78.92 ± 0.14	96.08 ± 0.07
3	<b>95.84 ± 0.17</b>	95.26 ± 0.01	79.00 ± 0.13	94.28 ± 0.08
4	<b>94.57 ± 0.28</b>	93.68 ± 0.01	78.81 ± 0.12	92.71 ± 0.10
5	<b>93.52 ± 0.24</b>	92.20 ± 0.02	78.64 ± 0.12	91.42 ± 0.11
6	<b>92.31 ± 0.19</b>	90.76 ± 0.02	78.49 ± 0.13	90.30 ± 0.12
7	<b>91.34 ± 0.30</b>	89.40 ± 0.01	78.23 ± 0.12	89.02 ± 0.14
8	<b>90.62 ± 0.29</b>	88.07 ± 0.01	77.88 ± 0.12	88.15 ± 0.13
9	<b>89.60 ± 0.39</b>	86.83 ± 0.01	77.71 ± 0.10	87.17 ± 0.11
10	<b>89.06 ± 0.28</b>	85.65 ± 0.02	77.36 ± 0.07	86.34 ± 0.14
11	<b>88.25 ± 0.33</b>	84.49 ± 0.02	77.09 ± 0.09	85.53 ± 0.12
12	<b>87.41 ± 0.35</b>	83.37 ± 0.02	76.65 ± 0.09	84.77 ± 0.11
13	<b>86.80 ± 0.31</b>	82.29 ± 0.02	76.48 ± 0.08	84.13 ± 0.14
14	<b>86.09 ± 0.40</b>	81.24 ± 0.02	76.01 ± 0.08	83.46 ± 0.13
15	<b>85.46 ± 0.25</b>	80.27 ± 0.02	75.71 ± 0.06	82.82 ± 0.12
16	<b>84.90 ± 0.34</b>	79.29 ± 0.02	75.35 ± 0.06	82.30 ± 0.17
17	<b>84.23 ± 0.34</b>	78.39 ± 0.02	75.01 ± 0.06	81.92 ± 0.12
18	<b>83.75 ± 0.40</b>	77.45 ± 0.03	74.64 ± 0.06	81.32 ± 0.13
19	<b>83.03 ± 0.31</b>	76.60 ± 0.02	74.33 ± 0.05	80.79 ± 0.12
20	<b>82.74 ± 0.33</b>	75.78 ± 0.02	73.99 ± 0.06	80.30 ± 0.11
21	<b>82.07 ± 0.35</b>	74.96 ± 0.02	73.71 ± 0.06	79.89 ± 0.12
22	<b>81.56 ± 0.33</b>	74.17 ± 0.02	73.40 ± 0.06	79.46 ± 0.13
23	<b>81.20 ± 0.33</b>	73.39 ± 0.02	73.03 ± 0.06	79.07 ± 0.12
24	<b>80.96 ± 0.30</b>	72.66 ± 0.02	72.77 ± 0.05	78.51 ± 0.12
25	<b>80.33 ± 0.42</b>	71.91 ± 0.02	72.45 ± 0.06	78.23 ± 0.12

Continued on Next Page...

Table C.2 – Continued

Load	FSAC	SPR	ACRWA	UCBRWA
26	<b>79.45 ± 0.35</b>	71.23 ± 0.02	72.13 ± 0.06	77.74 ± 0.11
27	<b>79.49 ± 0.33</b>	70.54 ± 0.02	71.83 ± 0.06	77.40 ± 0.11
28	<b>78.50 ± 0.31</b>	69.87 ± 0.02	71.56 ± 0.06	76.94 ± 0.13
29	<b>78.31 ± 0.33</b>	69.22 ± 0.03	71.24 ± 0.06	76.61 ± 0.11
30	<b>78.18 ± 0.37</b>	68.59 ± 0.02	70.98 ± 0.05	76.33 ± 0.11
31	<b>77.50 ± 0.37</b>	67.97 ± 0.03	70.63 ± 0.05	75.99 ± 0.11
32	<b>76.75 ± 0.44</b>	67.40 ± 0.03	70.40 ± 0.04	75.49 ± 0.11
33	<b>76.57 ± 0.39</b>	66.80 ± 0.02	70.10 ± 0.05	75.15 ± 0.09
34	<b>76.20 ± 0.32</b>	66.22 ± 0.02	69.83 ± 0.05	74.83 ± 0.12
35	<b>75.56 ± 0.34</b>	65.67 ± 0.02	69.57 ± 0.05	74.54 ± 0.10
36	<b>75.34 ± 0.42</b>	65.12 ± 0.03	69.28 ± 0.06	74.30 ± 0.09
37	<b>75.15 ± 0.35</b>	64.59 ± 0.02	69.01 ± 0.04	73.91 ± 0.10
38	<b>74.78 ± 0.39</b>	64.08 ± 0.03	68.70 ± 0.05	73.52 ± 0.11
39	<b>74.10 ± 0.34</b>	63.57 ± 0.02	68.48 ± 0.05	73.33 ± 0.12
40	<b>74.01 ± 0.37</b>	63.11 ± 0.02	68.20 ± 0.05	73.11 ± 0.09
41	<b>73.38 ± 0.34</b>	62.59 ± 0.03	67.89 ± 0.05	72.77 ± 0.09
42	<b>73.22 ± 0.31</b>	62.14 ± 0.02	67.66 ± 0.06	72.38 ± 0.08
43	<b>72.72 ± 0.43</b>	61.65 ± 0.03	67.36 ± 0.04	72.08 ± 0.12
44	<b>72.45 ± 0.31</b>	61.21 ± 0.03	67.11 ± 0.05	71.86 ± 0.11
45	<b>72.42 ± 0.32</b>	60.76 ± 0.02	66.87 ± 0.04	71.65 ± 0.08
46	<b>72.04 ± 0.30</b>	60.33 ± 0.02	66.64 ± 0.05	71.30 ± 0.09
47	<b>71.44 ± 0.30</b>	59.93 ± 0.02	66.36 ± 0.05	71.05 ± 0.06
48	<b>71.00 ± 0.35</b>	59.46 ± 0.03	66.08 ± 0.05	70.68 ± 0.08
49	<b>70.57 ± 0.26</b>	59.06 ± 0.02	65.78 ± 0.05	70.45 ± 0.09
50	<b>70.42 ± 0.36</b>	58.67 ± 0.02	65.51 ± 0.06	70.17 ± 0.08
51	<b>69.99 ± 0.30</b>	58.28 ± 0.03	65.19 ± 0.12	69.92 ± 0.06
52	<b>69.64 ± 0.28</b>	57.89 ± 0.03	64.44 ± 0.25	69.61 ± 0.07
53	69.23 ± 0.32	57.52 ± 0.03	63.69 ± 0.30	<b>69.39 ± 0.10</b>
54	<b>69.00 ± 0.31</b>	57.14 ± 0.03	62.96 ± 0.28	69.04 ± 0.09
55	68.49 ± 0.26	56.78 ± 0.03	62.26 ± 0.17	<b>68.79 ± 0.09</b>
56	68.15 ± 0.33	56.41 ± 0.02	61.97 ± 0.15	<b>68.46 ± 0.11</b>
57	68.07 ± 0.31	56.06 ± 0.03	61.46 ± 0.11	<b>68.27 ± 0.09</b>
58	67.69 ± 0.41	55.68 ± 0.03	61.05 ± 0.13	<b>67.93 ± 0.08</b>
59	67.19 ± 0.34	55.36 ± 0.03	60.68 ± 0.08	<b>67.68 ± 0.09</b>
60	66.96 ± 0.34	55.02 ± 0.03	60.32 ± 0.07	<b>67.32 ± 0.08</b>

Table C.3: Fixed Grid dataset of the Success ratio for all the tested algorithms on the large network topology.

Load	FSAC	SPR	ACRWA	UCBRWA
1	<b>99.38 ± 0.02</b>	97.19 ± 0.01	80.34 ± 0.15	92.60 ± 0.05
2	<b>98.71 ± 0.03</b>	94.04 ± 0.01	79.44 ± 0.17	85.97 ± 0.11
3	<b>98.05 ± 0.04</b>	91.16 ± 0.02	79.12 ± 0.20	81.41 ± 0.09
4	<b>97.42 ± 0.03</b>	88.53 ± 0.02	78.77 ± 0.13	77.91 ± 0.09
5	<b>96.69 ± 0.04</b>	86.11 ± 0.02	77.86 ± 0.15	75.07 ± 0.11
6	<b>95.94 ± 0.05</b>	83.87 ± 0.02	77.05 ± 0.13	72.98 ± 0.09
7	<b>95.12 ± 0.04</b>	81.78 ± 0.02	76.24 ± 0.17	71.14 ± 0.10
8	<b>94.31 ± 0.07</b>	79.81 ± 0.02	75.32 ± 0.13	69.52 ± 0.10

Continued on Next Page...

Table C.3 – Continued

Load	FSAC	SPR	ACRWA	UCBRWA
9	<b>93.48 ± 0.08</b>	77.96 ± 0.02	74.65 ± 0.12	68.11 ± 0.11
10	<b>92.60 ± 0.07</b>	76.23 ± 0.02	73.83 ± 0.15	66.90 ± 0.11
11	<b>91.81 ± 0.07</b>	74.60 ± 0.02	73.30 ± 0.10	65.83 ± 0.07
12	<b>90.83 ± 0.09</b>	73.08 ± 0.02	72.57 ± 0.09	64.71 ± 0.08
13	<b>89.98 ± 0.08</b>	71.60 ± 0.02	71.90 ± 0.10	63.85 ± 0.08
14	<b>89.06 ± 0.10</b>	70.22 ± 0.03	71.19 ± 0.11	63.02 ± 0.07
15	<b>88.09 ± 0.07</b>	68.93 ± 0.02	70.39 ± 0.09	62.32 ± 0.08
16	<b>87.04 ± 0.13</b>	67.68 ± 0.02	69.52 ± 0.08	61.57 ± 0.08
17	<b>86.18 ± 0.10</b>	66.49 ± 0.02	68.61 ± 0.07	60.79 ± 0.11
18	<b>85.18 ± 0.09</b>	65.33 ± 0.02	67.79 ± 0.09	60.41 ± 0.07
19	<b>84.17 ± 0.12</b>	64.26 ± 0.02	67.07 ± 0.07	59.77 ± 0.08
20	<b>83.29 ± 0.13</b>	63.21 ± 0.02	66.23 ± 0.09	59.20 ± 0.07
21	<b>82.46 ± 0.13</b>	62.22 ± 0.02	65.45 ± 0.10	58.73 ± 0.08
22	<b>81.35 ± 0.11</b>	61.25 ± 0.02	64.27 ± 0.17	58.22 ± 0.12
23	<b>80.33 ± 0.10</b>	60.31 ± 0.03	62.67 ± 0.28	57.66 ± 0.11
24	<b>79.45 ± 0.13</b>	59.43 ± 0.02	61.10 ± 0.26	57.32 ± 0.08
25	<b>78.61 ± 0.11</b>	58.59 ± 0.03	59.37 ± 0.29	56.93 ± 0.08
26	<b>77.60 ± 0.11</b>	57.75 ± 0.01	57.88 ± 0.25	56.53 ± 0.08
27	<b>76.70 ± 0.15</b>	56.96 ± 0.02	56.74 ± 0.26	56.11 ± 0.09
28	<b>75.86 ± 0.11</b>	56.17 ± 0.03	55.41 ± 0.24	55.77 ± 0.08
29	<b>74.85 ± 0.13</b>	55.43 ± 0.02	53.78 ± 0.23	55.31 ± 0.13
30	<b>73.89 ± 0.13</b>	54.70 ± 0.03	52.62 ± 0.21	55.00 ± 0.07
31	<b>73.04 ± 0.12</b>	54.00 ± 0.03	51.58 ± 0.16	54.64 ± 0.08
32	<b>72.02 ± 0.13</b>	53.35 ± 0.03	50.46 ± 0.28	54.26 ± 0.05
33	<b>71.28 ± 0.13</b>	52.71 ± 0.02	49.24 ± 0.22	53.85 ± 0.05
34	<b>70.44 ± 0.13</b>	52.06 ± 0.02	48.24 ± 0.21	53.62 ± 0.07
35	<b>69.58 ± 0.14</b>	51.44 ± 0.02	47.36 ± 0.13	53.29 ± 0.05
36	<b>68.69 ± 0.14</b>	50.86 ± 0.02	46.81 ± 0.11	53.06 ± 0.06
37	<b>67.89 ± 0.14</b>	50.27 ± 0.02	46.12 ± 0.08	52.72 ± 0.06
38	<b>67.08 ± 0.11</b>	49.71 ± 0.02	45.64 ± 0.07	52.36 ± 0.05
39	<b>66.32 ± 0.13</b>	49.14 ± 0.02	45.12 ± 0.07	52.14 ± 0.06
40	<b>65.48 ± 0.16</b>	48.61 ± 0.02	44.61 ± 0.05	51.82 ± 0.05
41	<b>64.60 ± 0.13</b>	48.08 ± 0.02	44.19 ± 0.07	51.58 ± 0.06
42	<b>63.96 ± 0.15</b>	47.59 ± 0.02	43.70 ± 0.09	51.31 ± 0.05
43	<b>63.10 ± 0.14</b>	47.08 ± 0.03	43.08 ± 0.15	50.89 ± 0.10
44	<b>62.21 ± 0.16</b>	46.61 ± 0.02	42.46 ± 0.18	50.75 ± 0.04
45	<b>61.61 ± 0.14</b>	46.13 ± 0.02	41.72 ± 0.22	50.49 ± 0.05
46	<b>61.13 ± 0.14</b>	45.68 ± 0.02	41.16 ± 0.13	50.26 ± 0.04
47	<b>60.25 ± 0.13</b>	45.21 ± 0.02	40.53 ± 0.11	50.00 ± 0.04
48	<b>59.52 ± 0.15</b>	44.78 ± 0.02	40.09 ± 0.11	49.71 ± 0.03
49	<b>58.75 ± 0.18</b>	44.35 ± 0.02	39.54 ± 0.10	49.47 ± 0.03
50	<b>58.01 ± 0.18</b>	43.94 ± 0.02	39.09 ± 0.09	49.19 ± 0.03
51	<b>57.56 ± 0.19</b>	43.52 ± 0.02	38.64 ± 0.08	48.88 ± 0.06
52	<b>56.91 ± 0.13</b>	43.11 ± 0.02	38.16 ± 0.07	48.68 ± 0.03
53	<b>56.20 ± 0.16</b>	42.74 ± 0.02	37.74 ± 0.07	48.44 ± 0.03
54	<b>55.57 ± 0.14</b>	42.37 ± 0.02	37.40 ± 0.07	48.19 ± 0.03
55	<b>54.86 ± 0.13</b>	41.96 ± 0.02	37.05 ± 0.07	47.91 ± 0.03
56	<b>54.42 ± 0.13</b>	41.59 ± 0.02	36.66 ± 0.05	47.65 ± 0.03
57	<b>53.82 ± 0.15</b>	41.25 ± 0.02	36.27 ± 0.04	47.36 ± 0.03
58	<b>53.40 ± 0.12</b>	40.90 ± 0.03	35.95 ± 0.06	47.07 ± 0.06
59	<b>52.62 ± 0.09</b>	40.56 ± 0.02	35.53 ± 0.05	46.79 ± 0.03
60	<b>51.98 ± 0.14</b>	40.21 ± 0.02	35.24 ± 0.05	46.46 ± 0.05

# Appendix D

## Appendix Flexible Spectrum Comparison Dataset

Table D.1: Flexible Spectrum dataset of the Success ratio for all the tested algorithms on the small network topology.

Load	FSAC	SPR	ACRWA	UCBRWA
2	<b>98.03 ± 0.05</b>	95.59 ± 0.01	57.52 ± 0.70	92.28 ± 0.06
4	<b>93.98 ± 0.15</b>	88.88 ± 0.02	53.85 ± 0.88	84.23 ± 0.08
6	<b>89.27 ± 0.20</b>	81.99 ± 0.03	51.77 ± 0.89	77.39 ± 0.11
8	<b>83.99 ± 0.31</b>	75.58 ± 0.03	49.66 ± 0.65	71.56 ± 0.12
10	<b>78.62 ± 0.34</b>	69.91 ± 0.03	46.84 ± 0.55	65.95 ± 0.13
12	<b>73.72 ± 0.35</b>	64.95 ± 0.03	45.00 ± 0.40	60.44 ± 0.12
14	<b>69.40 ± 0.38</b>	60.62 ± 0.03	43.70 ± 0.35	56.03 ± 0.12
16	<b>65.89 ± 0.33</b>	56.86 ± 0.02	42.82 ± 0.32	52.71 ± 0.14
18	<b>61.87 ± 0.48</b>	53.53 ± 0.03	41.81 ± 0.33	49.49 ± 0.16
20	<b>59.17 ± 0.40</b>	50.64 ± 0.02	41.25 ± 0.33	46.53 ± 0.12
22	<b>56.15 ± 0.35</b>	48.05 ± 0.02	40.24 ± 0.25	44.08 ± 0.14
24	<b>53.70 ± 0.44</b>	45.71 ± 0.03	39.82 ± 0.20	41.68 ± 0.15
26	<b>51.23 ± 0.34</b>	43.60 ± 0.02	38.61 ± 0.30	39.39 ± 0.18
28	<b>49.13 ± 0.34</b>	41.69 ± 0.03	37.73 ± 0.34	37.61 ± 0.23
30	<b>47.30 ± 0.32</b>	39.91 ± 0.03	36.48 ± 0.56	35.75 ± 0.26
32	<b>45.43 ± 0.30</b>	38.31 ± 0.03	35.68 ± 0.60	33.98 ± 0.22
34	<b>43.72 ± 0.36</b>	36.82 ± 0.02	35.16 ± 0.52	32.57 ± 0.22
36	<b>41.78 ± 0.25</b>	35.39 ± 0.02	33.78 ± 0.64	30.55 ± 0.22
38	<b>40.66 ± 0.27</b>	34.12 ± 0.02	33.22 ± 0.74	28.82 ± 0.23
40	<b>38.93 ± 0.33</b>	32.90 ± 0.03	31.65 ± 0.58	27.17 ± 0.31
42	<b>37.52 ± 0.36</b>	31.74 ± 0.02	31.24 ± 0.75	25.41 ± 0.23
44	<b>36.51 ± 0.37</b>	30.63 ± 0.03	29.90 ± 0.68	24.10 ± 0.30
46	<b>35.12 ± 0.30</b>	29.59 ± 0.02	28.97 ± 0.63	22.71 ± 0.18
48	<b>33.83 ± 0.32</b>	28.59 ± 0.02	28.07 ± 0.65	21.61 ± 0.25
50	<b>32.62 ± 0.24</b>	27.66 ± 0.03	26.67 ± 0.56	20.28 ± 0.29
52	<b>31.57 ± 0.27</b>	26.74 ± 0.02	25.90 ± 0.55	18.96 ± 0.25

Continued on Next Page...

APPENDIX D. APPENDIX FLEXIBLE SPECTRUM COMPARISON DATASET 181

Table D.1 – Continued

Load	FSAC	SPR	ACRWA	UCBRWA
54	<b>30.48 ± 0.25</b>	25.88 ± 0.02	24.33 ± 0.60	18.13 ± 0.21
56	<b>29.56 ± 0.27</b>	25.03 ± 0.02	23.72 ± 0.54	17.08 ± 0.28
58	<b>28.66 ± 0.20</b>	24.24 ± 0.02	22.58 ± 0.69	16.09 ± 0.19
60	<b>27.47 ± 0.30</b>	23.45 ± 0.02	22.19 ± 0.67	15.13 ± 0.25
62	<b>26.71 ± 0.21</b>	22.70 ± 0.02	20.96 ± 0.48	14.50 ± 0.27
64	<b>25.75 ± 0.19</b>	21.96 ± 0.02	20.43 ± 0.49	13.82 ± 0.25
66	<b>25.01 ± 0.22</b>	21.25 ± 0.02	19.62 ± 0.45	12.90 ± 0.26
68	<b>24.22 ± 0.26</b>	20.58 ± 0.02	18.54 ± 0.60	12.23 ± 0.26
70	<b>23.35 ± 0.19</b>	19.88 ± 0.02	18.05 ± 0.59	11.66 ± 0.25
72	<b>22.64 ± 0.22</b>	19.24 ± 0.02	17.23 ± 0.62	10.81 ± 0.22
74	<b>21.88 ± 0.25</b>	18.62 ± 0.01	16.34 ± 0.53	10.25 ± 0.20
76	<b>21.22 ± 0.19</b>	18.02 ± 0.02	15.73 ± 0.50	9.78 ± 0.20
78	<b>20.36 ± 0.22</b>	17.41 ± 0.02	14.90 ± 0.57	9.33 ± 0.26
80	<b>19.78 ± 0.16</b>	16.82 ± 0.01	14.67 ± 0.62	8.74 ± 0.23
82	<b>19.11 ± 0.22</b>	16.26 ± 0.02	13.85 ± 0.45	8.56 ± 0.19
84	<b>18.34 ± 0.21</b>	15.71 ± 0.02	13.24 ± 0.37	8.02 ± 0.22
86	<b>17.72 ± 0.20</b>	15.18 ± 0.02	12.45 ± 0.50	7.52 ± 0.23
88	<b>17.04 ± 0.18</b>	14.65 ± 0.02	11.68 ± 0.47	7.35 ± 0.22
90	<b>16.40 ± 0.19</b>	14.16 ± 0.02	11.54 ± 0.40	6.86 ± 0.20

Table D.2: Flexible Spectrum dataset of the Success ratio for all the tested algorithms on the medium network topology.

Load	FSAC	SPR	ACRWA	UCBRWA
2	<b>99.15 ± 0.03</b>	98.68 ± 0.01	80.33 ± 0.10	97.44 ± 0.02
4	<b>98.11 ± 0.04</b>	96.74 ± 0.01	79.24 ± 0.13	93.69 ± 0.04
6	<b>97.08 ± 0.05</b>	94.59 ± 0.01	77.67 ± 0.11	89.95 ± 0.06
8	<b>95.92 ± 0.04</b>	92.29 ± 0.02	75.79 ± 0.22	86.34 ± 0.06
10	<b>94.62 ± 0.07</b>	89.87 ± 0.02	74.06 ± 0.25	82.94 ± 0.07
12	<b>93.24 ± 0.08</b>	87.45 ± 0.02	72.49 ± 0.23	79.66 ± 0.07
14	<b>91.81 ± 0.07</b>	85.00 ± 0.02	70.65 ± 0.21	76.72 ± 0.10
16	<b>90.25 ± 0.11</b>	82.61 ± 0.03	68.80 ± 0.32	73.90 ± 0.11
18	<b>88.73 ± 0.11</b>	80.26 ± 0.03	67.28 ± 0.27	71.42 ± 0.09
20	<b>87.31 ± 0.12</b>	77.96 ± 0.03	65.52 ± 0.34	68.86 ± 0.11
22	<b>85.41 ± 0.12</b>	75.78 ± 0.03	64.27 ± 0.28	66.80 ± 0.12
24	<b>83.86 ± 0.15</b>	73.65 ± 0.03	62.47 ± 0.38	64.64 ± 0.11
26	<b>82.22 ± 0.15</b>	71.62 ± 0.02	61.32 ± 0.28	62.66 ± 0.13
28	<b>80.68 ± 0.16</b>	69.66 ± 0.03	60.02 ± 0.45	60.89 ± 0.10
30	<b>78.94 ± 0.21</b>	67.79 ± 0.03	58.32 ± 0.33	59.01 ± 0.12
32	<b>77.46 ± 0.17</b>	66.02 ± 0.02	57.63 ± 0.46	57.37 ± 0.14
34	<b>75.58 ± 0.17</b>	64.31 ± 0.03	56.63 ± 0.47	55.90 ± 0.14
36	<b>74.11 ± 0.16</b>	62.67 ± 0.03	55.33 ± 0.57	54.42 ± 0.12
38	<b>72.73 ± 0.16</b>	61.14 ± 0.03	54.75 ± 0.50	53.09 ± 0.15
40	<b>71.28 ± 0.20</b>	59.69 ± 0.03	54.12 ± 0.37	51.84 ± 0.14
42	<b>69.85 ± 0.17</b>	58.27 ± 0.03	53.21 ± 0.36	50.58 ± 0.13
44	<b>68.38 ± 0.17</b>	56.99 ± 0.02	52.24 ± 0.45	49.47 ± 0.14
46	<b>67.07 ± 0.20</b>	55.70 ± 0.02	51.38 ± 0.42	48.50 ± 0.11
48	<b>65.70 ± 0.17</b>	54.49 ± 0.03	50.73 ± 0.39	47.38 ± 0.15

Continued on Next Page...

APPENDIX D. APPENDIX FLEXIBLE SPECTRUM COMPARISON DATASET182

Table D.2 – Continued

Load	FSAC	SPR	ACRWA	UCBRWA
50	<b>64.41</b> ± 0.15	53.41 ± 0.02	50.24 ± 0.43	46.35 ± 0.12
52	<b>63.25</b> ± 0.19	52.28 ± 0.02	49.61 ± 0.27	45.69 ± 0.18
54	<b>62.03</b> ± 0.22	51.24 ± 0.02	48.67 ± 0.42	44.88 ± 0.14
56	<b>60.81</b> ± 0.17	50.29 ± 0.02	48.25 ± 0.39	43.90 ± 0.13
58	<b>59.71</b> ± 0.19	49.32 ± 0.03	47.65 ± 0.28	43.11 ± 0.14
60	<b>58.49</b> ± 0.20	48.45 ± 0.03	47.03 ± 0.36	42.64 ± 0.19
62	<b>57.56</b> ± 0.15	47.59 ± 0.02	46.67 ± 0.32	41.72 ± 0.16
64	<b>56.50</b> ± 0.25	46.78 ± 0.03	45.95 ± 0.37	41.28 ± 0.18
66	<b>55.71</b> ± 0.16	45.99 ± 0.03	45.45 ± 0.38	40.48 ± 0.17
68	<b>54.72</b> ± 0.16	45.27 ± 0.03	45.17 ± 0.27	39.91 ± 0.15
70	<b>53.86</b> ± 0.18	44.54 ± 0.03	44.51 ± 0.22	39.45 ± 0.16
72	<b>52.81</b> ± 0.20	43.87 ± 0.03	43.83 ± 0.41	38.89 ± 0.19
74	<b>51.95</b> ± 0.24	43.18 ± 0.03	43.34 ± 0.26	38.33 ± 0.16
76	<b>51.03</b> ± 0.18	42.56 ± 0.03	42.97 ± 0.33	37.57 ± 0.17
78	<b>50.62</b> ± 0.14	41.92 ± 0.03	42.72 ± 0.30	37.27 ± 0.18
80	<b>49.83</b> ± 0.20	41.37 ± 0.02	42.20 ± 0.29	36.71 ± 0.17
82	<b>48.86</b> ± 0.22	40.79 ± 0.02	41.65 ± 0.28	36.30 ± 0.18
84	<b>48.53</b> ± 0.17	40.24 ± 0.03	41.28 ± 0.31	35.85 ± 0.21
86	<b>47.64</b> ± 0.18	39.70 ± 0.03	41.00 ± 0.26	35.40 ± 0.19
88	<b>47.04</b> ± 0.19	39.20 ± 0.03	40.38 ± 0.40	34.90 ± 0.20
90	<b>46.21</b> ± 0.18	38.71 ± 0.03	39.84 ± 0.35	34.52 ± 0.19

Table D.3: Flexible Spectrum dataset of the Success ratio for all the tested algorithms on the large network topology.

Load	FSAC	SPR	ACRWA	UCBRWA
2	<b>97.74</b> ± 0.02	97.21 ± 0.01	73.63 ± 0.51	93.67 ± 0.04
4	<b>94.92</b> ± 0.03	93.26 ± 0.02	68.81 ± 0.32	85.51 ± 0.06
6	<b>91.73</b> ± 0.04	88.98 ± 0.02	64.07 ± 0.50	78.00 ± 0.07
8	<b>88.28</b> ± 0.05	84.63 ± 0.02	59.79 ± 0.58	71.55 ± 0.08
10	<b>84.71</b> ± 0.06	80.42 ± 0.02	56.38 ± 0.29	65.74 ± 0.10
12	<b>81.11</b> ± 0.05	76.43 ± 0.03	53.45 ± 0.53	60.92 ± 0.13
14	<b>77.63</b> ± 0.06	72.66 ± 0.02	50.48 ± 0.46	56.60 ± 0.09
16	<b>74.17</b> ± 0.06	69.14 ± 0.02	48.92 ± 0.44	52.96 ± 0.08
18	<b>70.98</b> ± 0.08	65.89 ± 0.03	46.44 ± 0.38	49.66 ± 0.13
20	<b>67.83</b> ± 0.05	62.88 ± 0.03	44.01 ± 0.55	46.75 ± 0.07
22	<b>64.98</b> ± 0.05	60.07 ± 0.03	43.28 ± 0.52	44.11 ± 0.11
24	<b>62.20</b> ± 0.08	57.47 ± 0.03	42.39 ± 0.36	41.91 ± 0.10
26	<b>59.62</b> ± 0.07	55.06 ± 0.02	40.64 ± 0.31	40.04 ± 0.10
28	<b>57.22</b> ± 0.06	52.79 ± 0.03	39.36 ± 0.44	38.23 ± 0.11
30	<b>55.06</b> ± 0.07	50.76 ± 0.03	38.57 ± 0.38	36.76 ± 0.13
32	<b>52.96</b> ± 0.07	48.80 ± 0.03	37.50 ± 0.37	35.33 ± 0.13
34	<b>50.99</b> ± 0.09	46.99 ± 0.03	36.69 ± 0.42	34.09 ± 0.11
36	<b>49.17</b> ± 0.07	45.33 ± 0.03	36.10 ± 0.39	32.95 ± 0.10
38	<b>47.54</b> ± 0.07	43.75 ± 0.03	35.38 ± 0.38	32.07 ± 0.12
40	<b>45.93</b> ± 0.09	42.31 ± 0.03	34.77 ± 0.41	31.15 ± 0.11
42	<b>44.48</b> ± 0.09	40.95 ± 0.03	34.32 ± 0.33	30.18 ± 0.13
44	<b>43.14</b> ± 0.08	39.67 ± 0.03	33.50 ± 0.28	29.50 ± 0.10

Continued on Next Page...



APPENDIX D. APPENDIX FLEXIBLE SPECTRUM COMPARISON DATASET183

Table D.3 – Continued

Load	FSAC	SPR	ACRWA	UCBRWA
46	<b>41.83 ± 0.08</b>	38.47 ± 0.02	32.56 ± 0.41	28.76 ± 0.11
48	<b>40.66 ± 0.11</b>	37.35 ± 0.02	32.23 ± 0.38	28.20 ± 0.09
50	<b>39.54 ± 0.09</b>	36.30 ± 0.02	31.71 ± 0.38	27.65 ± 0.09
52	<b>38.45 ± 0.09</b>	35.31 ± 0.03	31.35 ± 0.29	27.17 ± 0.06
54	<b>37.48 ± 0.10</b>	34.39 ± 0.02	30.98 ± 0.28	26.57 ± 0.07
56	<b>36.55 ± 0.07</b>	33.49 ± 0.02	30.22 ± 0.30	26.12 ± 0.11
58	<b>35.67 ± 0.07</b>	32.68 ± 0.02	29.84 ± 0.23	25.65 ± 0.08
60	<b>34.75 ± 0.09</b>	31.88 ± 0.02	29.26 ± 0.23	25.21 ± 0.13
62	<b>34.02 ± 0.07</b>	31.13 ± 0.02	29.08 ± 0.24	24.97 ± 0.08
64	<b>33.31 ± 0.07</b>	30.44 ± 0.02	28.64 ± 0.20	24.35 ± 0.09
66	<b>32.51 ± 0.06</b>	29.79 ± 0.02	28.32 ± 0.24	24.08 ± 0.08
68	<b>31.82 ± 0.09</b>	29.13 ± 0.02	27.81 ± 0.21	23.75 ± 0.08
70	<b>31.24 ± 0.07</b>	28.53 ± 0.02	27.33 ± 0.22	23.42 ± 0.07
72	<b>30.59 ± 0.09</b>	27.96 ± 0.02	27.28 ± 0.13	23.08 ± 0.09
74	<b>30.05 ± 0.08</b>	27.41 ± 0.02	26.52 ± 0.21	22.74 ± 0.09
76	<b>29.51 ± 0.09</b>	26.88 ± 0.02	26.44 ± 0.21	22.46 ± 0.08
78	<b>28.97 ± 0.08</b>	26.38 ± 0.02	25.90 ± 0.20	22.24 ± 0.10
80	<b>28.42 ± 0.07</b>	25.92 ± 0.02	25.61 ± 0.18	21.77 ± 0.10
82	<b>27.87 ± 0.09</b>	25.46 ± 0.02	25.25 ± 0.19	21.56 ± 0.09
84	<b>27.47 ± 0.08</b>	25.03 ± 0.02	24.74 ± 0.20	21.31 ± 0.08
86	<b>27.03 ± 0.09</b>	24.63 ± 0.02	24.33 ± 0.26	21.07 ± 0.08
88	<b>26.56 ± 0.08</b>	24.20 ± 0.02	24.33 ± 0.20	20.72 ± 0.10
90	<b>26.16 ± 0.10</b>	23.81 ± 0.02	23.90 ± 0.31	20.44 ± 0.08

# Appendix E

## IEEE (SSCI) 2016 Paper

This study investigated the use of the UCB1 formula in an ACO algorithm to determine which routes should be selected. UCB1 was incorporated into an ACO algorithm that allocates a path (from source to destination) and an appropriate wavelength to packets to be routed in a network, which employs Optical Burst Switching (OBS). The new algorithm was evaluated against an existing ant-based algorithm on three network topologies in order to determine its effectiveness. Results obtained indicated that the proposed algorithm outperformed all the tested algorithms in most scenarios.

This study was presented in a conference paper that was accepted for presentation at the 2016 IEEE Symposium Series on Computational Intelligence (IEEE SSCI 2016).

Gravett, A. S., du Plessis, M. C., Gibbon, T. B. (2016). Hybridising Ant Colony Optimisation with a Upper Confidence Bound Algorithm for Routing and Wavelength Assignment in an Optical Burst Switching Network. In 2016 IEEE Symposium Series on Computational Intelligence, pages 1-8.

# Appendix F

## Photonic Network Communications

This study described a distributed algorithm inspired by ACO for a solution to the problem of dynamic RWA with wavelength continuity constraint in OBS networks. The evaluation was conducted in a traditional ITU WDM network environment with limited number of wavelength channels and in a Flexible Spectrum network environment undergoing transmission impairments. The simulations in the Flexible Spectrum network environment aim to replicate both linear and non-linear effects. Under these effects, an optical BCP could be lost during traversal of the network with no measure in place to notify the network of the loss or to free up optical resource reservations. The OBS acknowledgement protocol has been modified in this work to account for a BCP failure by implementing a traversal acknowledgement to cater for its loss. The performance of the distributed ACO-based algorithm has been extensively evaluated on several network topologies and compared with that obtained by SPR and ACRWA. The results show that the distributed ant-based algorithm significantly improves the burst transmission success probability in the traditional ITU WDM network environment and provides a good solution in the Flexible Spectrum network environment undergoing transmission impairments.

This study has been submitted to Photonic Network Communications and has received positive feedback from the reviewers.

Gravett, A. S., du Plessis, M. C., Gibbon, T. B. (2017). A Distributed Ant-Based Algorithm for Routing and Wavelength Assignment in an Optical Switching Flexible Spectrum Network with Transmission Impairments. Manuscript submitted for publication.